PONTIFICIA
UNIVERSIDAD
CATÓLICA
DE CHILE

Facultad de Medicina

Departamento de Gastroenterología

ROLE OF EXTRACELLULAR VESICLES IN HYPOXIA-INDUCED HEPATIC INJURY IN NON-ALCOHOLIC FATTY LIVER DISEASE

por

ALEJANDRA HERNÁNDEZ VILLANUEVA

Tesis Doctoral presentada a la Facultad de Medicina de la Pontificia Universidad Católica de Chile para optar al grado académico de Doctor en Ciencias Médicas

Profesores guías

Dr. Marco Arrese, MD
Dr. Han Moshage, Prof

Abril 2020
Santiago-Chile

Se autoriza la reproducción total o parcial, con fines académicos, por cualquier medio o procedimiento, incluyendo la cita bibliográfica que acredita al trabajo y a su autor.

30 Abril 2020 ---------- 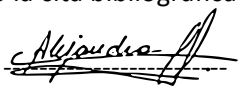

FECHA FIRMA

A mis padres por impulsarme a abrir mis alas y por confiar siempre en mí,

A toda mi familia por su amor incondicional,

A mis amigas del alma que son mi otra familia que elegí,

A mis profesores que les debo cada enseñanza y formación profesional,

A mi pololo por ser la alegría de mi vida,

A cada uno de ustedes…los quiero y llevo siempre en mi corazón.

Acknowledgements

This doctoral thesis was supported by the Chilean government through Fondo Nacional de Desarrollo Científico y Tecnológico (FONDECYT 1150327 and 1191145) and PhD fellowship from Comisión Nacional para la Investigación en Ciencia y Tecnología (CONICYT) and Vicerrectorate of Research and School of Medicine, PUC. Also, the support from the Abel Tasman Talent Program (ATTP) of the Graduate School of Medical Sciences and the University Medical Center Groningen (UMCG) from The Netherlands is gratefully acknowledged.

Abstract

Background: Nonalcoholic fatty liver disease (NAFLD) is considered the most common liver disease worldwide. Transition from steatosis to non-alcoholic steatohepatitis (NASH) is a key issue in NAFLD. Observations in patients with obstructive sleep apnea syndrome (OSAS), which is characterized by occurrence of intermittent hypoxia (IH), suggest that hypoxia contributes to develop NASH. Among other mechanisms, release of extracellular vesicles (EV) by injured hepatocytes has been implicated in NAFLD progression. **Aim:** In this thesis we aimed to investigate the role of hypoxia condition in modulation of steatosis and liver injury in both *in vitro* and *in vivo* models of NAFLD. Also we evaluated the cellular crosstalk between hypoxic and steatotic hepatocytes and non-parenchymal cells through EVs. **Methods:** Primary rat hepatocytes and hepatoma cell line HepG2 treated with free fatty acids (FFA) were subjected to chemically induced hypoxia (CH) using the hypoxia-inducible factor-1 alpha (HIF-1α) stabilizer cobalt chloride (CoCl2). Triglyceride (TG) content, oxidative stress, cell death rates, pro-inflammatory and pro-fibrotic cytokines, inflammasome components gene expression and protein levels of cleaved caspase-1 were assessed. Also, Kupffer cells (KC) and human stellate cell (LX-2) were treated with conditioned medium (CM) and EVs from hypoxic fat-laden hepatocytes. The choline deficient L-amino acid defined (CDAA)-fed mice model used to assess the effects of IH on experimental NAFLD. **Results:** Hepatocytes exposed to FFA and CoCl2 exhibited increased TG content and higher cell death rates as well as increased, oxidative stress and mRNA levels of pro-inflammatory, pro-fibrotic cytokines and inflammasome-components compared to non-treated hepatocytes. Protein levels of cleaved caspase-1 increased in CH-exposed hepatocytes and from EVs-hepatocytes. CM and EVs from hypoxic fat-laden hepatic cells evoked pro-inflammatory and pro-fibrotic phenotype in KC and LX-2 respectively. Livers from CDAA-fed mice exposed to IH exhibited increased of steatosis, portal inflammation, fibrosis, mRNA levels of pro-inflammatory, pro-fibrotic and inflammasome genes as well as increased levels of cleaved caspase-1 that correlated with an increase of circulating EV-caspase-1. **Conclusion:** Our findings in both *in vivo* and *in vitro* models of NAFLD/NASH indicate that hypoxia may increase liver injury and promote disease progression through amplification of inflammatory and fibrotic signals including inflammasome/caspase-1 activation. Hypoxia also promotes the release of EVs from hepatocytes contributing to cellular crosstalk with non-parenchymal cells by EVs-caspase-1-related mechanisms. These results suggest EVs and their content (caspase-1) as a potential novel biomarker in NAFLD and OSAS. Further characterization of EVs released under hypoxic conditions will allow the detailed delineation of their role in the promotion of steatosis, inflammation and fibrosis in the context of NAFLD and OSAS.

Resumen

Antecedentes: El hígado graso no alcohólico (HGNA) es actualmente la enfermedad hepática más prevalente en todo el mundo. Los mecanismos que subyacen a la transición de la esteatosis a la esteatohepatitis no alcohólica (EHNA) no está del todo comprendida. Observaciones clínicas en pacientes con el síndrome de la apnea obstructiva del sueño (SAOS), caracterizada por la presencia de hipoxia intermitente (HI), sugieren que esta condición contribuye al desarrollo de EHNA. Recientemente, el rol de las vesículas extracelulares (EV) desde hepatocitos esteatóticos ha sido estudiado en la progresión del daño en el HGNA. **Objetivo general:** Investigar si modelos experimentales de EHNA son más susceptibles a los efectos de hipoxia, y si tal condición promueve el aumento de EVs que señalizan a células no parenquimatosas. **Métodos:** Cultivo primario de hepatocitos y una línea celular HepG2 fueron tratados con ácidos grasos libres (FFA) y sometidos a hipoxia inducida químicamente (CH) usando cloruro de cobalto ($CoCl_2$). Se evaluó el contenido de triglicéridos (TG), el estrés oxidativo, muerte celular, la expression génica de citoquinas pro-inflamatorias, pro-fibróticas, y de los componentes del inflamasoma, incluída la caspasa-1 escindida. Las células de Kupffer (KC) y las células estrelladas humanas (LX-2) se trataron con medio condicionado (CM) y con EVs aisladas de hepatocitos. El modelo de ratones alimentados con L-aminoácido definido con deficiencia de colina (CDAA) se usó para evaluar los efectos de IH en HGNA experimental. **Resultados:** Los hepatocitos expuestos a FFA y $CoCl_2$ exhibieron un mayor contenido de TG, muerte celular, estrés oxidativo y un aumento en los niveles de la expression génica de citoquinas proinflamatorias, pro-fibróticas y de los componentes de inflamasoma en comparación con los hepatocitos no tratados. Los niveles de caspasa-1 escindida aumentaron en los hepatocitos expuestos a CH, así como en las EVs de los hepatocitos hipóxicos y estetaóticos. El CM y el mayor número de EVs de las células hepáticas hipóxicas tratadas con FFA promovieron un fenotipo pro-inflamatorio y pro fibrótico en las KC y LX-2 respectivamente. Los hígados de ratones alimentados con CDAA expuestos a IH mostraron un aumento en la esteatosis, en la inflamación y fibrosis que se correlacionó con un aumento de las EVs circulantes con cargo de caspasa-1. **Conclusión:** Nuestros hallazgos indican que los modelos experimentales de HGNA son más susceptibles a los efectos de la hipoxia que se correlacionan con el aumento de las EVs. La hipoxia promovió señales inflamatorias y fibróticas, incluida la activación del inflamasoma/caspasa-1 en hepatocitos cargados de grasa y en nuestro modelo in vivo de EHNA, contribuyendo a la diafonía celular con células no parenquimatosas por EVs-caspasa-1. Estos resultados proponen a las EVs, y su contenido (caspasa-1), como un nuevo biomarcador potencial en HGNA y SAOS.

TABLE OF CONTENTS **Page**

PREFACE & SCOPE OF THIS DOCTORAL THESIS

Preface

Non-alcoholic fatty liver disease (NAFLD) is a highly prevalent chronic liver disease that affects 30% of the general population. Of note, the incidence of NAFLD is steadily increasing due to its closed links with the obesity pandemic. NAFLD encompasses a pathological spectrum of liver lesions, ranging from isolated steatosis to an inflammatory condition termed non-alcoholic steatohepatitis (NASH), that can progress to liver fibrosis and subsequently to cirrhosis and hepatocellular carcinoma (HCC). Clinical observations have indicated that obstructive sleep apnea syndrome (OSAS) is a significant risk factor that predisposes patients to the progression of liver steatosis, inflammation and fibrosis. OSAS is a sleep breathing disorder characterized by intermittent hypoxia (IH) during sleep. It has been shown that IH in patients and in experimental rodent models is linked to oxidative stress, steatosis, inflammation and liver fibrosis.

In recent years, extracellular vesicles (EVs) have been implicated in intercellular communication in various pathophysiological conditions, including NASH. However, the mechanisms underlying the role of EVs in NASH in the context of (intermittent) hypoxia remains unexplored.

This doctoral thesis focuses on the role of extracellular vesicles in the pathogenesis of hypoxia-induced hepatic injury in different models of NASH. To validate our hypotheses we used *in vitro* models to investigate cellular crosstalk between fat-laden hepatocytes exposed to chemical hypoxia and non-parenchymal cells, such as hepatic stellate cells and Kupffer cells. Also, we used an *in vivo* model of NASH to evaluate whether IH promotes liver injury and increases circulating EVs. Our findings reveal new insights on the pathophysiological effects of hypoxia on lipotoxicity, inflammation and fibrosis. Moreover, we provide novel insights with regard to the presence of caspase-1 in EVs, suggesting caspase-1 as a potential novel biomarker to monitor NAFLD and OSA.

Scope of the thesis

The research described in this thesis focuses on the combination of lipotoxic and hypoxic conditions in *in vitro* and *in vivo* models of NASH. We investigated whether hypoxia promotes the activation of inflammatory and fibrotic pathways, with a special emphasis on inflammasome activation and the role of EVs in amplifying injury and evoking fibrogenesis through cellular crosstalk between hepatocytes and Kupffer cells and hepatic stellate cells respectively.

In **Chapter 1** we present a general introduction of NAFLD, intermittent hypoxia-related OSA, the role of EVs in NAFLD/NASH and the general aims of this thesis.

In **Chapter 2**, the role of EVs in liver (patho)physiology is reviewed and discussed *in-depth*, including their potential applications as biomarkers and therapeutics.

In **Chapter 3** we introduce our experimental *in vitro* model of NASH using primary rat hepatocytes exposed to free fatty acids (FFA) and subjected to chemically-induced hypoxia (CH) using the hypoxia-inducible factor 1 alpha (HIF-1α) stabilizer cobalt chloride ($CoCl_2$). We observed that hypoxia aggravates hepatocellular injury via a mechanism that involves inflammasome/caspase-1 activation in fat-laden hepatocytes and cellular crosstalk with Kupffer cells through EVs.

In **Chapter 4** we show studies evaluating whether IH has a pro-inflammatory effect using the CDAA-diet model of NASH. We observed that IH correlates with steatosis, inflammation and inflammasome/caspase-1 activation in our experimental model of NASH. Moreover, we observed that silencing of HIF-1α in hepatocytes abolished the induction of inflammasome-related genes in Kupffer cells. These data suggest that IH could be an aggravating factor in the progression of NASH via HIF-1α induction.

In **Chapter 5** we present experiments assesing the cellular crosstalk between hypoxic human HepG2 cells exposed to FFA and human hepatic LX-2 stellate cells. We observed that hypoxia exacerbates hepatocellular damage and pro-fibrotic signaling and that this is correlated with increased EVs release from fat-laden HepG2 cells. Interestingly, EVs from hypoxic fat-laden HepG2 evoked a pro-fibrotic response in LX-2 cells.

In **Chapter 6** we show data pointing to caspase-1 as one of the cargo components of EVs from both hypoxic fat-laden hepatocytes as well as from serum of mice fed the CDAA diet and exposed to IH.

Finally, in **Chapter 7** we summarize and discuss our results and provide an outlook for future studies.

Chapter 1

1. - GENERAL INTRODUCTION AND AIMS OF THE DOCTORAL THESIS

Non-alcoholic fatty liver disease (NAFLD) is the most common liver disease worldwide, affecting up to 30% of the current population (1). NAFLD is used as an umbrella term that describes a clinico-pathological entity defined by the presence of a spectrum of hepatic histological changes. Observed phenotypes vary in severity from non-inflammatory isolated steatosis (also termed non-alcoholic fatty liver [NAFL]) to a more aggressive form named steatohepatitis (or non-alcoholic steatohepatitis, NASH), which is characterized by inflammatory changes and hepatocellular ballooning associated with varying degrees of liver fibrosis (2,3). NASH is a multisystem disease associated with a significant risk for the development of cirrhosis and hepatocellular carcinoma, as well as liver transplantation and liver-related death (4,5).

The pathogenesis of NAFLD involves a complex interaction between nutritional factors, obesity, insulin resistance, changes in the microbiota, genetic and epigenetic factors. These factors are involved in the development and progression of steatosis resulting in an excessive accumulation of lipids, especially triglycerides, in the hepatocytes (6-8). Moreover, these factors contribute, either simultaneously or sequentially, to the inflammatory and fibrotic response of the liver to steatosis (9). At the cellular level, the increased influx of free fatty acids (FFA) into the liver exceeds the physiological capacity, leading to reactive oxygen species (ROS) overproduction, mitochondrial dysfunction and cellular death in a process called lipotoxicity, ultimately leading to inflammation and fibrosis (10,11).

Several studies have shown that lipotoxicity appears to be the central driver of hepatocellular damage that contributes to the inflammatory response and the development of liver fibrosis (12,13). The crosstalk between hepatocytes and non-parenchymal cells plays a crucial role in this inflammatory and fibrotic response (14-17). It is believed that fat-laden (steatotic) hepatocytes release damage signals to the extracellular environment, resulting in paracrine effects on neighboring cells such as resident macrophages of the liver (Kupffer cells) and stellate cells that promote the activation of inflammatory and fibrogenic pathways, respectively (18,19). In addition, fat-laden hepatocytes trigger various pathways leading to hepatocellular dysfunction by autocrine effects that initiate and perpetuate lipotoxicity (20-22).

In recent years, obstructive sleep apnea syndrome (OSAS), a common sleep disorder characterized by recurrent closure of the upper airways during sleep, has been associated with the development and progression of NAFLD (23) in both obese and non-obese subjects (24-25). The most noted hallmark of OSAS is intermittent hypoxia (IH), which leads to tissue hypoxia and can result in ROS

overproduction, mitochondrial dysfunction and inflammation (26). These events are also involved in the initiation of NASH (27). Several studies have indicated a link between OSAS or IH with increased liver TG accumulation in NAFLD through modulation of β-oxidation of fatty acids and *de novo* lipogenesis in hepatocytes (28-31). In addition, in experimental models of NASH it has been shown that mimicking OSAS with IH has pro-inflammatory effects as indicated by increased levels of inflammatory cytokines such as tumor necrosis factor alpha (TNF-α) and interleukin-6 (IL-6) (30, 31). Likewise, *in vitro* studies using hepatocytes demonstrated that hypoxia-inducible factor 1 alpha (HIF-1α) increases hepatocyte apoptosis and generation of pro-inflammatory signals in inflammatory cells (32-34). Moreover, a link between HIF-1α and hepatic inflammation and fibrosis has also been described in animal studies of IH (35-37). Taken together, the experimental evidence suggests that hypoxia, in a HIF-1α dependent manner, contributes to the transition from isolated steatosis to more advanced stages of NAFLD and can aggravate lipotoxicity, inflammation and/or fibrosise.

The pathophysiology of NASH is known to involve hepatocellular damage associated with lipotoxicity, triggering local inflammatory responses and contributing to liver fibrosis. However, there is a lack of knowledge regarding the mechanisms of the detrimental effect of hypoxia on fat-laden hepatocytes and the role of intercellular communication between hepatocytes and non-parenchymal cells types such as Kupffer and stellate cells.

Recent studies have indicated that extracellular vesicles (EVs) play a key role in intercellular communication in liver pathobiology (38-40). EVs are nanoparticles defined by a lipid bilayer (41,42), that contains a cargo able to evoke many effects on target cells in both physiological as well as pathophysiological settings. Classification of EVs depend on their size and site of biogenesis: Exosomes (40-150 nm) are released from multivesicular bodies, microvesicles (MVs) (50-1000 nm) are released from the budding plasma membrane and apoptotic bodies (50-5000 nm) are released from blebbing cells (42). Exosomes and MVs may contain a variety of bioactive molecules, including cytoplasmic proteins, lipids, specific lipid raft-interacting proteins, messenger RNAs, noncoding RNAs and metabolites (42). In general, apoptotic bodies are excluded from studies on EVs (41). EVs have been implicated in many pathophysiological processes and recently, the field has expanded into EV-based diagnostics, prognosis and therapeutics (42,43). Several research groups have demonstrated the involvement of EVs in intercellular communication in *in vivo* an *in vitro* models of liver diseases (42-46). Recent studies have shown that hepatocyte-derived EVs activate pro-inflammatory signals and pro-fibrotic signals in non-parenchymal cells (47,48). Additionally, increased levels of circulating EVs in *in vivo* models of NAFLD correlate with histologic features of NASH that indicate liver damage (41-43,49). Therefore, it is important to study the content of EVs that exert paracrine effects on target cells. Interestingly, recent data suggest that EVs released from fat-laden hepatocytes activate

the inflammasome via caspase-1 activation in hepatocytes and macrophages leading to an inflammatory response (50).

The NOD-like receptor Pyrin Domain Containing 3 (NLRP3) inflammasome is specific and critical for the activation of caspase-1 and the processing of pro-inflammatory cytokines. The NLRP3 inflammasome has recently been demonstrated to contribute to the transition from NAFLD to NASH (51.52). Studies have also shown that expression of inflammasome components is increased in mouse models of NASH and in humans with NASH (53,54). Moreover, downregulation of NLRP3 or caspase-1 inflammasome components alleviate hepatic steatosis, inflammation and fibrosis (55-57), suggesting that the inflammasome is a potential therapeutic target in NASH.

The research presented in this doctoral thesis investigates whether hypoxia exacerbates lipotoxicity in fat-laden hepatocytes and liver injury in a mice model of non-alcoholic steatohepatitis via the release of extracellular vesicles and cellular crosstalk between hepatocytes and non-parenchymal cells. Additionally, we examined inflammasome activation in conditions of hypoxia, both *in vitro* and *in vivo*. Taken together, the results of this thesis establish a link between extracellular vesicles and hepatocellular damage in hypoxia models that mimics OSA. This link involves EV-mediated intercellular communication between hepatocytes and non-parenchymal cells in non-alcoholic steatohepatitis.

2.- REFERENCES

1. Estes C, Razavi H, Loomba R, Younossi Z, Sanyal AJ. Modeling the epidemic of nonalcoholic fatty liver disease demonstrates an exponential increase in burden of disease. Hepatology 2018; 67:123-133.
2. Arab JP, Arrese M, Trauner M. Recent Insights into the Pathogenesis of Nonalcoholic Fatty Liver Disease. Annu Rev Pathol 2018; 13:321-350.
3. Koyama Y, Brenner DA. Liver inflammation and fibrosis. J. Clin. Investig 2017; 127:55-64
4. Sanyal AJ. Past, present and future perspectives in nonalcoholic fatty liver disease. Nat Rev Gastroenterol Hepatol 2019; 16: 377-386.
5. Younossi ZM. Non-alcoholic fatty liver disease - A global public health perspective. J Hepatol 2019; 70:531-544.
6. Goh GB, McCullough AJ. Natural history of nonalcoholic fatty liver disease. Dig. Dis. Sci 2016; 61:1226–33
7. Musso G, Cassader M, Gambino R. Non-alcoholic steatohepatitis: emerging molecular targets and therapeutic strategies. Nat. Rev. Drug. Discov. 2016; 15:249–74

8. Hardy T, Oakley F, Anstee QM, Day CP. Nonalcoholic fatty liver disease: pathogenesis and disease spectrum. Annu. Rev. Pathol. 2016; 11:451–96
9. Buzzetti E, Pinzani M, Tsochatzis EA. The multiple-hit pathogenesis of non-alcoholic fatty liver disease (NAFLD). Metabolism 2016; 65:1038–48
10. Kakisaka K, Cazanave SC, Fingas CD, Guicciardi ME, Bronk SF, Werneburg NW, Mott JL, et al. Mechanisms of lysophosphatidylcholine-induced hepatocyte lipoapoptosis. Am J Physiol Gastrointest Liver Physiol 2012;302:G77-84.
11. Hirsova P, Ibrahim SH, Gores GJ, Malhi H. Lipotoxic lethal and sublethal stress signaling in hepatocytes: relevance to NASH pathogenesis. J. Lipid Res. 2016; 57:1758–70
12. Geng Y, Hernandez A, Faber KN, de Meijier VE, Blokzijl H, Moshage H. Lipotoxicity in non-alcoholic fatty liver diseases: mechanisms and clinical implications. BBA-Mol Cell Biol l. October 2019. Submitted
13. Neuschwander-Tetri BA. Hepatic lipotoxicity and the pathogenesis of nonalcoholic steatohepatitis: the central role of nontriglyceride fatty acid metabolites. Hepatology 2020; 52:774–88
14. Wobser H., Dorn C., Weiss T. S., et al. Lipid accumulation in hepatocytes induces fibrogenic activation of hepatic stellate cells. Cell Research. 2009; 19:996–1005.
15. Brenner C., Galluzzi L., Kepp O., Kroemer G. Decoding cell death signals in liver inflammation. Journal of Hepatology. 2013; 59:583–594.
16. Lebensztejn D. M., Flisiak-Jackiewicz M., Białokoz-Kalinowska I., Bobrus-Chociej A., Kowalska I. Hepatokines and non-alcoholic fatty liver disease. Acta Biochimica Polonica. 2016;63:459–467.
17. Ganz M., Szabo G. Immune and inflammatory pathways in NASH. Hepatology International. 2013;7:771–781.
18. Wobser H, Dorn C, Weiss TS, Amann T, Bollheimer C, Büttner R, Schölmerich J, Hellerbrand C. Lipid accumulation in hepatocytes induces fibrogenic activation of hepatic stellate cells. Cell Res. 2009; 19:996-1005.
19. Wan J, Benkdane M, Teixeira-Clerc F, Bonnafous S, Louvet A, Lafdil F, Pecker F, Tran A, Gual P, Mallat A, Lotersztajn S, Pavoine C. M2 Kupffer cells promote M1 Kupffer cell apoptosis: a protective mechanism against alcoholic and nonalcoholic fatty liver disease. Hepatology. 2014; 59: 130-42.
20. Brenner C, Galluzzi L, Kepp O, Kroemer G. Decoding cell death signals in liver inflammation. J Hepatol. 2013; 59:583-94.
21. Liu J, Han L, Zhu L, Yu Y. Free fatty acids, not triglycerides, are associated with non-alcoholic liver injury progression in high fat diet induced obese rats. Lipids Health Dis. 2016 11; 15:27.

22. Bellanti F, Villani R, Facciorusso A, Vendemiale G, Serviddio G. Lipid oxidation products in the pathogenesis of non-alcoholic steatohepatitis. Free Radic Biol Med 2017;111:173-185.
23. Mesarwi, O, Loomba, R, Malhotra, A. Obstructive sleep apnea, hypoxia, and nonalcoholic fatty liver disease. Am J Respir Crit Care Med. 2019 1;199:830-841.
24. Chen LD, Zhang LJ, Lin XJ, Qi JC, Li H, Wu Z, Xu QZ, Huang YP, Lin L. Association between continuous positive airway pressure and serum aminotransferases in patients with obstructive sleep apnea. Eur Arch Otorhinolaryngol 2018; 275: 587-594.
25. Qi JC, Huang JC, Lin QC, Zhao JM, Lin X, Chen LD, Huang JF, Chen X. Relationship between obstructive sleep apnea and nonalcoholic fatty liver disease in nonobese adults. Sleep Breath 2016; 20: 529-535.
26. May AM, Mehra R. Obstructive sleep apnea: role of intermittent hypoxia and inflammation. Semin Respir Crit Care Med. 2014;35:531-44.
27. Noureddin M, Sanyal AJ. Pathogenesis of NASH: The Impact of Multiple Pathways. Curr Hepatol Rep. 2018;17:350-360.
28. Buttacavoli M, Gruttad'Auria CI, Olivo M, Virdone R, Castrogiovanni A, Mazzuca E, Marotta AM, Marrone O, Madonia S, Bonsignore MR. Liver Steatosis and Fibrosis in OSA patients After Longterm CPAP Treatment: A Preliminary Ultrasound Study. Ultrasound Med Biol 2016; 42: 104-109.
29. Aron-Wisnewsky J, Minville C, Tordjman J, Levy P, Bouillot JL, Basdevant A, Bedossa P, Clement K, Pepin JL. Chronic intermittent hypoxia is a major trigger for non-alcoholic fatty liver disease in morbid obese. J Hepatol 2012; 56: 225-233.
30. Briancon-Marjollet A, Monneret D, Henri M, et al. Intermittent hypoxia in obese Zucker rats: cardiometabolic and inflammatory effects. Exp Physiol. 2016; 101:1432-1442.
31. Kang HH, Kim IK, Lee HI, et al. Chronic intermittent hypoxia induces liver fibrosis in mice with diet-induced obesity via TLR4/MyD88/MAPK/NF-kB signaling pathways. Biochem Biophys Res Commun. 2017; 490:349-355.
32. Shi YF, Fong CC, Zhang Q, Cheung PY, Tzang CH, Wu RS, Yang M. Hypoxia induces the activation of human hepatic stellate cells LX-2 through TGF-beta signaling pathway. FEBS Lett 2007;581:203-210.
33. Copple BL, Bai S, Burgoon LD, Moon JO. Hypoxia-inducible factor-1alpha regulates the expression of genes in hypoxic hepatic stellate cells important for collagen deposition and angiogenesis. Liver Int 2011;31:230-244.
34. Roth KJ, Copple BL. Role of Hypoxia-Inducible Factors in the Development of Liver Fibrosis. Cell Mol Gastroenterol Hepatol 2015;1:589-597.

35. Savransky V, Bevans S, Nanayakkara A, Li J, Smith PL, Torbenson MS, Polotsky VY. Chronic intermittent hypoxia causes hepatitis in a mouse model of diet-induced fatty liver. Am J Physiol Gastrointest Liver Physiol 2007; 293: G871-877.
36. Moon JO, Welch TP, Gonzalez FJ, Copple BL. Reduced liver fibrosis in hypoxia-inducible factor-1alpha-deficient mice. Am J Physiol Gastrointest Liver Physiol 2009; 296: G582-592.
37. Mesarwi OA, Shin MK, Bevans-Fonti S, Schlesinger C, Shaw J, Polotsky VY. Hepatocyte Hypoxia Inducible Factor-1 Mediates the Development of Liver Fibrosis in a Mouse Model of Nonalcoholic Fatty Liver Disease. PLoS One 2016; 11: e0168572.
38. Hirsova P, Ibrahim SH, Verma VK, Morton LA, Shah VH, LaRusso NF, Gores GJ, Malhi H. Extracellular vesicles in liver pathobiology: Small particles with big impact. Hepatology (Baltimore, Md) 64: 2219-2233, 2016.
39. Stahl PD, and Raposo G. Extracellular Vesicles: Exosomes and Microvesicles, Integrators of Homeostasis. Physiology 2019; 34: 169-177.
40. Arrese M, Eguchi A, Feldstein AE. Circulating microRNAs: emerging biomarkers of liver disease. Semin Liver Dis 2015;35:43-54
41. Malhi H. Emerging Role of Extracellular Vesicles in Liver Diseases. Am J Physiol Gastrointest Liver Physiol 2019; 317: G739–G749.
42. Szabo G, Momen-Heravi F. Extracellular vesicles in liver disease and potential as biomarkers and therapeutic targets. Nat Rev Gastroenterol Hepatol 2017; 14: 455-466.
43. Arab JP, Reyes D, Lapitz A, Moshage H, Bañales JM, Arrese M.Extracellular Vesicles in NAFLD/ALD: From Pathobiology to Therapy. Hernández A, Cells. 2020 Mar 27;9(4):E81
44. Kakazu E, Mauer AS, Yin M, and Malhi H. Hepatocytes release ceramide-enriched pro-inflammatory extracellular vesicles in an IRE1alpha-dependent manner. J Lipid Res 2016; 57: 233-245.
45. Povero D, Eguchi A, Li H, Johnson CD, Papouchado BG, Wree A, Messer K, and Feldstein AE. Circulating extracellular vesicles with specific proteome and liver microRNAs are potential biomarkers for liver injury in experimental fatty liver disease. PLoS One 2014; 9: e11365.
46. Povero D, Eguchi A, Niesman IR, Andronikou N, de Mollerat du Jeu X, Mulya A,Berk M, Lazic M, Thapaliya S, Parola M, Patel HH, and Feldstein AE. Lipid-induced toxicity stimulates hepatocytes to release angiogenic microparticles that require Vanin-1 for uptake by endothelial cells. Sci Signal 2013; 6: ra88.
47. Hirsova P, Ibrahim SH, Krishnan A, Verma VK, Bronk SF, Werneburg NW, Charlton MR, et al. Lipid-Induced Signaling Causes Release of Inflammatory Extracellular Vesicles From Hepatocytes. Gastroenterology 2016;150:956-967.

48. Lee YS, Kim SY, Ko E, Lee JH, Yi HS, Yoo YJ, Je J, et al. Exosomes derived from palmitic acid-treated hepatocytes induce fibrotic activation of hepatic stellate cells. Sci Rep 2017;7:3710.
49. Welsh JA, Scorletti E, Clough GF, Englyst NA, and Byrne CD. Leukocyte extracellular vesicle concentration is inversely associated with liver fibrosis severity in NAFLD. J Leukoc Biol 2018; 104: 631-639.
50. Cannito S, Morello E, Bocca C, Foglia B, Benetti E, Novo E, Chiazza F, et al. Microvesicles released from fat-laden cells promote activation of hepatocellular NLRP3 inflammasome: A pro-inflammatory link between lipotoxicity and non-alcoholic steatohepatitis. PLoS One 2017;12:e0172575.
51. Wan X, Xu C, Yu C, Li Y. Role of NLRP3 Inflammasome in the Progression of NAFLD to NASH. Can J Gastroenterol Hepatol. 2016;2016:6489012.
52. Luan J, Ju D. Inflammasome: A Double-Edged Sword in Liver Diseases. Front Immunol. 2018;9:2201.
53. Wree A, McGeough MD, Inzaugarat ME, Eguchi A, Schuster S, Johnson CD, Peña CA, Geisler LJ, Papouchado BG, Hoffman HM, Feldstein AE. NLRP3 inflammasome driven liver injury and fibrosis: Roles of IL-17 and TNF in mice. Hepatology. 2018 ; 67:736-749.
54. Wree A, McGeough MD, Peña CA, Schlattjan M, Li H, Inzaugarat ME, Messer K, Canbay A, Hoffman HM, Feldstein AE. NLRP3 inflammasome activation is required for fibrosis development in NAFLD. J Mol Med (Berl). 2014;92:1069-82.
55. Dixon LJ, Berk M, Thapaliya S, Papouchado BG, Feldstein AE. Caspase-1-mediated regulation of fibrogenesis in diet-induced steatohepatitis. Lab Invest. 2012; 92:713-23.
56. Yang G, Lee HE, Lee JY. A pharmacological inhibitor of NLRP3 inflammasome prevents non-alcoholic fatty liver disease in a mouse model induced by high fat diet. Sci Rep. 2016; 6: 24399
57. Cabrera D, Wree A, Povero D, Solís N, Hernandez A, Pizarro M, Moshage H, Torres J, Feldstein AE, Cabello-Verrugio C, Brandan E, Barrera F, Arab JP, Arrese M. Andrographolide Ameliorates Inflammation and Fibrogenesis and Attenuates Inflammasome Activation in Experimental Non-Alcoholic Steatohepatitis. Sci Rep 2017 14;7:3491.

Chapter 2

EXTRACELLULAR VESICLES IN NAFLD/ALD: FROM PATHOBIOLOGY TO THERAPY

ABSTRACT

In recent years, knowledge on the biology and pathobiology of extracellular vesicles (EVs) has exploded. EVs are submicron membrane-bound structures secreted from different cell types containing a wide variety of bioactive molecules [i.e., proteins, lipids, and nucleic acids (coding and non-coding RNA, and mitochondrial DNA]. EVs have important functions in cell- to-cell communication and are found in a wide variety of tissues and body fluids. Better delineation of EVs structure and advances in the isolation and characterization of their cargo have allowed to explore diagnostic and therapeutic implications of these particles. In the field of liver diseases, EVs are emerging as key players in pathogenesis of both alcoholic liver disease (ALD) and nonalcoholic liver disease (NAFLD), the most prevalent liver diseases worldwide and their complications, including development of hepatocellular carcinoma. In these diseases, stressed/damaged hepatocytes release large quantities of EVs that contribute to the occurrence of inflammation, fibrogenesis and angiogenesis that are key pathobiological processes in liver disease progression. Moreover, the specific molecular signatures of released EVs in biofluids have allowed to consider EVs as promising candidates to serve as disease biomarkers. Also, different experimental studies have shown that EVs may have potential for therapeutic use as a liver-specific delivery method of different agents taking advantage of their hepatocellular uptake through interactions with specific receptors. In this review, we will focus on the most recent findings concerning the role of EVs as new structures mediating autocrine and paracrine intercellular communication in both ALD and NAFLD as well as their potential use as biomarkers of disease severity and progression. Emerging therapeutic applications of EVs in these liver diseases are also examined and the potential for successful transition from bench to clinic.

1. - INTRODUCTION

Knowledge of the pathobiology of extracellular vesicles (EVs) has expanded significantly in the last decade (1, 2). Indeed, significant advances have been made in delineating the mechanisms of assembly and release of EVs as well as their subsequent membrane fusion with target cells (3, 4). Moreover, powerful analytical techniques have made possible the extensive characterization of the cargo of EVs that includes a myriad of molecules including growth factors, metabolic enzymes, microRNAs and transcription factors, certain proteins, lipids and metabolites, among others, that modulate intercellular and inter-organ communication (3, 5, 6). Of note, high-throughput datasets of vesicular components are now available in public databases, which strongly supports EV research (7, 8).

Novel insights into the biology of EVs show that these particles regulate critical biological functions and may act as contributors to disease pathogenesis and may also serve as disease biomarkers in virtue of the relative simplicity of EVs isolation from different biofluids (9). In addition, EVs are gaining interest from a therapeutic point of view due to their potential as a unique drug delivery system (10).

In the field of hepatology EVs have recently emerged as novel players in the pathogenesis and progression of several conditions (11-13) including the two most common liver diseases world-wide: non-alcoholic liver disease (NAFLD) and alcoholic liver disease (ALD) (14). Specifically, recent studies point to a significant role of EVs in modulating injury, amplifying inflammation and promoting liver fibrosis in both NAFLD and ALD (15-17). Since information on this topic is dynamic and rapidly evolving, we aim to provide an up-to-date overview of the current knowledge on the role of EVs in the context of both NAFLD and ALD with emphasis on their potential diagnostic and therapeutic impact in these diseases. We exclude from this review data regarding EVs in liver cancer since this has been recently reviewed elsewhere (18, 19).

2. - GENERAL CONCEPTS OF EV IN THE LIVER: EVs BIOGENESIS, SECRETION AND CARGO

Details on the formation and secretion pathways of EVs have been recently reviewed elsewhere (15, 20, 21) and can also be found in other contributions in this special issue of Cells (22). Only basic concepts will be provided here as well as information on aspects that are of particular importance for liver physiology and pathophysiology.

In general, EVs are classified according to size and biogenetic pathway, such as exosomes, microvesicles and apoptotic bodies (23). Exosomes are bilayer lipid vesicles with a diameter of 30-150 nm that are derived from endosomal multivesicular bodies (MVBs) (15, 23). Its formation results from the invagination of the plasma membrane (early endosome) and the subsequent fusion of endocytic vesicles mediated by the endosomal sorting complex responsible for transport (ESCRTs) and other components (such as ceramides and tetraspanins) (24). The MVBs can release the intraluminal vesicles known as exosomes by the fusion of MVBs to the plasma membrane, a process mediated in part by Rab GTPases (25). Microvesicles (MVs) have a diameter of 50-1000 nm and originate from the plasma membrane by budding and fission followed by release into the extracellular space (15, 23). MVs contain a subset of cell surface proteins depending on the composition of the parental plasma membrane (26, 27). Apoptotic bodies have a diameter of 100-5000 nm and originate from the budding of cell membranes and may contain nuclear material, which is quickly phagocytosed during programmed cell death (15, 28). Unlike exosomes and MVs, the role of apoptotic bodies is not related to intercellular communication. Therefore, when studying EVs under cellular damage conditions, apoptotic bodies are excluded (29).

All EVs transport a variety of bioactive molecules, including cytoplasmic proteins, lipids, specific lipid raft-interacting proteins, messenger RNA (mRNA), microRNA (miRNA), ribosomal RNA (rRNA), transfer RNA

(tRNA), noncoding RNAs (ncRNAs), DNA, mitochondrial DNA (mtDNA) and metabolites (24, 30). Lipidomic analysis has shown that EVs, independently of their biogenesis, contain a myriad of lipids such as cholesterol, sphingomyelin, ceramide, saturated fatty acids, phosphatidylcholine, phosphatidylethanolamine and phosphatidylserine (4, 23, 29, 30). In addition, proteomic analysis has shown that EVs contains different types of proteins, such as heat shock proteins (Hsp70 and Hsp90), tetraspanins (CD9, CD63, CD81, CD82), endosomal sorting complex proteins required for transport (Alix and Tsg101), receptors including epidermal growth factor receptor (EGFR), membrane trafficking proteins (GTPases, Flotillin and Annexins), cytoskeletal proteins (tubulin and actin) and cytosolic proteins (5, 26). Of note, the cargo of EVs varies depending not only on their cellular origin but also on the condition under which they are released (i.e. physiological vs. pathological).

In the liver, both parenchymal (hepatocytes) and non-parenchymal cells (i.e. hepatic stellate cells, endothelial, cholangiocytes, Kupfer cells and liver endothelial cells) have been found to release EVs in both physiological and pathological states (20). However, information on target cell repertoire, receptors or other specific actions is still limited and incomplete. It has been shown that healthy hepatocytes produce limited amounts of exosomes containing proteins potentially relevant for cell survival, growth and proliferation (31), whereas stressed hepatocytes boost exosome release (32) and enrich their content in specific proteins, lipids and microRNAs that modulate the transcriptional program of neighboring hepatocytes and non-parenchymal cells, thus modulating inflammation and fibrosis which are critical for the progression of liver diseases (Figure 1). Interestingly recent evidence suggests that EVs from fat-laden hepatocyte can also signal to other organs such as adipose tissue influencing adipogenesis and tissue remodeling (33).

2.2 EVs and liver inflammation

Hepatocellular damage determines the release of a number of signals into the extracellular environment that can contribute to tissue inflammation (34). Some of these signals (collectively termed damage-associated molecular patterns [DAMPs]) are packaged in EVs and signal between hepatocytes and non-parenchymal cells such as liver-resident macrophages (Kupffer cells, KC) (35). Indeed, EVs may evoke synthesis and release of proinflammatory cytokines such as pro-interleukin (IL)-1b and IL-6 (36) by KCs, thus contributing to local inflammation (37). Also, EVs released from hepatocytes can promote the recruitment of additional immune cells (i.e. proinflammatory monocyte-derived macrophages) into the liver maintaining and amplifying inflammation. EVs can also signal to endothelial cells and can contribute to vascular inflammation (38). Furthermore, to add complexity, EVs can also be secreted from other cells and influence liver inflammation. In this regard, some evidence suggests that platelet-derived EVs may have

proinflammatory effects in the liver but this needs further confirmation (39, 40). Finally, it has also been shown that EVs are released from monocytic cells and induce polarization towards the anti-inflammatory M2 phenotype of neighboring naive monocytes by delivering cargo miR-27a, thus contributing to resolution of inflammation (41). Collectively, these findings suggest that EVs released from injured hepatocytes have an important role in modulating the inflammatory response during liver damage through intercellular communication between different cell types with potential contributions from other cell-derived EVs (35). Specific mechanisms involved in NAFLD and ALD are reviewed below.

2.3 EVs and liver fibrosis

Persistent liver fibrogenesis and the development of cirrhosis are responsible for the liver-related morbidity and mortality associated with chronic liver diseases (42). Activation or trans-differentiation of HSCs resulting in insoluble collagen deposition and distortion of the normal macro- and micro-anatomical structure of the liver is the major driver of liver fibrogenesis (43). The role of paracrine signals originating from injured epithelial cells (hepatocytes) that can directly or indirectly induce HSC activation has been recognized in recent years (44). In this regard, EVs seem to play a role as shown by previous reported studies. Of note, lipid-induced hepatocyte-derived EVs seem to regulate HSC activation by shuttling specific microRNAs (i.e. miR-128-3p) that suppress PPAR-γ expression in HSC leading to a marked increase of profibrogenic gene expression (45). Other authors have shown that internalization of endothelial-derived exosomes by HSCs enhances cell migration in a process mediated by sphingosine 1-phosphate (S1P) (46). Additionally, intercellular communication between quiescent and activated HSCs via exosomes can also modulate fibrosis. In this regard, a role for shuttled microRNA 214 (miR-214) in regulating the expression of alpha-smooth muscle actin and collagen in activated HSCs has been demonstrated (47, 48). Moreover, EVs derived from non-resident cells such as platelets or granulocytes have been shown to increase angiogenesis and to have procoagulant properties, thus promoting fibrogenesis (49, 50). These findings suggest that EVs appear to be key modulators in fibrosis as signals from both parenchymal and non-parenchymal liver cells can either drive or slow down HSC activation. In addition, circulating EVs may be used as a biomarker of hepatic fibrosis and have potential implications for the development of novel anti-fibrotic targets (51) as reviewed in the following sections.

3. - EVs AS BIOMARKERS IN LIVER DISEASES

Dynamic changes of EV generation in pathological conditions and the accessibility to measure and analyze them in biological samples (i.e. blood, urine, bile and other biofluids) render EVs good candidates as disease biomarkers. The relative accessibility for testing and performing repeated measurements over time could facilitate early diagnosis, disease monitoring and development of personalized medicine.

Furthermore, refinement of techniques allowing isolation and in depth characterization of EV cargoes can lead to identification of disease-specific molecular signatures or profiles and provide ample opportunities for EVs to be used as suitable, non-invasive biomarkers (52).

EVs have been studied as potential biomarkers of liver injury in the setting of ALD, NAFLD, drug-induced liver disease and cholangiopathies (13, 27, 53, 54) as well as diagnostic tools for liver cancer (i.e. hepatocellular carcinoma and cholangiocarcinoma) (19, 54). In this regard, determination of the number of circulating EVs and the use of nucleic acid based, lipid-based and protein-based diagnostics have been performed to measure EVs enriched in liver-derived DNA, microRNAs, lipids or proteins (13, 27). However, before implementing EV-based biomarkers in the clinic, standardization of sample processing (i.e. collection, transportation, storage and handling) and assay systems is needed as well as large replicative studies to allow EV molecular signatures to be conclusively linked to specific liver diseases. Recent advances related to NAFLD and ALD are reviewed below.

4. - THERAPEUTIC POTENCIAL OF EVs

From a therapeutic perspective, EVs either unmodified or engineered, can be utilized for therapeutic purposes (55). With regard to liver diseases, efforts have been focused on two major areas: a) the use of EVs as delivery vehicles of drugs to the liver (56) and b) the use of EVs themselves as therapeutic agents to stimulate liver regeneration, modulate inflammation, reduce liver fibrosis or halt hepatocarcinogenesis (57, 58). The former approach involves the use of different techniques to load EVs with a desired cargo (i.e. miRNA, siRNA, chemotherapeutic agents) to act as a "Trojan horse" on target cells. Theoretically, membrane properties of EVs allow organ and cell-specific delivery, immune-evasion and targeting of distinct intracellular trafficking pathways. However, a number of challenges related to the manufacturing of EVs (i.e. production, coating, loading, etc.) still need to be solved before controlled clinical studies can be carried out (59, 60). With regard to the use of EVs as therapeutic agents, most of the available evidence has been generated using mesenchymal stem cell (MSC)-derived EVs obtained from human umbilical cord or human embryos that have been tested in numerous preclinical liver disease models (i.e. carbon tetrachloride, thioacetamide, D-galactosamine/TNF-α-induced lethal hepatic failure and bile duct ligation) with promising results. Data for NAFLD and ALD are more limited and are reviewed in the corresponding sections below.

A third, and still nascent, approach related to EV-based therapy is based on the concept that interfering with EVs secretion or uptake may attenuate harmful effects on target cells (11, 61). In this regard, several pharmacological agents are being explored that have been shown to inhibit EV trafficking, modify lipid metabolism or decrease EVs secretion. However, the complexity of EVs biogenesis poses significant

challenges to the development of specific agents able to block EVs production selectively [see ref. (61) for an in-depth review of this topic].

5. - EVs IN NAFLD

A number of studies have demonstrated a role of EVs in both pathogenesis and progression of NAFLD (14, 15). Triggering of inflammation and fibrosis development are key for progression from isolated steatosis (also referred as NAFL or non-NASH fatty liver) to nonalcoholic steatohepatitis (NASH), which is hallmarked by the presence of hepatocyte ballooning as reflect of ongoing liver injury and death (36). Data from different diet-induced animal models of NASH have shown that EV concentration increases with disease progression in a time-dependent manner.(17, 62, 63). This seems to be a response to the accumulation of toxic lipids and their downstream mediators in the liver, which increase the capacity of hepatocytes to form and release different types of EVs (37, 62-64). *In vitro* treatment of hepatocytes with non-esterified fatty acids evokes the release of EVs containing numerous molecules including C-X-C motif ligand 10 (CXCL10), sphingosine-1-phosphate (S1P), mitochondrial DNA (mtDNA), micro-RNAs, ceramides and tumor necrosis factor-related apoptosis-inducing ligand (TRAIL) (15). These molecules may amplify inflammation through multiple mechanisms such as macrophage activation and monocyte chemotaxis as well as inflammasome activation and modulation of the NF-κB pathway in target cells (64, 65). As mentioned earlier, EVs may be released by different mechanisms including a caspase-3-dependent mechanism (63) or activation of death receptor 5 (DR5) in hepatocytes. Hepatocyte-derived EVs are able to induce expression of pro-inflammatory cytokines and promote M1 polarization of hepatic macrophages (37, 66). Of note, CXCL10-bearing EVs can also serve as chemotactic stimuli for macrophages as shown recently (64). Moreover, EVs released from hepatocytes can contribute to hepatic recruitment of monocyte-derived macrophages by promoting monocyte adhesion via integrin β1 (ITGβ1)-dependent mechanisms as shown in murine NASH (67). Additional stimuli can also stimulate EVs release from hepatocytes. In this regard, it has been observed that hypoxia determines that fat-laden hepatocytes release EVs able to signal KC evoking proinflammatory phenotypes in this cells, a phenomena that may explain may underlie the aggravating effect of obstructive sleep apnea syndrome on NAFLD (68). Thus, it seems clear that lipotoxic injury of hepatocytes determines EVs release, promoting inflammation through activation and recruitment of macrophages (14) with clear implications for the triggering of inflammation in NAFLD/NASH (36). In addition, hepatocyte-derived EVs may promote HSC activation (45, 69) in experimental models of NAFLD/NASH. Interestingly, both mouse and human HSCs release EVs that target hepatocytes and HSCs themselves (47, 48, 70). Collectively, these data implicate EVs as part of the cellular events triggering hepatic fibrogenesis, a key process in NAFLD progression (71). In addition to signaling to macrophages and HSCs, EVs may act on

endothelial cells (38, 63) promoting vascular inflammation with potential implications for NAFLD-related atherosclerosis. In this regard, it has been shown that EVs carrying miR-1 as cargo mediates proinflammatory effects in endothelial cells in mice via downregulation of KLF4 and activation of the NF-κB pathway (38). Finally, other organ-derived EVs (i.e. visceral adipose tissue-derived exosomes) can contribute to NAFLD pathogenesis and progression and influence fibrogenic pathways in both hepatocytes and HSCs (72) underscoring the role of other insulin-sensitive organs in NAFLD.

Studies carried out in mouse models of NASH have shown that total circulating EVs and particularly hepatocyte-derived EVs are elevated early in the disease process while other cell-derived EVs (i.e. macrophage- and neutrophil-derived EVs) appear in the circulation later, likely reflecting the ongoing inflammatory process (62, 73). Proteomic profiling of circulating EVs in experimental NAFLD has been demonstrated to allow differentiation between NAFLD *vs.* control animals (17). These findings underscore the potential of EVs as minimally invasive biomarkers for NAFLD (74), which are urgently for clinical trials and in the clinic. Since circulating EVs (mainly exosomes) are also increased in human NAFLD and have been found by some authors to correlate with disease histological features (75), EVs analysis in serum involving quantitative and qualitative determinations (including cell surface markers assessment and measurement of different cargoes [i.e. proteins, lipids and microRNAs]) is now a focus of intense research. Several studies have been published in this regard showing that the number of CD14+ and CD16+ EVs is inversely associated with the severity of NAFLD-related liver fibrosis, while also increasing the diagnostic capability of the enhanced liver fibrosis score (LFS) in patients with NAFLD (AUC: 0.948 and 0.967 for CD14+ and CD16+ EVs, respectively, vs 0.915 for LFS alone) (76). Other efforts include detection of circulating EVs containing C16:0 ceramide- and S1P-enriched lipid species that progressively increase in the plasma of obese patients with simple steatosis and in NASH patients with early fibrosis (62). Unfortunately, diagnostic accuracy of these determinations remains incompletely explored in the field of NAFLD/NASH and rigorous validation of this approach is needed (13, 74). Moreover, significant challenges remain regarding isolation, reproducibility and definition of normal controls (13, 77).

Therapeutic efforts involving EVs in the field of NAFLD/NASH are nascent. Attempts to halt inflammation and fibrosis in rodent models of NAFLD/NASH using EVs as therapeutic agents have been published recently. EVs obtained from amnion-derived MSC (AMSC) to treat rats with either NASH or liver fibrosis induced by the hepatic toxicant CCL4. AMSC-EVs were given intravenously in one or two doses and amelioration of inflammation and fibrogenesis was observed (78). More recently, human liver stem cells (HLSCs)-derived EVs have been used to treat mice with diet-induced steatohepatitis (79). The authors found that EV-HLSC treatment significantly downregulated hepatic pro-fibrotic and pro-inflammatory gene expression and ameliorated the histological abnormalities in

mice with NASH. Proteomic analysis of EV-HLSCs showed that their cargo included various anti-inflammatory proteins such as Interleukin-10, that may contribute to the observed beneficial effects. These results underscore the concept that EVs can be exploited for therapy in NAFLD/NASH.

6. - EVs AND ALD

Recent studies have focused on the role of EVs in ALD (11, 14, 80, 81). Both hepatocyte and monocyte-derived EVs have been postulated to regulate macrophage differentiation, thereby promoting inflammation in alcoholic hepatitis (AH) (24, 41, 53, 69, 82). Several molecules have been proposed to be responsible for EV-mediated cell-to-cell signaling, including miRNAs (in particular, miR-122 and miR-155) (41, 81, 83-88). The CD40 ligand was proposed as an EV cargo that could promote macrophage activation in vitro and in vivo in experimental models of AH (81). Also, in a mouse model of ALD involving gastric infusion of ethanol, a microRNA barcode (let7f, miR-29a, and miR-340) that can be detected in blood, which is specific for alcohol-related liver injury (16).

From a clinical point of view, there is currently no biomarker able to assess early stages of ALD. EVs have been shown to correlate with the diagnosis and prognosis of alcoholic hepatitis (89). Additionally, EVs have been proposed as potential biomarkers to differentiate mild and severe forms of ALD and their cargo, such as sphingolipids, to discriminate between different liver disease etiologies (89). Early identification of these subjects might lead to timely intervention in the disease process. At present, the diagnosis of AH relies on a history of alcohol consumption in a compatible clinical scenario. There are no biomarkers which permit the early diagnosis of AH in “at-risk” populations nor screening tests that can anticipate those at risk for more severe manifestations of AH. This at-risk group is particularly important to identify since there is no effective therapy for severe AH and efforts to avoid it could be implemented. Several clinical prognostic markers have been proposed but the variables used reflect the severity of liver disease. These indices (i.e. the Maddrey discriminant function, model for end-stage liver disease (MELD) and the Lille Score) are based on the non-specific biochemical assessment of liver and renal function and rely heavily on serum total bilirubin, prothrombin time, and creatinine (90). The reliance on bilirubin limits their diagnostic utility, as specificity is confounded by hyperbilirubinemia in co-existent cholestatic liver diseases such as drug-induced liver disease or cholestatic hepatitis such as primary sclerosing cholangitis and primary biliary cholangitis. None of these prognostic scores utilizes a pathophysiologically validated biomarker that reflects the underlying molecular and signaling mechanisms of the disease. Furthermore, the inflammatory response is predictive of mortality but is not taken into account in mathematical models. They can identify subjects at highest mortality risk with an area under the receiver operating curve (AUROC) of under 0.8; ideal survival models should have an AUROC >0.8 (91). The reason these scores are imperfect may be that they are not based on pathophysiologic mechanisms that mediate liver injury. Liver biopsy, the gold

standard for diagnosis of AH, remains underutilized due to the concurrent coagulopathy, which greatly increases the risk of biopsy-related complications (92). Liver biopsy-based hepatic histology score performs as an AUROC of 0.73 in predicting 90-day mortality (91). In this regard the use of EVs as biomarker in AH is promising. Thus, it has been recently reported that the total number of EVs was significantly increased in patients with AH and that two microRNAs (i.e. miRNA-192 and miRNA-30a) were significantly increased in plasma of subjects with AH (82). Most recently, EVs have been used as a surrogate marker of improvement in clinical trials of patients with AH (93). Further studies will be required to validate EV as a biomarker for AH diagnosis and/or prognosis.

7. - CONCLUDING REMARKS AND FUTURE PERSPECTIVES

The field of EVs in fatty liver diseases is rapidly evolving as the important functions of these particles in cell-to-cell communication and in the pathogenesis of both ALD and NAFLD, the most prevalent liver diseases worldwide, are unveiled. The release of large quantities of EVs by stressed/damaged hepatocytes contributes to inflammation, fibrogenesis and angiogenesis, fueling liver disease progression and provides opportunities for intervention. The identification of specific molecular signatures of released EVs is promising in the search for disease-specific biomarkers although more data is needed to validate these markers in larger cohorts and in a rigorous manner. EVs may have potential for therapeutic use but this field is still nascent. More research is needed for a successful transition of current EVs knowledge from the bench to the clinic.

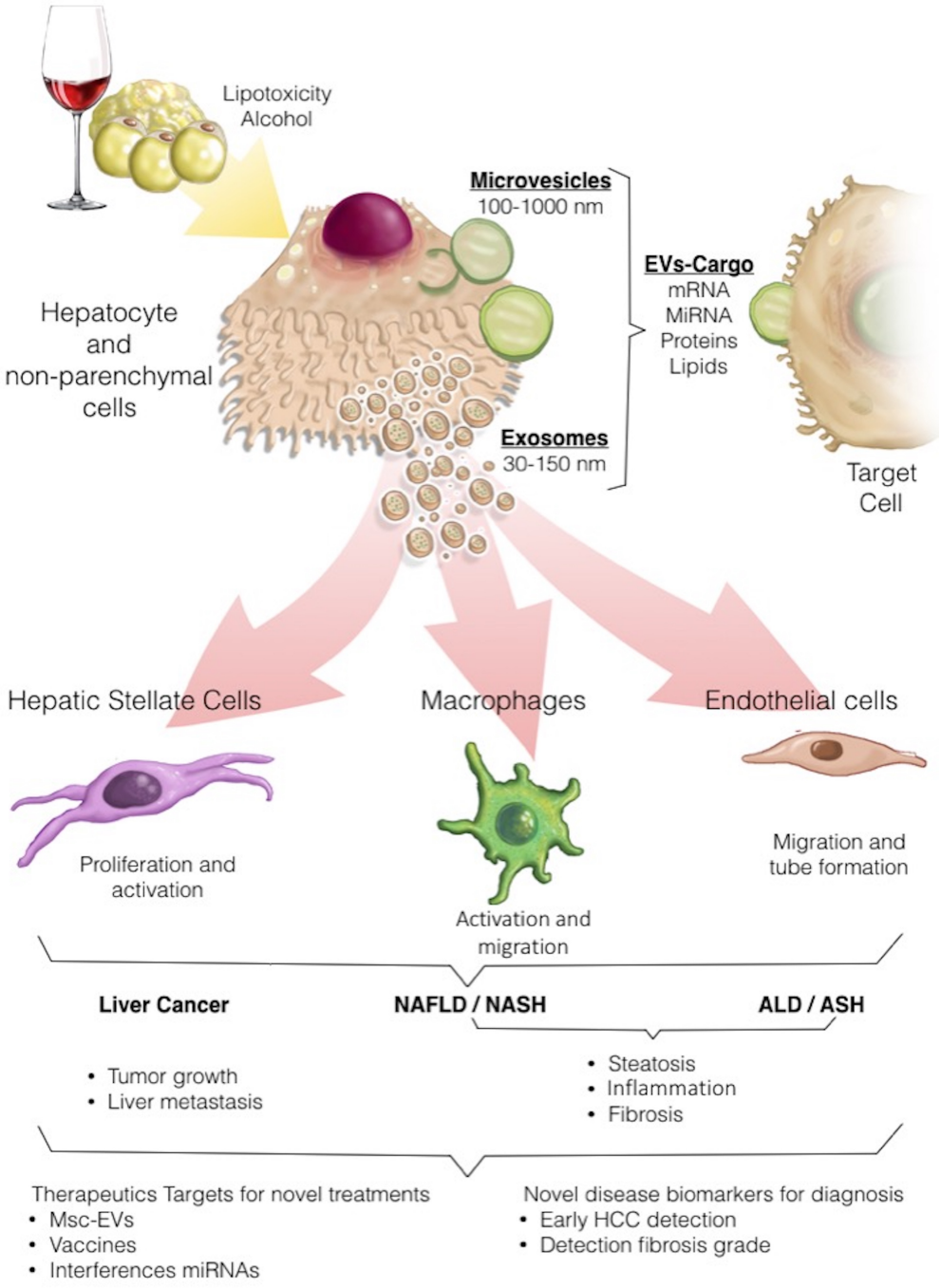

Figure 1. Extracellular vesicles (EVs) can be released by hepatocytes upon lipotoxic or alcohol-induced injury. EVs cargoes include a myriad of molecules that can act on target cells evoking inflammatory and fibrogenic events and promoting neoplastic transformation thus contributing to the progression of both alcoholic liver disease (ALD) and nonalcoholic liver disease (NAFLD) to their inflammatory and more aggressive forms nonalcoholic steatohepatitis (NASH) and alcoholic steatohepatitis (ASH).

8. - REFERENCES

1. Stahl PD, Raposo G. Extracellular Vesicles: Exosomes and Microvesicles, Integrators of Homeostasis. Physiology (Bethesda). 2019;34(3):169-77.

2. Cocucci E, Racchetti G, Meldolesi J. Shedding microvesicles: artefacts no more. Trends Cell Biol. 2009;19(2):43-51.

3. Abels ER, Breakefield XO. Introduction to Extracellular Vesicles: Biogenesis, RNA Cargo Selection, Content, Release, and Uptake. Cell Mol Neurobiol. 2016;36(3):301-12.

4. van Niel G, D'Angelo G, Raposo G. Shedding light on the cell biology of extracellular vesicles. Nat Rev Mol Cell Biol. 2018;19(4):213-28.

5. Kowal J, Arras G, Colombo M, Jouve M, Morath JP, Primdal-Bengtson B, et al. Proteomic comparison defines novel markers to characterize heterogeneous populations of extracellular vesicle subtypes. Proc Natl Acad Sci U S A. 2016;113(8):E968-77.

6. Zivko C, Fuhrmann G, Luciani P. Liver-derived extracellular vesicles: A cell by cell overview to isolation and characterization practices. Biochim Biophys Acta Gen Subj. 2020:129559.

7. Kim DK, Lee J, Kim SR, Choi DS, Yoon YJ, Kim JH, et al. EVpedia: a community web portal for extracellular vesicles research. Bioinformatics. 2015;31(6):933-9.

8. Kim DK, Kang B, Kim OY, Choi DS, Lee J, Kim SR, et al. EVpedia: an integrated database of high-throughput data for systemic analyses of extracellular vesicles. J Extracell Vesicles. 2013;2.

9. Shao H, Im H, Castro CM, Breakefield X, Weissleder R, Lee H. New Technologies for Analysis of Extracellular Vesicles. Chem Rev. 2018;118(4):1917-50.

10. Maas SLN, Breakefield XO, Weaver AM. Extracellular Vesicles: Unique Intercellular Delivery Vehicles. Trends Cell Biol. 2017;27(3):172-88.

11. Urban SK, Mocan T, Sanger H, Lukacs-Kornek V, Kornek M. Extracellular Vesicles in Liver Diseases: Diagnostic, Prognostic, and Therapeutic Application. Semin Liver Dis. 2019;39(1):70-7.

12. Lemoinne S, Thabut D, Housset C, Moreau R, Valla D, Boulanger CM, et al. The emerging roles of microvesicles in liver diseases. Nat Rev Gastroenterol Hepatol. 2014;11(6):350-61.

13. Szabo G, Momen-Heravi F. Extracellular vesicles in liver disease and potential as biomarkers and therapeutic targets. Nat Rev Gastroenterol Hepatol. 2017;14(8):455-66.

14. Eguchi A, Feldstein AE. Extracellular vesicles in non-alcoholic and alcoholic fatty liver diseases. Liver Res. 2018;2(1):30-4.

15. Malhi H. Emerging role of extracellular vesicles in liver diseases. Am J Physiol Gastrointest Liver Physiol. 2019;317(5):G739-G49.

16. Eguchi A, Lazaro RG, Wang J, Kim J, Povero D, Willliams B, et al. Extracellular vesicles released by hepatocytes from gastric infusion model of alcoholic liver disease contain a MicroRNA barcode that can be detected in blood. Hepatology. 2017;65(2):475-90.

17. Povero D, Eguchi A, Li H, Johnson CD, Papouchado BG, Wree A, et al. Circulating extracellular vesicles with specific proteome and liver microRNAs are potential biomarkers for liver injury in experimental fatty liver disease. PLoS One. 2014;9(12):e113651.

18. Xie F, Feng S, Yang H, Mao Y. Extracellular vesicles in hepatocellular cancer and cholangiocarcinoma. Ann Transl Med. 2019;7(5):86.

19. Sasaki R, Kanda T, Yokosuka O, Kato N, Matsuoka S, Moriyama M. Exosomes and Hepatocellular Carcinoma: From Bench to Bedside. Int J Mol Sci. 2019;20(6).

20. Sung S, Kim J, Jung Y. Liver-Derived Exosomes and Their Implications in Liver Pathobiology. Int J Mol Sci. 2018;19(12).

21. Latifkar A, Hur YH, Sanchez JC, Cerione RA, Antonyak MA. New insights into extracellular vesicle biogenesis and function. J Cell Sci. 2019;132(13).

22. Doyle LM, Wang MZ. Overview of Extracellular Vesicles, Their Origin, Composition, Purpose, and Methods for Exosome Isolation and Analysis. Cells. 2019;8(7).

23. Moran L, Cubero FJ. Extracellular vesicles in liver disease and beyond. World J Gastroenterol. 2018;24(40):4519-26.

24. Devhare PB, Ray RB. Extracellular vesicles: Novel mediator for cell to cell communications in liver pathogenesis. Mol Aspects Med. 2018;60:115-22.

25. Hirsova P, Ibrahim SH, Verma VK, Morton LA, Shah VH, LaRusso NF, et al. Extracellular vesicles in liver pathobiology: Small particles with big impact. Hepatology. 2016;64(6):2219-33.

26. Haraszti RA, Didiot MC, Sapp E, Leszyk J, Shaffer SA, Rockwell HE, et al. High-resolution proteomic and lipidomic analysis of exosomes and microvesicles from different cell sources. J Extracell Vesicles. 2016;5:32570.

27. Banales JM, Feldstein AE, Sanger H, Lukacs-Kornek V, Szabo G, Kornek M. Extracellular Vesicles in Liver Diseases: Meeting Report from the International Liver Congress 2018. Hepatol Commun. 2019;3(2):305-15.

28. Aizawa S, Brar G, Tsukamoto H. Cell Death and Liver Disease. Gut Liver. 2019.

29. Thery C, Witwer KW, Aikawa E, Alcaraz MJ, Anderson JD, Andriantsitohaina R, et al. Minimal information for studies of extracellular vesicles 2018 (MISEV2018): a position statement of the International Society for Extracellular Vesicles and update of the MISEV2014 guidelines. J Extracell Vesicles. 2018;7(1):1535750.

30. Royo F, Gil-Carton D, Gonzalez E, Mleczko J, Palomo L, Perez-Cormenzana M, et al. Differences in the metabolite composition and mechanical properties of extracellular vesicles secreted by hepatic cellular models. J Extracell Vesicles. 2019;8(1):1575678.

31. Nojima H, Freeman CM, Schuster RM, Japtok L, Kleuser B, Edwards MJ, et al. Hepatocyte exosomes mediate liver repair and regeneration via sphingosine-1-phosphate. J Hepatol. 2016;64(1):60-8.

32. Chen L, Chen R, Kemper S, Brigstock DR. Pathways of production and delivery of hepatocyte exosomes. J Cell Commun Signal. 2018;12(1):343-57.

33. Zhao Y, Zhao MF, Jiang S, Wu J, Liu J, Yuan XW, et al. Liver governs adipose remodelling via extracellular vesicles in response to lipid overload. Nat Commun. 2020;11(1):719.

34. Arrese M, Cabrera D, Kalergis AM, Feldstein AE. Innate Immunity and Inflammation in NAFLD/NASH. Dig Dis Sci. 2016;61(5):1294-303.

35. Sato K, Kennedy L, Liangpunsakul S, Kusumanchi P, Yang Z, Meng F, et al. Intercellular Communication between Hepatic Cells in Liver Diseases. Int J Mol Sci. 2019;20(9).

36. Schuster S, Cabrera D, Arrese M, Feldstein AE. Triggering and resolution of inflammation in NASH. Nat Rev Gastroenterol Hepatol. 2018;15(6):349-64.

37. Hirsova P, Ibrahim SH, Krishnan A, Verma VK, Bronk SF, Werneburg NW, et al. Lipid-Induced Signaling Causes Release of Inflammatory Extracellular Vesicles From Hepatocytes. Gastroenterology. 2016;150(4):956-67.

38. Jiang F, Chen Q, Wang W, Ling Y, Yan Y, Xia P. Hepatocyte-derived extracellular vesicles promote endothelial inflammation and atherogenesis via microRNA-1. J Hepatol. 2020;72(1):156-66.

39. Antwi-Baffour S, Adjei J, Aryeh C, Kyeremeh R, Kyei F, Seidu MA. Understanding the biosynthesis of platelets-derived extracellular vesicles. Immun Inflamm Dis. 2015;3(3):133-40.

40. Balaphas A, Meyer J, Sadoul K, Fontana P, Morel P, Gonelle-Gispert C, et al. Platelets and Platelet-Derived Extracellular Vesicles in Liver Physiology and Disease. Hepatol Commun. 2019;3(7):855-66.

41. Saha B, Momen-Heravi F, Kodys K, Szabo G. MicroRNA Cargo of Extracellular Vesicles from Alcohol-exposed Monocytes Signals Naive Monocytes to Differentiate into M2 Macrophages. J Biol Chem. 2016;291(1):149-59.

42. Lee YA, Wallace MC, Friedman SL. Pathobiology of liver fibrosis: a translational success story. Gut. 2015;64(5):830-41.

43. Friedman SL. Hepatic stellate cells: protean, multifunctional, and enigmatic cells of the liver. Physiol Rev. 2008;88(1):125-72.

44. Higashi T, Friedman SL, Hoshida Y. Hepatic stellate cells as key target in liver fibrosis. Adv Drug Deliv Rev. 2017;121:27-42.

45. Povero D, Panera N, Eguchi A, Johnson CD, Papouchado BG, de Araujo Horcel L, et al. Lipid-induced hepatocyte-derived extracellular vesicles regulate hepatic stellate cell via microRNAs targeting PPAR-gamma. Cell Mol Gastroenterol Hepatol. 2015;1(6):646-63 e4.

46. Wang R, Ding Q, Yaqoob U, de Assuncao TM, Verma VK, Hirsova P, et al. Exosome Adherence and Internalization by Hepatic Stellate Cells Triggers Sphingosine 1-Phosphate-dependent Migration. J Biol Chem. 2015;290(52):30684-96.

47. Chen L, Charrier A, Zhou Y, Chen R, Yu B, Agarwal K, et al. Epigenetic regulation of connective tissue growth factor by MicroRNA-214 delivery in exosomes from mouse or human hepatic stellate cells. Hepatology. 2014;59(3):1118-29.

48. Charrier A, Chen R, Chen L, Kemper S, Hattori T, Takigawa M, et al. Exosomes mediate intercellular transfer of pro-fibrogenic connective tissue growth factor (CCN2) between hepatic stellate cells, the principal fibrotic cells in the liver. Surgery. 2014;156(3):548-55.

49. Owens AP, 3rd, Mackman N. Microparticles in hemostasis and thrombosis. Circ Res. 2011;108(10):1284-97.

50. Valla DC. Thrombosis and anticoagulation in liver disease. Hepatology. 2008;47(4):1384-93.

51. Chen L, Brenner DA, Kisseleva T. Combatting Fibrosis: Exosome-Based Therapies in the Regression of Liver Fibrosis. Hepatol Commun. 2019;3(2):180-92.

52. Clayton A, Buschmann D, Byrd JB, Carter DRF, Cheng L, Compton C, et al. Summary of the ISEV workshop on extracellular vesicles as disease biomarkers, held in Birmingham, UK, during December 2017. J Extracell Vesicles. 2018;7(1):1473707.

53. Cho YE, Song BJ, Akbar M, Baek MC. Extracellular vesicles as potential biomarkers for alcohol- and drug-induced liver injury and their therapeutic applications. Pharmacol Ther. 2018;187:180-94.

54. Arbelaiz A, Azkargorta M, Krawczyk M, Santos-Laso A, Lapitz A, Perugorria MJ, et al. Serum extracellular vesicles contain protein biomarkers for primary sclerosing cholangitis and cholangiocarcinoma. Hepatology. 2017;66(4):1125-43.

55. Murphy DE, de Jong OG, Brouwer M, Wood MJ, Lavieu G, Schiffelers RM, et al. Extracellular vesicle-based therapeutics: natural versus engineered targeting and trafficking. Exp Mol Med. 2019;51(3):32.

56. Villa F, Quarto R, Tasso R. Extracellular Vesicles as Natural, Safe and Efficient Drug Delivery Systems. Pharmaceutics. 2019;11(11).

57. Balaphas A, Meyer J, Sadoul R, Morel P, Gonelle-Gispert C, Buhler LH. Extracellular vesicles: Future diagnostic and therapeutic tools for liver disease and regeneration. Liver Int. 2019;39(10):1801-17.

58. Borrelli DA, Yankson K, Shukla N, Vilanilam G, Ticer T, Wolfram J. Extracellular vesicle therapeutics for liver disease. J Control Release. 2018;273:86-98.

59. Gao J, Dong X, Wang Z. Generation, purification and engineering of extracellular vesicles and their biomedical applications. Methods. 2019.

60. Patel DB, Santoro M, Born LJ, Fisher JP, Jay SM. Towards rationally designed biomanufacturing of therapeutic extracellular vesicles: impact of the bioproduction microenvironment. Biotechnol Adv. 2018;36(8):2051-9.

61. Catalano M, O'Driscoll L. Inhibiting extracellular vesicles formation and release: a review of EV inhibitors. Journal of Extracellular Vesicles. 2019 (in press).

62. Kakazu E, Mauer AS, Yin M, Malhi H. Hepatocytes release ceramide-enriched pro-inflammatory extracellular vesicles in an IRE1alpha-dependent manner. J Lipid Res. 2016;57(2):233-45.

63. Povero D, Eguchi A, Niesman IR, Andronikou N, de Mollerat du Jeu X, Mulya A, et al. Lipid-induced toxicity stimulates hepatocytes to release angiogenic microparticles that require Vanin-1 for uptake by endothelial cells. Sci Signal. 2013;6(296):ra88.

64. Ibrahim SH, Hirsova P, Tomita K, Bronk SF, Werneburg NW, Harrison SA, et al. Mixed lineage kinase 3 mediates release of C-X-C motif ligand 10-bearing chemotactic extracellular vesicles from lipotoxic hepatocytes. Hepatology. 2016;63(3):731-44.

65. Cannito S, Morello E, Bocca C, Foglia B, Benetti E, Novo E, et al. Microvesicles released from fat-laden cells promote activation of hepatocellular NLRP3 inflammasome: A pro-inflammatory link between lipotoxicity and non-alcoholic steatohepatitis. PLoS One. 2017;12(3):e0172575.

66. Liu XL, Pan Q, Cao HX, Xin FZ, Zhao ZH, Yang RX, et al. Lipotoxic Hepatocyte-Derived Exosomal miR-192-5p Activates Macrophages via Rictor/Akt/FoxO1 Signaling in NAFLD. Hepatology. 2019.

67. Guo Q, Furuta K, Lucien F, Gutierrez Sanchez LH, Hirsova P, Krishnan A, et al. Integrin beta1-enriched extracellular vesicles mediate monocyte adhesion and promote liver inflammation in murine NASH. J Hepatol. 2019;71(6):1193-205.

68. Hernandez A, Geng Y, Sepulveda R, Solis N, Torres J, Arab JP, et al. Chemical Hypoxia induces pro-inflammatory signals in fat-laden hepatocytes and contributes to cellular crosstalk with Kupffer cells through extracellular vesicles. BBA - Molecular Basis of Disease (in press). 2020.

69. Lee YS, Kim SY, Ko E, Lee JH, Yi HS, Yoo YJ, et al. Exosomes derived from palmitic acid-treated hepatocytes induce fibrotic activation of hepatic stellate cells. Sci Rep. 2017;7(1):3710.

70. Chen L, Chen R, Kemper S, Charrier A, Brigstock DR. Suppression of fibrogenic signaling in hepatic stellate cells by Twist1-dependent microRNA-214 expression: Role of exosomes in horizontal transfer of Twist1. Am J Physiol Gastrointest Liver Physiol. 2015;309(6):G491-9.

71. Schuppan D, Surabattula R, Wang XY. Determinants of fibrosis progression and regression in NASH. J Hepatol. 2018;68(2):238-50.

72. Koeck ES, Iordanskaia T, Sevilla S, Ferrante SC, Hubal MJ, Freishtat RJ, et al. Adipocyte exosomes induce transforming growth factor beta pathway dysregulation in hepatocytes: a novel paradigm for obesity-related liver disease. J Surg Res. 2014;192(2):268-75.

73. Li J, Liu H, Mauer AS, Lucien F, Raiter A, Bandla H, et al. Characterization of Cellular Sources and Circulating Levels of Extracellular Vesicles in a Dietary Murine Model of Nonalcoholic Steatohepatitis. Hepatol Commun. 2019;3(9):1235-49.

74. Ban LA, Shackel NA, McLennan SV. Extracellular Vesicles: A New Frontier in Biomarker Discovery for Non-Alcoholic Fatty Liver Disease. Int J Mol Sci. 2016;17(3):376.

75. Kornek M, Lynch M, Mehta SH, Lai M, Exley M, Afdhal NH, et al. Circulating microparticles as disease-specific biomarkers of severity of inflammation in patients with hepatitis C or nonalcoholic steatohepatitis. Gastroenterology. 2012;143(2):448-58.

76. Welsh JA, Scorletti E, Clough GF, Englyst NA, Byrne CD. Leukocyte extracellular vesicle concentration is inversely associated with liver fibrosis severity in NAFLD. J Leukoc Biol. 2018;104(3):631-9.

77. Momen-Heravi F, Szabo G. Extracellular Vesicles and Exosomes: Biology and Pathobiology. In: ARIAS IM, ALTER HJ, BOYER JL, COHEN DE, SHAFRITZ DA, THORGEIRSSON SS, et al., editors. The Liver: Biology and Pathobiology. Hoboken, NJ, USA: Wiley-Blackwell; 2020. p. 1022-8.

78. Ohara M, Ohnishi S, Hosono H, Yamamoto K, Yuyama K, Nakamura H, et al. Extracellular Vesicles from Amnion-Derived Mesenchymal Stem Cells Ameliorate Hepatic Inflammation and Fibrosis in Rats. Stem Cells Int. 2018;2018:3212643.

79. Bruno S, Pasquino C, Herrera Sanchez MB, Tapparo M, Figliolini F, Grange C, et al. HLSC-Derived Extracellular Vesicles Attenuate Liver Fibrosis and Inflammation in a Murine Model of Non-alcoholic Steatohepatitis. Mol Ther. 2019.

80. Rahman MA, Patters BJ, Kodidela S, Kumar S. Extracellular Vesicles: Intercellular Mediators in Alcohol-Induced Pathologies. J Neuroimmune Pharmacol. 2019.

81. Verma VK, Li H, Wang R, Hirsova P, Mushref M, Liu Y, et al. Alcohol stimulates macrophage activation through caspase-dependent hepatocyte derived release of CD40L containing extracellular vesicles. Journal of hepatology. 2016;64(3):651-60.

82. Momen-Heravi F, Saha B, Kodys K, Catalano D, Satishchandran A, Szabo G. Increased number of circulating exosomes and their microRNA cargos are potential novel biomarkers in alcoholic hepatitis. J Transl Med. 2015;13:261.

83. Bala S, Petrasek J, Mundkur S, Catalano D, Levin I, Ward J, et al. Circulating microRNAs in exosomes indicate hepatocyte injury and inflammation in alcoholic, drug-induced, and inflammatory liver diseases. Hepatology. 2012;56(5):1946-57.

84. Momen-Heravi F, Bala S, Kodys K, Szabo G. Exosomes derived from alcohol-treated hepatocytes horizontally transfer liver specific miRNA-122 and sensitize monocytes to LPS. Sci Rep. 2015;5:9991.

85. Csak T, Bala S, Lippai D, Satishchandran A, Catalano D, Kodys K, et al. microRNA-122 regulates hypoxia-inducible factor-1 and vimentin in hepatocytes and correlates with fibrosis in diet-induced steatohepatitis. Liver Int. 2015;35(2):532-41.

86. Li HD, Du XS, Huang HM, Chen X, Yang Y, Huang C, et al. Noncoding RNAs in alcoholic liver disease. J Cell Physiol. 2019.

87. Lamichhane TN, Leung CA, Douti LY, Jay SM. Ethanol Induces Enhanced Vascularization Bioactivity of Endothelial Cell-Derived Extracellular Vesicles via Regulation of MicroRNAs and Long Non-Coding RNAs. Sci Rep. 2017;7(1):13794.

88. Brandon-Warner E, Feilen NA, Culberson CR, Field CO, deLemos AS, Russo MW, et al. Processing of miR17-92 Cluster in Hepatic Stellate Cells Promotes Hepatic Fibrogenesis During Alcohol-Induced Injury. Alcohol Clin Exp Res. 2016;40(7):1430-42.

89. Arab JP, Verma V, Martin-Mateos R, Simonetto D, Kamath PS, Gores GJ, et al. Extracellular Vesicle C16 Ceramide and S1P Content in Alcoholic Hepatitis Correlates with Disease Severity and Resolution. Gastroenterology. 2018;154(6):S-1120.

90. Singal AK, Shah VH. Therapeutic Strategies for the Treatment of Alcoholic Hepatitis. Seminars in liver disease. 2016;36(1):56-68.

91. Altamirano J, Miquel R, Katoonizadeh A, Abraldes JG, Duarte-Rojo A, Louvet A, et al. A histologic scoring system for prognosis of patients with alcoholic hepatitis. Gastroenterology. 2014;146(5):1231-9 e1-6.

92. Arab JP, Barrera F, Arrese M. The Evolving Role of Liver Biopsy in Non-alcoholic Fatty Liver Disease. Ann Hepatol. 2018;17(6):899-902.

93. Arab JP, Sehrawat TS, Simonetto DA, Verma VK, Feng D, Tang T, et al. An Open Label, Dose Escalation Study To Assess The Safety And Efficacy Of IL-22 Agonist F-652 In Patients With Alcoholic Hepatitis. Hepatology. 2019.

Chapter 3

CHEMICAL HYPOXIA INDUCES PRO-INFLAMMATORY SIGNALS IN FAT-LADEN HEPATOCYTES AND CONTRIBUTES TO CELLULAR CROSSTALK WITH KUPFFER CELLS THROUGH EXTRACELLULAR VESICLES

ABSTRACT

Background: Obstructive sleep apnea syndrome (OSAS), which is characterized by occurrence of intermittent hypoxia (IH), is an aggravating factor of non-alcoholic fatty liver disease (NAFLD). We investigated the effects of hypoxia in both in vitro and in vivo models of NAFLD. **Methods:** Primary rat hepatocytes treated with free fatty acids (FFA) were subjected to chemically induced hypoxia (CH) using the hypoxia-inducible factor-1 alpha (HIF-1α) stabilizer cobalt chloride (CoCl2). Triglyceride (TG) content, mitochondrial superoxide production, cell death rates, pro-inflammatory cytokines and inflammasome components gene expression and protein levels of cleaved caspase-1 were assessed. Also, Kupffer cells (KC) were treated with conditioned medium (CM) and extracellular vesicles (EVs) from hypoxic fat-laden hepatocytes and the choline deficient L-amino acid defined (CDAA)-fed mice model used to assess the effects of IH on experimental NAFLD in vivo. **Results:** CH induced a 2-fold increase in HIF-1α protein levels. Hepatocytes exposed to FFA and CoCl2 exhibited increased TG content and higher cell death rates as well as increased mitochondrial superoxide production and mRNA levels of pro-inflammatory cytokines and of inflammasome-components interleukin-1β, NLRP3 and ASC. Protein levels of cleaved caspase-1 increased in CH-exposed hepatocytes. CM and EVs from hypoxic fat-laden hepatic cells evoked a pro-inflammatory phenotype in KC. Livers from CDAA-fed mice exposed to IH exhibited increased mRNA levels of pro-inflammatory and inflammasome genes as well as increased levels of cleaved caspase-1. **Conclusion:** Hypoxia promotes inflammatory signals including inflammasome/caspase-1 activation in fat-laden hepatocytes and contributes to cellular crosstalk with Kupffer cells by release of EVs. These mechanisms may underlie the aggravating effect of OSAS on NAFLD.

1. - INTRODUCTION

In recent years, obstructive sleep apnea syndrome (OSAS), a common sleep disorder characterized by recurrent closure of the upper airways during sleep, has been suggested to modulate the severity of different metabolic disorders (1, 2). The hallmark of OSAS is the occurrence of intermittent hypoxia (IH) leading to tissue hypoxia and promoting oxidative stress, inflammation and a myriad of multi-organ pathophysiological effects (3). Among conditions in which OSAS acts as both a potential inducer and as an aggravating factor is non-alcoholic fatty liver disease (NAFLD), the commonest liver disease worldwide (4-6). NAFLD describes a clinicopathological entity defined by the presence of a spectrum of hepatic histological changes ranging in severity from isolated steatosis (also termed non-

alcoholic fatty liver [NAFL]) to steatohepatitis (named non-alcoholic steatohepatitis, NASH) through to advanced fibrosis and cirrhosis (7, 8). Development of steatosis is closely linked to both overweight and obesity as well as to insulin resistance and transition from isolated steatosis to more advanced stages of the disease occurs only in a minority of NAFLD patients. Multiple factors influence NAFLD development and progression including individual's genetic background, environmental factors and the presence of a myriad of comorbidities including OSAS (6, 9).

The main mechanisms of hepatocellular damage in NAFLD include those related to lipotoxicity, mitochondrial dysfunction, formation of reactive oxygen species, endoplasmic reticulum stress and disturbed autophagy ultimately leading to hepatocyte injury and death that triggers hepatic inflammation, hepatic stellate cell activation, and progressive fibrogenesis, thus driving disease progression (8, 10-12). In addition, recent studies have shown that inflammasome activation is also one of the key events in NAFLD progression (13-15). Specifically, the NOD-like receptor Pyrin Domain Containing 3 (NLRP3) inflammasome has been recognized to be involved in the progression of liver damage in experimental *in vitro* (hepatocytes and immune liver cells) and *in vivo* models of NASH (16-18) and also in human studies (19). NLRP3 inflammasome mediates the maturation of inactive pro-caspase-1 into active cleaved caspase-1, which cleaves gasdermin D (GSDMD) that in turn determine the activation of the pro-inflammatory cytokines interleukin [IL]-1β and IL-18, which amplify the pathological phenomena in NAFLD by promoting inflammation and pyroptotic cell death (20). Of note, the progression of damage in NAFLD also involves the participation of other liver-resident cells such as macrophages or Kupffer cells (KC) as well as the recruitment of inflammatory cells from the periphery (21-23).

With regard to the pathophysiological connections between OSAS and NAFLD, existing data indicate that OSAS may relate to both NAFLD occurrence as well as disease progression. Of note, several studies have shown that IH is able to induce metabolic alterations such as insulin resistance and increased liver triglyceride (TG) accumulation as well as increased oxidative stress and increased inflammation, which are related to steatosis development and hepatocellular damage, respectively (24-26). Hepatic TG accumulation in the setting of OSAS may result from hypoxia-related changes in lipid metabolic pathways such as a decrease in fatty acid β-oxidation and increased *de novo* lipogenesis (5, 27). Also, IH has been shown to promote pro-inflammatory effects in animal models of NAFLD modulating inflammatory cytokine production (i.e. tumor necrosis factor-alpha [TNF-α] and IL-6) (28, 29). Although some studies suggest a relevant role of hypoxia, likely through induction of the hypoxia inducible factor 1 alpha (HIF-1α), in promoting hepatocellular cell death and the generation of pro-inflammatory signals in several experimental settings (30), assessment of these phenomena in the context of NAFLD has been less explored (5, 31).

In the present study, we aimed to assess the effects of hypoxia on cellular lipid accumulation, hepatocellular death and pro-inflammatory signals including those related to the NLRP3 inflammasome leading to caspase-1 activation in *in vitro* and *in vivo* models of NAFLD. Moreover, we explored whether hypoxia modulates cellular crosstalk between hepatocytes and resident macrophages (i.e. KCs) in the setting of NAFLD and if this crosstalk involves the release of extracellular vesicles (EVs) from hepatocytes. Of note, EVs have been recently recognized as playing an important role in amplifying the inflammatory response in NASH (32, 33) but few data exist on the potential role of hypoxia in modulating their release. We found that hypoxia induces hepatocellular damage in fat-laden hepatocytes that involves NLRP3 inflammasome-associated caspase-1 activation and increased mitochondrial superoxide production leading to increase cell death rates by multiple mechanisms including apoptosis and pyroptosis. Also, hypoxia contributes to evoking a pro-inflammatory response in Kupffer cells by a mechanism that involves EVs release from fat-laden hepatocytes. These observations partially clarify the mechanisms underlying the aggravating effect of OSAS on NAFLD**.**

2. - MATERIALS AND METHODS

2.1 Animals

Specified pathogen-free male Wistar rats (220–250 g; Charles River Laboratories Inc., Wilmington, MA, USA) and male C57bl6 mice [purchased from Jackson Laboratories (Bar Harbor, ME, USA)] were used in the present study. Animals were housed under standard laboratory conditions with free access to standard laboratory chow diet and water. All experiments were carried out according to the Dutch and Chilean laws on the welfare of laboratory animals and guidelines of the local institutional animal care and use committees of the Pontificia Universidad Católica de Chile and ethics committee of University of Groningen for care and use of laboratory animals. All efforts were made to minimize animals suffering and to reduce the number of animals used.

2.2 Cell isolation techniques, culture conditions, cell surface markers detection and use of liver-derived cell lines

To conduct the experiments described below we used both primary rat hepatocytes and KC. Isolation techniques used are described elsewhere (34, 35) and in the Supplementary material file. Details of culture conditions and KC cell surface markers detection are also provided in that section. The human hepatocellular carcinoma cell line HepG2 (American Type Culture Collection [ATCC] HB-8065, Manassas, VA, USA) was used to carry out experiments involving EVs isolation after treatment with FFA. Culture conditions are described in the supplementary material file.

2.3 Treatment with free fatty acids and chemical hypoxia induction

In order to assess the effects of hypoxia in fat-laden liver cells, hepatocytes were incubated with a mixture of free fatty acids (FFA) consisting of oleic acid (500 µmol/L) and palmitic acid (250 µmol/L) in an aqueous solution of BSA as described (36). Incubations were carried out with or without Cobalt (II) chloride (CoCl2; Sigma Aldrich, Saint Louis, MO, USA) (200 µmol/L) for 24 hours to induce chemical hypoxia (37). CoCl2 is a well-known hypoxia-mimetic agent, that mimics hypoxia/ischemic conditions by stabilization of hypoxia-inducible factor HIF-1α (38). Control cells were treated with BSA alone. To obtain the corresponding conditioned medium (CM), after treatment, hepatocyte culture medium was replaced by FBS-free medium for an additional 24 hours. CM from different treatments were added to KC for 24 hours in order to explore the possibility that hypoxia modulates hepatocytes-KC cellular crosstalk.

2.4 Oil red O cell staining and TG measurement

Primary rat hepatocytes cultured on glass cover slides were treated with FFA and CoCl2 for 24 h. Hepatocytes were then washed with phosphate-buffered saline (PBS) twice, and then fixed with 4% formalin for 10 minutes. Cells were washed with 60% isopropanol twice and stained with oil-red-O solution for 10 minutes at room temperature. Then, cells were washed with 60% isopropanol and washed in distilled water for 5 minutes. Then cells were incubated with hematoxylin/eosin solution for 1 minute and washed with distilled water for 5 minutes. Slices were mounted using 1 drop of glycerin-gelatin solution. Stained lipid droplets in cells were examined using a slide scanner, NanozoomerTM (Hamamatsu Photonics K.K., Shizuoka, Japan). Intracellular TG content was determined using TG Quantification Assay kit (ab65336, Abcam, Cambridge, UK) according to the manufacturer's instructions and normalized to protein concentration.

2.5 Apoptosis measurement

Caspase-3 fluorometric assay was used to determine apoptosis induced by FFA and/or CoCl2 in freshly isolated mouse hepatocytes. After treatment, hepatocytes were scraped and cell lysates were obtained by three cycles of freezing (−196°C) in liquid nitrogen and thawing (37°C) followed by centrifugation for 5 minutes at 13,000g. Caspase-3 enzyme activity was assayed as described previously (39). Arbitrary units of fluorescence (AUF) were quantified in a spectrofluorometer at an excitation wavelength of 380 nm and an emission wavelength of 430 nm.

2.6 Assessment of cell death associated to disrupted cellular membrane integrity

SYTOXTM Green nucleic acid stain (Invitrogen, S7020, Carlsbad, CA, USA) was used to determine cell death induced by FFA and/or CoCl2 in hepatocytes (40). Cells were cultured in 12-well plates. After

treatment, diluted SYTOX Green solution (1:40.000/HBSS) was added to the plates for at least 15 minutes at 37°C, 5% CO2. SYTOXTM Green enters the cell upon loss of membrane integrity and binds to DNA acting as a counterstain that can be analyzed when excited at 488 nm. A Leica fluorescence microscope was used at that wavelength of for detection of necrotic cells, which were quantified using Image J software. Lactate dehydrogenase (LDH) release was assessed as described in the Supplementary materials file. Additionally, we assessed the caspase-cleaved gasdermin-N domain (GSDMD-N) to confirm pyroptotic cell death by Western blot to evaluate the occurrence of pyroptotic cell death (19).

2.7 Mitochondrial superoxide detection

At the end of 24h-long incubations, hepatocytes were washed once with warm HBSS followed by incubation with 200 nmol/L MitoSOX™ Red Molecular Probes (InvitrogenTM, Carlsbad, CA,USA) in William's E medium for 15 min at 37°C protected from light in order to detect mitochondrial superoxide production (41). Then, cells were washed with warm HBSS and mounted onto glass slides using DAPI staining solution (InvitrogenTM, Carlsbad, CA,USA). The fluorescence analyses were immediately recorded using a fluorescent microscope at a wavelength of 510/580 nm (Ex/Em) by a Leica microscope (Leica Microsystems GmbH, Wetzlar, Germany). Quantification of fluorescence in microscopic images of MitoSOX was performed using Image J software.

2.8 Western Blot analyses and antibodies

Protein levels expression were detected by total cell lysate subjected to western blot as previous described (42). The following antibodies were used: Monoclonal mouse anti-HIF1α 1:1000 (Abcam, USA); monoclonal mouse anti-GSDMDC1 1:500 (Santa Cruz Biotechnology, Dallas, TX, USA); polyclonal rabbit anti-CASP-3 (Cell Signaling Technology, Leiden, The Netherlands); monoclonal mouse anti-CASP1 1:500 (Santa Cruz Biotechnology, Dallas, TX, USA); monoclonal mouse anti-CD81 1:1000 (InvitrogenTM, Carlsbad, CA,USA) and monoclonal rabbit anti-Bcl-2 1:1000 (Abcam, UK) were used in combination with appropriate peroxidase-conjugated secondary antibodies. Monoclonal mouse anti-tubulin or actin were used as loading controls (Sigma, Life Sciences, Merck KGaA, Darmstadt, German). Blots were analyzed in a ChemiDoc XRS system (Bio-Rad, Hercules, CA, USA). Protein band intensities were quantified by ImageLab software (BioRad, Hercules, CA, USA).

2.9 RNA isolation and quantitative real-time reverse transcription polymerase chain reaction (qRT-PCR)

Total RNA was isolated with TRI-reagent (Sigma-Aldrich, Saint Louis, MO, USA) according to the manufacturer's instructions. Quantification of RNA was measured with the Nanodrop

spectrophotometer (Thermo Scientific, Wilmington, DE, USA). Reverse transcription (RT) was performed using 2.5 µg of total RNA. Quantitative Real Time PCR (qRT-PCR) was carried out in a StepOnePlus™ (96-well) PCR System (Applied Biosystems, Thermofisher, Waltham, MA, USA) using TaqMan method or SYBR Green method. The sequences of the probes and primer sets are described in the Supplementary materials file. mRNA levels were normalized to the housekeeping gene 18S and further normalized to the mean expression level of the control group. Relative gene expression was calculated via the 2 ddCT.

2.10 Enzyme-linked immunosorbent assay (ELISA) of Interleukin-1beta

Levels of pro-inflammatory cytokine of IL-1β in primary rat KC were assessed by the ELISA kit (ab100768, Abcam, Cambridge, UK), according to the manufacturer's instructions.

2.11 EVs isolation and characterization

EVs were collected from culture media of HepG2 cells as described previously (43) and summarized in the Supplementary materials file. Nanoparticle tracking analysis (NTA) was performed using NanoSight NS300 instrumentation (Marvel, Egham, UK) that uses both light scattering and Brownian motion analysis for nanoparticle characterization. We further caharacterized EVs using Transmission electron microscopy. Sample preparation and details of these analysis are described in the Supplementary materials file.

2.12 Treatment of KC cells with and extracellular vesicles

Rat primary KC were incubated with FBS-free William's E medium and exposed to 15 µg of EVs that were isolated from HepG2 cells treated with CoCl2 + FFA for 24h. After 24h of EVs treatment, KC were harvested to continue with analyses by quantitative PCR.

2.13 Effects of intermittent hypoxia in experimental NASH

Animal experiments were approved by the institutional animal care and use committee (Comité de ética y bienestar Animal, Escuela de Medicina, Pontificia Universidad Católica de Chile, CEBA 100623003). Male C57BL/6 mice aged 10 weeks at the beginning of the study and divided into four experimental groups (n = 4–8) receiving either choline-deficient amino acid-defined (CDAA) diet (Catalog # 518753, Dyets Inc. Bethlehem, PA) to induce NASH or the choline-supplemented L-amino acid defined (CSAA, Catalog # 518754, Dyets Inc. Bethlehem, PA) diet as control for 22 weeks as previously described (16, 44). Animals were exposed to IH or normoxia (chambers 41x22x35 cm, COY lab products™, Grass Lake, MI, USA) during the last 12 weeks of the experimental or control feeding period. IH regimen consisted in 30 events/hour of hypoxic exposures for 8 hour/day during the rest

cycle, between 9 am and 5 pm. This cycle was repeated 7 days a week for 12 consecutive weeks. After ending the study, mice were anesthetized (ketamine 60 mg/kg plus xylazine 10 mg/kg intraperitoneally) and then euthanized by exsanguination. Serum and liver tissue samples were collected and processed or stored at −80 °C until analyzed. Gene expression and protein analyses were carried out as described above. Positive control of hypoxia induction was evaluated by measurement of hepatic gene expression of HIF-1α.

2.14 Histological Studies

Liver steatosis was analyzed on paraformaldehyde-fixed liver sections stained with Oil Red-O staining that show lipid deposits in red color on frozen 7 μm liver cryosections. A blinded pathologist (J.T.) assigned a score for steatosis, inflammation and fibrosis as described (44). Scores were given as it follows: Steatosis: grade 0, none present; grade 1, steatosis of ≤25% of parenchyma; grade 2, steatosis of 26–50% of parenchyma; grade 3, steatosis of 51–75% of parenchyma; grade 4, steatosis of ≥76% of parenchyma and inflammation: grade 0, no inflammatory foci; grade 1, 1–5 inflammatory foci per high power field; grade 2, >5 inflammatory foci/high power field. Fibrosis was estimated qualitatively in Sirius red-stained samples.

2.15 Hepatic triglyceride determination

Hepatic triglyceride content (HTC) was using 40-50 mg of homogenized liver tissue in 1.5 ml of a CHCl3-CH3OH mixture (2:1, v/v), followed by a Folch extraction described previously (16, 31).

2.16 Statistical Analyses

Analyses were performed using GraphPad software (version 5.03, GraphPad Software Inc., CA, USA). Statistical analyses were performed using one-way analysis of variance (ANOVA) with a post-hoc Bonferroni correction with multiple-comparison test or by parametric t-tests when needed. All the results are presented as a mean of at least 3 independent experiments ± SEM. Values were represented as absolute number, normalized data respect to control or percentage for categorical variables. Regarding in vitro assays, independent experiments means different cell plates harvested from at least three animals. Regarding in vivo assays, independent experiments means at least three different animal samples. All the results were analyzed and plotted using GraphPad software (version 5.03, GraphPad Software Inc., CA, USA). Statistics with a value of $p<0.05$ were considered significant.

3. - RESULTS

3.1 Hypoxia induces HIF-1α and promotes the increase of lipid droplets in fat-laden hepatocytes: To investigate whether hypoxia exacerbates lipotoxicity in an *in vitro* model of experimental NASH, we

treated fat-laden primary rat hepatocytes with CoCl2, a hypoxia mimetic agent that promotes the accumulation of HIF-1α (45, 46). As expected, chemical hypoxia increased protein levels of HIF-1α in both control and fat-laden hepatocytes as determined by Western Blot technique (Figure 1). Interestingly, we also observed an increase in the number of intracellular lipid droplets, determined by Oil Red O staining (Figure 2a) and of hepatocyte TG content (Figure 2b) after treatment with a mixture of FFA, which was higher in cells concomitantly treated with CoCl2 indicating that the hypoxic condition promotes an increase intracellular lipid deposition in this model.

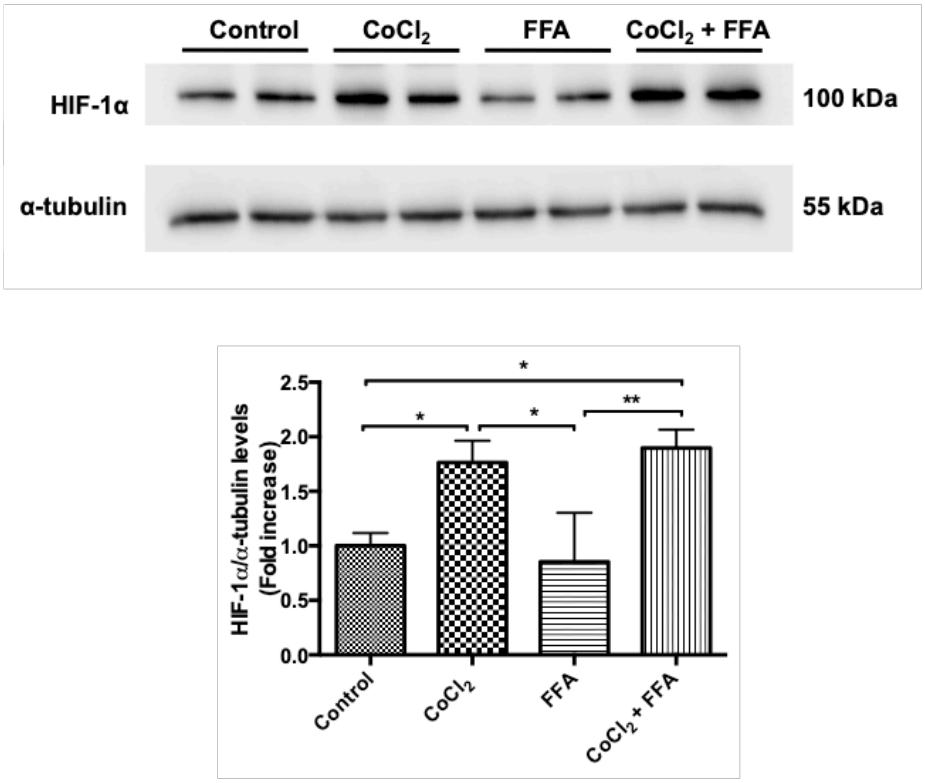

Figure 1. Chemical hypoxia stabilizes HIF-1α. Primary hepatocytes were incubated for 24 h with oleic acid and palmitic acid (2:1 ratio) (FFA) in the presence or absence of CoCl2 200 µmol/L. Protein levels of HIF-1α was determined by Western Blot as described in Material and Methods. α-Tubulin was used as loading control. Data were shown as mean ± SEM (n ≥ 3) * indicates $P < 0.05$ and ** indicates $P < 0.01$.

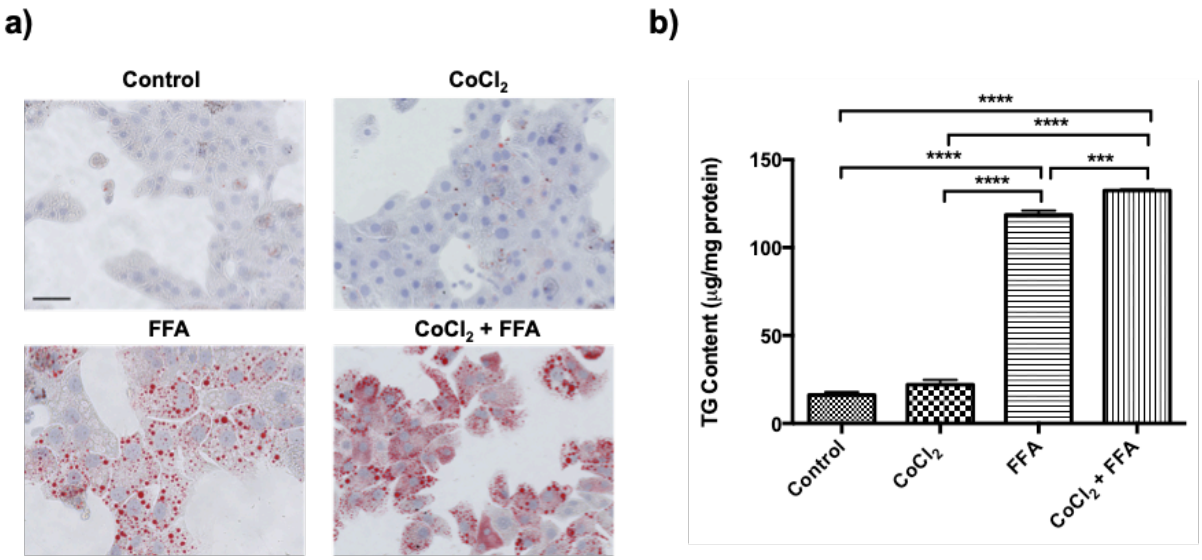

Figure 2. Steatosis *in vitro*: Free fatty acids and chemical hypoxia treatment increase the content of triglycerides. Primary hepatocytes were incubated for 24h with oleic acid and palmitic acid (2:1 ratio) (FFA) in the presence or absence of CoCl2 200 µmol/L. a) Oil Red O staining (scale bar: 40 µm) and b) Triglycerides (TG) content were measured as described in Materials and Methods. Data were shown as mean ± SEM (n ≥ 3) *** indicates P < 0.005 and **** indicates P < 0.001.

3.2 Hypoxia increases apoptotic and pyroptotic cell death in fat-laden hepatocytes: To evaluate whether the induction of chemical hypoxia exacerbates lipotoxic cell damage and death, we determined protein levels and activity of caspase-3 to assess apoptotic cell death and used SYTOX™ Green nucleic acid stain and LDH leakage to evaluate cell death associated to disrupted cellular membrane integrity. Additionally, we assessed the caspase-cleaved gasdermin-N domain (GSDMD-N) to evaluate pyroptotic cell death (19). While CoCl2 did not influence cleaved caspase-3 and caspase 3 activity in normal hepatocytes, steatotic hepatocytes undergoing chemical hypoxia displayed a two-fold increase in cleaved caspase-3 (Figure 3a) and six-fold increase in caspase-3 activity (Figure 3b) compared to control cells. Of note, treatment with a mixture of FFA alone led to a two-fold increase (n.s.) in caspase 3 activity suggesting that chemical hypoxia exacerbates lipotoxicity and apoptotic cell death in fat-laden hepatocytes. Also, using SYTOX™ Green nucleic acid stain (Figure 4a) and measurement of cellular LDH leakage (Figure 4b), we found that chemical hypoxia also increased cell death rate associated to losing plasma membrane integrity of fat-laden hepatocytes compared to control cells or cells treated only with FFA. Furthermore, protein levels of GSDMD-N, which is considered a pyroptosis executor (19), increased three-fold in hypoxic fat-laden hepatocytes compared to control cells (Figure 4c).

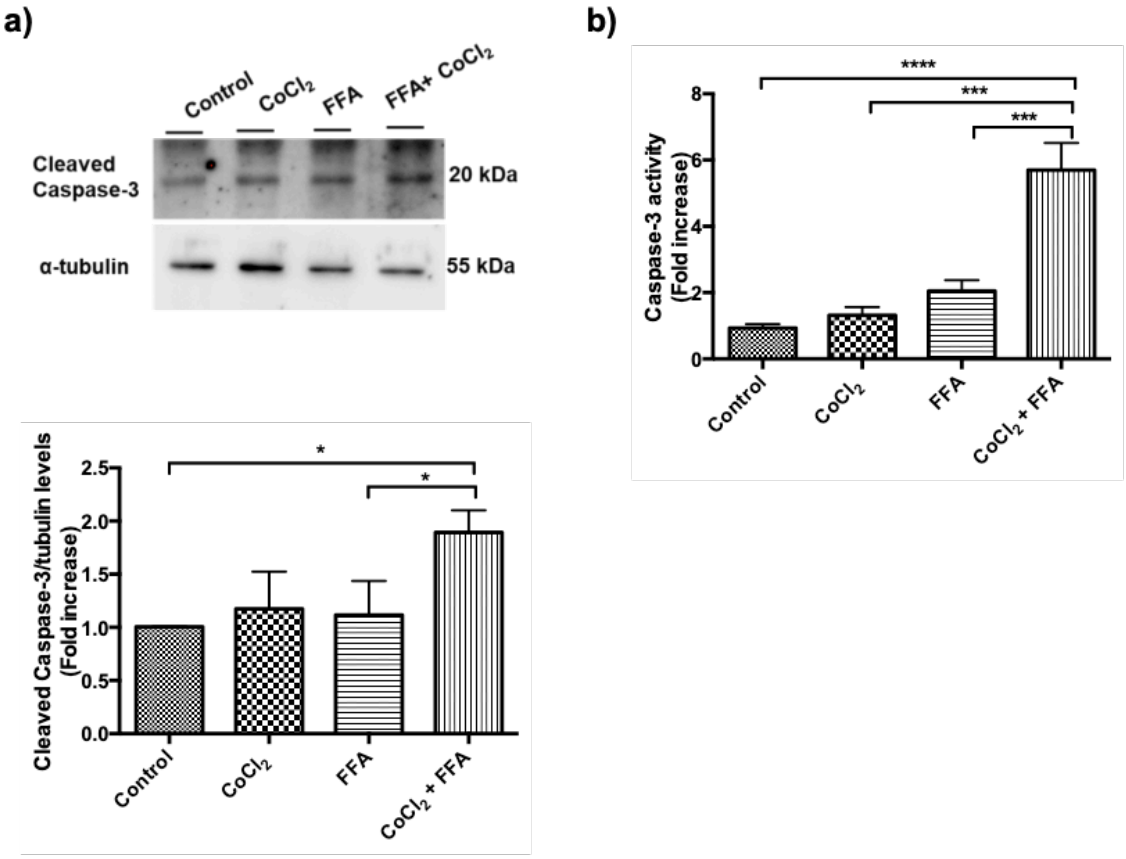

Figure 3. Chemical hypoxia promotes apoptotic cell death evaluate by a) cleaved Caspase-3 and b) Caspase-3 activity in fat-laden hepatocytes. Primary hepatocytes were incubated for 24h with oleic acid and palmitic acid (2:1 ratio) (FFA) in the presence or absence of CoCl2 200 µmol/L**.** a) Cleaved Caspase-3 protein levels and b) Caspase-3 activity were measured as described in Materials and Methods. Data were shown as mean ± SEM (n ≥ 3) * indicates $P < 0.05$; *** indicates $P < 0.005$ and **** indicates $P < 0.001$.

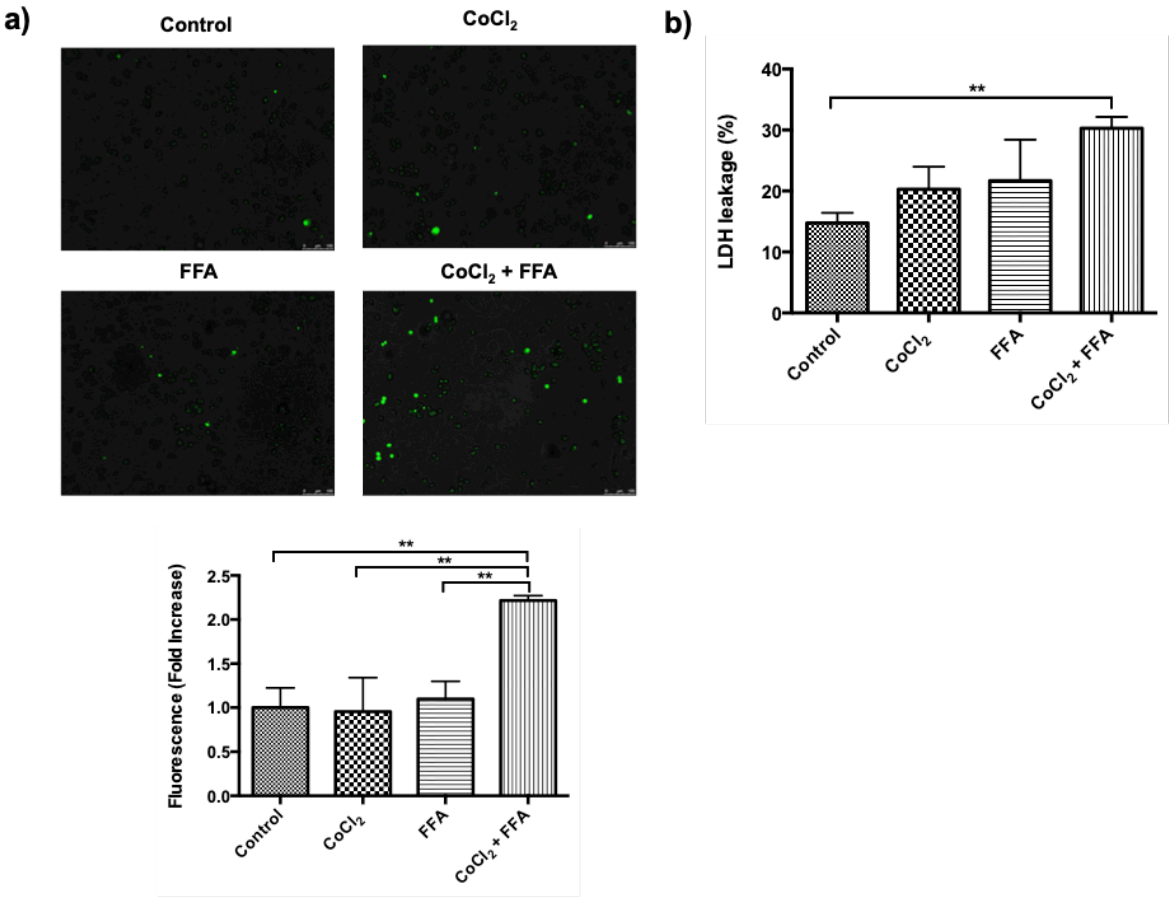

Figure 4. Hypoxia promotes pyroptotic cell death evaluate by a) SYTOX green, b) Lactate dehydrogenase leakage and c) Gasdermin-N in fat-laden hepatocytes. Primary hepatocytes were incubated for 24h with oleic acid and palmitic acid (2:1 ratio) (FFA) in the presence or absence of CoCl2 200 µmol/L**.** a) Sytox green (Representative images and quantification), b) LDH leakage percentage and c) GSDMD-N protein levels determinated by Western Blot were measured as described in Materials and Methods. Data were shown as mean ± SEM (n ≥ 3) * indicates P < 0.05 and ** indicates P < 0.01.

3.3 Hypoxia increases superoxide production by mitochondria in steatosis in vitro: Recent studies on the pathogenesis of NASH have described an important role for mitochondrial oxidative stress (47-50). To evaluate this issue, we examined the levels of mitochondrial superoxide generation in fat-laden hepatocytes treated with CoCl2. Fat-laden hepatocytes undergoing hypoxia exhibited ten-fold higher levels of mitochondrial superoxide fluorescence determined by MitoSOX™ compared to control cells. CoCl2 or FFA treatment alone did not determine significant changes in MitoSOX™ fluorescence intensity (Figure 5). These data indicate that chemical hypoxia in fat-laden hepatocytes promotes oxidative stress by an increase of mitochondrial superoxide production.

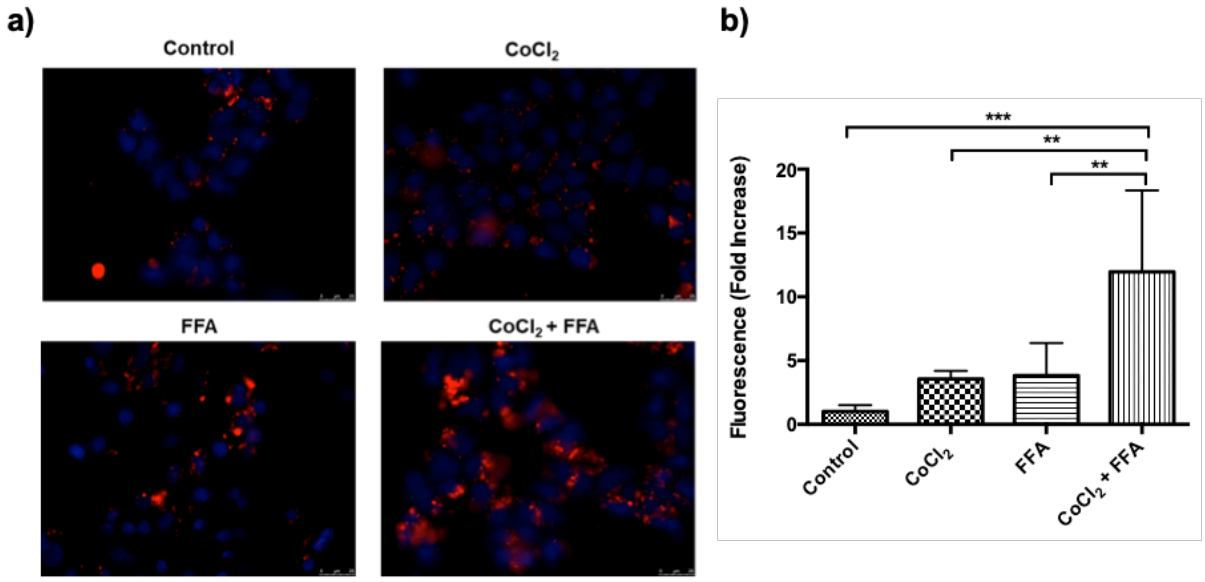

Figure 5. Hypoxia increases mitochondrial superoxide levels in steatotic hepatocytes. Primary hepatocytes were incubated for 24h with oleic acid and palmitic acid (2:1 ratio) (FFA) in the presence or absence of CoCl2 200 µmol/L. Superoxide generation by mitochondria was determined using MitoSOX™ fluorogenic probe as described in Materials and Methods. Data were shown as mean ± SEM (n ≥ 3) ** indicates $P < 0.01$ and *** indicates $P < 0.005$.

3.4 Effect of CoCl2-induced chemical hypoxia on the expression of pro-inflammatory cytokines and inflammasome components in fat-laden hepatocytes: To evaluate whether chemical hypoxia promotes an inflammatory phenotype in fat-laden hepatocytes, we measured mRNA levels of the pro-inflammatory cytokines TNF-a, IL-6 as well as of NLRP3 inflammasome components in cultured cells treated or not with FFA and CoCl2. As shown in figure 6, steatotic hepatocytes treated with CoCl2 displayed a marked increase in mRNA levels of IL-1β (2.5-fold), TNF-α (2-fold), and of IL-6 (9-fold) compared to non-treated cells. Also, mRNA levels of NLRP3 and Apoptosis-Associated Speck-Like Protein Containing CARD (ASC) were also significantly increased in fat-laden hepatocytes undergoing hypoxia compared with cells treated solely with FFA (Figure 6).

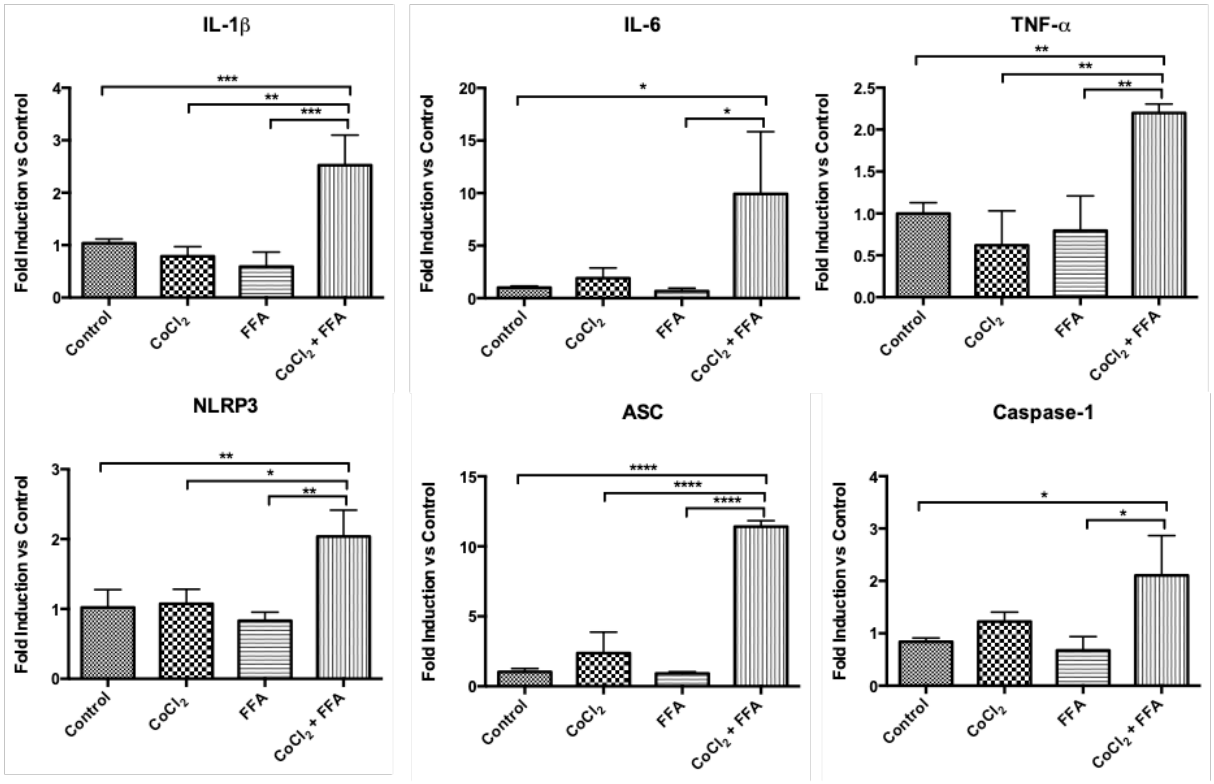

Figure 6. Hypoxia increases the expression of pro-inflammatory cytokines in steatotic hepatocytes. Primary hepatocytes were incubated for 24h with oleic acid and palmitic acid (2:1 ratio) (FFA) in the presence or absence of CoCl2 200 µmol/L. mRNA levels of IL-1β, TNF-α and IL-6 were measured as described in Materials and Methods. Data were shown as mean ± SEM (n ≥ 3) * indicates P < 0.05; ** indicates P < 0.01; *** indicates P < 0.005 and **** indicates P < 0.001.

3.5 CoCl2-treatment of fat-laden hepatocytes increases protein expression of caspase-1: The inflammasome is a multiprotein complex needed for caspase-1 processing and the subsequent activation of the inflammatory cytokines IL-1β and IL-18, which has been involved in the pathogenesis of NAFLD/NASH (20). Therefore, we examined the protein expression of caspase-1 in both freshly isolated control hepatocytes and hepatocytes treated with FFA as described above treated or not with CoCl2 in order to explore the effects of chemical hypoxia on inflammasome activation. While FFA treatment did not influence protein expression of caspase-1, CoCl2 treatment increased the protein levels of pro-caspase-1 (inactive form) and cleaved caspase-1 (p20 and p10 active forms) in hepatocytes irrespective if they were fat-laden or not (Figure 7) These data suggest that chemical hypoxia is able to activate the inflammasome complex in hepatocytes resulting in caspase-1 activation.

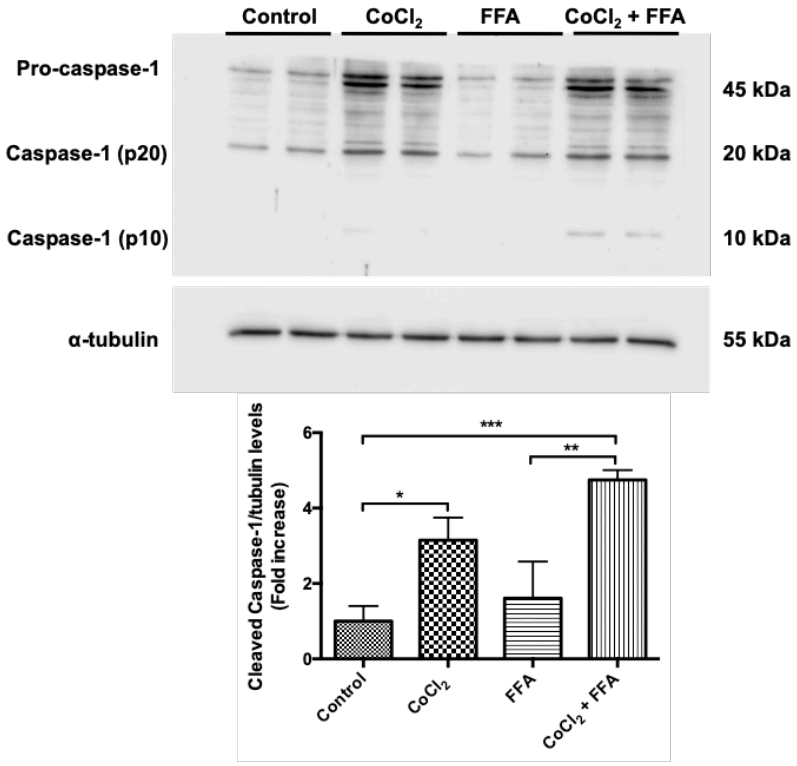

Figure 7. Hypoxia increases cleaved caspase-1 protein levels in steatotic hepatocytes. Primary hepatocytes were incubated for 24h with oleic acid and palmitic acid (2:1 ratio) (FFA) in the presence or absence of CoCl2 200 µmol/L. Protein levels of pro-caspase-1 and cleaved caspase-1 (p10 and p20) were determinated by Western Blot as described in Materials and Methods. α-Tubulin was used as loading control. The sum of p20 and p10 caspase-1 was calculated to determine the generation of cleaved Caspase-1. Data were shown as mean ± SEM (n ≥ 3) * indicates P < 0.05; ** indicates P < 0.01 and *** indicates P < 0.005.

3.6 Conditioned medium of steatotic hepatocytes subjected to hypoxia increases pro-inflammatory cytokines in Kupffer cells: To explore whether hypoxic, fat-laden hepatocytes can trigger pro-inflammatory responses in KC, we performed experiments exploring the effects of exposing KCs to CM obtained from fat-laden hepatocytes undergoing chemical hypoxia. We first profiled isolated KC assessing the expression of two typical macrophage markers [CD-68 as macrophage marker and CD-163 as KC marker (51)] by immunofluorescence (Figure 8) confirming the quality of KC isolation. Then, we observed that CM from steatotic hepatocytes subjected to hypoxia increases KC's mRNA levels of pro-inflammatory genes and decreased mRNA levels of the anti-inflammatory cytokine IL-10, without affecting gene expression of the classic KC M2 marker gene arginase-1 (Arg-1) (Figure 9a). Furthermore, protein levels of IL-1β were significantly higher in KC treated with CM from fat-laden hepatocytes undergoing chemical hypoxia compared with all other groups (Figure 9b). Treatment of cultured rat KC with CM obtained from hepatocytes treated with FFA alone also resulted in higher protein levels of IL-1β in KC compared to control cells (Figure 9b) but this effect

was less intense than that observed with CM from steatotic hepatocytes undergoing chemical hypoxia, suggesting that hypoxia exacerbates the expression of this pro-inflammatory cytokine. These data support the hypothesis that hypoxic and steatotic hepatocytes release signals that promote a pro-inflammatory phenotype in KC.

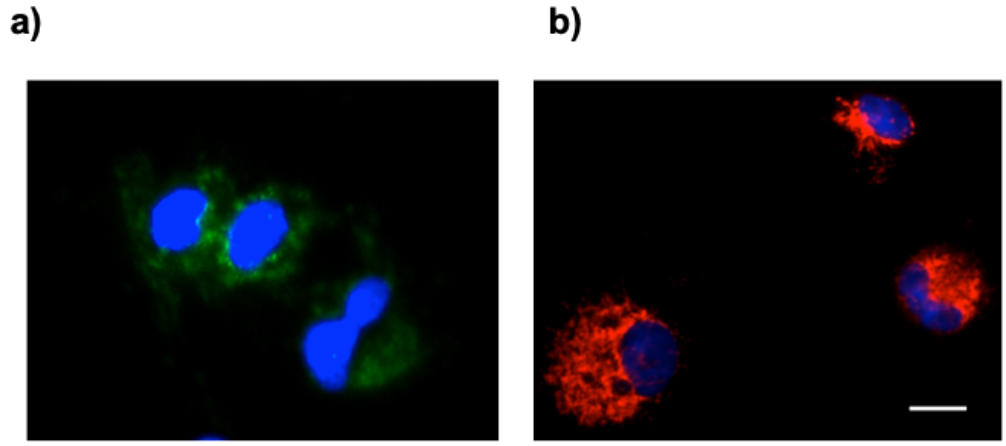

Figure 8. Characterization of Kupffer cells by immunofluorescence. Protein expression of specific Kupffer cell green fluorescent marker CD163 (A) and macrophage red fluorescent marker CD68 (B) were determined by immunofluorescence and nuclei were stained blue with DAPI as described in Materials and Methods (Supplementary materials). Scale bar: 10 µm

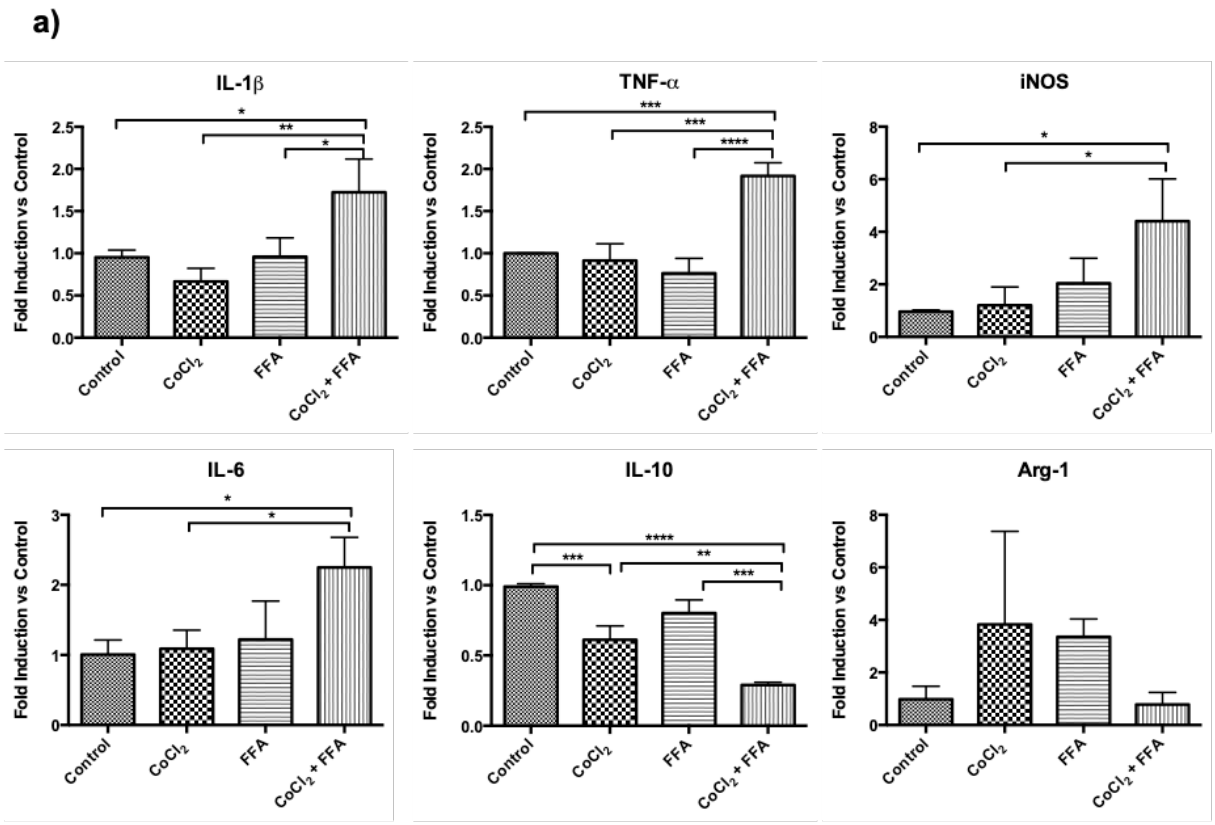

b)

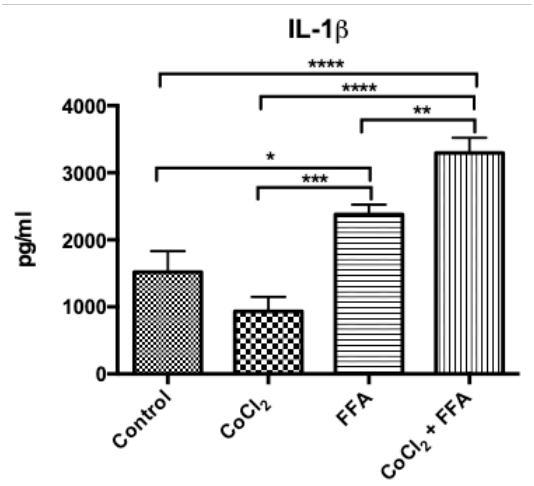

Figure 9. Conditioned medium of steatotic hepatocytes subjected to hypoxia increases a) pro-inflammatory genes and) IL-1β protein levels in Kupffer cells. Culture medium of primary hepatocytes was replaced 24 hours after treatment by FFA and CoCl2-free medium for an additional 24 hours (conditioned medium; CM). Kupffer cells were treated for 24 hours with the CM from hepatocytes. a) mRNA levels of IL-1β, TNF-α, iNOS, IL-6, IL-10 and Arg-1 and b) IL-1β protein levels by ELISA were measured as described in Materials and Methods. Data were shown as mean ± SEM (n ≥ 3) * indicates P < 0.05; ** indicates P < 0.01; *** indicates P < 0.005; **** indicates P < 0.001.

3.7 Extracellular vesicles increased in CM from fat-laden hepatocellular cell line exposed to CoCl2 and promoted pro-inflammatory genes expression in KC: To explore if EVs released from fat-laden hepatocytes undergoing hypoxia play a role in promoting a pro-inflammatory effects in KC, EVs were collected from culture media obtained from cultured HepG2 cells. We first explored if CM from HepG2 cells exposed to the different treatments evoked proinflammatory signals in KC. Results of these experiments are shown in Supplementary figure 2. As shown in this figure, similar to the effects observed in experiments involving hepatocytes, CM did determine increased expression of proinflammatory genes in KC, a decrease in the expression of IL-10 and had no effect on Arginase-1 expression. We then explored the effects of HepG2-derived EVs on KC and compared the observed effects with the effect of treatment with the EVs-free fraction. We first characterized EVs by transmission electron microscopy as well as by Western blot detection of the presence of the EVs marker CD81 and the absence of the mitochondrial protein Bcl-2 in all EV fractions (Figure 10a and Supplementary Figure 1). Of note, the size and concentration of HepG2-derived EVs were determined by NTA. Interestingly, we found an increase of EVs in culture media from fat-laden cells exposed to CoCl2 (6.0×10^{11} particles/mL) compared to culture media from control cells (9.5×10^{10} particles/mL) (Figure 10b). As shown in this figure, the average size of EVs obtained from culture media of control

cells was 150 nm while those EVs obtained from fat-laden HEPG2 cells undergoing CoCl2 was 130 nm (n.s.). Next, we examined the response of KCs to treatment with HepG2-derived EVs. EVs from steatotic HepG2 cells treated with CoCl2 determined a marked increase in mRNA levels in KC of the following proinflammatory genes: IL-1β (2.0-fold), TNF-α (2.5-fold), iNOS (1.6-fold) and of IL-6 (2.2-fold) in comparison to treatment with EVs from non-treated cells, without affecting significantly gene expression of IL-10 and Arg-1 (Figure 10c). However, EV-free CM, as negative control to evaluate the specific effect of EVs, promoted an increased on iNOS gene expression in KC (1.4-fold), demonstrating that CM EV-free may contains soluble substances that induce the expression of this specific pro-inflammatory cytokine. Of note, treatment of KC with EVs obtained from HepG2 cells treated with FFA or CoCl2 alone did not evoke significant changes in KC expression of pro-inflammatory genes (Supplementary Figure 3).

a)

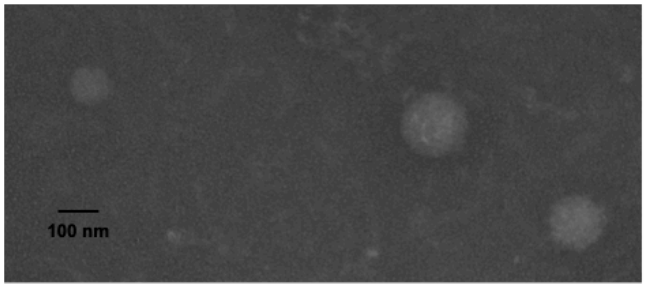

b)

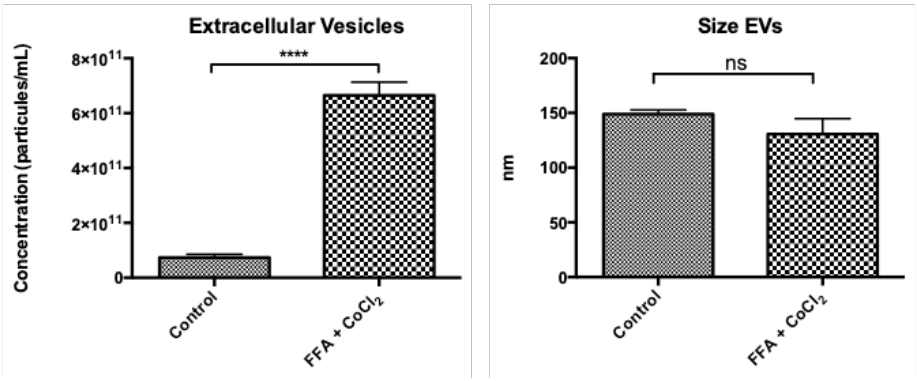

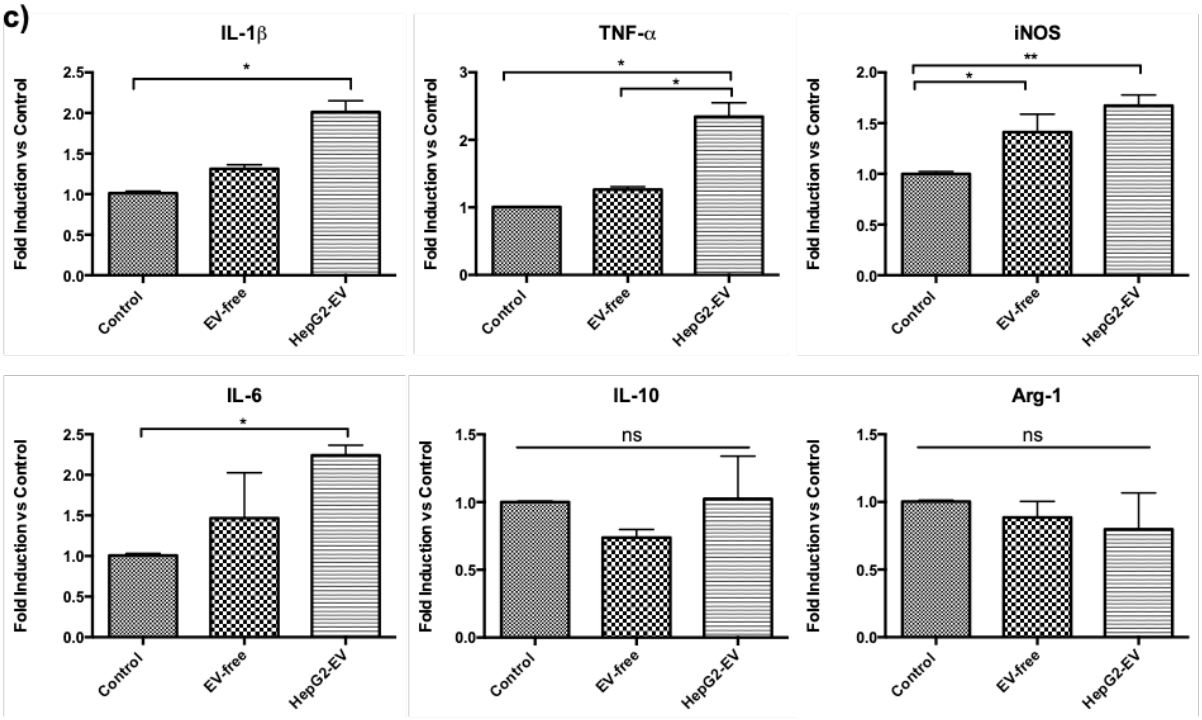

Figure 10. EVs obtained from culture media of fat-laden HepG2 cells exposed to CoCl2 increases pro-inflammatory genes in Kupffer Cells. KC was treated with EV-free CM, as negative control, and with 15 µg of EVs isolated from HepG2 cells that had been treated with CoCl2 + FFA for 24h. mRNA levels of IL-1β, TNF-α, iNOS, IL-6, IL-10 and Arg-1 were measured as described in Materials and Methods. Data were shown as mean ± SEM (n ≥ 3) * indicates P < 0.05; ** indicates P < 0.01; *** indicates P < 0.005; **** indicates P < 0.001.

3.8 Intermittent hypoxia in an experimental model of diet-induced non-alcoholic steatohepatitis increases the inflammatory phenotype: To validate our *in vitro* findings, we investigated the effect of IH for 12 weeks in an animal model, the CDAA diet-induced NASH (16). To evaluate steatosis, liver sections were stained with Oil red O staining (Figure 11a) (Abcam, Cambridge, UK). Steatosis, inflammation and fibrosis was graded blindly by an experienced pathologist (J.T.) according to the NAS score. Specifically, the amount of steatosis (percentage of hepatocytes containing fat droplets) was scored as 0 (<5%), 1 (5–33%), 2 (>33–66%) and 3 (>66%). Although pathological scoring suggested a higher degree of steatosis in animals on CDAA diet and exposed to hypoxia compared to control animals and compared to animals on CDAA diet and normoxic conditions (Figure 11b), we did not observed significant differences in the hepatic TG levels between the CDAA-fed mice groups (Figure 11c). Also, no differences were found in NAS score when comparing CDAA-fed groups. However, mRNA levels of pro-inflammatory genes and NLRP3 inflammasome components significantly increased in animals with hypoxia on CDAA diet compared to all other groups (Figure 12). Finally, we tested the caspase-1 protein levels, which significantly increases in animals with

hypoxia on CDAA diet (Figure 13). With these results, we verified that hypoxia promotes an aggravated the inflammatory phenotype in NASH and specifically influences inflammasome activation.

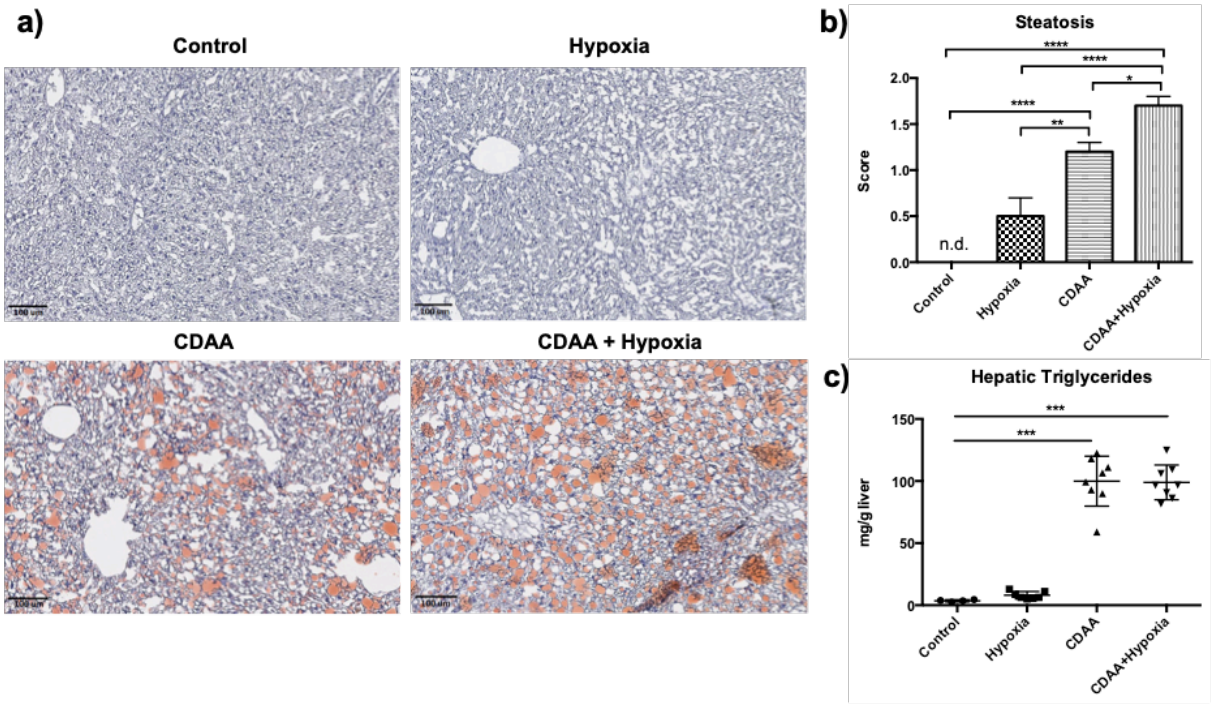

Figure 11. Intermittent hypoxia increased steatosis in mice with CDAA-induced liver injury determined by Oil Red-O staining, without changes in hepatic triglycerides. Mice were placed on choline-supplemented L-amino acid defined (CSAA) diet as control, or defined diet with choline deficiency amino acids (CDAA) for 22 weeks to induce liver injury and intermittent hypoxia (IH) or normoxia was applied for the last 12 weeks of the diet as described in Materials and Methods. a) Liver sections were stained with Oil Red O and analyzed by a pathologist in a blinded fashion to determine b) steatosis score as described in Materials and Methods. c) Hepatic Triglycerides was measured as described in Materials and Methods. Data were shown as mean ± SEM ($n \geq 3$) ** indicates $P < 0.01$; *** indicates $P < 0.005$ and **** indicates $P < 0.001$.

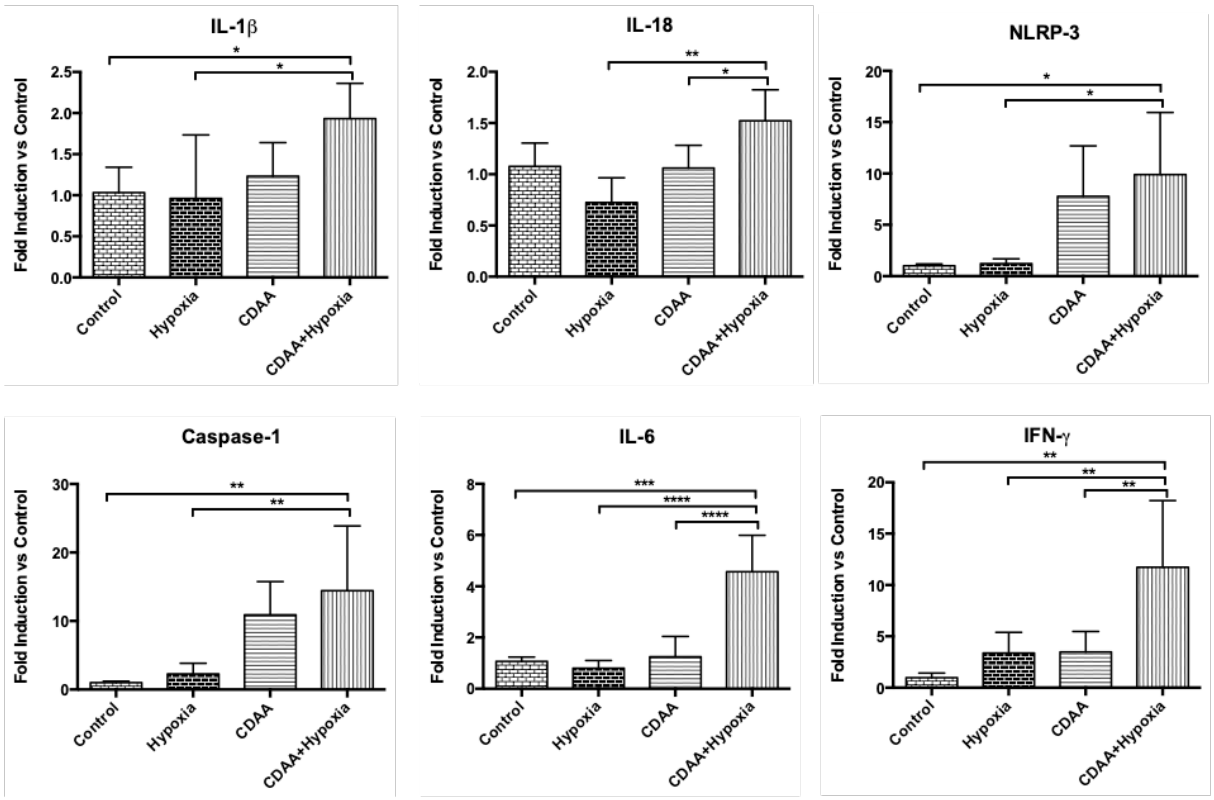

Figure 12. Intermittent hypoxia in mice with CDAA-induced liver injury increases the expression of pro-inflammatory cytokines and inflammasome components. The mice were placed on choline-supplemented L-amino acid defined (CSAA) diet as control, or defined diet with choline deficiency amino acids (CDAA) for 22 weeks to induce liver injury and intermittent hypoxia (IH) or normoxia was applied for the last 12 weeks of the diet as described in Materials and Methods. mRNA levels of IL-1β, IL-18, NLRP3, caspase-1, IL-6 and IFN-γ were measured as described in Materials and Methods. Data were shown as mean ± SEM (n ≥ 3) * indicates P < 0.05; ** indicates P < 0.01; *** indicates P < 0.005; **** indicates P < 0.001.

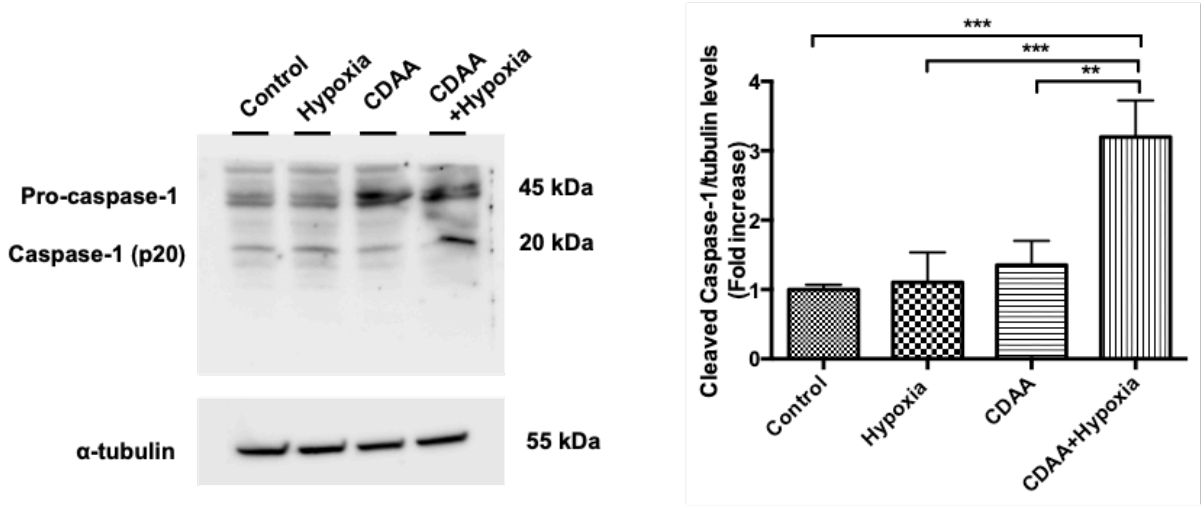

Figura 13. Intermittent hypoxia in mice with CDAA-induced liver injury increases cleaved caspase-1. The mice were placed on choline-supplemented L-amino acid defined (CSAA) diet as control, or defined diet with choline deficiency amino acids (CDAA) for 22 weeks to induce liver injury and intermittent hypoxia (IH) or normoxia was applied for the last 12 weeks of the diet as described in Materials and Methods. Protein levels of pro-caspase-1 and cleaved caspase-1 (p10 and p20) were determined by Western Blot as described in Materials and Methods. α-Tubulin was used as a loading control. The sum of p20 and p10 caspase-1 was calculated to determine the generation of cleaved caspase-1. Data were shown as mean ± SEM (n ≥ 3) ** indicates $P < 0.01$ and *** indicates $P < 0.005$.

4. - DISCUSSION

NAFLD represents a highly frequent cause of liver disease, which is closely associated with obesity and insulin resistance (7, 52). Clinical observations suggest that patients with OSAS have a greater predisposition to develop NAFLD and NASH, the aggressive form of NAFLD, which is characterized by the presence of necro-inflammatory and fibrotic phenomena in the liver (5). Several studies have shown that OSAS, mainly through the occurrence of IH, can modulate hepatocellular damage by triggering proinflammatory and profibrotic signals (25, 26), but pathways underlying this effects are ill-defined. The present study used cellular models of NAFLD/NASH to explore potential synergistic interactions between hypoxia and FFA exposure. To that end, the hypoxia mimetic agent CoCl2 was used to treat fat-laden hepatocytes. Our findings suggest that indeed hypoxia determines a further increase in cellular TG content in FFA treated hepatocytes as well as increased mRNA levels of pro-inflammatory cytokines as well as those of the NLRP3 inflammasome components. These phenomena were also associated with increased mitochondrial superoxide levels and increased rates of cell death due to apoptosis and disruption of cell membrane, likely pyroptosis as suggested by the increase in GSDMD levels. Moreover, conditioned medium obtained from hypoxic fat-laden hepatocytes promoted an inflammatory phenotype in KC, which is known to be decisive for the amplification of the pathological phenomenon of NASH (12, 23). Additionally, in order to determine if the observed effects on KC could be mediated by EVs release from hepatocytes, we conducted further experiments in the human hepatoma cell line HepG2. We choose this approach for practical reasons since using this cell line the EVs isolation efficiency is high. Our results showed that treatment of HepG2 with FFA and CoCl2 determines an increase in the release of EVs to the medium and that these EVs also evoke a pro-inflammatory response in rat KC in line with previous observations showing that released EVs from fat-laden hepatocytes can act in in macrophages and contribute to pro-inflammatory response in a paracrine fashion (15).

Finally, we found correlates of our *in vitro* NASH model findings in an animal model of NASH induced by feeding a CDAA diet. In the latter experiments, we also confirmed that IH promotes NLRP3

inflammasome activation in the setting of NASH. Collectively taken, these findings indicate that hypoxia may influence NAFLD development and progression by acting at different levels including promotion of further lipid accumulation as well as enhancement of liver inflammation and hepatocellular death. Of note, recent rodent studies indicate that hypoxia may be also linked to liver fibrosis, a key prognostic feature of NASH (8). In fact, Mersarwi et al. demonstrated that HIF-1α deletion in hepatocytes protects against the development of liver fibrosis in a mouse model of NAFLD (53). This observation adds to our data and support the concept that hypoxia contributes to NAFLD progression influencing critical steps of the disease.

Experimental data on the effects of hypoxia in NAFLD models is scarce and mainly restricted to whole animal studies (53, 54). No data is available on the effects of hypoxia in cellular models of NAFLD/NASH (36). To assess this, we used the hypoxia mimetic compound CoCl2, which induces chemical hypoxia by stabilizing HIF-1α and 2α (38). This model is well accepted and has several advantages over alternatives such as the hypoxia chamber or a CO_2 incubator with regulated oxygen levels, which are less available, most costly and provide a less stable experimental conditions (38). CoCl2 has been previously used in normal isolated hepatocytes (38, 45) but not in fat-laden cells underlying the novelty of our approach. Of note, previous studies as well as experiments of our laboratory on hepatocyte cell lines have demonstrated the non-toxic effect of CoCl2 at concentrations not exceeding 400 µmol/L for 24 hours as previously described (55). On the other hand, FFA treatment using combination of OA and PA effectively induced TG accumulation in the absence of lipoapoptosis (56). In spite of these advantages and, although CoCl2-induced chemical hypoxia is a suitable model to assess the effects of hypoxia in cellular models, we acknowledge that this model reproduces only some of the effects generated by a decrease in oxygen supply, which limit the generalizability of our results until they are confirmed in other models.

The observed hypoxia-related increases in intracellular lipid droplets and TG content in fat-laden hepatocytes is consistent with previous studies that indicate that hypoxia, through HIF-1α, promotes an increase in lipid biosynthesis causing TG accumulation (57, 58). We did not observe a marked increase in lipid content in cells treated solely with CoCl2, which may relate to length of treatment and experimental conditions. We also did not find an increase in the in vivo CDAA-feeding NASH model. We think that this may be related to the fact that this particular model determines severe steatosis and inflammation (59) and that therefore is difficult to observe subtle changes.

With regard to the effects of chemical hypoxia on cell death of FFA treated hepatocytes, qualitative determination of apoptosis, necrosis and pyroptosis using determination of caspase-3 cleavage, caspase-3 activity, SYTOX green staining, LDH release and GSDMD-N were carried out as performed

in previous studies (56, 60). While, treatment with CoCl2 or FFA alone did not induce a significant increase in apoptosis compared to control conditions, CoCl2 treatment of fat-laden hepatocytes did increase cleaved caspase-3 and caspase-3 activity reflecting ongoing apoptosis. The same observation was made regarding cell death associated to a disrupted plasma membrane, by SYTOX Green and LDH leakage measure, as an increased number of necrotic death cells was observed in steatotic hepatocytes subjected to hypoxia. Given the fact that hypoxia was associated to increase of GSDMD cleavage and up-regulation of inflammasome components, it is likely that pyroptosis also contributed to cell death of fat-laden hepatocytes undergoing chemical hypoxia. Of note, it has been suggested that pyroptosis may be an inflammatory link related to the progression from bland steatosis to NASH, as NLRP3 activation is not present in animal model of isolated steatosis without inflammation (61). Additionally, we observed a significant increase in mitochondrial superoxide levels in the fat-laden hepatocytes exposed to chemical hypoxia. Interestingly, increased mitochondrial superoxide generation has been correlated to mitochondrial dysfunction, oxidative damage, cellular death and pro-inflammatory effects in NASH (49, 62). Thus, this synergistic effect of hypoxia and FFA in hepatocytes with regard to mitochondrial superoxide generation, likely contributes to the observed increase in cell death when hepatocytes are exposed to both stimuli.

In addition to the observed effects on cell death and oxidative stress, chemical hypoxia also induced the expression of several inflammatory cytokines, including TNF-a, IL-6 and IL-1β, as well as of the components of the NLRP3 inflammasome (caspase-1, NLRP3 and ASC), in steatotic hepatocytes. The NLRP3 inflammasome activates pro-caspase-1 into active caspase-1 (p10 and p20 cleaved caspase-1) that in turn cleaves pro-IL-1β into the mature form of IL-1β promoting amplification of liver inflammation and cell death (12). In recent years, caspase-1 has been studied extensively and has been shown to contribute to liver damage during the development of NASH (63, 64) and several studies have shown protective effects against liver damage when caspase-1 is inhibited (63). In our study, we evaluated the protein levels of caspase-1 (pro-caspase -1 and active cleaved-caspase-1) in hepatocytes. An increase in the total level of pro-caspase-1 was observed in hypoxic hepatocytes and hypoxic hepatocytes treated with FFA compared to the control conditions. Interestingly, cleaved-p-20 and p-10, the active isoforms of caspase-1, were only detected in hypoxic hepatocytes treated with FFA. These results are consistent with the observed up-regulation of inflammasome components and similar to those obtained by other authors in prostate epithelial cells undergoing hypoxia, showing increased NLRP3 inflammasome activation as determined by increased cellular levels of cleaved caspase-1 (65). Taken together, our results suggest that the induction of hypoxia in hepatocytes promotes susceptibility to damage by FFA, resulting in increased caspase-3 mediated

apoptosis, (secondary) necrosis, pyroptosis and an inflammatory phenotype, characterized by increased expression of pro-inflammatory genes and protein levels of caspase-1.

Kupffer cells (KC) are involved in the pathogenesis of various liver diseases, including steatohepatitis (66). However, their role in the context of hepatocellular damage due to hypoxia remains poorly explored. KC are derived from circulating monocytes and, once established in the liver, fulfill multiple functions related to the immune system. KC maintain constant paracrine communication with neighboring hepatocytes, stellate cells and endothelial cells through the signals that they receive from the extracellular environment (66). To verify the paracrine involvement of KC with steatotic hepatocytes in the context of hypoxia, KC were exposed to conditioned medium of hepatocytes subjected to different treatments. We documented that conditioned medium from steatotic and hypoxic hepatocytes induced a pro-inflammatory profile in KC. These novel results correlate well with recent studies showing micro-RNA-mediated cellular crosstalk between hepatocytes treated with ethanol and monocytes/ macrophages (67). As mentioned before, hepatocytes are able to modulate signaling pathways in macrophages, stellate cells and endothelial cells in a paracrine manner by cytokines, micro-RNAs and EVs (32). Our experiments involving isolation of EVs from HEPG2 cells strongly suggest that EVs participate in the cellular communication between steatotic and hypoxic hepatocytes and KC. This observations may have diagnostic and therapeutic implications (33).

In the present study, we also explored whether IH influences hepatic steatosis and the pro-inflammatory phenotype in an *in vivo* model of NASH. To this end, we assessed the effects of hypoxia for 22 weeks in CDAA-fed mice by evaluating liver histology and hepatic mRNA levels of pro-inflammatory cytokines. Our results showed a worsening of histological steatosis in CDAA-fed mice subjected to IH compared to those animals that did not undergo hypoxic conditions. However, we did not observe a corresponding increase in thepatic TG content. We think that this may be related to the fact that this particular model determines severe steatosis and inflammation (59) and that therefore is difficult to observe subtle changes.

With regard to inflammatory markers, CDAA-fed mice exposed to IH exhibited an increase of all inflammasome components (IL-1β, IL-18, NLRP3 and caspase-1) and other pro-inflammatory cytokines (IL-6, IFN-γ). Also, active caspase-1 level protein increased in livers from CDAA-fed mice exposed to IH, which correlates with the findings in the *in vitro* model. These observations support the concept that hypoxia may contribute to liver damage in the setting of NAFLD by activating the NLRP3 inflammasome. A recent study showing that IH activates the NLRP3 inflammasome in kidneys, which result in progressive renal injury (68) provides support to this notion. Although not explored in

this study, this might have implications not only for hepatocellular injury but also for liver fibrosis development and hepatocarcinogenesis (69, 70).

In summary, our results in *in vitro* and *in vivo* models of NAFLD/NASH support the notion that hypoxia plays an aggravating role in the setting of excessive lipid load in liver cells by influencing lipid deposition, hepatocellular death and pro-inflammatory signals, involving NLRP3 inflammasome activation. Moreover, our novel findings demonstrate that hypoxia modulates cellular crosstalk between steatotic hepatocytes and inflammatory cells (KCs). Future studies should focus on the characterization of the extracellular environment of hypoxic and steatotic hepatocytes to identify the hypoxia-specific factors and the mechanisms of hepatocellular damage at play in NASH.

5. - SUPPLEMENTARY FIGURES

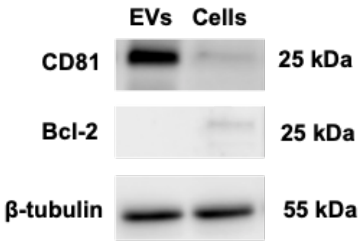

Figure S1. Characterization of HepG2-EV. EVs were characterized in culture medium from control HepG2 cells by detection of EV-positive marker CD81 and EV negative mitochondrial marker Bcl-2 by Western blot as described in Material and Methods.

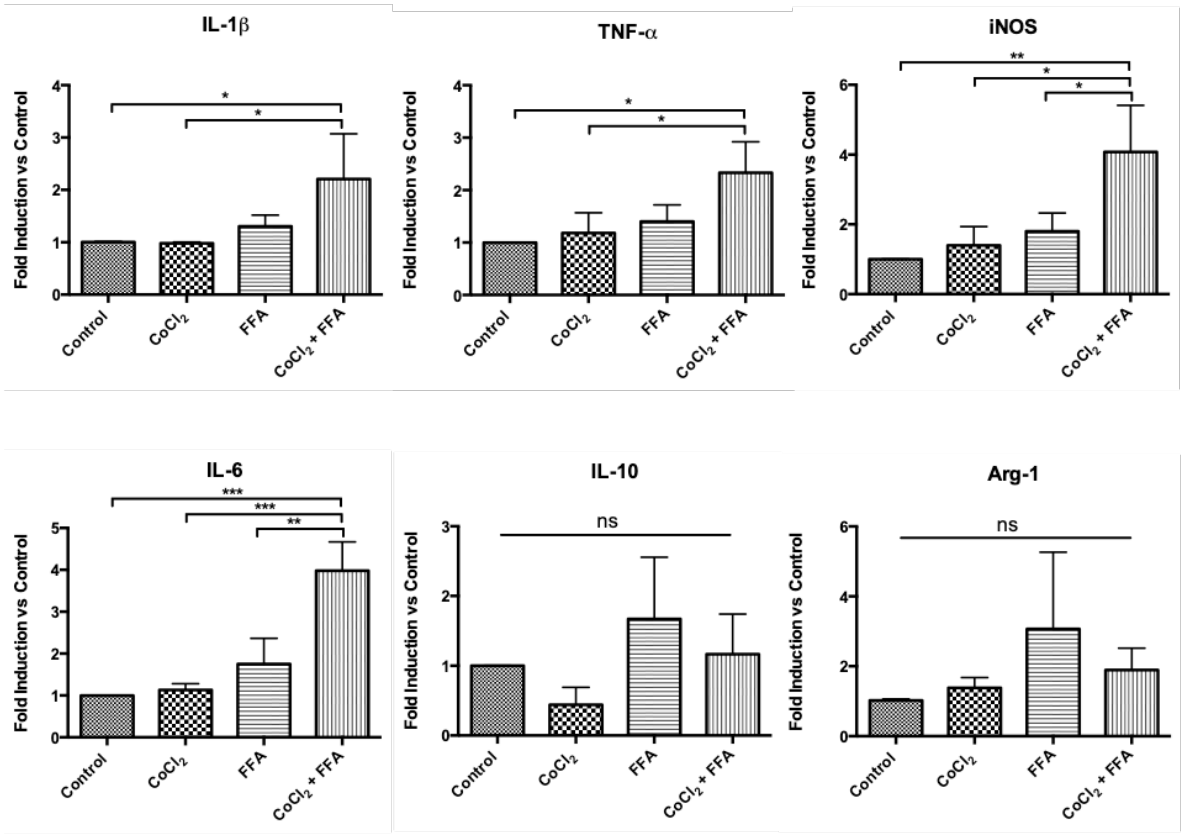

Figure S2. Conditioned medium of steatotic HepG2 cells subjected to hypoxia increases pro-inflammatory genes in Kupffer cells. Culture medium of HepG2 cells was replaced 24 hours after treatment by FFA and CoCl2-free medium for an additional 24 hours (conditioned medium; CM). Kupffer cells were treated for 24 hours with the CM from HepG2 cells. mRNA levels of IL-1β, TNF-α, iNOS, IL-6, IL-10 and Arg-1 were measured as described in Materials and Methods. Data were shown as mean ± SEM (n ≥ 3) *indicates P < 0.05; ** indicates P < 0.01; *** indicates P < 0.005.

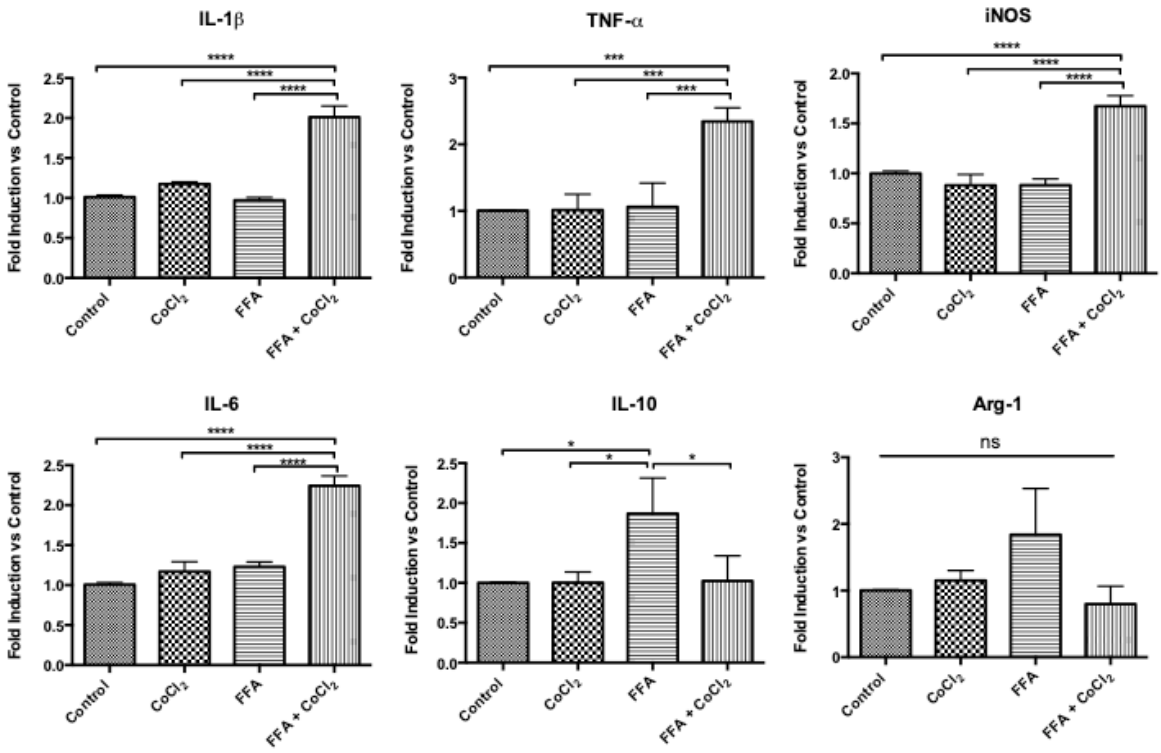

Figure S3. EVs obtained from culture media of fat-laden HepG2 cells exposed to CoCl2 increases proinflammatoyry genes in Kupffer cells. KC cells were exposed to 15 μg of EVs that were isolated from HepG2 cells that had been treated with CoCl2, FFA and CoCl2 + FFA for 24h. mRNA levels of IL-1β, TNF-α, iNOS, IL-6, IL-10 and Arg-1 were measured as described in Materials and Methods. Data were shown as mean ± SEM (n ≥ 3) *indicates P < 0.05; *** indicates P < 0.005; **** indicates P < 0.001.

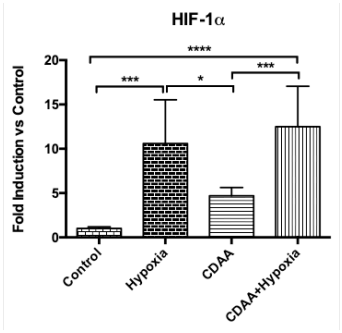

Figure S4. Intermittent hypoxia in mice increases the gene expression of HIF-1α. The mice were placed on choline-supplemented L-amino acid defined (CSAA) diet as control, or defined diet with choline deficiency amino acids (CDAA) for 22 weeks to induce liver injury and intermittent hypoxia (IH) or normoxia was applied for the last 12 weeks of the diet as described in Materials and Methods. mRNA levels of HIF-1α was measured as described in Materials and Methods. Data were shown as mean ± SEM (n ≥ 3) * indicates P < 0.05; *** indicates P < 0.005; **** indicates P < 0.001.

6. - REFERENCES

1. Drager LF, Lopes HF, Maki-Nunes C, Trombetta IC, Toschi-Dias E, Alves MJ, Fraga RF, et al. The impact of obstructive sleep apnea on metabolic and inflammatory markers in consecutive patients with metabolic syndrome. PLoS One 2010;5:e12065.
2. Gaines J, Vgontzas AN, Fernandez-Mendoza J, Bixler EO. Obstructive sleep apnea and the metabolic syndrome: The road to clinically-meaningful phenotyping, improved prognosis, and personalized treatment. Sleep Med Rev 2018;42:211-219.
3. Dempsey JA, Veasey SC, Morgan BJ, O'Donnell CP. Pathophysiology of sleep apnea. Physiol Rev 2010;90:47-112.
4. Agrawal S, Duseja A, Aggarwal A, Das A, Mehta M, Dhiman RK, Chawla Y. Obstructive sleep apnea is an important predictor of hepatic fibrosis in patients with nonalcoholic fatty liver disease in a tertiary care center. Hepatol Int 2015;9:283-291.
5. Mesarwi OA, Loomba R, Malhotra A. Obstructive Sleep Apnea, Hypoxia, and Nonalcoholic Fatty Liver Disease. Am J Respir Crit Care Med 2019;199:830-841.
6. Parikh MP, Gupta NM, McCullough AJ. Obstructive Sleep Apnea and the Liver. Clin Liver Dis 2019;23:363-382.
7. Rinella ME. Nonalcoholic fatty liver disease: a systematic review. JAMA 2015;313:2263-2273.
8. Arab JP, Arrese M, Trauner M. Recent Insights into the Pathogenesis of Nonalcoholic Fatty Liver Disease. Annu Rev Pathol 2018;13:321-350.
9. Chalasani N, Younossi Z, Lavine JE, Charlton M, Cusi K, Rinella M, Harrison SA, et al. The diagnosis and management of nonalcoholic fatty liver disease: Practice guidance from the American Association for the Study of Liver Diseases. Hepatology 2018;67:328-357.
10. Noureddin M, Sanyal AJ. Pathogenesis of NASH: The Impact of Multiple Pathways. Curr Hepatol Rep 2018;17:350-360.
11. Ibrahim SH, Hirsova P, Gores GJ. Non-alcoholic steatohepatitis pathogenesis: sublethal hepatocyte injury as a driver of liver inflammation. Gut 2018;67:963-972.
12. Schuster S, Cabrera D, Arrese M, Feldstein AE. Triggering and resolution of inflammation in NASH. Nat Rev Gastroenterol Hepatol 2018;15:349-364.
13. Wree A, McGeough MD, Pena CA, Schlattjan M, Li H, Inzaugarat ME, Messer K, et al. NLRP3 inflammasome activation is required for fibrosis development in NAFLD. J Mol Med (Berl) 2014;92:1069-1082.
14. Wree A, Eguchi A, McGeough MD, Pena CA, Johnson CD, Canbay A, Hoffman HM, et al. NLRP3 inflammasome activation results in hepatocyte pyroptosis, liver inflammation, and fibrosis in mice. Hepatology 2014;59:898-910.

15. Cannito S, Morello E, Bocca C, Foglia B, Benetti E, Novo E, Chiazza F, et al. Microvesicles released from fat-laden cells promote activation of hepatocellular NLRP3 inflammasome: A pro-inflammatory link between lipotoxicity and non-alcoholic steatohepatitis. PLoS One 2017;12:e0172575.

16. Cabrera D, Wree A, Povero D, Solis N, Hernandez A, Pizarro M, Moshage H, et al. Andrographolide Ameliorates Inflammation and Fibrogenesis and Attenuates Inflammasome Activation in Experimental Non-Alcoholic Steatohepatitis. Sci Rep 2017;7:3491.

17. Csak T, Ganz M, Pespisa J, Kodys K, Dolganiuc A, Szabo G. Fatty acid and endotoxin activate inflammasomes in mouse hepatocytes that release danger signals to stimulate immune cells. Hepatology 2011;54:133-144.

18. Mridha AR, Wree A, Robertson AAB, Yeh MM, Johnson CD, Van Rooyen DM, Haczeyni F, et al. NLRP3 inflammasome blockade reduces liver inflammation and fibrosis in experimental NASH in mice. J Hepatol 2017;66:1037-1046.

19. Xu B, Jiang M, Chu Y, Wang W, Chen D, Li X, Zhang Z, et al. Gasdermin D plays a key role as a pyroptosis executor of non-alcoholic steatohepatitis in humans and mice. J Hepatol 2018;68:773-782.

20. Guo H, Callaway JB, Ting JP. Inflammasomes: mechanism of action, role in disease, and therapeutics. Nat Med 2015;21:677-687.

21. Cha JY, Kim DH, Chun KH. The role of hepatic macrophages in nonalcoholic fatty liver disease and nonalcoholic steatohepatitis. Lab Anim Res 2018;34:133-139.

22. Yu Y, Liu Y, An W, Song J, Zhang Y, Zhao X. STING-mediated inflammation in Kupffer cells contributes to progression of nonalcoholic steatohepatitis. J Clin Invest 2019;129:546-555.

23. Arrese M, Cabrera D, Kalergis AM, Feldstein AE. Innate Immunity and Inflammation in NAFLD/NASH. Dig Dis Sci 2016;61:1294-1303.

24. Drager LF, Li J, Reinke C, Bevans-Fonti S, Jun JC, Polotsky VY. Intermittent hypoxia exacerbates metabolic effects of diet-induced obesity. Obesity (Silver Spring) 2011;19:2167-2174.

25. Savransky V, Nanayakkara A, Vivero A, Li J, Bevans S, Smith PL, Torbenson MS, et al. Chronic intermittent hypoxia predisposes to liver injury. Hepatology 2007;45:1007-1013.

26. Savransky V, Reinke C, Jun J, Bevans-Fonti S, Nanayakkara A, Li J, Myers AC, et al. Chronic intermittent hypoxia and acetaminophen induce synergistic liver injury in mice. Exp Physiol 2009;94:228-239.

27. Liu Y, Ma Z, Zhao C, Wang Y, Wu G, Xiao J, McClain CJ, et al. HIF-1alpha and HIF-2alpha are critically involved in hypoxia-induced lipid accumulation in hepatocytes through reducing PGC-1alpha-mediated fatty acid beta-oxidation. Toxicol Lett 2014;226:117-123.

28. Briancon-Marjollet A, Monneret D, Henri M, Joyeux-Faure M, Totoson P, Cachot S, Faure P, et al. Intermittent hypoxia in obese Zucker rats: cardiometabolic and inflammatory effects. Exp Physiol 2016;101:1432-1442.

29. Kang HH, Kim IK, Lee HI, Joo H, Lim JU, Lee J, Lee SH, et al. Chronic intermittent hypoxia induces liver fibrosis in mice with diet-induced obesity via TLR4/MyD88/MAPK/NF-kB signaling pathways. Biochem Biophys Res Commun 2017;490:349-355.

30. Ju C, Colgan SP, Eltzschig HK. Hypoxia-inducible factors as molecular targets for liver diseases. J Mol Med (Berl) 2016;94:613-627.

31. van der Graaff D, Kwanten WJ, Francque SM. The potential role of vascular alterations and subsequent impaired liver blood flow and hepatic hypoxia in the pathophysiology of non-alcoholic steatohepatitis. Med Hypotheses 2019;122:188-197.

32. Eguchi A, Feldstein AE. Extracellular vesicles in non-alcoholic and alcoholic fatty liver diseases. Liver Res 2018;2:30-34.

33. Malhi H. Emerging role of extracellular vesicles in liver diseases. Am J Physiol Gastrointest Liver Physiol 2019;317:G739-G749.

34. Moshage H, Casini A, Lieber CS. Acetaldehyde selectively stimulates collagen production in cultured rat liver fat-storing cells but not in hepatocytes. Hepatology 1990;12:511-518.

35. Damba T, Zhang M, Buist-Homan M, van Goor H, Faber KN, Moshage H. Hydrogen sulfide stimulates activation of hepatic stellate cells through increased cellular bio-energetics. Nitric Oxide 2019;92:26-33.

36. Chavez-Tapia NC, Rosso N, Tiribelli C. In vitro models for the study of non-alcoholic fatty liver disease. Curr Med Chem 2011;18:1079-1084.

37. Pecoraro M, Pinto A, Popolo A. Inhibition of Connexin 43 translocation on mitochondria accelerates CoCl2-induced apoptotic response in a chemical model of hypoxia. Toxicol In Vitro 2018;47:120-128.

38. Munoz-Sanchez J, Chanez-Cardenas ME. The use of cobalt chloride as a chemical hypoxia model. J Appl Toxicol 2019;39:556-570.

39. Schoemaker MH, Conde de la Rosa L, Buist-Homan M, Vrenken TE, Havinga R, Poelstra K, Haisma HJ, et al. Tauroursodeoxycholic acid protects rat hepatocytes from bile acid-induced apoptosis via activation of survival pathways. Hepatology 2004;39:1563-1573.

40. Chan LL, McCulley KJ, Kessel SL. Assessment of Cell Viability with Single-, Dual-, and Multi-Staining Methods Using Image Cytometry. Methods Mol Biol 2017;1601:27-41.

41. Wang G, Memin E, Murali I, Gaspers LD. The effect of chronic alcohol consumption on mitochondrial calcium handling in hepatocytes. Biochem J 2016;473:3903-3921.

42. Woudenberg-Vrenken TE, Conde de la Rosa L, Buist-Homan M, Faber KN, Moshage H. Metformin protects rat hepatocytes against bile acid-induced apoptosis. PLoS One 2013;8:e71773.

43. Thery C, Amigorena S, Raposo G, Clayton A. Isolation and characterization of exosomes from cell culture supernatants and biological fluids. Curr Protoc Cell Biol 2006;Chapter 3:Unit 3 22.

44. Pizarro M, Solis N, Quintero P, Barrera F, Cabrera D, Rojas-de Santiago P, Arab JP, et al. Beneficial effects of mineralocorticoid receptor blockade in experimental non-alcoholic steatohepatitis. Liver Int 2015;35:2129-2138.

45. Suzuki E, Matsunaga T, Aonuma A, Sasaki T, Nagata K, Ohmori S. Effects of hypoxia-inducible factor-1alpha chemical stabilizer, CoCl(2) and hypoxia on gene expression of CYP3As in human fetal liver cells. Drug Metab Pharmacokinet 2012;27:398-404.

46. Wu D, Yotnda P. Induction and testing of hypoxia in cell culture. J Vis Exp 2011.

47. Sun Q, Gao W, Loughran P, Shapiro R, Fan J, Billiar TR, Scott MJ. Caspase 1 activation is protective against hepatocyte cell death by up-regulating beclin 1 protein and mitochondrial autophagy in the setting of redox stress. J Biol Chem 2013;288:15947-15958.

48. Egnatchik RA, Leamy AK, Noguchi Y, Shiota M, Young JD. Palmitate-induced activation of mitochondrial metabolism promotes oxidative stress and apoptosis in H4IIEC3 rat hepatocytes. Metabolism 2014;63:283-295.

49. Garcia-Ruiz C, Fernandez-Checa JC. Mitochondrial Oxidative Stress and Antioxidants Balance in Fatty Liver Disease. Hepatol Commun 2018;2:1425-1439.

50. Masarone M, Rosato V, Dallio M, Gravina AG, Aglitti A, Loguercio C, Federico A, et al. Role of Oxidative Stress in Pathophysiology of Nonalcoholic Fatty Liver Disease. Oxid Med Cell Longev 2018;2018:9547613.

51. He Y, Sadahiro T, Noh SI, Wang H, Todo T, Chai NN, Klein AS, et al. Flow cytometric isolation and phenotypic characterization of two subsets of ED2(+) (CD163) hepatic macrophages in rats. Hepatol Res 2009;39:1208-1218.

52. Younossi ZM. Non-alcoholic fatty liver disease - A global public health perspective. J Hepatol 2019;70:531-544.

53. Mesarwi OA, Shin MK, Bevans-Fonti S, Schlesinger C, Shaw J, Polotsky VY. Hepatocyte Hypoxia Inducible Factor-1 Mediates the Development of Liver Fibrosis in a Mouse Model of Nonalcoholic Fatty Liver Disease. PLoS One 2016;11:e0168572.

54. Chen J, Chen J, Fu H, Li Y, Wang L, Luo S, Lu H. Hypoxia exacerbates nonalcoholic fatty liver disease via the HIF-2alpha/PPARalpha pathway. Am J Physiol Endocrinol Metab 2019;317:E710-E722.

55. Kong D, Zhang F, Shao J, Wu L, Zhang X, Chen L, Lu Y, et al. Curcumin inhibits cobalt chloride-induced epithelial-to-mesenchymal transition associated with interference with TGF-beta/Smad signaling in hepatocytes. Lab Invest 2015;95:1234-1245.

56. Ricchi M, Odoardi MR, Carulli L, Anzivino C, Ballestri S, Pinetti A, Fantoni LI, et al. Differential effect of oleic and palmitic acid on lipid accumulation and apoptosis in cultured hepatocytes. J Gastroenterol Hepatol 2009;24:830-840.

57. Mylonis I, Simos G, Paraskeva E. Hypoxia-Inducible Factors and the Regulation of Lipid Metabolism. Cells 2019;8.

58. Mylonis I, Sembongi H, Befani C, Liakos P, Siniossoglou S, Simos G. Hypoxia causes triglyceride accumulation by HIF-1-mediated stimulation of lipin 1 expression. J Cell Sci 2012;125:3485-3493.

59. Jahn D, Kircher S, Hermanns HM, Geier A. Animal models of NAFLD from a hepatologist's point of view. Biochim Biophys Acta Mol Basis Dis 2019;1865:943-953.

60. Moravcova A, Cervinkova Z, Kucera O, Mezera V, Rychtrmoc D, Lotkova H. The effect of oleic and palmitic acid on induction of steatosis and cytotoxicity on rat hepatocytes in primary culture. Physiol Res 2015;64 Suppl 5:S627-636.

61. Wu J, Lin S, Wan B, Velani B, Zhu Y. Pyroptosis in Liver Disease: New Insights into Disease Mechanisms. Aging Dis 2019;10:1094-1108.

62. Mari M, Caballero F, Colell A, Morales A, Caballeria J, Fernandez A, Enrich C, et al. Mitochondrial free cholesterol loading sensitizes to TNF- and Fas-mediated steatohepatitis. Cell Metab 2006;4:185-198.

63. Dixon LJ, Flask CA, Papouchado BG, Feldstein AE, Nagy LE. Caspase-1 as a central regulator of high fat diet-induced non-alcoholic steatohepatitis. PLoS One 2013;8:e56100.

64. Tang Y, Cao G, Min X, Wang T, Sun S, Du X, Zhang W. Cathepsin B inhibition ameliorates the non-alcoholic steatohepatitis through suppressing caspase-1 activation. J Physiol Biochem 2018;74:503-510.

65. Panchanathan R, Liu H, Choubey D. Hypoxia primes human normal prostate epithelial cells and cancer cell lines for the NLRP3 and AIM2 inflammasome activation. Oncotarget 2016;7:28183-28194.

66. Guillot A, Tacke F. Liver Macrophages: Old Dogmas and New Insights. Hepatol Commun 2019;3:730-743.

67. Momen-Heravi F, Saha B, Kodys K, Catalano D, Satishchandran A, Szabo G. Increased number of circulating exosomes and their microRNA cargos are potential novel biomarkers in alcoholic hepatitis. J Transl Med 2015;13:261.

68. Wu X, Chang SC, Jin J, Gu W, Li S. NLRP3 in fl ammasome mediates chronic intermittent hypoxia-induced renal injury implication of the microRNA-155/FOXO3a signaling pathway. J Cell Physiol 2018;233:9404-9415.

69. Alegre F, Pelegrin P, Feldstein AE. Inflammasomes in Liver Fibrosis. Semin Liver Dis 2017;37:119-127.

70. Wei Q, Mu K, Li T, Zhang Y, Yang Z, Jia X, Zhao W, et al. Deregulation of the NLRP3 inflammasome in hepatic parenchymal cells during liver cancer progression. Lab Invest 2014;94:52-62.

Chapter 4

INTERMITTENT HYPOXIA INCREASES PRO-INFLAMMATORY SIGNALING AND CASPASE-1 ACTIVATION IN EXPERIMENTAL NON-ALCOHOLIC STEATOHEPATITIS

ABSTRACT

Background: Progression from isolated steatosis (IS) to non-alcoholic steatohepatitis (NASH) is a key event in the pathogenesis of non-alcoholic fatty liver disease (NAFLD). Recent observations in patients with obstructive sleep apnea syndrome (OSAS), suggest that intermittent hypoxia (IH) may contribute to disease progression. IH could play a role in hepatic inflammation but the mechanism is unclear. We investigated the effects of IH on liver injury in experimental NASH. **Methods:** C57BL6 mice were fed a choline-deficient and amino acid-defined (CDAA) diet for 22 weeks with or without IH for the last 12 weeks. Serum levels of aminotransferases, insulin and glucose were measured and hepatic steatosis and inflammation scored histologically. Hepatic triglyceride content (HTC), caspase-1 activation and hepatic mRNA levels of pro-inflammatory and inflammasome-related genes were assessed. The hepatic cells line HepG2 was used to assess the effects of chemical hypoxia induced by the HIF-1α stabilizer $CoCl_2$ in hepatic macrophages (Kupffer cells; KC). **Results:** IH increased steatosis, portal inflammation, hepatic expression of pro-inflammatory and inflammasome-related genes in the NASH model. Hepatic caspase-1 activation increased significantly with IH in CDAA-fed animals. These results correlated with the expression of pro-inflammatory genes and caspase-1 activation in hypoxic and fat-laden HepG2 cells. The silencing of HIF-1α using siRNA in HepG2 prevented the increased expression of inflammasome-related genes in KC. **Conclusion:** Hypoxia promotes steatosis, inflammation and inflammasome/caspase-1 activation in experimental NASH. The silencing of HIF-1α in hypoxic fat-laden HepG2 cells prevents inflammasome-activation in Kupffer Cells. These data identify hypoxia as a promoter of NASH in a mechanism that involves caspase-1 and HIF-1α activation. Our findings warrant further studies to understand the role of caspase-1 in NAFLD and IH-related OSAS.

1.- INTRODUCTION

Non-alcoholic fatty liver disease (NAFLD) is characterized by increased deposition of lipids in the liver in the absence of significant alcoholic intake (1,2). NAFLD is considered a serious public health problem with an estimated prevalence of 25–30% worldwide (2,3). Histologically, NAFLD encompasses a spectrum of structural and functional alterations of the liver ranging from isolated steatosis without inflammation or fibrosis to non-alcoholic steatohepatitis (NASH), which is characterized by steatosis, necro-inflammatory changes and hepatocyte cell death leading to liver

fibrosis (3). Given the morbidity and mortality associated with NASH, understanding the mechanisms underlying the development of NASH is a relevant and urgent issue.

In recent years, obstructive sleep apnea syndrome (OSAS), a common sleep disorder characterized by recurrent closure of the upper airways during sleep, has been linked to the severity of NAFLD (4,5). The most important hallmark of OSAS is the intermittent hypoxia (IH), leading to tissue hypoxia and oxidative stress, inflammation and other pathophysiological effects (6). In rodent models, IH has been linked to insulin resistance, dysregulation of hepatic lipid metabolism, mitochondrial dysfunction and hepatic steatosis and fibrosis (7-9). Interestingly, *in vitro* and *in vivo* studies have indicated a role of the transcription factor hypoxia-inducible factor 1 alpha (HIF-1α) in the accumulation of lipids in hepatocytes and the induction of pro-inflammatory and pro-fibrotic signals (10-13). However, it is still not well understood how hypoxic events of OSAS can enhance the development and/or progression of NAFLD.

The activation of the inflammasome has been reported to be a major contributor to inflammation and cell death in the development of chronic liver diseases (14-16). Specifically, the NOD-like receptor Pyrin Domains Containing 3 (NLRP3) inflammasome is composed of a sensor protein NLRP3 responsible for caspase-1 activation which triggers the maturation and secretion of the pro-inflammatory cytokine IL-1β which in turn promotes subsequent chronic inflammation-related signaling (17).

In the present study, we used a NASH model by feeding mice the choline-deficient amino acid-defined (CDAA) diet for 22 weeks and studied the effects of IH during the last 12 weeks in this model. We found that IH promoted an inflammatory phenotype that correlated with increased signaling via the inflammasome pathway. In addition, we explored whether a chemical inducer of hypoxia modulates inflammasome activation and cellular crosstalk between fat-laden hepatocytes and inflammatory cells (i.e. KCs) via the transcription factor HIF-1α. Our findings establish the role of hypoxia in the pro-inflammatory phenotype and caspase-1/inflammasome activation in the context of NAFLD.

2.-MATERIALS AND METHODS

2.1 Animals

Animal experiments were approved by the institutional animal care and use committee (Comité de ética y bienestar Animal, Escuela de Medicina, Pontificia Universidad Católica de Chile, CEBA 100623003). Male C57BL/6 mice aged 10 weeks at the beginning of the study and divided into four experimental groups (n = 4–8) receiving either choline-deficient amino acid-defined (CDAA) diet

(Catalog # 518753, Dyets Inc. Bethlehem, PA) to induce NASH or the choline-supplemented L-amino acid defined (CSAA, Catalog # 518754, Dyets Inc. Bethlehem, PA) diet as control for 22 weeks as previously described (18,19). Animals were exposed to IH or normoxia (chambers 41x22x35 cm, COY lab products™) during the last 12 weeks of the experimental or control feeding period. The regimen of IH consisted of 30 events/hour during the light phase for 8 hour/day during the rest cycle, between 9 am and 5 pm. This cycle was repeated 7 days a week for 12 consecutive weeks. After ending the study, mice were anesthetized (ketamine 60 mg/kg plus xylazine 10 mg/kg intraperitoneally) and then euthanized by exsanguination. Serum and liver tissue samples were collected and processed or stored at −80 °C until analyzed. Gene expression and protein analyses were carried out as described above.

2.2 Histological Studies

Liver specimens from the right lobe of all mouse livers were analyzed in paraformaldehyde-fixed 4 µm tissue sections stained with hematoxylin/eosin. Steatosis, inflammation and ballooning were graded blindly by an experienced pathologist (J.T.) using the NAFLD activity score (NAS) (20). Specifically, the following scores were given: Steatosis (percentage of hepatocytes containing lipid droplets) was scored as 0 (<5%), 1 (5–33%), 2 (>33–66%) and 3 (>66%). Hepatocyte ballooning was classified as 0 (none present), 1 (few) or 2 (many cells/prominent ballooning). Foci of lobular inflammation were scored as 0 (no inflammatory foci), 1 (<2 foci per 200× field), 2 (2–4 foci per 200× field) and 3 (>4 foci per 200× field). Finally, the NAFLD activity score (NAS) was computed from the grades for steatosis, inflammation and ballooning.

2.3 Biochemical determinations

Serum alanine aminotransferase (ALT) was quantified using a commercial kit from Kovalent Ltd. (Rio de Janeiro, Brazil). Serum insulin and serum glucose were quantified using a commercial ELISA kit (Merck, EZRMI-13K). Hepatic triglyceride content (HTC) was quantified using 40-50 mg of homogenized liver tissue in 1.5 ml of a $CHCl_3$/CH_3OH mixture (2:1, v/v), followed by a Folch extraction as described previously (21).

2.4 RNA isolation and quantitative real-time reverse transcription polymerase chain reaction (qRT-PCR)

Total RNA was isolated from frozen liver tissue using SV total RNA Isolation kit (Promega, Madison, WI, USA). The quantity and purity of RNA was verified using a NanoDrop ND-1000 spectrophotometer (NanoDrop Technologies, Wilmington, DE, USA) by measuring absorbance at 260 and 280 nm. The cDNA synthesis was performed with 1.0 µg of RNA using the ImProm-II ™ reverse

transcription system (Promega, Madison, WI, USA). Real-Time qPCR was carried out in a StepOnePlus™ (96-well) PCR System (Applied Biosystems, Thermofisher) using Taqman probes obtained from ThermoFisher Scientific (Applied Biosystems ™ TaqMan® Gene Expression Assays). mRNA levels were normalized to the housekeeping gene 18S and further normalized to the mean expression level of the control group. Relative gene expression was calculated using the ΔCt method. The sequences of the probes and primer sets are described in the Supplementary Material.

2.5 Caspase-1 activity

Liver tissue or cell lysate were assayed for caspase-1 activity by their ability to cleave a fluorescent CASP-1 substrate, following the manufacturer's instructions (Abcam, USA).

2.6 Western Blot analyses

Hepatic tissue samples were lysed with a commercial kit of RIPA Buffer (Cell Signaling Technology, 9806S). Total amount of protein in lysates was measured by Bio-Rad protein assay (Bio-Rad; Hercules, CA, USA). For Western blot, 30-50 µg protein was resolved on Mini-PROTEAN® TGX Stain-Free™ Precast Gels (BioRad, UK, Oxford). Semi dry-blotting was performed using Trans-Blot Turbo Midi Nitrocellulose Membrane with Trans-Blot Turbo System Transfer (BioRad, UK, Oxford). Ponceau S 0.1% w/v (Sigma) staining was used to confirm protein transfer. Monoclonal mouse anti-CASP1 1:500 (Santa Cruz, INC) was used in combination with appropriate peroxidase-conjugated secondary antibodies. Monoclonal mouse anti-tubulin was used as loading controls (Sigma, USA).The blots were analyzed in a ChemiDoc XRS system (BioRad, Hercules, CA, USA). Protein band intensities were quantified by ImageLab software (BioRad, Hercules, CA, USA).

2.7 Treatment with free fatty acids and chemical hypoxia induction in human hepatocellular carcinoma cell line

In order to assess the effect of hypoxia in fat-laden liver cells, the human hepatocellular carcinoma cell line HepG2 (ATCC, USA) was cultured in Dulbecco's modified Eagle medium (1X) + GlutaMAX™- I (DMEM, 10569010, Gibco) supplemented with 10% fetal bovine serum (FBS; Gibco) and 1% penicillin-streptomycin (Gibco) at 37°C and 5% CO_2. All cells were plated in a cell culture plate at least 24h -36h before treatment. Upon reaching 80% confluency, the cells were incubated with a mixture of free fatty acids (FFA) consisting of oleic acid (500 µmol/L) and palmitic acid (250 µmol/L) in an aqueous solution of bovine serum albumin (BSA) as described previously (22). Incubations were carried out with or without Cobalt(II) chloride ($CoCl_2$; Sigma Aldrich) (200 µmol/L) for 24 hours to induce chemical hypoxia (23). $CoCl_2$ is a well-known hypoxia-mimetic agent by stabilization of hypoxia-inducible factor (HIF)-1α (24). Control cells were treated with BSA alone.

2.8 Kupffer cell isolation

Kupffer cells (KC) were isolated from the non-parenchymal cell fraction obtained during hepatocyte isolation. The supernatant was subjected to different low-speed centrifugation steps at 4°C and the final cell pellet resuspended in Hank's Balanced Salt Solution (HBSS) (Gibco, California, USA) supplemented with 0.3% bovine serum albumin (BSA). KC were purified using the 20% density gradient medium OptiPrepTM (Sigma-Aldrich). After different low-speed centrifugations, the final pellet was resuspended in HBSS supplemented with 10% FBS and seeded on tissue culture plastic to allow cells to attach. After the attachment period, KC were cultured in William's E medium supplemented with 50 µg/ml of gentamycin, 10% FBS and 1% of p/s/f for 18 hours until the start of the experiments.

2.9 Transfection of HepG2 cell line with HIF-1α small interfering RNA or control small interfering RNA

HepG2 cells were grown to approximately 60% confluency in 6-well plates before transfection and treatments. Small interfering RNA (esiRNA) was employed to silence HIF-1α in HepG2 cells (EHU151981, Sigma-Aldrich) using standard Lipofectamine (Lipo3000, Invitrogen) in OPTI-MEM™ I medium at a final concentration of 100 nmol/L according to the manufacturer's protocol. Cells were transfected with EGFP siRNA as control (EHUEGFP, Sigma-Aldrich). Experiments were performed after 24 hours of transfection for 24 hours. The efficiency of transfection was determined by quantitative RT-PCR and Western blot for HIF-1α (Supplementary Material). To obtain the corresponding conditioned medium (CM), hepatocyte culture medium was replaced by FBS-free medium after treatment for an additional 24 hours. CM from different treatments were added to KC for 24 hours.

2.10 Statistical Analyses

Analyses were performed using GraphPad software (version 5.03, GraphPad Software Inc., CA, USA). All results are presented as a mean of at least 3 independent experiments ± SEM or as absolute number or percentage for categorical variables. The statistical significance of differences between the means of the experimental groups was evaluated using one-way analysis of variance (ANOVA) with a post-hoc Bonferroni multiple-comparison test; $P<0.05$ was considered as statistically significant.

3.- RESULTS

3.1 Intermittent hypoxia promotes portal inflammation in CDAA diet-fed mice: To investigate the effect of IH on animals with NASH, we used C57BL/6J male mice fed the CDAA-diet for 22 weeks as model of NASH. IH was applied during the last 12 weeks. As presented in Fig. 1a, IH did neither increase VAT weight in the control group nor in the CDAA-fed group. In contrast, the CDAA-diet increased VAT weight both in the IH group as well as in the non-IH group. The CDAA-diet also increased insulin level, but only in the IH group. There were no significant differences in body weight, liver weight, glycemia, and ALT between the different groups. As expected, steatosis, ballooning, portal inflammation and hepatic TG content increased in CDAA diet-fed mice compared to both control and hypoxia groups. Interestingly, liver histology showed more steatosis and portal inflammation in CDAA diet-fed mice exposed to IH compared to all other groups. In addition, CDAA diet-fed mice exposed to IH increased significantly hepatic TG compared to control animals. Finally, NAS score increased significantly in CDAA diet-fed mice and CDAA diet-fed mice exposed to IH compared to control. These results confirm that hypoxia promotes liver steatosis, but does not correlate with hepatic TG content. Moreover hypoxia aggravated portal inflammation in the animal model of NASH.

a)

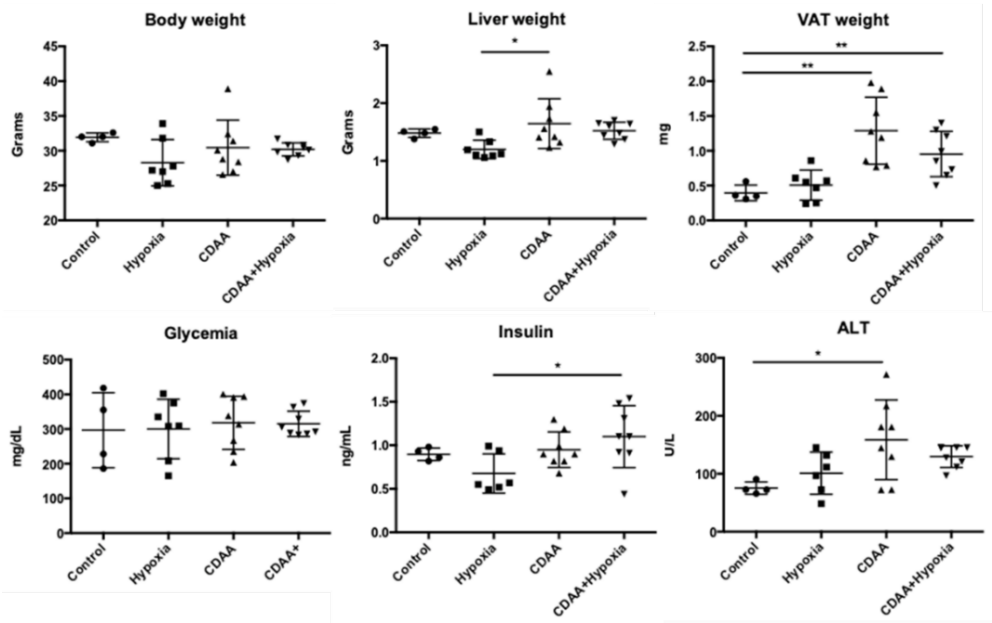

b)

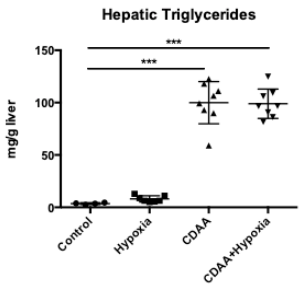

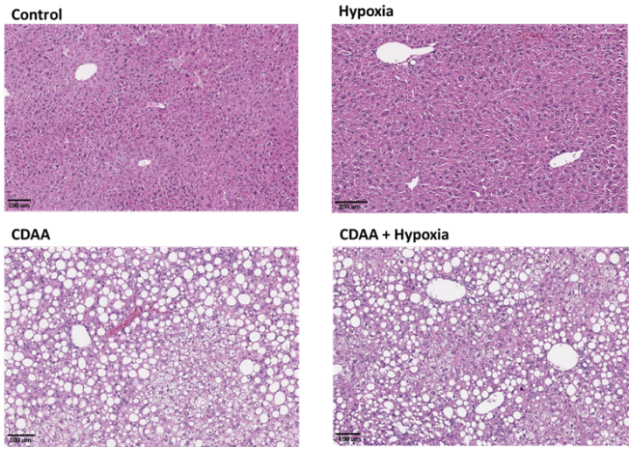

	Control	Hypoxia	CDAA	CDAA+ Hypoxia
Steatosis	0±0	0.5±0.2	1.2±0.1 [b,c]	1.7±0.1 [b,d,e]
Ballooning	0±0	0.4±0.2	1.4±0.2 [b,c]	0.9±0.1 [a]
Portal Inflammation	0±0	0.2±0.1	1.2±0.2 [b,c]	2.0±0.2 [b,d,e]
NAS	0±0	1.1±0.5	5.1±0.5 [b,d]	6.4±0.4 [b,d]

Figure 1. Intermittent Hypoxia promotes steatosis and portal inflammation in CDAA diet-fed mice. The mice were placed on choline-supplemented L-amino acid defined (CSAA) diet as control, or choline deficient L-amino acid defined diet (CDAA) for 22 weeks to induce liver injury and intermittent hypoxia (IH) or normoxia was applied for the last 12 weeks of the diet as described in Materials and Methods. A. Body weight; Liver Weight; Visceral Adipose Tissue (VAT) weight; Glycemia; Insulin; Alanine aminotransferase (ALT) B. Histology of liver tissue (Hematoxilin/eosin staining); Hepatic Triglycerides content and NAFLD activity score (NAS). Hematoxilin/eosin liver samples were analyzed in a double blind manner by a pathologist for steatosis, inflammation, ballooning and determination of NAS. Representative histology of hematoxilin/eosin staining of liver samples from differents mice groups. Values represent mean ± SEM (n= 4-8). Statistical significance was evaluated using ANOVA with a post-hoc Bonferroni multiple-comparison test (*$p \leq 0.05$; **$p \leq 0.01$; **$p \leq 0.005$). "a" $P<0.01$ and "b" $P<0.001$ represents statistical significance when comparing Control to CDAA or CDAA+Hypoxia groups. "c" $P<0.01$ and "d" $P<0.001$ represents statistical significance when comparing Hypoxia to CDAA or CDAA+Hypoxia groups. "e" $P<0.05$ represents statistical significance when comparing CDAA to CDAA+Hypoxia group.

3.2 Intermittent hypoxia increases pro-inflammatory cytokines and inflammasome components in mice with NASH: To determine the effect of hypoxia on mice with NASH, pro-inflammatory gene expression was measured in liver tissue by RT-qPCR. HIF-1α was determined to confirm the induction of hypoxia. As expected, HIF-1α expression was increased in both groups exposed to IH (Fig.2). Next, tumor necrosis factor-α (TNF-α), interleukin-6 (IL-6) and interferon-γ (IFN-γ) were analyzed (Fig.2).

TNF-α tended to increase in CDAA diet-fed mice independent of IH exposure, but the difference was not statistically significant. IL-6 and IFN-γ gene expression was significantly increased in CDAA diet-fed mice exposed to IH compared to all other groups. We also studied gene expression of the inflammasome components interleukin-1β (IL-1β), interleukin-18 (IL-18), NLRP-3 and caspase-1 in liver tissue by RT-qPCR (Fig.3). Interestingly, IL-1β, NLRP-3 and caspase-1 increased in CDAA diet-fed animals exposed to IH compared to the control and hypoxia groups and IL-18 increased in CDAA diet-fed mice exposed to IH compared to the CDAA and hypoxia groups. These data suggest that hypoxia promotes a pro-inflammatory phenotype, including inflammasome activation in mice with NASH.

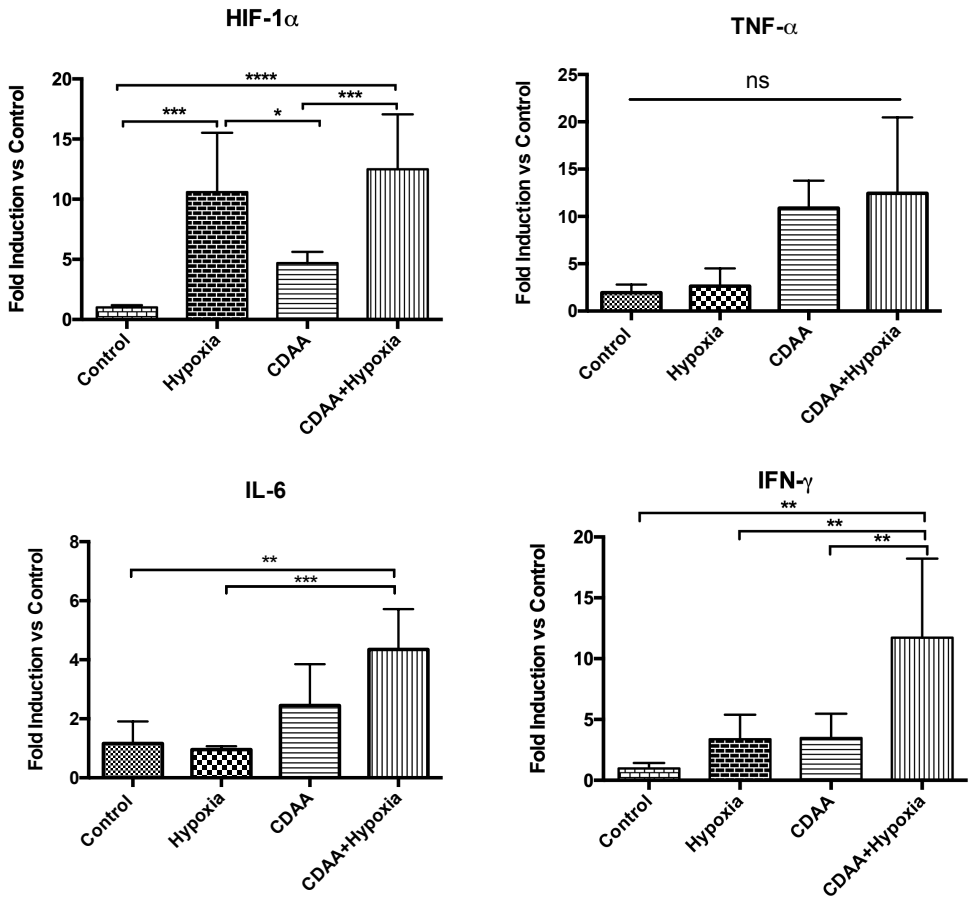

Figure 2. Intermittent hypoxia in mice with CDAA-induced liver injury increases the expression of pro-inflammatory genes. The mice were placed on choline-supplemented L-amino acid defined (CSAA) diet as control or choline deficient L-amino acid defined diet (CDAA) for 22 weeks to induce liver injury and intermittent hypoxia (IH) or normoxia was applied for the last 12 weeks of the diet as described in Materials and Methods. mRNA levels of HIF-1α, TNF-α, IL-6 and IFN-γ were measured as described in Materials and Methods. Data were shown as mean ± SEM (n ≥ 3) *indicates P < 0.05; **indicates P < 0.01; *** indicates P < 0.005; **** indicates P < 0.001.

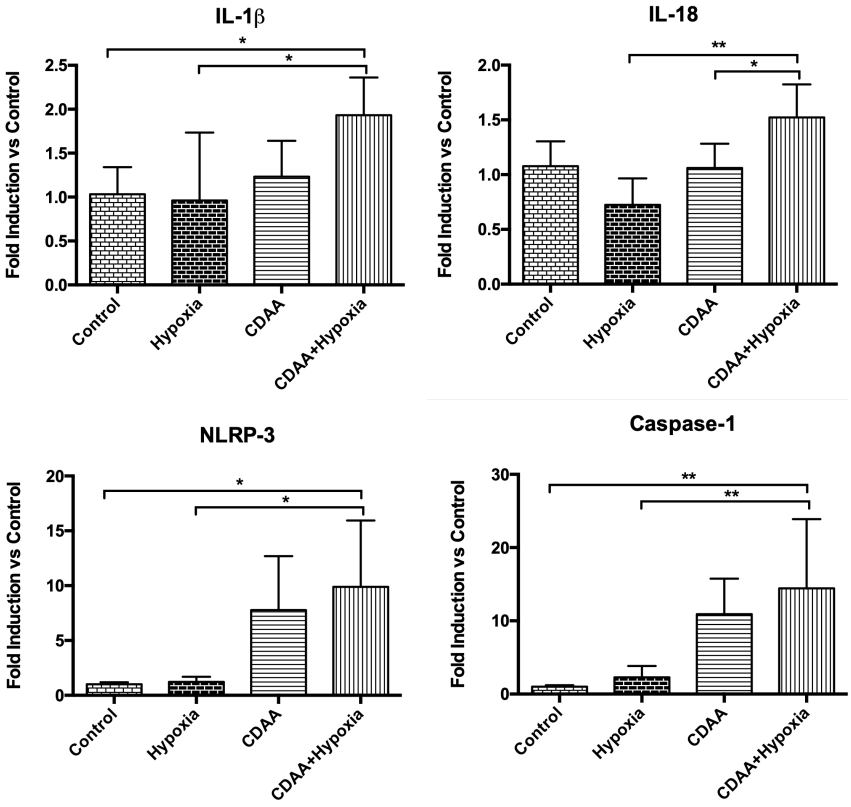

Figure 3. Intermittent hypoxia in mice with CDAA-induced liver injury increases the expression of inflammasome components. The mice were placed on choline-supplemented L-amino acid defined (CSAA) diet as control or choline-deficient, L-amino acid defined (CDAA) diet for 22 weeks to induce liver injury and intermittent hypoxia (IH) or normoxia was applied for the last 12 weeks of the diet as described in Materials and Methods. mRNA levels of IL-1β, IL-18, NLRP3 and caspase-1 were measured as described in Materials and Methods. Data were shown as mean ± SEM (n ≥ 3) *indicates $P < 0.05$; **indicates $P < 0.01$.

3.3 Intermittent hypoxia increases and activates caspase-1 protein in animals with NASH: To evaluate inflammasome activation, we determinated the level of cleaved caspase-1 in liver samples by Western blot and caspase-1 activity assay as described in Materials and Methods. We observed a significantly increased protein level of cleaved caspase-1 (Casp-1 p20) compared to all other groups (Fig.4a). Moreover, caspase-1 activity in liver samples was increased in animals with NASH exposed to IH compared to the control group (Fig. 4b). Taken together, these results confirm that hypoxia aggravates inflammation in an *in vivo* model of NASH by inflammasome activation and activation of caspase-1.

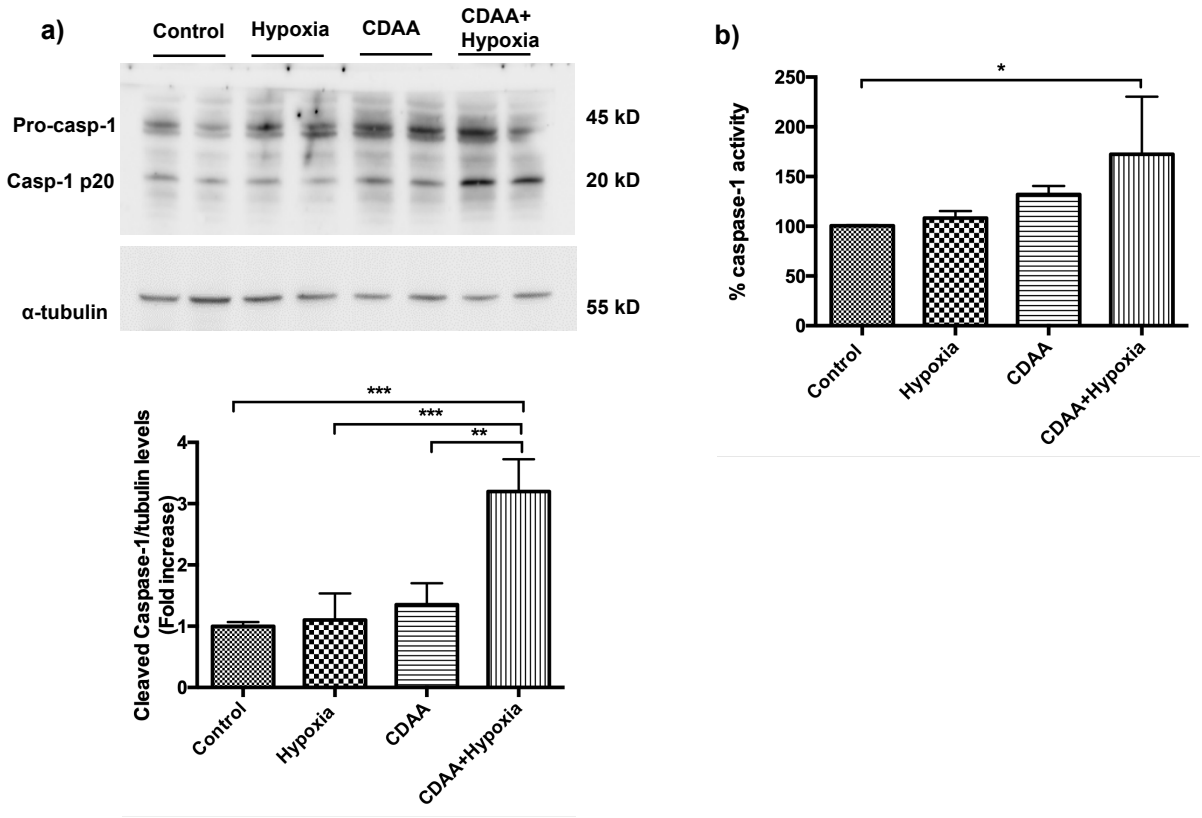

Figure 4. Intermittent hypoxia in mice with CDAA-induced liver injury increases a) caspase-1 protein levels and b) caspase-1 activity in the liver. Protein levels of pro-caspase-1 and cleaved caspase-1 (p10 and p20) were determined by Western blot as described in Materials and Methods. α-Tubulin was used as loading control. The total amount of p20 caspase-1 was calculated to determine the generation of cleaved caspase-1. Data were shown as mean ± SEM (n ≥ 3) *indicates P < 0.05; **indicates P < 0.01; *** indicates P < 0.005.

3.4 Hypoxia increases expression of pro-inflammatory genes and inflammasome/caspase-1 levels in an in vitro model of NASH: To further characterize our findings in the *in vivo* model of NASH, we evaluated whether the HIF-1α stabilizer $CoCl_2$ increases the expression of inflammatory genes and inflammasome components in fat-laden liver cells. HepG2 cells were treated with $CoCl_2$ and FFAs to mimick hypoxia and steatosis *in vitro* as described in Materials and Methods. Figure 5 shows that hypoxia increased expression of pro-inflammatory genes like TNF-α and IFN-γ in fat-laden HepG2 cells. Furthermore, $CoCl_2$ increased expression of inflammasome components like IL-1β, IL-18, NLRP3 and Caspase-1, in fat-laden HepG2 cells. Finally, inflammasome activation was determined by measuring cleaved caspase-1 levels in HepG2 cells by Western blot as well as caspase-1 activity. The increased protein level of cleaved caspase-1 (Fig. 6a) and increased caspase-1 activity (Fig.6b) confirmed that the HIF-1α stabilizer $CoCl_2$ could promote inflammasome activation in fat-laden HepG2 cells.

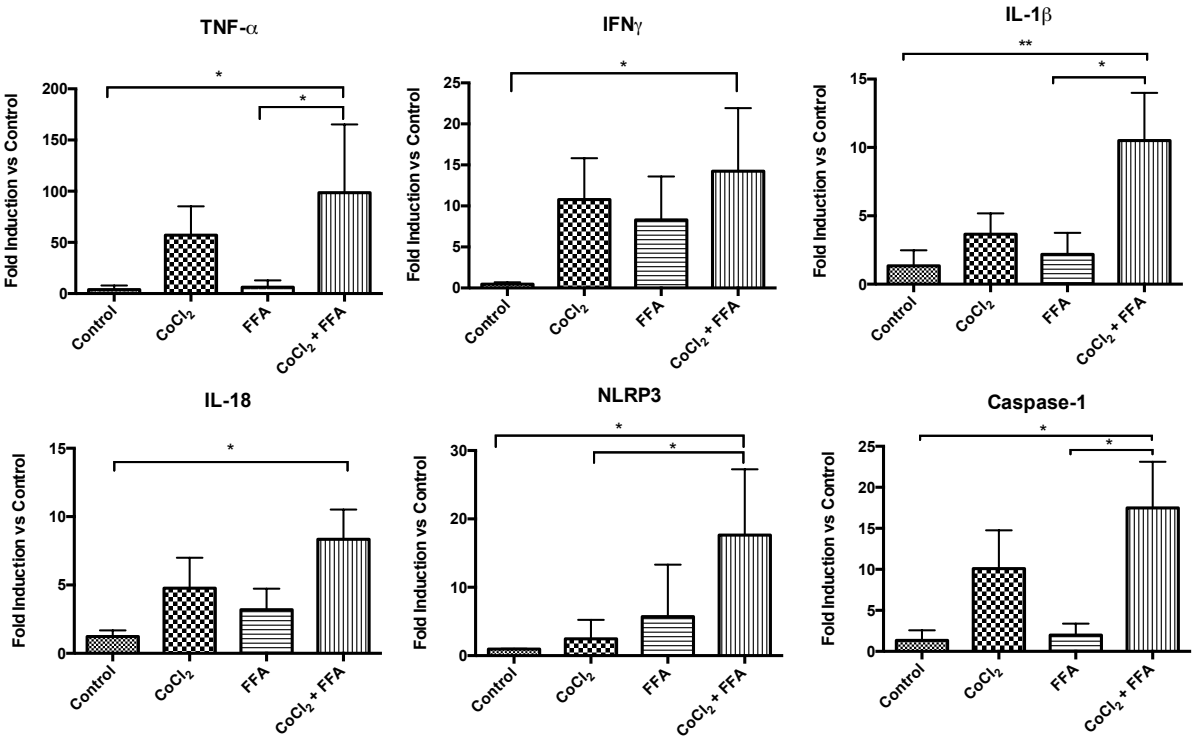

Figure 5. Hypoxia increases the expression of pro-inflammatory genes and inflammasome components in an *in vitro* model of NASH. HepG2 cells were incubated for 24h with oleic acid and palmitic acid (2:1 ratio) (FFA) in the presence or absence of $CoCl_2$ 200 µmol/L. mRNA levels of TNF-α IFN-γ, IL-1β, IL-18, NLRP3 and Caspase-1 were measured as described in Materials and Methods. Data were shown as mean ± SEM (n ≥ 3) * indicates P < 0.05; **indicates P < 0.01.

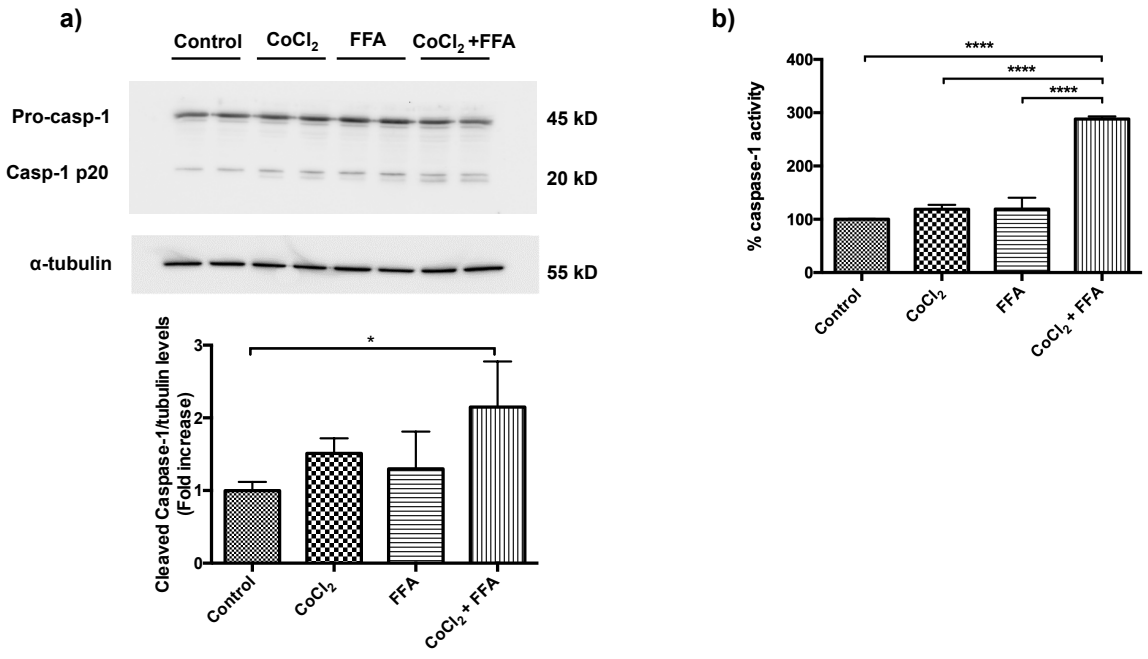

Figure 6. Hypoxia increases inflammasome caspase-1 level in an *in vitro* model of NASH a) protein levels of pro-caspase-1 and cleaved caspase-1. b) activity of caspase-1. HepG2 cells were incubated for 24h with oleic acid and palmitic acid (2:1 ratio) (FFA) in the presence or absence of $CoCl_2$ 200 µmol/L. Protein levels of pro-caspase-1 and cleaved caspase-1 (p20) were determined by Western blot as described in Materials and Methods. α-Tubulin was used as loading control. Total p20 caspase-1 was calculated to determine the generation of cleaved caspase-1. Data were shown as mean ± SEM (n ≥ 3) * indicates P < 0.05; **** indicates P < 0.001.

3.5 Silencing of HIF-1α in hypoxic and fat-laden HepG2 prevents inflammasome activation in hepatic macrophages: To explore whether hypoxic and fat-laden HepG2 cells can increase expression of inflammasome-related genes in hepatic resident macrophages, we isolated primary rat Kupffer cells (KC) and investigated whether inflammasome activation in KCs depends on HIF-1α in fat-laden hepatocytes. Conditioned medium from steatotic HepG2 cells treated with $CoCl_2$ increased mRNA levels of NLRP3, Apoptosis-Associated Speck-Like Protein Containing CARD (ASC), Caspase-1 and IL-1β in KC. The increase of these genes was abolished by HIF-1α knock-down in steatotic HepG2 cells treated with $CoCl_2$ (Figure 7). Taken together, our results suggest a cellular crosstalk between hepatocytes and macrophages in hypoxia, which is dependent on HIF-1α activation in hepatocytes, that promotes a inflammatory phenoptype in NASH thought inflammasome activation.

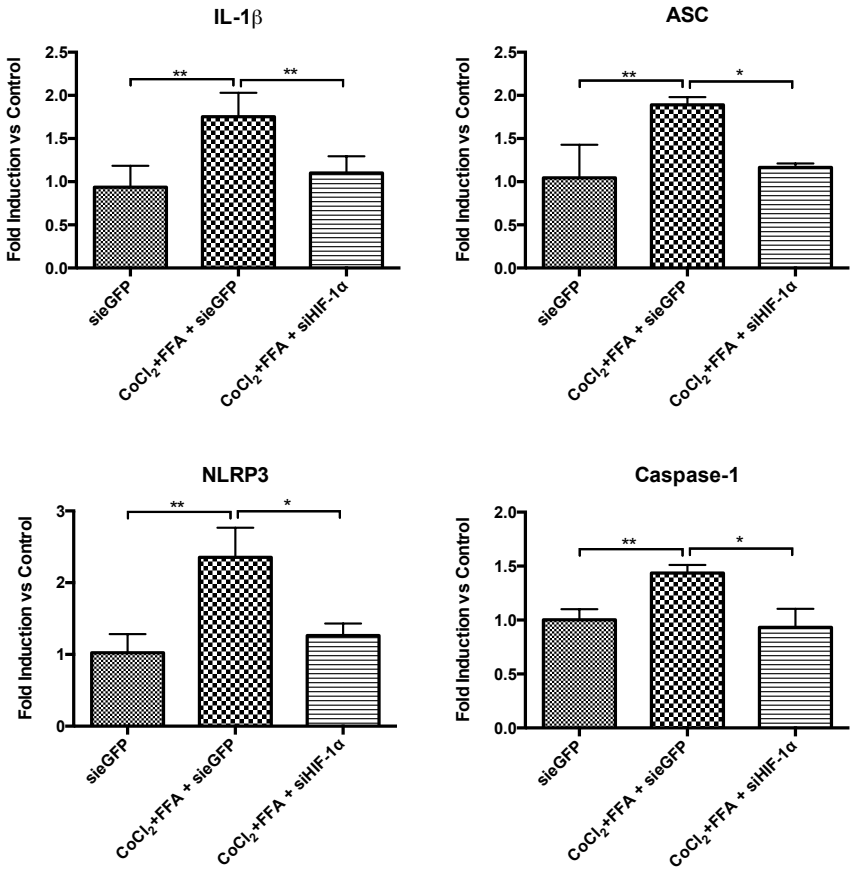

Figure 7. Silencing of HIF-1α prevents inflammasome activation in hepatic macrophages. Culture medium of hypoxic fat-laden HepG2 cells transfected with negative control siRNA (sieGFP) or HIF-1α siRNA (siHIF-1α) was replaced after 24 hours of treatment by fresh medium without FFA and $CoCl_2$. Cells were cultured for another 24 hours and the conditioned medium (CM) was collected. Kupffer cells were treated for 24 hours with CM from HepG2 cells. mRNA levels of IL-1β, ASC, NLRP3 and Caspase-1 were measured as described in Materials and Methods. Data were shown as mean ± SEM ($n \geq 3$) * indicates $P < 0.05$; ** indicates $P < 0.01$.

4.- DISCUSSION

The present study demonstrates that intermittent hypoxia (IH) promotes a pro-inflammatory phenotype, portal inflammation and activation of the inflammasome in the CDAA diet model of NASH. Moreover, we established an association between HIF-1α and caspase-1/inflammasome activation in an *in vitro* model of hypoxia and steatosis that involves crosstalk between hepatocytes and Kupffer cells (KC). These results demonstrate for the first time a link between hypoxia and inflammasome activation as a possible mechanism in the progression of NAFLD.

Our *in vivo* study in mice fed a CDAA-diet showed a significant increase in levels of serum ALT and hepatic TG compared to animals fed a normal diet as described previously (19,25). IH did not induce a significant increase in serum ALT and hepatic TG in mice on a CDAA diet compare to normoxic CDAA-diet fed mice. However, liver histology showed more steatosis in CDAA-diet fed animals subjected to IH compared to normoxic CDAA-diet fed animals. This is in line with another study that demonstrated that IH induced the expression of genes related to hepatic lipid biosynthesis, but does not exacerbate the pre-existing hyperlipidemia and metabolic disturbances in a model of fatty liver (26). A possible explanation is that steatosis not only involves the accumulation of triglycerides, but also other types of lipids such as cholesterol (27). Future studies, such as the use of a high fat diet in an animal model, will be necessary to verify the effect of hypoxia in a NASH model with less liver damage.

Histological examination showed more portal inflammation in CDAA diet-fed mice exposed to IH compared to all other groups. Also, NAS scores were significantly increased in CDAA diet-fed mice and CDAA diet-fed mice exposed to IH compared to control groups. These results suggest that hypoxia can promote steatosis and portal inflammation in an animal model of NASH. A recent study showed that hepatocytes accumulation of oxidized lipids, specifically low-density lipoproteins, promotes portal inflammation and activation of Kupffer cells, triggering an inflammatory response in fatty liver (28). Therefore, we analyzed the expression of pro-inflammatory cytokines and inflammasome components in our *in vivo* model. We demonstrated a significant increase in the

hepatic mRNA expression of the pro-inflammatory cytokines IL-6 and IFN-γ in the CDAA-fed diet group exposed to IH compared to all others groups. In addition, we observed that IH further increased hepatic mRNA expression of inflammasome components in the CDAA-fed diet group compared to the control group. These findings, in the context of hypoxia, are consistent with previous studies that demonstrated a correlation between inflammasome activation and liver inflammation and fibrosis (19,25,29). NLRP3 inflammasome activation drives the cleavage and activation of caspase-1 resulting in maturation of effector pro-inflammatory cytokines such as pro-IL-1β and pro-IL-18 (30). IL-1β is one of the key factors in the maintenance and progression of the inflammatory and fibrogenic phenotype in advanced stages of NASH (25,31).

In the present study, we also analyzed the hepatic protein levels of active caspase-1 to corroborate our findings on the gene expression levels of inflammasome components. We observed significantly increased protein levels of caspase-1 and increased caspase-1 activity in hypoxic CDAA-diet fed mice. Based on our results on the role of the inflammasome/caspase-1 activation in inflammatory signaling in the liver during hypoxia, the role of HIF-1α in the pro-inflammatory phenotype and caspase-1 activation in an *in vitro* model of steatosis was investigated in more detail. Fat-ladenHepG2 cells treated with $CoCl_2$, which stabilizes the HIF-1α protein, showed a significant increase in the gene expression of various pro-inflammatory cytokines compared to steatotic HepG2 or non-treated cells. In addition, gene expression of inflammasome components in fat-laden HepG2 cells treated with $CoCl_2$ was increased compared to the control groups and this increase correlated with increased protein levels and activity of caspase-1. These results are in line with our previous study in primary rat-hepatocytes where we demonstrated that hypoxia induces NLRP3 inflammasome-associated caspase-1 activation and increased cell death, contributing to a pro-inflammatory phenotype in KC (32). We also demonstrated cellular cross-talk between hepatocytes and Kupffer cells: conditioned medium from fat-laden hepatocytes treated with $CoCl_2$ increased the gene expression of inflammasome components and the inflammatory phenotype of KCs. This effect is dependent on intact HIF1α signaling in hepatocytes as shown by experiments in which HIF1α was genetically silenced. Our interpretation of these findings is that hypoxia promotes an inflammatory phenotype in steatotic hepatocytes and, via intercellular communication between hepatocytes and non-parenchymal cells, also a pro-inflammatory phenotype in Kupffer cells, which contributes to the pathogenesis of NAFLD. In line with this, several studies suggested that KC drive inflammasome activation although in these studies the modulating role of hypoxia remained unexplored (28,33-35). These novel findings are supported by a recent *in vivo* study in which HIF-1α was demonstrated to be an important regulator of macrophage-dependent hepatic injury, suggesting that HIF-1α may be a novel therapeutic target for the treatment of chronic liver disease (36). Furthermore, a paracrine

mechanism has recently been described involving the activation of KC by factors released from damaged hepatocytes, creating a feedback loop amplifying inflammasome activation of hepatocytes and hepatic inflammation and injury (37).

In summary, our findings demonstrate that hypoxia plays a crucial role in exarcerbating steatosis, inflammasome activation and inflammation in NASH. Furthermore, our *in vitro* results demonstrate that this aggravating effect of hypoxia may be due to increased, HIF-1α dependent, inflammasome and caspase-1 activation in Kupffer cells.

5.- REFERENCES

1. Bedossa P. Pathology of non-alcoholic fatty liver disease. Liver Int 2017;37:85-89.
2. Younossi ZM, Koenig AB, Abdelatif D, Fazel Y, Henry L, Wymer M. Global epidemiology of nonalcoholic fatty liver disease-Meta-analytic assessment of prevalence, incidence, and outcomes. Hepatology 2016;64:73-84.
3. Arab JP, Arrese M, Trauner M. Recent insights into the pathogenesis of non-alcoholic fatty liver disease. Annual Review of Pathology Mechanisms of Disease 2018 13: 321-350
4. Agrawal S, Duseja A, Aggarwal A, Das A, Mehta M, Dhiman RK, Chawla Y. Obstructive sleep apnea is an important predictor of hepatic fibrosis in patients with nonalcoholic fatty liver disease in a tertiary care center. Hepatol Int 2015;9:283-291.
5. Mesarwi OA, Loomba R, Malhotra A. Obstructive Sleep Apnea, Hypoxia, and Nonalcoholic Fatty Liver Disease. Am J Respir Crit Care Med. 2019;199:830-841
6. Drager LF, Lopes HF, Maki-Nunes C, Trombetta IC, Toschi-Dias E, Alves MJ, Fraga RF, Jun JC, Negrão CE, Krieger EM, Polotsky VY, Lorenzi-Filho G.The impact of obstructive sleep apnea on metabolic and inflammatory markers in consecutive patients with metabolic syndrome. PLoS One 2010 11; 5:e12065
7. Savransky V, Nanayakkara A, Vivero A, Li J, Bevans S, Smith PL, Torbenson MS, et al. Chronic intermittent hypoxia predisposes to liver injury. Hepatology 2007;45:1007-1013.
8. Savransky V, Reinke C, Jun J, Bevans-Fonti S, Nanayakkara A, Li J, Myers AC, et al. Chronic intermittent hypoxia and acetaminophen induce synergistic liver injury in mice. Exp Physiol 2009;94:228-239.
9. Drager LF, Li J, Reinke C, Bevans-Fonti S, Jun JC, Polotsky VY. Intermittent hypoxia exacerbates metabolic effects of diet-induced obesity. Obesity (Silver Spring) 2011;19:2167-2174.
10. Liu Y, Ma Z, Zhao C, Wang Y, Wu G, Xiao J, McClain CJ, et al. HIF-1alpha and HIF-2alpha are critically involved in hypoxia-induced lipid accumulation in hepatocytes through reducing PGC-1alpha-mediated fatty acid beta-oxidation. Toxicol Lett 2014;226:117-123.

11. Mesarwi OA, Shin MK, Bevans-Fonti S, Schlesinger C, Shaw J, Polotsky VY. Hepatocyte Hypoxia Inducible Factor-1 Mediates the Development of Liver Fibrosis in a Mouse Model of Nonalcoholic Fatty Liver Disease. PLoS One. 2016;11:e0168572.
12. Briancon-Marjollet A, Monneret D, Henri M, Joyeux-Faure M, Totoson P, Cachot S, Faure P, et al. Intermittent hypoxia in obese Zucker rats: cardiometabolic and inflammatory effects. Exp Physiol 2016;101:1432-1442.
13. Kang HH, Kim IK, Lee HI, Joo H, Lim JU, Lee J, Lee SH, et al. Chronic intermittent hypoxia induces liver fibrosis in mice with diet-induced obesity via TLR4/MyD88/MAPK/NF-kB signaling pathways. Biochem Biophys Res Commun 2017;490:349-355.
14. Wan X, Xu C, Yu C, Li Y. Role of NLRP3 Inflammasome in the Progression of NAFLD to NASH. Can J Gastroenterol Hepatol. 2016;2016:6489012.
15. Alegre F, Pelegrin P, Feldstein AE. Inflammasomes in Liver Fibrosis. Semin Liver Dis 2017;3:119-127.
16. Luan J, Ju D. Inflammasome: A Double-Edged Sword in Liver Diseases. Front Immunol. 2018;9:2201.
17. Guo H, Callaway JB, Ting JP. Inflammasomes: mechanism of action, role in disease, and therapeutics. Nat Med. 2015;21677-87
18. Pizarro M, Solis N, Quintero P, Barrera F, Cabrera D, Rojas-de Santiago P, Arab JP, et al. Beneficial effects of mineralocorticoid receptor blockade in experimental non-alcoholic steatohepatitis. Liver Int 2015;35:2129-2138.
19. Cabrera D, Wree A, Povero D, Solís N, Hernandez A, Pizarro M, Moshage H, Torres J, Feldstein AE, Cabello-Verrugio C, Brandan E, Barrera F, Arab JP, Arrese M. Andrographolide Ameliorates Inflammation and Fibrogenesis and Attenuates Inflammasome Activation in Experimental Non-Alcoholic Steatohepatitis. Sci Rep 2017;7:3491.
20. Kleiner, D. E. et al. Design and validation of a histological scoring system for nonalcoholic fatty liver disease. Hepatology 2005; 41:1313–1321
21. Carr TP, Andresen CJ, Rudel LL. Enzymatic determination of triglyceride, free cholesterol, and total cholesterol in tissue lipid extracts. Clin Biochem 1993; 26: 39–42.
22. Chavez-Tapia NC, Rosso N, Tiribelli C. In vitro models for the study of non-alcoholic fatty liver disease. Curr Med Chem 2011;18:1079-1084.
23. Pecoraro M, Pinto A, Popolo A. Inhibition of Connexin 43 translocation on mitochondria accelerates CoCl2-induced apoptotic response in a chemical model of hypoxia. Toxicol In Vitro 2018;47:120-128.
24. Munoz-Sanchez J, Chanez-Cardenas ME. The use of cobalt chloride as a chemical hypoxia model. J Appl Toxicol 2019;39:556-570.

25. Wree A, McGeough MD, Peña CA, Schlattjan M, Li H, Inzaugarat ME, Messer K, Canbay A, Hoffman HM, Feldstein AE. NLRP3 inflammasome activation is required for fibrosis development in NAFLD. J Mol Med (Berl). 2014;92:1069-82.
26. Li, J., et al., Intermittent hypoxia induces hyperlipidemia in lean mice.Circ Res 2005; 97:698-706
27. Ioannou GN, Haigh WG, Thorning D, Savard C. Hepatic cholesterol crystals and crown-like structures distinguish NASH from simple steatosis. J Lipid Res. 2013;54:1326-34.
28. Ho CM, Ho SL, Jeng YM, Lai YS, Chen YH, Lu SC, Chen HL, Chang PY, Hu RH, Lee PH. Accumulation of free cholesterol and oxidized low-density lipoprotein is associated with portal inflammation and fibrosis in nonalcoholic fatty liver disease. J Inflamm (Lond) 2019;16:7.
29. Miura K, Yang L, van Rooijen N, Brenner DA, Ohnishi H, Seki E. Toll-like receptor 2 and palmitic acid cooperatively contribute to the development of nonalcoholic steatohepatitis through inflammasome activation in mice. Hepatology 2013; 57:577-89.
30. Strowig T, Henao-Mejia J, Elinav E, Flavell R. Inflammasomes in health and disease. Nature 2012; 481:278-86.
31. Mridha AR, Wree A, Robertson AAB, Yeh MM, Johnson CD, Van Rooyen DM, Haczeyni F, Teoh NC, Savard C, Ioannou GN, Masters SL, Schroder K, Cooper MA, Feldstein AE, Farrell GC. NLRP3 inflammasome blockade reduces liver inflammation and fibrosis in experimental NASH in mice. J Hepatol. 2017;66:1037-1046.
32. Hernandez A. Geng Y, Sepulveda R, Solis N, Torres, J, et al. Chemical Hypoxia induces pro-inflammatory signals in fat-laden hepatocytes and contributes to cellular crosstalk with Kupffer cells. Molecular Basis of Disease, Nov 2019 Submitted
33. Dixon L, Berk M, Thapaliya S, Papouchado B, Feldstein A. Caspase 1-mediated regulation of fibrogenesis in diet-induced steatohepatitis. Lab Invest. 2012; 92: 713–723.
34. Bieghs V, Walenbergh SM, Hendrikx T, et al. Trapping of oxidized LDL in lysosomes of Kupffer cells is a trigger for hepatic inflammation. Liver Int 2013;33:1056–1061.
35. Zhang J, Zhang K, Li Z, Guo B. ER Stress-induced Inflammasome Activation Contributes to Hepatic Inflammation and Steatosis. J Clin Cell Immunol. 2016;7: 457.
36. Copple BL, Kaska S, Wentling C. Hypoxia-inducible factor activation in myeloid cells contributes to the development of liver fibrosis in cholestatic mice. Pharmacol Exp Ther 2012; 341:307-16.
37. Zhang LY, Zhan DL, Chen YY, Wang WH, He CY, Lin Y, Lin YC, Lin ZN. Aflatoxin B1 enhances pyroptosis of hepatocytes and activation of Kupffer cells to promote liver inflammatory injury via dephosphorylation of cyclooxygenase-2: an in vitro, ex vivo and in vivo study. Arch Toxicol. 2019; 14.

Chapter 5

EXTRACELLULAR VESICLES DERIVED FROM FAT LADEN HYPOXIC HEPATOCYTES PROMOTE A PRO-FIBROTIC PHENOTYPE IN HEPATIC STELLATE CELLS

ABSTRACT

Background: Transition from steatosis to non-alcoholic steatohepatitis (NASH) is a key issue in Non-alcoholic fatty liver disease (NAFLD). Observations in patients with obstructive sleep apnea syndrome (OSAS), suggest that hypoxia contributes to progression to NASH and liver fibrosis and the release of extracellular vesicles (EV) by injured hepatocytes has been implicated in NAFLD progression. **Aim:** to evaluate the effects of hypoxia on pro-fibrotic response and the release of EV in NAFLD and to assess cellular crosstalk between hepatocytes and human hepatic stellate cells (LX-2). **Methods:** HepG2 cells were treated with free fatty acids and subjected to chemically-induced hypoxia (CH) using the hypoxia-inducible factor-1alpha (HIF-1α) stabilizer cobalt chloride ($CoCl_2$). Lipid droplets, oxidative stress, apoptosis and pro-fibrotic-associated genes were assessed. EVs were isolated by ultracentrifugation. LX-2 cells were treated with EVs from hepatocytes and pro-fibrogenic-associated markers were determined. CDAA-fed mice model was used to assess the effects of intermittent hypoxia (IH) on experimental NASH. **Results:** CH-treatment in fat-laden HepG2 cells increased the steatosis, oxidative stress, apoptosis, pro-fibrotic gene expression and increased the release of EV compared to non-treated HepG2 cells. Treatment of LX2 cells with EV from fat-laden hypoxic hepatocytes increased pro-fibrotic markers compared to EVs from non-treated hepatocytes. CDAA-fed animals exposed to IH exhibited increased fibrosis that correlated with an increase of circulating EV. **Conclusion:** Hypoxia promotes hepatocellular damage and pro-fibrotic signaling that correlates with increases of EV release from hepatocytes and from our *in vivo* model of NASH. EV from hypoxic fat-laden hepatocytes evoke pro-fibrotic responses in LX-2 cells.

1. - INTRODUCTION

Non-alcoholic fatty liver disease (NAFLD) is currently the most common liver disease and is a major global health problem (1). NAFLD is characterized by fat accumulation in the liver which may progress to hepatitis, cirrhosis and liver-related morbidity and mortality (2). Recent evidence suggests that saturated fatty acids (FFAs) contribute to the phenomenon of lipotoxicity and can trigger inflammation in the liver and an abnormal wound-healing response or fibrosis leading to the development of non-alcoholic steatohepatitis (NASH) (3-5).

It is still not clear why some patients with fatty liver develop advanced stages of NASH more rapidly and severely than others. Clinical observations in patients who suffer from Obstructive Sleep Apnea

syndrome (OSAS) have revealed that these patients have a higher risk of developing more severe NAFLD associated with significant liver damage (6,7). The pathophysiology of this condition is characterized by intermittent airway obstruction that alters gas exchange leading to periodic hypoxia (8). Several studies have demonstrated that hypoxia induces metabolic alterations such as insulin resistance, increased oxidative stress, increased liver triglyceride accumulation and increased inflammation, hepatocellular damage and fibrogenesis (9-14).

During hypoxia, the transcription factor hypoxia inducible factor 1 alpha (HIF-1α) is stabilized and translocated to the nucleus to activate its target genes by means of binding of HIF-1α to Hypoxia Responsive Elements (HREs) located in the target gene promoters (15). These target genes modify hepatocyte lipid metabolism and also energy metabolism, cell survival, inflammation and fibrosis (16-18). In rodent models of NASH, intermittent hypoxia was shown to have a pro-inflammatory and pro-fibrotic effect as indicated by increased levels of NF-κB-dependent inflammatory cytokines, such as TNF-α, IL-6 and IL-1β, and an increased expression of collagen type I in the liver (20,21). Likewise, *in vitro* studies using hepatocytes and stellate cells showed that HIF-1α can modulate pro-fibrogenic signaling (17,21-23), which could be key for the development and progression of NASH.

The involvement of extracellular vesicles (EVs) in the progression of NAFLD has been studied recently in *in vitro* and *in vivo* models (24-27). EVs are classified according to their size and biogenetic origin, e.g. exosomes and microvesicles (28). Exosomes are small particles (50 to 150 nm) released after the fusion of multivesicular bodies. Microvesicles are directly released from the cell membrane and have a size of 100 to 1000 nm (28). In our study, we do not distinguish between microvesicles and exosomes and we will therefore use the term "EVs" for both. EVs play an important role in cellular communication in normal physiological and pathophysiological situations due to their content of proteins, mRNAs and/or lipids (29). There are enough evidence that indicate the involvement of EVs in NASH (30,31), but their role in the context of hypoxia and effects on non-parenchymal cells, notably stellate cells, the principal cell type involved in matrix deposition in fibrogenesis, remains to be elucidated.

Therefore, the aim of this study was to test the hypothesis that hypoxia leads to hepatocellular damage that involves release of EVs that have a pro-fibrotic effect on stellate cells. We used both *in vitro* and *in vivo* model to test this hypothesis.

2.- MATERIALS AND METHODS

2.1 Animals

Animal experiments were approved by the institutional animal care and use committee (Comité de ética y bienestar Animal, Escuela de Medicina, Pontificia Universidad Católica de Chile, CEBA 100623003). Male C57BL/6 mice aged 10 weeks at the beginning of the study and divided into four experimental groups (n = 4-8) receiving either choline-deficient amino acid-defined (CDAA) diet (Catalog # 518753, Dyets Inc. Bethlehem, PA) to induce NASH or the choline-supplemented L-amino acid defined (CSAA, Catalog # 518754, Dyets Inc. Bethlehem, PA) diet as control for 22 weeks as previously described (32,33). Animals were exposed to IH or normoxia (chambers 41x22x35 cm, COY lab products™, Grass Lake, MI, USA) during the last 12 weeks of the experimental or control feeding period. IH regimen consisted of a reduction of fraction of inspired oxygen (FiO_2) from 0.21 to 0.07 over a 30 seconds period and then reoxygenation to 0.21 FiO_2 in the subsequent 30 seconds period. This regimen was performed for 30 events/hour of hypoxic exposure for 8 hour/day during the rest cycle, between 9 am and 5 pm. The cycle was repeated 7 days a week for 12 consecutive weeks. After ending the study, mice were anesthetized (ketamine 60 mg/kg plus xylazine 10 mg/kg intraperitoneally) and then euthanized by exsanguination. Serum and liver tissue samples were collected and processed or stored at −80 °C until analyzed.

2.2 Histological studies

Liver fibrosis was analyzed on paraformaldehyde-fixed liver sections stained with Sirius Red on frozen 7 µm liver cryosections. Staining was quantitated by digital image analysis (ImageJ, NIH, US) as previously described (32).

2.3 Cell culture and treatment with free fatty acids and chemical hypoxia induction

The human hepatocellular carcinoma cell line HepG2 (ATCC, USA) was cultured in Dulbecco's modified Eagle medium (1X) + GlutaMAX™- I (DMEM, 10569010, Gibco) supplemented with 10% fetal bovine serum (FBS; Gibco) and 1% penicillin-streptomycin (Gibco) at 37°C and 5% CO_2. All cells were plated in a cell culture plate at least 24h-36h before treatment. Upon reaching 80% confluence, the cells were incubated with a mixture of free fatty acids (FFA) consisting of oleic acid (500 µmol/L) and palmitic acid (250 µmol/L) in an aqueous solution of bovine serum albumin (BSA) as described (34). Incubations were carried out with or without Cobalt(II) chloride ($CoCl_2$; Sigma Aldrich) (200 µmol/L) for 24 hours to induce chemical hypoxia (35). $CoCl_2$ is a well-known hypoxia-mimetic agent by stabilization of hypoxia-inducible factor (HIF)-1α (36). Control cells were treated with BSA alone.

2.4 Western blot analyses

Cell lysates were resolved on Mini-PROTEAN® TGX Stain-Free™ Precast Gels (BioRad, UK, Oxford). Semi dry-blotting was performed using Trans-Blot Turbo Midi Nitrocellulose Membrane with Trans-Blot Turbo System Transfer (BioRad). Ponceau S 0.1% w/v (Sigma) staining was used to confirm protein transfer. Anti-HIF1α (610958, Biosciences), anti-CASP1 (SC-56036, Santa Cruz), anti-CD81 (10630D, Invitrogen), anti-Bcl-2 (ab32370, Abcam), anti-Type I Collagen (1310-01; Southern Biotech) and anti-αSMA (A5228, Sigma) were used in combination with appropriate peroxidase-conjugated secondary antibodies. Tubulin (T9026, Sigma) or actin (A5228, Sigma) were used as loading controls. The blots were analyzed in a ChemiDoc XRS system (Bio-Rad). Protein band intensities were quantified by ImageLab software (BioRad).

2.5 Nile red staining

Intracellular lipid droplets in the HepG2 cells were detected with Nile Red fluorescent probe (N1142, Thermo Fisher). HepG2 cells were grown in 96-well plates and treated with FFA and/or $CoCl_2$. After treatment, the cells were washed twice with PBS and stained with Nile Red solution for 10 min in the dark. The cells were then washed twice with PBS and stained with Hoechst dye (33342, Thermo Fisher). The fluorescence intensity of each well was analyzed with excitation/emission wavelength at 488 nm/550 nm using a microplate reader. The fluorescence images were recorded using an inverted fluorescence microscope

2.6 Determination of reactive oxygen species

The intracellular generation of reactive oxygen species (ROS) in HepG2 cells was monitored with DCFH-DA fluorescent probe. HepG2 cells were grown in 96-well plates and treated with FFA and/or $CoCl_2$. Cells were washed twice with PBS and incubated with the cell permeable reagent 2',7'–dichlorofluorescin diacetate (DCFDA; Abcam, USA) for 45 min. Cells were then washed twice with PBS and the fluorescence intensity of each well was analyzed with excitation/emission wavelength at 495 nm/529 nm using a microplate reader.

2.7 Apoptosis measurement

Caspase-3 fluorometric assay was used to determine apoptosis induced by FFA and/or $CoCl_2$ in HepG2 cells. After treatment, HepG2 were scraped and cell lysates were obtained by three cycles of freezing (−80°C) and thawing (37°C) followed by centrifugation for 5 minutes at 13,000g. Caspase-3 enzyme activity was assayed as described previously (37). The arbitrary units of fluorescence (AUF) was quantified in a spectrofluorometer at an excitation wavelength of 380 nm and an emission wavelength of 430 nm.

2.8 Assessment of cell death associated to disrupted cellular membrane integrity

SYTOX® Green nucleic acid stain (Invitrogen, S7020) was used to determine cell death induced by FFA and/or $CoCl_2$ in HepG2 (38). Cells were cultured in 12-well plates. After treatment, diluted Sytox Green solution (1:40.000/PBS) was added to the cells for at least 15 minutes at 37°C, 5% CO_2. Necrotic cells have ruptured plasma membranes, allowing entrance of non-cell permeable Sytox Green into the cells and binding to nucleic acids. Necrosis was determined using a Leica fluorescence microscope at a wavelength of 488 nm.

2.9 RNA isolation and quantitative real-time reverse transcription polymerase chain reaction (qRT-PCR)

HepG2 cells were harvested on ice and washed twice with ice-cold PBS. Total RNA was isolated with TRI-reagent (Sigma) according to the manufacturer's instructions. Reverse transcription (RT) was performed using 2.5 µg of total RNA, 1X RT buffer (500 mmol/l Tris-HCl [pH 8.3]; 500 mmol/l KCl; 30 mmol/l $MgCl_2$; 50 mmol/l DTT), 1 mmol/l deoxynucleotides triphosphate (dNTPs, Sigma), 10 ng/µl random nanomers (Sigma), 0.6 U/µl RNaseOUT™ (Invitrogen) and 4 U/µl M-MLV reverse transcriptase (Invitrogen) in a final volume of 50 µl. The cDNA synthesis program was 25°C/10 min, 37°C/60 min and 95°C/5 min. Complementary DNA (cDNA) was diluted 20X in nuclease-free water. Real-Time qPCR was carried out in a StepOnePlus™ (96-well) PCR System (Applied Biosystems, Thermofisher) using TaqMan probes. The sequences of the probes and primer sets are described in Supplementary Material. For qPCR, 2X reaction buffer (dNTPs, HotGoldStar DNA polymerase, 5 mmol/L $MgCl_2$) (Eurogentec, Belgium, Seraing), 5 µmol/L fluorogenic probe and 50 µmol/L of sense and antisense primers (Invitrogen) were used. mRNA levels were normalized to the housekeeping gene 18S and further normalized to the mean expression level of the control group.

2.10 Extracellular vesicles isolation

For EV collection, HepG2 cells were grown in culture dishes of 100 mm to obtain 70 ml of serum-free conditioned medium (devoid of CoCl2 or FFA) after different treatments for an additional 24 hours. EVs were isolated from conditioned medium by differential ultracentrifugation (UCF Thermo-Sorvall 80wx+) according to a modified previous protocol (39). A total volume of 70 ml medium per treatment was depleted of cells and cell debris by consecutive, low-speed centrifugations (2,000 × g for 30 min and 12,000 × g for 45 min). The resulting supernatants were carefully collected and centrifuged for 70 min at 120,000 × g at 4 °C. Pellets from this centrifugation step were washed in PBS, pooled and centrifuged again for 60 min at 100,000 × g at 4°C. For EV collection from animals, serum samples were reconstituted in a total volume of 4.4 mL and were centrifugated at 2,000 × g for 30 min and 10,000 × g for 30 min. The resulting supernatants were carefully collected and

centrifuged for 70 min at 120,000 × g at 4°C. Pellets from this centrifugation step were washed in PBS, pooled and centrifuged again for 60 min at 100,000 × g at 4°C. The obtained pellets from HepG2 cells or serum were resuspended in lysis buffer or PBS solution depending on subsequent experiments and stored in aliquots at -80 °C. Protein concentration in EV pellet were measured using BCA protein assay kit (Pierce, Rockford, IL).

2.11 Nanoparticle tracking analysis

Concentration and size distribution of isolated EVs were assessed by nanoparticle tracking analysis (NTA) using NanoSight NS300 instrumentation (Marvel, Egham, UK). EV samples were diluted with PBS to a concentration of 10^8 to 10^9 particles/mL in a total volume of 1 ml. Each sample was continuously run through a flow-cell top-plate set up at 18°C using a syringe pump. At least three videos of 20 seconds documenting Brownian motion of nanoparticles were recorded and at least 1000 of completed tracks were analyzed by NanoSight software (NTA v3.2).

2.12 Transmission electron microscopy

Isolated EVs were fixed in 2% paraformaldehyde in 0.1 M phosphate buffer overnight at 4°C. The samples were then placed on Formvar/Carbon 300 Mesh (FCF300-CU, EMS) grid and air dried for 10 min. The grids were first contrasted with uranyl-oxalate solution and then contrasted and embedded in a mixture of 4% uranyl acetate. The grids were air dried and visualized with a Philips Tecnai 12 (Biotwin, Eindhoven, Netherlands) electron microscope at 80 kV. The images were captured with the software Item Olympus Soft Imaging Solutions (Windows NT 6.1).

2.13 Treatment of LX-2 cells with extracellular vesicles

To investigate the crosstalk between EVs from HepG2 and LX-2 human hepatic stellate cells, a typical cell line to study hepatic fibrogenesis (40), LX-2 cells were treated with isolated EVs. LX-2 cells were cultured in DMEM supplemented with 10% FBS and 1% penicillin-streptomycin at 37°C and 5% CO_2. All cells were plated in a cell culture plate at least 24-36 h before treatment. Upon reaching 80% confluence, the cells were incubated with FBS-free medium and exposed to 15 µg of EVs that were isolated from HepG2 cells that had been treated with $CoCl_2$, FFA and $CoCl_2$ + FFA for 24h. After 24h of EVs treatment, LX-2 cells were harvested to continue with analyses by quantitative PCR, Western Blot and immunofluorescence.

2.14 Immunofluorescence microscopy

LX-2 cells were grown on glass cover slips placed in 12-well plates. After treatment, culture media were removed and cover slips were carefully washed twice with PBS. Cells were then fixed using a 4%

paraformaldehyde solution in PBS for 10 min at room temperature and washed twice with PBS. Permeabilization was performed by incubation of the samples for 10 minutes in 0.1% Triton X-100 (Sigma). The cells were washed twice with PBS and incubated with 2% BSA (Sigma) in PBS/0.1% Tween 20 (Sigma) solution for 30 minutes to block non-specific binding sites. Goat anti-Type I Collagen (1310-01; Southern Biotech) was used at a dilution of 1:200 in 2% BSA/PBS in a humidified chamber for 1 hour at room temperature. Samples were subsequently washed twice with 2% BSA/PBS. Finally, cells were incubated with rabbit anti-goat Alexa Fluor® 568 at a dilution of 1:500 in 2% BSA/PBS for 30 min at room temperature in the dark. Slides were mounted with ProLong antifade with DAPI (Molecular Probes) and images were evaluated using fluorescence microscopy and analyzed by Leica ALS AF Software (Leica).

2.15 Statistical analyses

Analyses were performed using GraphPad software (version 5.03, GraphPad Software Inc., CA, USA). All results are presented as a mean of at least 3 independent experiments ± SEM or as absolute number or percentage for categorical variables. The statistical significance of differences between the means of the experimental groups was evaluated using one-way analysis of variance (ANOVA) with a post-hoc Bonferroni multiple-comparison test; $P<0.05$ was considered as statistically significant.

3. - RESULTS

3.1 Chemical hypoxia increases lipid droplet content in fat laden hepatocytes: To investigate whether hypoxia exacerbates lipid accumulation in an *in vitro* model of experimental NASH, we treated HepG2 cells with $CoCl_2$, a hypoxia mimetic agent that promotes the accumulation of HIF-1α. HepG2 cells treated with $CoCl_2$ showed a significant increase of HIF-1α, independent of treatment with FFA (Figure 1). To induce steatosis, HepG2 cells were treated with a mixture of oleic acid and palmitic acid (FFA) as described previously (41). Hepatocytes showed increased formation of lipid droplets (Figure 2a). Interestingly, a significant increase in the content of lipid droplets was observed in the steatotic hepatocytes treated with the chemical inducer of hypoxia (Figure 2b), indicating that hypoxia increases steatosis in this model.

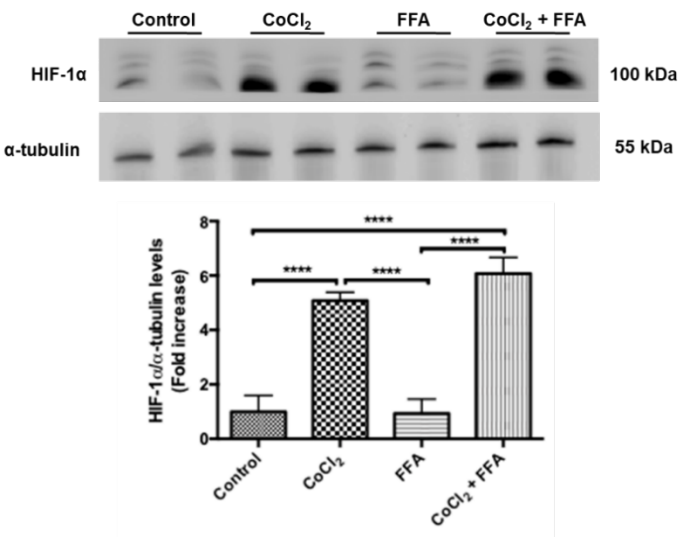

Figure 1. Chemical hypoxia stabilizes HIF-1α. HepG2 cells were incubated for 24h with oleic acid and palmitic acid 2:1 (FFA) in the presence or absence of $CoCl_2$ 200 µmol/L. Protein levels of HIF-1α were determined by Western Blot as described in Material and Methods. α-Tubulin was used as loading control. Data were shown as mean ± SEM (n ≥ 3) **** indicates P < 0.001.

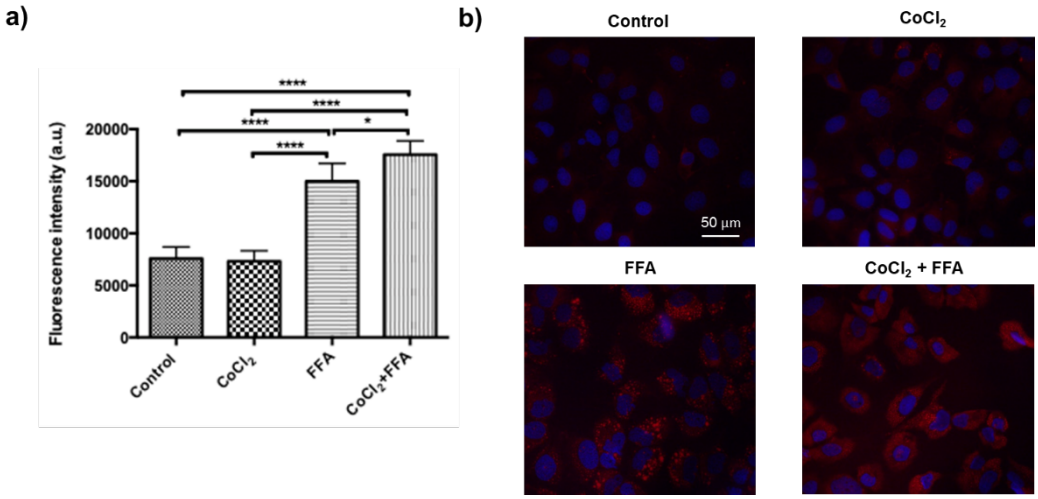

Figure 2. Hypoxia aggravates FFA-induced steatosis *in vitro*. HepG2 cells were incubated for 24h with oleic acid and palmitic acid 2:1 (FFA) in the presence or absence of $CoCl_2$ 200 µmol/L. Lipid droplets content was measured by a) Fluorescence intensity and b) Fluorescence images of Nile Red as described in Material and Methods. Data were shown as mean ± SEM (n ≥ 3) * indicates P < 0.05; **** indicates P < 0.001.

3.2 Hypoxia increases oxidative stress and apoptotic cell death in fat laden hepatocytes: To evaluate whether the induction of hypoxia exacerbates damage by lipotoxicity, we determined the generation of reactive oxygen species (ROS) and the extent of cell death. The increase in ROS was evaluated using the fluorogenic dye DCF. The results indicated a significant increase in ROS in each of the treatments compared to the control (Figure 3). Furthermore, hypoxia exacerbates the increase in ROS in steatotic HepG2 cells compared to the hypoxic and FFA conditions separately.

Apoptotic cell death was evaluated by measuring the activity of caspase-3. The results demonstrate that hypoxia in steatotic HepG2 cells induces apoptotic lipotoxicity compared to control cells. (Figure 4a). Hypoxia or steatosis alone did not induce apoptotic cell death. Lipotoxicity was also evaluated by Sytox Green assay to detect cell death associated to disrupted cellular membrane integrity. The different treatments in HepG2 cells did not induce any necrotic cell death (Figure 4b).

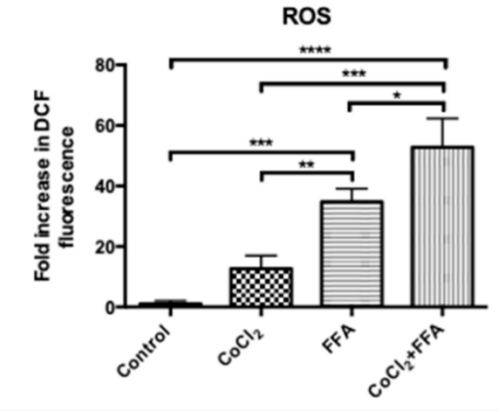

Figure 3. Hypoxia increases the production of reactive oxygen species in steatotic HepG2 cells. HepG2 cells were incubated for 24h with oleic acid and palmitic acid 2:1 (FFA) in the presence or absence of $CoCl_2$ 200 µmol/L. Reactive oxygen species (ROS) were measured as described in Material and Methods. Data were shown as mean ± SEM (n ≥ 3) * indicates P < 0.05; ** indicates P < 0.01; *** indicates P < 0.005; **** indicates P < 0.001.

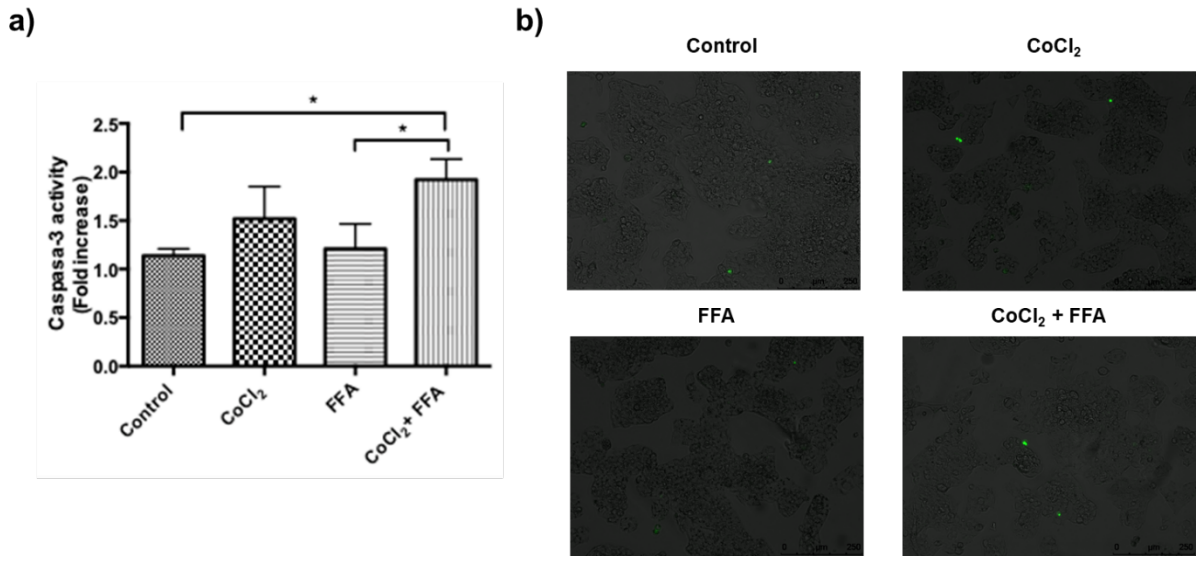

Figure 4. Hypoxia and steatosis in vitro promote apoptotic cell death but do not promote necrotic cell death. HepG2 cells were incubated for 24h with oleic acid and palmitic acid 2:1 (FFA) in the presence or absence of $CoCl_2$ 200 µmol/L. Caspase-3 activity and necrosis were measured as described in Material and Methods. Data were shown as mean ± SEM (n ≥ 3) * indicates P < 0.05

3.3 Hypoxia induces the expression of pro-fibrotic cytokines: To evaluate whether hypoxia promotes a profibrotic phenotype in fat laden HepG2 cells, we measured the mRNA levels of different profibrotic cytokines. We demonstrate that chemical hypoxia in fat laden hepatocytes significantly increases mRNA levels of profibrotic cytokines. Expression of some genes was also increased in hepatocytes treated only with $CoCl_2$ (Figure 5).

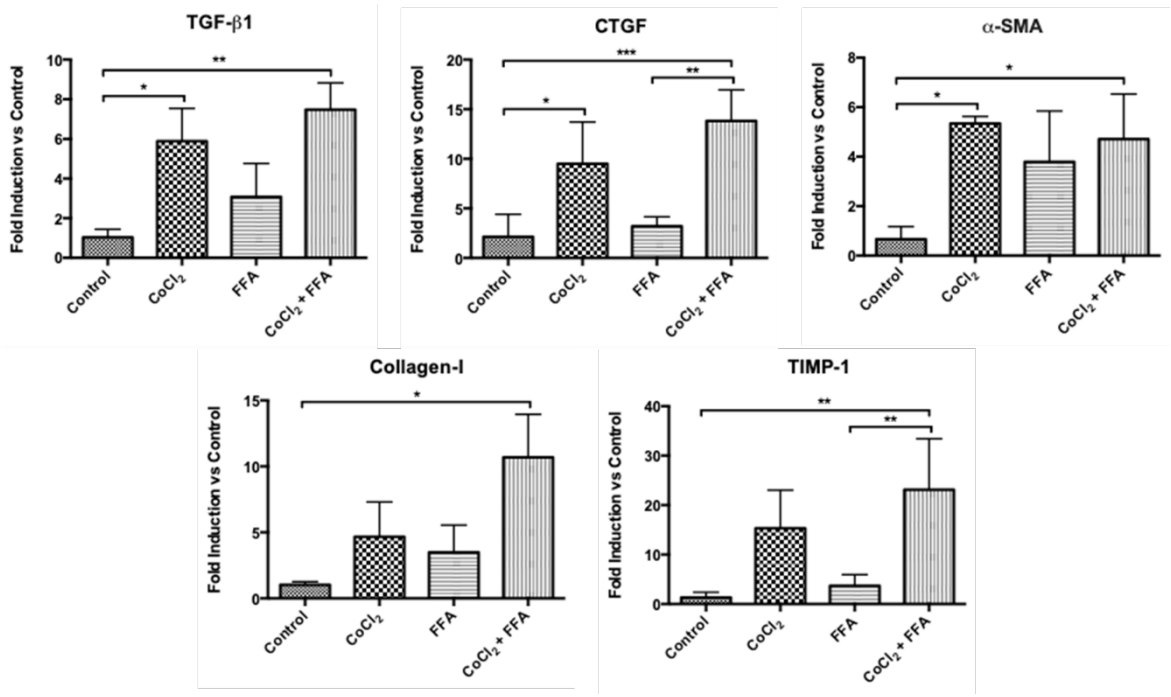

Figure 5. Hypoxia increases the expression of pro-fibrotic cytokines in steatotic HepG2 cells. HepG2 cells were incubated for 24h with oleic acid and palmitic acid 2:1 (FFA) in the presence or absence of $CoCl_2$ 200 µmol/L. mRNA levels of TGF-β1, CTGF, collagen-I, α-SMA and TIMP-1 were measured as described in Material and Methods. Data were shown as mean ± SEM (n ≥ 3) * indicates P < 0.05; ** indicates P < 0.01; *** indicates P < 0.005

3.4 Increased number of EVs in hepatocyte conditioned medium in hypoxic and steatotic conditions: To better characterize the involvement of hepatocytes in the promotion of the pro-fibrotic phenotype and possible crosstalk with stellate cells, we assessed EVs from conditioned medium of HepG2 cells (HepG2-EV) following different treatments. After isolation of EVs from conditioned medium, we characterized EVs according to previous guidelines (42) by their typical structure visualized by TEM (Figure 6a) and detection of EV positive marker CD81 and EV negative marker Bcl-2

(mitochondrial marker) by Western blotting (Figure 6b). Also, the size (around 100-150 nm) and concentration of HepG2-EV (Figure 6c) were determined by NTA. Notably, the fat laden-hepatocytes in the presence of $CoCl_2$ showed a significant increase in the concentration of HepG2-EV compared to all conditions (Figure 7). These results suggest that steatotic and hypoxic conditions in HepG2 cells can modulate the release of EVs.

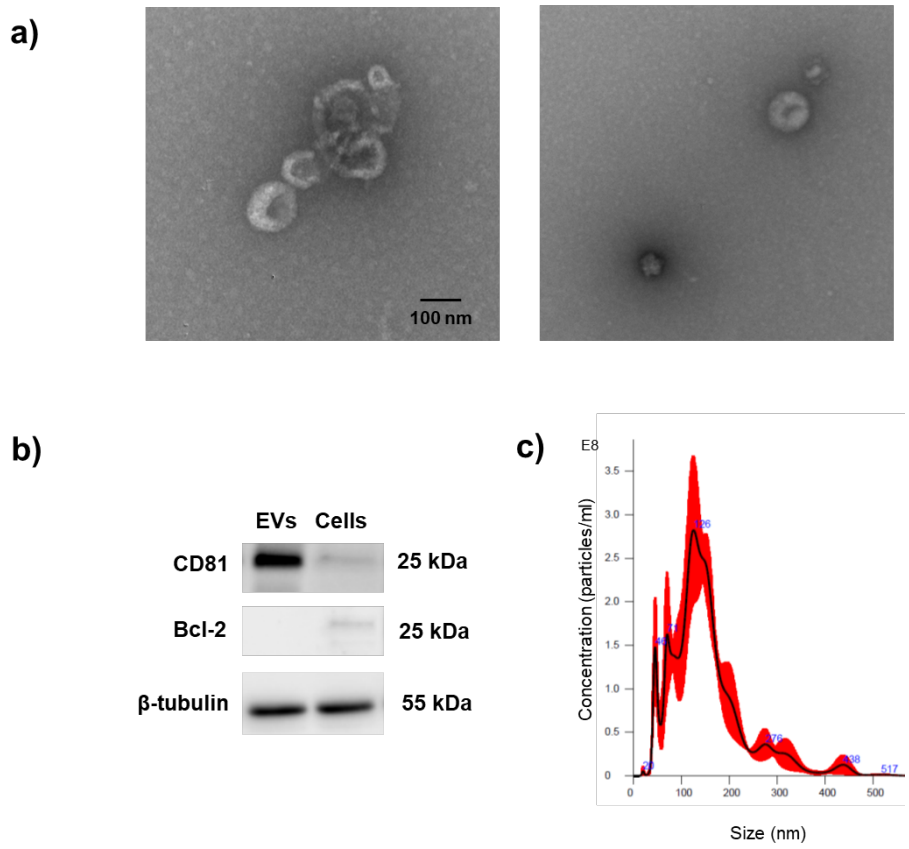

Figure 6. Characterization of HepG2-EV. EVs were characterized in conditioned medium from control HepG2 cells by a) transmission electron microscopy; b) detection of EV-positive marker CD81 and EV negative mitochondrial marker Bcl-2 by Western blot c) size distribution by NTA as described in Material and Methods.

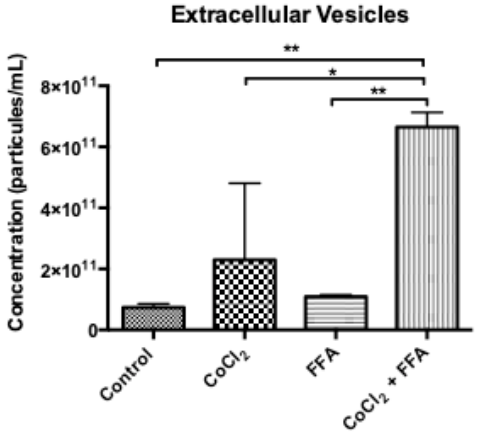

Figure 7. EV release is increased in hepatocyte conditioned medium in hypoxic and steatotic conditions *in vitro*. EV quantification in conditioned medium from HepG2 after different treatments performed by NTA as described in Material and Methods. Data were shown as mean ± SEM (n ≥ 3) * indicates P < 0.05; ** indicates P < 0.01.

3.5 HepG2-EVs from steatotic and hypoxic conditions promote a pro-fibrotic phenotype in stellate cells: To evaluate whether HepG2-EVs have a direct effect on stellate cells we used the human stellate cell line LX-2. LX-2 cells were stimulated with 15 µg/ml of HepG2-EV from each treatment and mRNA and protein levels of some pro-fibrotic cytokines were evaluated. As shown in Figure 8, HepG2-EVs from steatotic and hypoxic condition significantly increase the gene expression of TGF-β-1, CTGF, collagen-I and α-SMA in LX-2 cells. The results also suggest an additive effect of FFA and $CoCl_2$ to promote a pro-fibrotic phenotype in LX-2 cells. Interestingly, a similar result was observed in a confirmatory experiment assessing protein levels of collagen-I (Figure 9a-9c) and α-SMA (Figure 9b) in LX-2 cells treated with HepG2-EVs from steatotic and hypoxic condition.

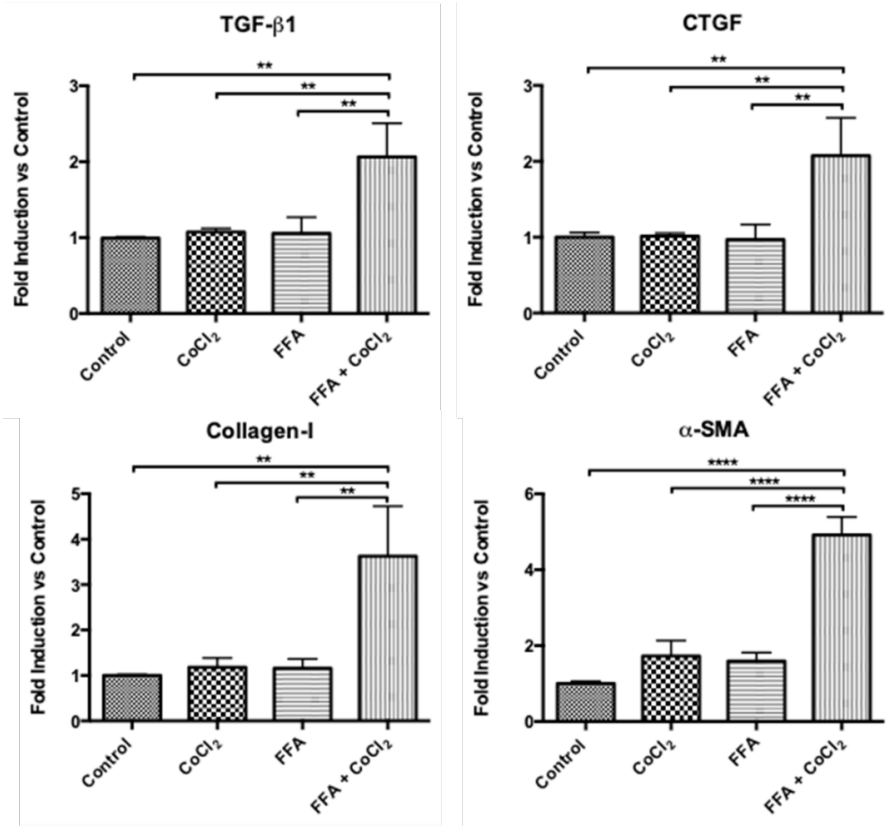

Figure 8. HepG2-derived EVs increase the expression of profibrotic cytokines in LX-2 cells. LX-2 cells were exposed to 15 µg of EVs that were isolated from HepG2 cells that had been treated with $CoCl_2$, FFA and $CoCl_2$ + FFA for 24h. mRNA levels of TGF-β1, CTGF, Collagen-I and α-SMA were measured as described in Material and Methods. Data were shown as mean ± SEM (n ≥ 3) ** indicates P < 0.01; **** indicates P < 0.001.

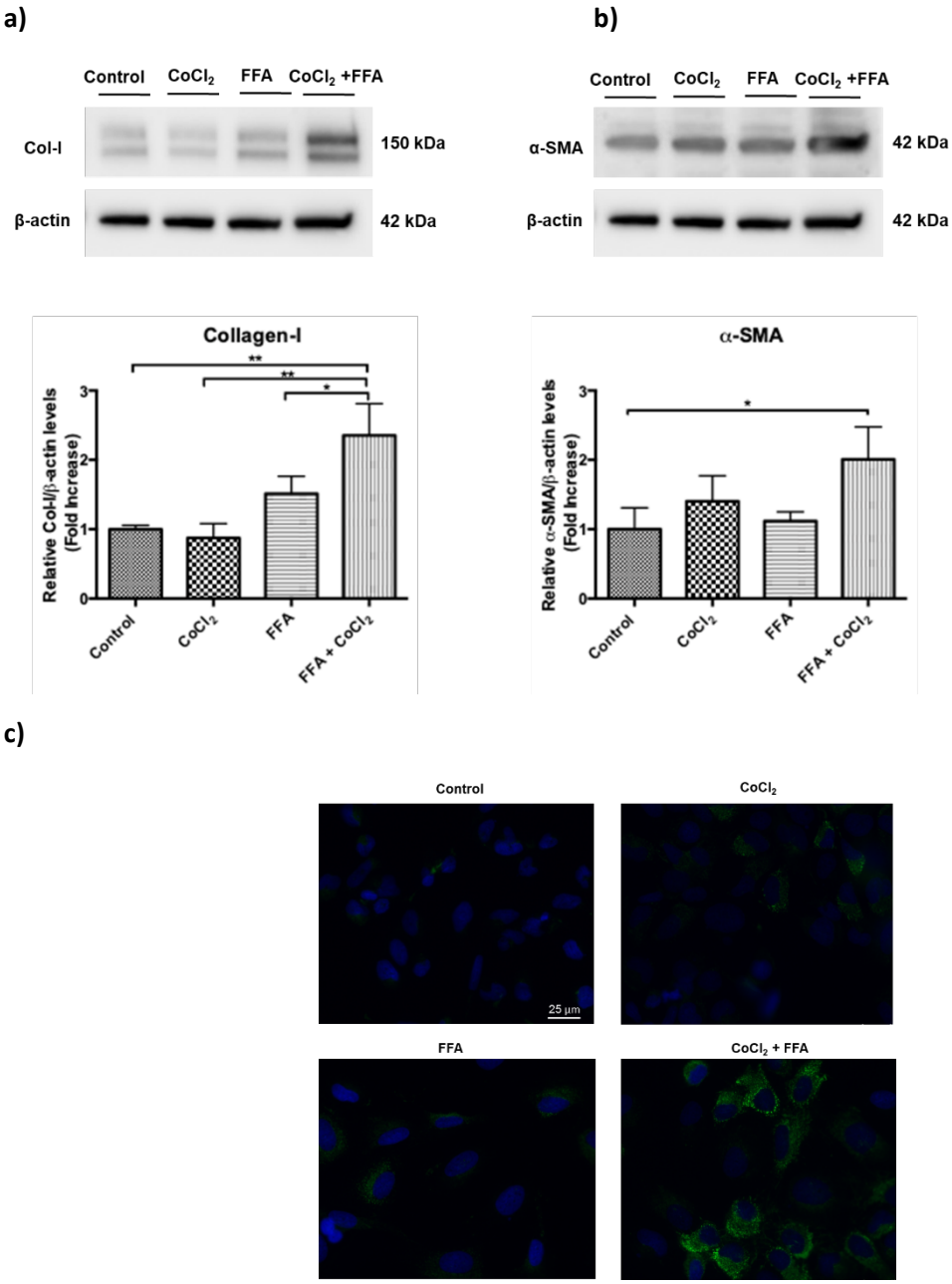

Figure 9. EVs derived from steatotic and hypoxic HepG2 cells increases the expression of profibrotic proteins in stellate cells. LX-2 cells were exposed to 15 µg of EVs that were isolated from HepG2 cells that had been treated with $CoCl_2$, FFA and $CoCl_2$ + FFA for 24h. Protein levels of a) Collagen-I and b) α-SMA were determined by Western blot as described in Materials and Methods. β-Actin was used as loading control. c) Intracellular Collagen-I expression was determined by immunofluorescence as described in Materials and Methods. Data were shown as mean ± SEM (n ≥ 3) * indicates $P < 0.05$; ** indicates $P < 0.01$; *** indicates $P < 0.005$.

.

3.6 Hypoxia promotes a pro-fibrotic phenotype and correlates with increased release of EVs in an in vivo model of NASH: To validate the previous results in an *in vivo* model, CDAA diet feeding for 22-weeks was used to induce NASH and an intermittent hypoxia regimen was applied for the last 12 weeks. As expected, CDAA diet-fed mice showed significant liver fibrosis as shown by conventional Sirius Red staining (Figure 10a). Interestingly, collagen deposition area of IH-treated mice with NASH was even further increased compared with CDAA diet-group, indicating a pro-fibrotic action of hypoxia. In addition, as shown in Figure 10b, IH significantly increased hepatic mRNA levels of several markers of fibrogenesis induced by the CDAA diet including TGF-β1, CTGF, collagen-I, α-SMA, TIMP-1 and MCP-1. Finally, EVs were isolated from mice serum to determine the concentration of EVs in each experimental group. As shown in Figure 10c, CDAA diet-fed mice exhibited a significant increase of EVs when exposed to IH compared to control or CDAA diet-fed mice under normoxic conditions. These results suggest a strong correlation between the induction of hypoxia with the increase of the EVs and the promotion of a more pro-fibrotic phenotype in an *in vivo* model of NASH.

a)

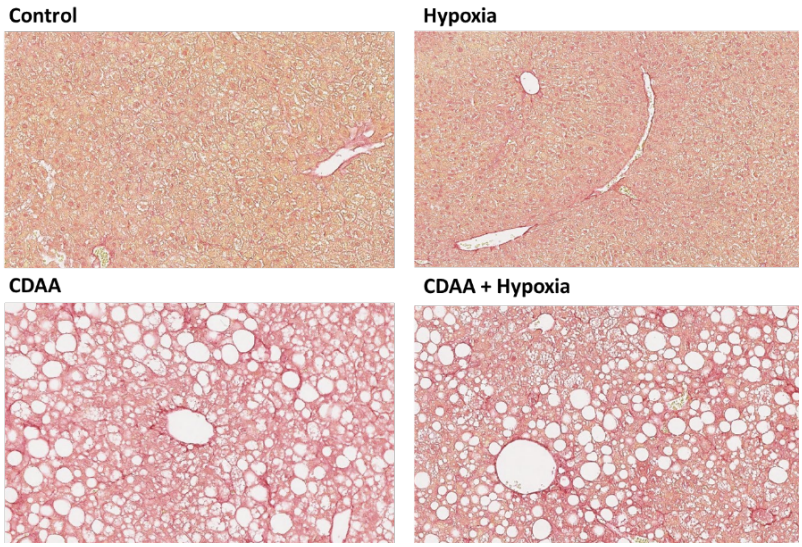

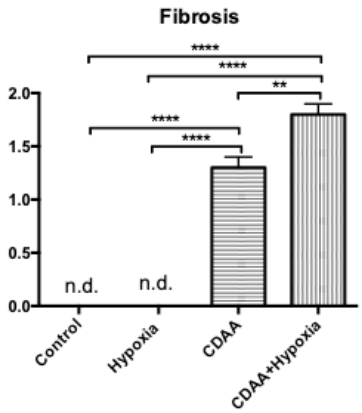

b)

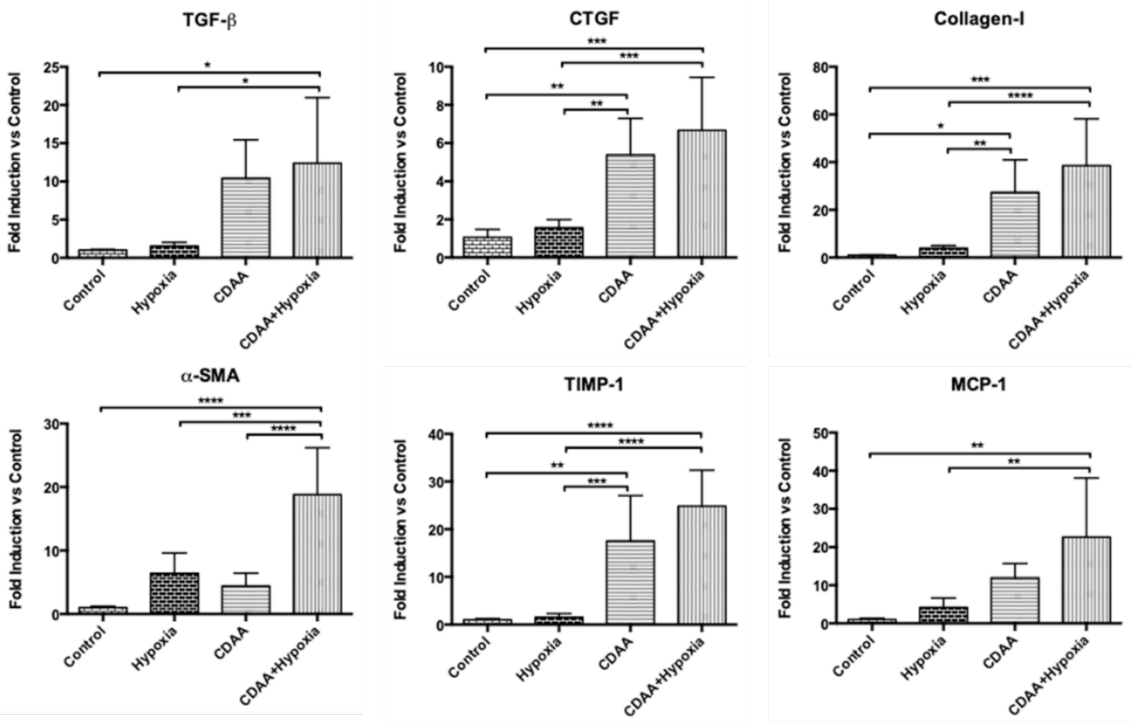

c)

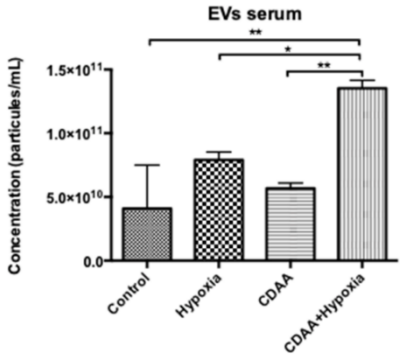

Figure 10. Intermittent hypoxia promotes a pro-fibrotic phenotype in mice with NASH and correlates with increased levels of EVs *in vivo*. The mice were placed on choline-supplemented L-amino acid defined (CSAA) diet as control, or defined diet with choline deficiency amino acids (CDAA) for 22 weeks to induce liver injury. Intermittent hypoxia (IH) or normoxia was applied for the last 12 weeks of the diet as described in Materials and Methods. a) Liver sections stained with Sirius Red from mice fed control diet, intermittent hypoxia and/or choline-deficient amino acid-defined (CDAA) diet. In addition, fibrosis area was quantified using digital image analysis of the red-stained area in Sirius red-stained samples (ImageJ, NIH, US); mRNA levels of pro-fibrotic cytokines were determined by RT-qPCR as described in Materials and Methods; c) quantification of EVs from serum samples was determined by NTA as described in Materials and Methods. Data were shown as mean ± SEM ($n \geq 3$) * indicates $P < 0.05$; ** indicates $P < 0.01$; *** indicates $P < 0.005$; **** indicates $P < 0.001$.

4. - DISCUSSION

In recent years, the mechanisms underlying the progression of NAFLD/NASH have been thoroughly studied. The early stages of NAFLD are characterized by fat accumulation in the liver resulting in steatosis that can progress to hepatocellular damage and inflammation in a condition termed NASH (2,5). Moreover, some patients develop liver fibrosis associating with increased mortality due to risk of HCC development (43). Interestingly, clinical studies have indicated that obstructive sleep apnea (OSA) is a new predictive factor of hepatic fibrosis in patients with NAFLD (44-46). Recent research has provided evidence regarding the role of hypoxia, a hallmark of OSA, in the development of liver injury and hepatic fibrosis in animal models of NAFLD (17,19,47). However, there are still major gaps in our understanding of the progression of NASH to fibrosis, e.g. the cellular mechanism underlying the crosstalk between hepatocytes and stellate cells, the principal non-parenchymal cell responsible for liver scar formation (48). In this study, we demonstrate that hypoxia, induced by a HIF-1α chemical stabilizer in fat-laden hepatocytes, promotes hepatocellular damage, increases pro-fibrogenic gene expression and increases the release of extracellular vesicles (EVs). Furthermore, EVs from hypoxic and steatotic hepatocytes promote mRNA and protein expression of important fibrosis markers in stellate cells.

In the present study, our *in vitro* model of steatosis was key to the analysis of hypoxia induced by the hypoxia mimetic $CoCl_2$, a HIF-1 stabilizer. We used the human hepatocyte cell line HepG2, in which the effectiveness of the hypoxia mimetic was evaluated through the quantification of HIF-1α levels, which increased due to the intracellular stabilization, as described in other *in vitro* studies (49,50). We showed that treatment with palmitic acid (PA) and oleic acid (OA) (1: 2) increased the content of lipid droplets in hepatocytes in the absence of lipotoxicity. Previous studies have shown that OA promotes steatosis in hepatocytes, both in primary hepatocyte culture and in hepatoma cell lines, while PA induces a cytotoxic response (51,52). Our results are in line with a previous report using a combination of both fatty acids, using a higher OA concentration, that promoted an anti-apoptotic effect and triglyceride accumulation (51). Interestingly, the hypoxia mimetic $CoCl_2$ increased the content of lipid droplets compared to HepG2 cells without hypoxia, as determined via quantification of Nile Red fluorescence. These results are supported by an *in vivo* study indicating that hypoxia, via HIF-1α, promotes an increase in lipid biosynthesis in steatotic conditions (53). Hepatocyte cell death by apoptosis was measured using caspase-3 and as expected, treatment with FFA alone did not induce cell death. However, HepG2 cells exposed to the combination of $CoCl_2$ and FFA presented an increase of caspase-3 activity that correlated with an increase in oxidative stress compared to the control group. Unexpectedly, HepG2 cells treated with FFAs also increased ROS compared to $CoCl_2$ and control groups. A recent study demonstrated that OA prevents ROS production in HepG2 cells

treated with PA (54). Likewise, another study showed that FFA treatment of HepG2 cells induced TNF-α generation, which is an important mediator in hepatic steatohepatitis and liver injury (55). Additional studies to further delineate the mechanism, such as measurement of mitochondrial ROS production, remain to be performed. We also analyzed hepatocyte cell death associated to disrupted cellular membrane integrity (necrosis) using SytoxGreen®. None of the treatments we applied induced a significant increase in necrosis. The divergent results of apoptosis and necrosis can be explained by the fact that different stimuli may induced different modes of cell death in different cell types (56). Taken together, our findings indicate that hypoxia promotes lipotoxicity as determined by the increase in hepatocellular apoptosis and oxidative stress.

To evaluate the possible damaging effects of hypoxia in fat-laden hepatocytes, we measured gene expression of pro-inflammatory and pro-fibrotic cytokines. As expected and in accordance with our previous results, the condition of hypoxia in steatotic hepatocytes increased the expression of TNF-α, IFN-γ, IL-1β, IL-18, TGF-β1, CTGF, collagen-I, α-SMA and TIMP-1. Interestingly, some pro-fibrotic genes such as TGF-β1, CTGF and α-SMA, increased in hypoxic HepG2 cells in the absence of FFAs. Previous data have demonstrated that the induction of HIF-1α in hepatocytes actives TGF-β signaling and promotes fibrogenesis in the liver (21, 22). To evaluate the role of EVs in this model, we checked the amount of EVs released in the culture medium and we observed an increase after treatment of HepG2 cells with CoCl2 and FFA compared to all other groups. EVs, comprising exosomes and microparticles, are small structures surrounded by membrane and released from the cells to the extracellular environment. EVs have a pathophysiological role in various diseases, including NASH and other chronic liver diseases (30,31,57). We performed a characterization of the isolated EVs from HepG2 cells using positive and negative markers by Western blotting and determinate EV size by NTA. Finally, isolated EVs from control hepatocytes were directly visualized using TEM.

Previous studies have demonstrated that during hepatocellular damage, hepatocytes release EVs that modulate pro-inflammatory and pro-fibrotic signaling in non-parenchymal liver cells (25, 58-61). To confirm whether EVs from our model of hypoxic and steatotic hepatocytes promote a pro-fibrotic phenotype in non-parenchymal liver cells, we used the human stellate cell line LX-2. EVs derived from $CoCl_2$-treated fat-laden hepatocytes increased gene expression of pro-fibrotic cytokines such as TGF-β1, CTGF, collagen-I and α-SMA in LX-2 cells compared to all other groups. In addition, protein expression of collagen-I and α-SMA was analyzed in LX-2 cells treated with EVs from HepG2 cells. Both pro-fibrotic proteins increased when LX-2 cells were treated with EVs derived from $CoCl_2$-treated steatotic hepatocytes. This interesting result suggests that the EV-cargo in our model is an important topic for future analysis. Recent studies that support our findings show that palmitic acid increased EVs from hepatocytes and change their miRNA cargo inducing pro-fibrogenic signals to

HSCs (60). Another study, providing similar results, indicated that EVs from lipotoxic hepatocytes activate HSCs via miRNA-128-3p (25).

The exact relation(s) between intermittent hypoxia, a hallmark of OSAS, and NAFLD/NASH progression, particularly with regard to liver fibrosis development, remains incompletely understood. We found that intermittent hypoxia promotes a pro-fibrotic phenotype in our CDAA diet-fed animal model and increases circulating levels of EVs. Histological examination showed more fibrosis, as determined by Sirius red staining, was significantly increased in CDAA diet-fed mice and CDAA diet-fed mice exposed to IH compared to control groups. In line with this, a recent study demonstrated that accumulation of oxidized lipids, specifically low-density lipoproteins, in hepatocytes, promotes fibrosis associated with progressive NAFLD (62). With regard to the increase of circulating EVs, previous studies have demonstrated that IH mimicking OSA alters EV generation and release as well as EV-cargo and function, promoting pathophysiology in different *in vivo* models (63-65). This important finding correlates with our in vitro results and provide evidence for a novel pro-fibrotic mechanism, involving EVs. Next challenge will be identified if the most of circulating EVs are derived from liver or from other specific cell source and identify gene and proteins cargo, including membrane surface composition.

Some limitations regarding our study is the used of $CoCl_2$ as hypoxia mimicking agent instead of performing the cell culture under real hypoxia, because a hypoxia incubator is not available in our laboratory to carry out cell culture to isolate the EVs. However, $CoCl_2$-induced chemical hypoxia model is well accepted and provide a more stable experimental conditions that are extrapolable to real hypoxia (35,36,49). Of note,a recent previous study of our laboratory on primary rat hepatocyte demonstrated that $CoCl_2$ is able to induce hypoxia, like demonstrated by HIF-1α increased expression, without affecting cell viability (61). Future studies will be neccessary to performance in real hypoxic conditions to understand the impact of hypoxia in the context of NASH and the mechanisms underlying hypoxia-induced EVs.

In conclusion hypoxia promoted hepatocellular damage and increased pro-fibrotic genes that correlates with increases of EVs derived from hepatocytes and from our *in vivo* model of NASH. Moreover, EVs from hypoxic fat-laden hepatocytes promoted a pro-fibrotic responses in LX-2 cells, showing a novel cell to cell communication in this model. Finally, mice model of NASH exposed to intermittent hypoxia presented a pro-fibrotic phenotype that correlate with increased of circulating of EVs. Future work should focus on analysis to profile the genomic, transcriptomic, proteomic an lipidomic cargo into EVs-derived from cells and biological fluids from rodents models under hypoxia condition that could be promotes fibrosis profile in the setting of NAFLD and OSAS.

5. - REFERENCES

1. Drescher HK, Weiskirchen S, Weiskirchen R. Current Status in Testing for Nonalcoholic Fatty Liver Disease (NAFLD) and Nonalcoholic Steatohepatitis (NASH). Cells 2019;8.pii E845.

2. Arab JP, Arrese M, Trauner M. Recent insights into the pathogenesis of non-alcoholic fatty liver disease. Annual Review of Pathology Mechanisms of Disease 2018;13:321-350.

3. Trauner, M.; Arrese, M.; Wagner, M. Fatty liver and lipotoxicity. Biochim. Biophys. Acta 2010;1801:299-310.

4. Hirsova P, Ibrahim SH, Gores GJ, Malhi H. Lipotoxic lethal and sublethal stress signaling in hepatocytes: relevance to NASH pathogenesis.J Lipid Res 2016;57:1758-1770.

5. Schuster S, Cabrera D, Arrese M, Feldstein AE. Triggering and resolution of inflammation in NASH. Nat Rev Gastroenterol Hepatol 2018;15:349-364.

6. Agrawal S, Duseja A, Aggarwal A, Das A, Mehta M, Dhiman RK, Chawla Y. Obstructive sleep apnea is an important predictor of hepatic fibrosis in patients with nonalcoholic fatty liver disease in a tertiary care center. Hepatol Int 2015;9:283-291.

7. Mesarwi OA, Loomba R, Malhotra A. Obstructive Sleep Apnea, Hypoxia, and Nonalcoholic Fatty Liver Disease. Am J Respir Crit Care Med. 2019;199:830-841.

8. Dempsey JA, Veasey SC, Morgan BJ, O'Donnell CP. Pathophysiology of sleep apnea. Physiol Rev 2010;90:47-112.

9. Savransky V, Nanayakkara A, Vivero A, Li J, Bevans S, Smith PL, Torbenson MS, et al. Chronic intermittent hypoxia predisposes to liver injury. Hepatology 2007;45:1007-1013.

10. Savransky V, Reinke C, Jun J, Bevans-Fonti S, Nanayakkara A, Li J, Myers AC, et al. Chronic intermittent hypoxia and acetaminophen induce synergistic liver injury in mice. Exp Physiol 2009;94:228-239.

11. Drager LF, Lopes HF, Maki-Nunes C, Trombetta IC, Toschi-Dias E, Alves MJ, Fraga RF, Jun JC, Negrão CE, Krieger EM, Polotsky VY, Lorenzi-Filho G.The impact of obstructive sleep apnea on metabolic and inflammatory markers in consecutive patients with metabolic syndrome. PLoS One 2010;5:e12065.

12. Drager LF, Li J, Reinke C, Bevans-Fonti S, Jun JC, Polotsky VY. Intermittent hypoxia exacerbates metabolic effects of diet-induced obesity. Obesity (Silver Spring) 2011;19:2167-2174.

13. Paschetta E, Belci P, Alisi A, Liccardo D, Cutrera R, Musso G, Nobili V. OSAS-related inflammatory mechanisms of liver injury in nonalcoholic fatty liver disease. Mediators Inflamm 2015;2015:815721.

14. Archontogeorgis K, Nena E, Papanas N, Rizzo M, et al. Metabolic Syndrome and Vitamin D Levels in Patients with Obstructive Sleep Apnea Syndrome. Metab Syndr Relat Disord 2018;16:190-196.

15. Nakayama K. Cellular signal transduction of the hypoxia response. J Biochem 2009;146:757-65.

16. Liu Y, Ma Z, Zhao C, Wang Y, Wu G, Xiao J, McClain CJ, et al. HIF-1alpha and HIF-2alpha are critically involved in hypoxia-induced lipid accumulation in hepatocytes through reducing PGC-1alpha-mediated fatty acid beta-oxidation. Toxicol Lett 2014;226:117-123.

17. Mesarwi OA, Shin MK, Bevans-Fonti S, Schlesinger C, Shaw J, Polotsky VY.Hepatocyte Hypoxia Inducible Factor-1 Mediates the Development of Liver Fibrosis in a Mouse Model of Nonalcoholic Fatty Liver Disease. PLoS One 2016;11:e0168572.

18. Briancon-Marjollet A, Monneret D, Henri M, Joyeux-Faure M, Totoson P, Cachot S, Faure P, et al. Intermittent hypoxia in obese Zucker rats: cardiometabolic and inflammatory effects. Exp Physiol 2016;101:1432-1442.

19. Kang HH, Kim IK, Lee HI, Joo H, Lim JU, Lee J, Lee SH, et al. Chronic intermittent hypoxia induces liver fibrosis in mice with diet-induced obesity via TLR4/MyD88/MAPK/NF-kB signaling pathways. Biochem Biophys Res Commun 2017;490:349-355.

20. Wu W, Li W, Wei J, Wang C, Yao Y, et al. Chronic intermittent hypoxia accelerates liver fibrosis in rats with combined hypoxia and nonalcoholic steatohepatitis via angiogenesis rather than endoplasmic reticulum stress. Acta Biochim Biophys Sin (Shanghai) 2019;51:159-1672.

21. Shi YF, Fong CC, Zhang Q, Cheung PY, Tzang CH, Wu RS, Yang M. Hypoxia induces the activation of human hepatic stellate cells LX-2 through TGF-beta signaling pathway. FEBS Lett 2007;581:203-210.

22. Copple BL, Bustamante JJ, Welch TP, Kim ND, Moon JO. Hypoxia-inducible factor-dependent production of profibrotic mediators by hypoxic hepatocytes. Liver Int 2009;29:1010-21.

23. Copple BL, Bai S, Burgoon LD, Moon JO. Hypoxia-inducible factor-1alpha regulates the expression of genes in hypoxic hepatic stellate cells important for collagen deposition and angiogenesis. Liver Int 2011;31:230-244.

24. Povero D, Eguchi A, Li H, Johnson CD, Papouchado BG, Wree A, Messer K, et al. Circulating extracellular vesicles with specific proteome and liver microRNAs are potential biomarkers for liver injury in experimental fatty liver disease. PLoS One 2014;9:e113651.

25. Povero D, Panera N, Eguchi A, Johnson CD, Papouchado BG, de Araujo Horcel L, Pinatel EM, et al. Lipid-induced hepatocyte-derived extracellular vesicles regulate hepatic stellate cell via microRNAs targeting PPAR-gamma. Cell Mol Gastroenterol Hepatol 2015;1:646-663.

26. Hirsova P, Ibrahim SH, Krishnan A, Verma VK, Bronk SF, Werneburg NW, Charlton MR, et al. Lipid-Induced Signaling Causes Release of Inflammatory Extracellular Vesicles From Hepatocytes. Gastroenterology 2016;150:956-967.

27. Cannito S, Morello E, Bocca C, Foglia B, Benetti E, Novo E, et al. Microvesicles released from fat-laden cells promote activation of hepatocellular NLRP3 inflammasome: A pro-inflammatory link between lipotoxicity and non-alcoholic steatohepatitis. PLoS One 2017;12:e0172575.

28. van Niel G, D'Angelo G, Raposo G. Shedding light on the cell biology of extracellular vesicles. Nat Rev Mol Cell Biol 2018;19:213-228.

29. Devhare PB, Ray RB. Extracellular vesicles: Novel mediator for cell to cell communications in liver pathogenesis. Mol Aspects Med 2018;60:115-122.

30. Pradip B. Devhare, Ratna B. Ray. Extracellular vesicles: Novel mediator for cell to cell communications in liver pathogenesis. Mol Aspects Med 2018;60:115-122.

31. Hernández A, Arab JP, Reyes D, Lapitz A, Moshage H, Bañales JM, Arrese M Extracellular Vesicles in NAFLD/ALD: From Pathobiology to Therapy. Cells. 2020 Mar 27;9(4). pii: E817.

32. Pizarro M, Solis N, Quintero P, Barrera F, Cabrera D, Rojas-de Santiago P, Arab JP, et al. Beneficial effects of mineralocorticoid receptor blockade in experimental nonalcoholic steatohepatitis. Liver Int 2015;35:2129-2138.

33. Cabrera D, Wree A, Povero D, Solis N, Hernandez A, Pizarro M, Moshage H, et al. Andrographolide Ameliorates Inflammation and Fibrogenesis and Attenuates Inflammasome Activation in Experimental Non-Alcoholic Steatohepatitis. Sci Rep 2017;7:3491.

34. Chavez-Tapia NC, Rosso N, Tiribelli C. In vitro models for the study of non-alcoholic fatty liver disease. Curr Med Chem 2011;18:1079-1084.

35. Pecoraro M, Pinto A, Popolo A. Inhibition of Connexin 43 translocation on mitochondria accelerates CoCl2-induced apoptotic response in a chemical model of hypoxia. Toxicol In Vitro 2018;47:120-128.

36. Munoz-Sanchez J, Chanez-Cardenas ME. The use of cobalt chloride as a chemical hypoxia model. J Appl Toxicol 2019;39:556-570.

37. Schoemaker MH, de la Rosa L C, Buist-Homan M, et al. Tauroursodeoxycholic Acid protects Rat hepatocytes from Bile Acid-induced apoptosis via activation of survival pathways. Hepatology 2004;39:1563-1573.

38. Chan LL, McCulley KJ, Kessel SL. Assessment of Cell Viability with Single-, Dual-, and Multi-Staining Methods Using Image Cytometry. Methods Mol Biol 2017;1601:27-41.

39. Thery C, Amigorena S, Raposo G, Clayton A. Isolation and characterization of exosomes from cell culture supernatants and biological fluids. Curr Protoc Cell Biol 2006;3:22.

40. Xu L, Hui AY, Albanis E, Arthur MJ, O'Byrne SM, Blaner WS, Mukherjee P, Friedman SL, Eng FJ. Human hepatic stellate cell lines, LX-1 and LX-2: new tools for analysis of hepatic fibrosis. Gut 2005;54:142-51.

41. Feldstein AE, Canbay A, Guicciardi ME, Higuchi H, Bronk S, Gores G. Diet associated hepatic steatosis sensitizes to fas mediated liver injury in mice. J Hepatol 2003;39:978-983.

42. Théry C, Witwer KW, Aikawa E, Alcaraz MJ, Anderson JD, et al. Minimal information for studies of extracellular vesicles 2018 (MISEV2018): a position statement of the International Society for Extracellular Vesicles and update of the MISEV2014 guidelines. J Extracell Vesicles 2018;7:1535750.

43. Vilar-Gomez E, Calzadilla-Bertot L, Wai-Sun Wong V, Castellanos M, Aller-de la Fuente R, et al. Fibrosis Severity as a Determinant of Cause-Specific Mortality in Patients With Advanced Nonalcoholic Fatty Liver Disease: A Multi-National Cohort Study. Gastroenterology. 2018;155:443-457.

44. Mesarwi OA, Shin MK, Drager LF, Bevans-Fonti S, Jun JC, Putcha N, Torbenson MS, Pedrosa RP, Lorenzi-Filho G, Steele KE, Schweitzer MA, Magnuson TH, Lidor AO, Schwartz AR, Polotsky VY. Lysyl Oxidase as a Serum Biomarker of Liver Fibrosis in Patients with Severe Obesity and Obstructive Sleep Apnea. Sleep 2015;38:1583-91.

45. Buttacavoli M, Gruttad'Auria CI, Olivo M, Virdone R, Castrogiovanni A, Mazzuca E, Marotta AM, Marrone O, Madonia S, Bonsignore MR. Liver Steatosis and Fibrosis in OSA patients After Long-term CPAP Treatment: A Preliminary Ultrasound Study. Ultrasound Med Biol 2016;42:104-9.

46. Mesarwi OA, Loomba R, Malhotra A. Obstructive Sleep Apnea, Hypoxia, and Nonalcoholic Fatty Liver Disease. Am J Respir Crit Care Med 2019;199:830-841.

47. Feng SZ, Tian JL, Zhang Q, Wang H, Sun N, Zhang Y, Chen BY. An experimental research on chronic intermittent hypoxia leading to liver injury. Sleep Breath 2011;15:493-502.

48. Friedman S.L. Hepatic stellate cells: protean, multifunctional, and enigmatic cells of the liver. Physiol Rev 2008;88:125-172.

49. Jeon YJ, Song KS, Han HJ, et al. Rosmarinic acid inhibits chemical hypoxia-induced cytotoxicity in primary cultured rat hepatocytes. Arch Pharm Res 2014;37:907-15.

50. Marin JJG, Lozano E, Perez MJ. Lack of mitochondrial DNA impairs chemical hypoxia-induced autophagy in liver tumor cells through ROS-AMPK-ULK1 signaling dysregulation independently of HIF-1α. Free Radic Biol Med 2016;101:71-84.

51. Ricchi M, Odoardi MR, Carulli L, et al. Differential effect of oleic and palmitic acid on lipid accumulation and apoptosis in cultured hepatocytes. J Gastroenterol Hepatol 2009;24:830-40.

52. Moravcova A, Cervinkova Z, Kucera O, Mezera V, Rychtrmoc D, Lotkova H. The effect of oleic and palmitic acid on induction of steatosis and cytotoxicity on rat hepatocytes in primary culture. Physiol Res 2015;64:S627-636.

53. Li, J., et al., Chronic Intermittent Hypoxia Upregulates Genes of Lipid Biosynthesis in Obese Mice. J Appl Physiol .2005;99:1643-8.

54. Chen X, Li L, Liu X, Luo R, Liao G, Li L, Liu J, Cheng J, Lu Y, Chen Y. Oleic acid protects saturated fatty acid mediated lipotoxicity in hepatocytes and rat of non-alcoholic steatohepatitis. Life Sci 2018;203:291-304.

55. Feldstein AE, Werneburg NW, Canbay A, Guicciardi ME, Bronk SF, Rydzewski R, Burgart LJ, Gores GJ. Free fatty acids promote hepatic lipotoxicity by stimulating TNF-alpha expression via a lysosomal pathway. Hepatology 2004;40:185-94.

56. Malhi H, Gores GJ, Lemasters JJ. Apoptosis and necrosis in the liver: a tale of two deaths? Hepatology 2006;43:S31-44.

57. Payance A, Silva-Junior G, Bissonnette J, et al. Hepatocyte Microvesicle Levels Improve Prediction of Mortality in Patients With Cirrhosis. Hepatology 2018;68:1508-1518.

58. Povero D, Eguchi A, Niesman IR, Andronikou N, de Mollerat du Jeu X, Mulya A, Berk M, Lazic M, Thapaliya S, Parola M, Patel HH, Feldstein AE Lipid-induced toxicity stimulates hepatocytes to release angiogenic microparticles that require Vanin-1 for uptake by endothelial cells. Sci Signal 2013;6:ra88.

59. Momen-Heravi F, Bala S, Kodys K, Szabo G. Exosomes derived from alcohol-treated hepatocytes horizontally transfer liver specific miRNA-122 and sensitize monocytes to LPS. Sci Rep 2015;5:9991.

60. Lee Y, Kim S, Ko E, Lee JH, Yi HS,Yoo Y, Je J, et al. Exosomes derived from palmitic acid-treated hepatocytes induce fibrotic activation of hepatic stellate cells. Sci Rep 2017;7:3710.

61. Hernández A, Geng Y, Sepulveda R, Solis N, Torres J, et al. Chemical Hypoxia induces pro-inflammatory signals in fat-laden hepatocytes and contributes to cellular crosstalk with Kupffer cells. Biochim Biophys Acta Mol Basis Dis. 2020;1866:165753

62. Almendros, I., Y. Wang, L. Becker, F.E. Lennon, J. Zheng, B.R. Coats, K.S. Schoenfelt, A. Carreras, F. Hakim, S.X. Zhang, R. Farre, and D. Gozal. Intermittent hypoxia-induced changes in tumor-associated macrophages and tumor malignancy in a mouse model of sleep apnea. Am J Respir Crit Care Med 2014;189:593-601.

63. Ho CM, Ho SL, Jeng YM, Lai YS, Chen YH, Lu SC, Chen HL, Chang PY, Hu RH, Lee PH. Accumulation of free cholesterol and oxidized low-density lipoprotein is associated with portal inflammation and fibrosis in nonalcoholic fatty liver disease. J Inflamm (Lond) 2019;16:7.

64. Luo, Y., H.Y. Dong, B. Zhang, Z. Feng, Y. Liu, Y.Q. Gao, M.Q. Dong, and Z.C. Li. miR-29a-3p attenuates hypoxic pulmonary hypertension by inhibiting pulmonary adventitial fibroblast activation. Hypertension 2015;65:414-420.

65. Khalyfa, A., R. Cortese, Z. Qiao, H. Ye, R. Bao, J. Andrade, and D. Gozal. Late gestational intermittent hypoxia induces metabolic and epigenetic changes in male adult offspring mice. J Physiol 2017;595:2551-2568.

Chapter 6

CASPASE-1 IN EXTRACELLULAR VESICLES DERIVED FROM HYPOXIC, FAT-LADEN HEPATOCYTES PROMOTES INFLAMMASOME ACTIVATION IN KUPFFER CELLS

ABSTRACT

Background: Intercellular crosstalk between hepatocytes and non-parenchymal cells is an important factor in the pathogenesis and progression of non-alcoholic fatty liver disease (NAFLD). Extracellular Vesicles (EV) play an important role in intercellular crosstalk in the context of liver diseases, including NAFLD. Clinical observations have indicated that Obstructive sleep apnea (OSA) is an aggravating factor in NAFLD. Hypoxia is the hallmark of OSAS, however, whether hypoxia modulates the crosstalk between hepatocytes and non-parenchymal cells, in particular Kupffer cells (KCs), has not been investigated yet. **Aim:** to investigate whether hypoxia modulates hepatocellular damage and intercellular crosstalk in the context of NAFLD and whether EVs and inflammasomes are involved in this modulation. **Methods:** Primary rat hepatocytes and the human hepatoma cell line HepG2 were treated with free fatty acids (FFAs) and chemical hypoxia (CH) was induced by cobalt (II)chloride ($CoCl_2$). Triglyceride content (TG), pyroptotic cell death (LDH release), mitochondrial superoxide generation and inflammasome-related gene expression were assessed in hypoxic fat-laden hepatocytes and in liver tissue. Intermittent Hypoxia (IH) was applied to mice fed a CDAA diet (NASH model). EVs were isolated from conditioned medium (CM) or serum by ultracentrifugation and characterized by nanoparticle tracking and electron microscopy. Cleaved caspase-1 and caspase-1 activity were measured by Western blot and enzymatic assay respectively. **Results:** Chemical hypoxia in fat-laden hepatocytes increased TG content, LDH release, superoxide generation, expression of inflammasome-related genes and release of EVs compared to non-treated hepatocytes. These results correlated with the *in vivo* results. Treatment of KC cells with EVs from fat-laden hypoxic hepatocytes increased pro-inflammatory and inflammasome-related gene expression in KCs compared to KC treated with EVs from non-treated hepatocytes. Cleaved caspase-1 content and activity of caspase-1 was increased in EVs from hypoxic fat-laden hepatocytes and from serum of CDAA-fed animals exposed to IH. **Conclusion:** Our findings indicate that hypoxia induces the release of EVs from fat-laden hepatocytes promoting the inflammatory phenotype in Kupffer cells via a caspase-1/inflammasome-mediated mechanism. These findings suggest EVs and their content (caspase-1) as a potential novel biomarker in NAFLD and OSAS.

1.- INTRODUCTION

Significant advances have been made in understanding the importance of intercellular communication between hepatocytes and non-parenchymal cells in the pathogenesis of liver diseases (1,2). In particular in the pathophysiology of non-alcoholic steatohepatitis (NASH), the inflammatory and progressive form of non-alcoholic fatty liver disease (NAFLD), Kupffer cells (KCs), the liver-resident macrophages, are considered to play a key role in the inflammatory response and disease progression (2,3). Indeed, it has been demonstrated that KC activation promotes steatosis, inflammation and fibrosis in NASH (4-7). An early event in the pathogenesis of NAFLD is the increased accumulation of lipids in the liver, in particular in hepatocytes. This lipid accumulation promotes cytotoxic effects known as lipotoxicity, resulting in hepatocellular damage and triggering of inflammatory signaling (8-10). Emerging data suggest that lipotoxic hepatocytes release extracellular vesicles (EV) to neighboring target cells in an autocrine/paracrine manner and in this way promote liver damage (11). EVs are 50-150 nanometer-sized vesicles released after the fusion of multivesicular bodies or directly from the cell membrane (12). Their cargo is diverse and may contain proteins, various RNA species and/or lipids (13).

Several studies have indicated the importance of EVs in the crosstalk between injured hepatocytes and KCs (14-17). Moreover, increased levels of EVs have been reported in serum of mice and humans with NASH and these levels correlate with histological liver inflammation and macrophage activation (18-21). Recent data have also indicated that injured hepatocytes release inflammasome components into the extracellular environment, providing a mechanism to spread inflammasome signaling to adjacent cells (22,23). The activation of the inflammasome promotes the maturation and release of pro-inflammatory interleukins via activation of caspase-1. The active caspase-1 is composed of a tetramer containing two 20 kDa fragments and two 10 kDa fragments (24). The activation of caspase-1 initiates a novel form of programmed necrotic cell death named pyroptosis. Pyroptotic cells release proinflammatory cytokines like IL-1β and IL-18 and the intracellular enzyme lactate dehydrogenase (LDH) via gasdermin-dependent pores in the plasma membrane (25,26). Recent studies have indicated that caspase-1 activation plays an important role in inflammation and fibrosis in NASH (27,28). A recent study reported the presence of caspase-1 in EVs released from monocytes that induced endothelial cell death in a model of lung injury (29). However, the presence and role of caspase-1 in EVs in the context of NASH has not been studied yet.

Emerging evidence from clinical studies indicates that intermittent hypoxia (IH), the principal pathophysiological factor in obstructive sleep apnea (OSA), aggravates NAFLD (30). Indeed, there is substantial evidence from rodent models and human subjects that IH associated with OSA increases

hepatic triglyceride (TG) levels and exacerbates inflammation and fibrosis in NASH (31-35). Although the precise molecular mechanisms underlying the aggravating effect of IH on NASH have not been elucidated yet, the activation of the transcription factor hypoxia inducible factor 1 alpha (HIF-1α) appears to be an important factor. Hepatic HIF-1α activation increases steatosis and promotes pro-inflammatory and pro-fibrotic signaling pathways (35-38).

Taken together, there is strong evidence that hypoxia via HIF-1α and Inflammasome/Caspase-1 activation is an aggravating factor in NASH. However, it is still not fully understood whether caspase-1 participates in hypoxia-induced liver injury.

In the present study we have investigated the role of hypoxia and EVs in *in vivo* and *in vitro* models of NASH. We demonstrate that hypoxia increases mRNA levels of inflammasome components, caspase-1 activation, incorporation of caspase-1 in EVs and cellular crosstalk between hypoxic, fat laden-hepatocytes and Kupffer cells.

2.- MATERIALS AND METHODS

2.1 Animals

Specified pathogen-free male Wistar rats (220–250 g; Charles River Laboratories Inc., Wilmington, MA, USA) and male C57bl6 mice [purchased from Jackson Laboratories (Bar Harbor, ME)] were used. Animals were housed under standard laboratory conditions with free access to standard laboratory chow diet and water. All experiments were carried out according to the Dutch and Chilean laws on the welfare of laboratory animals and guidelines of the local institutional animal care and use committees of the Pontificia Universidad Católica de Chile and ethics committee of the University of Groningen for care and use of laboratory animals. All efforts were made to minimize animal suffering and to reduce the number of animals used.

2.2 Hepatocyte isolation

Primary hepatocytes were isolated using a two-step collagenase perfusion method as described previously (39). Trypan blue staining was used as viability test and only hepatocyte isolations with a viability above 85% were used. The animals were housed in a 12 hours light-dark cycle, with free access to chow and water and treated following the guidelines of the local committee for care and use of laboratory animals from the University of Groningen. After isolation, 750.000 cells/mL were cultured in collagen-coated plates with William's E medium (Gibco, California, USA), supplemented with 5% fetal bovine serum (FBS, Gibco), 50 µg/ml gentamycin (BioWhittaker, Verviers) and 50 nmol/l dexamethasone (Sigma) for 4 hours at 37°C and 5% CO_2 to allow cells to attach. After the

attachment period, hepatocytes were cultured in William's E medium supplemented with 50 µg/ml gentamycin, 10% FBS and 1% of p/s/f for 18 hours until the start of the experiments.

2.3 Kupffer cell isolation

Kupffer cells were isolated from the non-parenchymal cell fraction obtained during the hepatocyte isolation. The supernatant was subjected to different low-speed centrifugations at 4°C and resuspending the pellets in Hank's Balanced Salt Solution (HBSS) (Gibco, California, USA) supplemented with 0.3% bovine serum albumin (BSA). KC were purified using a 20% of density gradient medium OptiPrepTM (Sigma-Aldrich). After different low-speed centrifugations, the final pellet was dissolved in HBSS supplemented with 10% FBS to allow cells to attach. After the attachment period, KC were cultured in William's E medium supplemented with 50 µg/ml gentamycin, 10% FBS and 1% of p/s/f for 18 hours until the start of the experiments.

2.4 HepG2 hepatoma cell line

The human hepatocellular carcinoma cell line HepG2 (ATCC, USA) was cultured in Dulbecco's modified Eagle medium (1X) + GlutaMAX™- I (DMEM, 10569010, Gibco) supplemented with 10% fetal bovine serum (FBS; Gibco) and 1% penicillin-streptomycin (Gibco) at 37°C and 5% CO_2. All cells were plated in a cell culture plate at least 24 h -36 h before treatment upon reaching 80% confluence.

2.5 Treatment with free fatty acids and chemical hypoxia

In order to assess the effects of hypoxia on fat-laden liver cells, rat hepatocytes or HepG2 cells were incubated with a mixture of free fatty acids (FFA) consisting of oleic acid (500 µmol/L) and palmitic acid (250 µmol/L) in an aqueous solution of BSA as described (41). Incubations were carried out with or without Cobalt(II)chloride ($CoCl_2$; Sigma Aldrich) (200 µmol/L) for 24 hours to induce chemical hypoxia (40). $CoCl_2$ is a well-known hypoxia-mimetic agent, that mimics hypoxia/ischemic conditions by stabilization of hypoxia-inducible factor HIF-1α (42). Control cells were treated with BSA alone. To obtain the corresponding conditioned medium (CM), the hepatocyte culture medium was replaced after treatment by FBS-free medium for an additional 24 hours.

2.6 Effects of intermittent hypoxia in experimental NASH

Animal experiments were approved by the institutional animal care and use committee (Comité de ética y bienestar Animal, Escuela de Medicina, Pontificia Universidad Católica de Chile, CEBA 100623003). Male C57BL/6 mice aged 10 weeks at the beginning of the study were divided into four experimental groups (n = 4–8) receiving either choline-deficient amino acid-defined (CDAA) diet (Catalog # 518753, Dyets Inc. Bethlehem, PA) to induce NASH or the choline-supplemented L-amino

acid defined (CSAA, Catalog # 518754, Dyets Inc. Bethlehem, PA) diet as control for 22 weeks as previously described (43, 44). Animals were exposed to IH or normoxia (chambers 41x22x35 cm, COY lab products™, Grass Lake, MI, USA) during the last 12 weeks of the experimental or control feeding period. IH regimen consisted of 30 events/hour of hypoxic exposures for 8 hour/day during the rest cycle, between 9 am and 5 pm. This cycle was repeated 7 days a week for 12 consecutive weeks. At the end of the study, mice were anesthetized (ketamine 60 mg/kg plus xylazine 10 mg/kg intraperitoneally) and then euthanized by exsanguination. Serum and liver tissue samples were collected and processed or stored at −80 °C until analyzed. Gene expression and protein analyses were carried out as described above.

2.7 Western Blot analyses

Protein lysates were collected by scraping cells in lysis buffer (HEPES 25 mmol/L, KAc 150 mmol/L, EDTA pH 8.0 2mmol/L, NP-40 0.1%, NaF 10 mmol/L, PMSF 50 mmol/L, aprotinin 1 µg/µL, pepstatin 1 µg/µL, leupeptin 1 µg/µL, DTT 1 mmol/L). Total amount of protein in lysates was measured by Bio-Rad protein assay (Bio-Rad; Hercules, CA, USA). For Western blot, 30-50 µg protein was resolved on Mini-PROTEAN® TGX Stain-Free™ Precast Gels (BioRad, UK, Oxford). Semi dry-blotting was performed using Trans-Blot Turbo Midi Nitrocellulose Membrane with Trans-Blot Turbo System Transfer (BioRad). Ponceau S 0.1% w/v (Sigma) staining was used to confirm protein transfer. Monoclonal mouse anti-HIF1α 1:1000 (Abcam, USA), polyclonal rabbit anti-ASGPR1 1:1000 (Novus, USA) and monoclonal mouse anti-CASP1 1:500 (Santa Cruz, INC) were used in combination with appropriate peroxidase-conjugated secondary antibodies. Monoclonal mouse anti-tubulin or actin were used as loading controls (Sigma, USA). The blots were analyzed in a ChemiDoc XRS system (Bio-Rad). Protein band intensities were quantified by ImageLab software (BioRad).

2.8 Nile red staining and Triglycerides assay

Intracellular lipid droplets in the HepG2 cells were detected with Nile Red fluorescent probe (N1142, Thermo Fisher). HepG2 cells were grown in 96-well plates and treated with FFA and/or $CoCl_2$. After treatment, the cells were washed twice with PBS and stained with Nile Red solution for 10 min in the dark. The cells were then washed twice with PBS and stained with Hoechst dye (33342, Thermo Fisher). The fluorescence intensity of each well was analyzed with excitation/emission wavelength at 488 nm/550 nm using a microplate reader. The fluorescence images were recorded using an inverted fluorescence microscope. For TG assay, primary hepatocytes cultured in 12-well plates were treated with FFA and $CoCl_2$ for 24 h. Intracellular TG content was determined using Triglyceride Quantification Assay kit (Abcam, ab65336) according to the manufacturer's instructions and normalized to protein concentration.

2.9 Lactate dehydrogenase (LDH) release assay

Necrotic cell death was quantified by LDH measurement in primary hepatocytes and HepG2 cells as previously described (45). Briefly, the LDH release or leakage was calculated as the percentage of the activity of LDH released in the medium vs. the total LDH activity, both in the medium and cell lysates. The LDH activity was measured spectrophotometrically at 340 nm using a Bio-Tek Epoch2 microplate reader (Bio-Tek Instruments, Inc., Bad Friedrichshall, Germany).

2.10 Mitochondrial superoxide detection

HepG2 cells cultured on glass cover slides were treated with FFA and/or $CoCl_2$ for 24 h. At the end of treatment, hepatocytes were washed once with warm HBSS followed by incubation with 200 nmol/L MitoSOX™ Red (to detect mitochondrial superoxide) (Molecular Probes; Invitrogen) in William's E medium for 15 min at 37°C protected from light. Then, cells were washed with warm HBSS and mounted onto glass slides using DAPI staining solution (Invitrogen). The fluorescence analyse was immediately recorded using a fluorescent microscope at a wavelength of 510/580 nm (Ex/Em) by a Leica microscope. Quantification of fluorescence in microscopic images of MitoSOX was performed using ImageJ software.

2.11 RNA isolation and quantitative real-time reverse transcription polymerase chain reaction (qRT-PCR)

After treatment, HepG2 cells and rat hepatocytes were harvested on ice and washed twice with ice-cold PBS. Total RNA was isolated with TRI-reagent (Sigma) according to the manufacturer's instructions. Reverse transcription (RT) was performed using 2.5 µg of total RNA, 1X RT buffer (500 mmol/l Tris-HCl [pH 8.3]; 500 mmol/l KCl; 30 mmol/l MgCl2; 50 mmol/l DTT), 1 mmol/l deoxynucleotides triphosphate (dNTPs, Sigma), 10 ng/µl random nanomers (Sigma), 0.6 U/µl RNaseOUT™ (Invitrogen) and 4 U/µl M-MLV reverse transcriptase (Invitrogen) in a final volume of 50 µl. The cDNA synthesis program was 25°C/10 min, 37°C/60 min and 95°C/5 min. Complementary DNA (cDNA) was diluted 20X in nuclease-free water. Real-Time qPCR was carried out in a StepOnePlus™ (96-well) PCR System (Applied Biosystems, Thermofisher) using TaqMan probes. The sequences of the probes and primer sets are described in Supplementary Material. For qPCR, 2X reaction buffer (dNTPs, HotGoldStar DNA polymerase, 5 mmol/l MgCl2) (Eurogentec, Belgium, Seraing), 5 µmol/l fluorogenic probe and 50 µmol/l of sense and antisense primers (Invitrogen) were used. mRNA levels were normalized to the housekeeping gene 18S and further normalized to the mean expression level of the control group. Relative gene expression was calculated using the ΔCt method. The sequences of the probes and primer sets are described in the Supplementary Material.

2.12 Extracellular vesicles isolation

For EV collection, HepG2 cells were grown in culture dishes of 100 mm to obtain 70 ml of serum-free conditioned media after 24 hours of treatment. EVs were isolated from conditioned medium by differential ultracentrifugation (UCF Thermo-Sorvall 80wx+) according to a modified protocol described previously (46). A total volume of 70 ml medium per treatment was depleted of cells and cell debris by consecutive, low-speed centrifugations (2,000 × g for 30 min and 12,000 × g for 45 min). The resulting supernatants were carefully collected and centrifuged for 70 min at 120,000 × g at 4 °C. Pellets from this centrifugation step were washed in PBS, pooled and centrifuged again for 60 min at 100,000 × g at 4 °C. For EV collection from serum, samples were reconstituted in a total volume of 4.4 mL and centrifugated at 2,000 × g for 30 min and 10,000 × g for 30 min. The resulting supernatants were carefully collected and centrifuged for 70 min at 120,000 × g at 4 °C. Pellets from this centrifugation step were washed in PBS, pooled and centrifuged again for 60 min at 100,000 × g at 4 °C. The obtained pellets from HepG2 cells or serum were resuspended in lysis buffer or PBS depending on subsequent experiments and stored in aliquots at -80 °C. Protein from HepG2-derived EVs or serum-derived EVs were obtained using the Total Exosome Protein Isolation kit (Invitrogen). Protein concentration in EV pellets were measured using BCA protein assay kit (Pierce, Rockford, IL).

2.13 Nanoparticle tracking analysis

Concentration and size distribution of isolated EVs were assessed by nanoparticle tracking analysis (NTA) using NanoSight NS300 instrumentation(Marvel, Egham, UK). EV samples were diluted with PBS to a concentration of 10^8 to 10^9 particles/mL in a total volume of 1 ml. Each sample was continuously run through a flow-cell top-plate set up at 18°C using a syringe pump. At least three videos of 20 seconds documenting Brownian motion of nanoparticles were recorded and at least 1000 completed tracks were analyzed by NanoSight software (NTA v3.2).

2.14 Transmission electron microscopy

Isolated EVs were fixed in 2% paraformaldehyde in 0.1 M phosphate buffer overnight at 4 °C. The samples were then placed on Formvar/Carbon 300 Mesh (FCF300-CU, EMS) grid and air dried for 10 min. The grids were first contrasted with uranyl-oxalate solution and then contrasted and embedded in a mixture of 4% uranyl acetate. The grids were air dried and visualized with a Philips Tecnai 12 (Biotwin, Eindhoven, Netherlands) electron microscope at 80 kV. The images were captured with the software Item Olympus Soft Imaging Solutions (Windows NT 6.1).

2.15 Treatment of Kupffer cells with extracellular vesicles

Rat primary Kupffer cells (KCs) were incubated with FBS-free William's E medium and exposed to 15 µg of EVs isolated from HepG2 cells treated with $CoCl_2$, FFA or $CoCl_2$ + FFA for 24h. After 24h of treatment, KCs were harvested.

2.16 Caspase-1 activity

HepG2-derived EVs or serum-derived EVs were assayed for their ability to cleave a fluorescent CASP-1 substrate, following the manufacturer's instructions (Abcam, USA).

2.17 Statistical analyses

Analyses were performed using GraphPad software (version 5.03, GraphPad Software Inc., CA, USA). All results are presented as a mean of at least 3 independent experiments ± SEM or as absolute number or percentage for categorical variables. The statistical significance of differences between the means of the experimental groups was evaluated using one-way analysis of variance (ANOVA) with a post-hoc Bonferroni multiple-comparison test; $P<0.05$ was considered as statistically significant.

3.- RESULTS

3.1 Chemical hypoxia stabilizes HIF-1α and promotes accumulation of lipids droplets, mitochondrial superoxide formation and necrotic cell death in fat-laden hepatocytes: To investigate whether hypoxia exacerbates lipotoxicity, fat-laden primary rat hepatocytes and HepG2 cells were treated with $CoCl_2$, a hypoxia mimetic agent that promotes the accumulation HIF-1α. $CoCl_2$ increased protein levels of HIF-1α in both control and fat-laden hepatocytes (Figure 1a). Cells treated with FFA accumulated more lipids compared to non-treated cells, as indicated by Nile Red staining and triglyceride determination (Figure 1c). Lipid accumulation was further enhanced by treatment with $CoCl_2$ indicating that hypoxia exarcebates steatosis in hepatocytes.

We next determined the effect of hypoxia and steatosis on necrotic cell death and mitochondrial superoxide generation. Hypoxia increased LDH release by 105.4% % and 135.7% in fat-laden rat-hepatocytes and fat-laden HepG2 cells respectively, compared to controls. Mitochondrial superoxide generation was significantly increased in hypoxic cells compared to controls and was even further increased by the combination of steatosis and hypoxia (figure 1E). These data indicate that chemical hypoxia promotes oxidative stress via increased mitochondrial superoxide generation and that steatosis further enhances this mitochondrial oxidative stress.

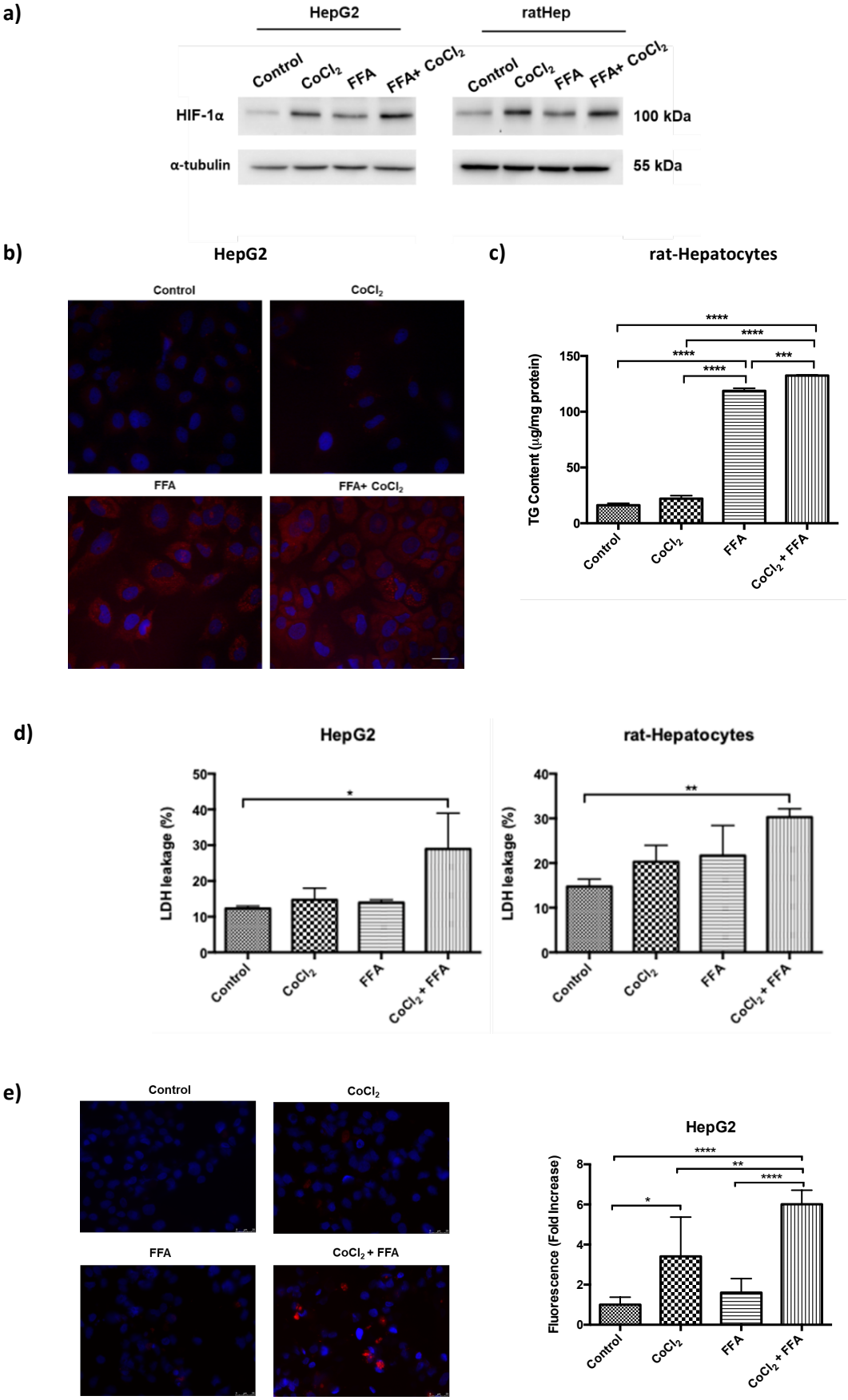
a)
HepG2
ratHep
Control
CoCl2
FFA
FFA+ CoCl2
HIF-1α
α-tubulin
100 kDa
55 kDa
b)
HepG2
Control
CoCl2
FFA
FFA+ CoCl2
c)
rat-Hepatocytes
TG Content (µg/mg protein)
d)
HepG2
rat-Hepatocytes
LDH leakage (%)
e)
Control
CoCl2
FFA
CoCl2 + FFA
HepG2
Fluorescence (Fold Increase)

Figure 1. Chemical hypoxia stabilizes HIF-1α, increases triglyceride content, necrotic cell death and mitochondrial superoxide generation in steatotic hepatocytes. HepG2 cells and primary rat hepatocytes were incubated for 24 h with oleic acid and palmitic acid (2:1 ratio) (FFA) in the presence or absence of $CoCl_2$ (200 µmol/L. a) Protein levels of HIF-1α were determined by Western Blot as described in Material and Methods. α-tubulin was used as loading control. b) Nile Red was used to obtain fluorescent images of intracellular lipid droplets in HepG2 cells and c) Rat hepatocytes were used to measure triglyceride (TG) content as described in Materials and Methods. d) Necrosis was quantified by LDH leakage shown as a percentage of total LDH release in the medium and e) Superoxide generation by mitochondria was determined using MitoSOX™ fluorogenic probe as described in Materials and Methods. Data were shown as mean ± SEM (n ≥ 3) * indicates P < 0.05; ** indicates P < 0.01; *** indicates P < 0.005; **** indicates P < 0.001.

3.2 Effect of chemical hypoxia on inflammasome-related gene expression in fat-laden hepatocytes: To evaluate whether hypoxia promotes the inflammatory phenotype in fat-laden hepatocytes, we measured the mRNA levels of inflammasome-related genes. In accordance to previous data, fat-laden and hypoxic hepatocytes exhibit increased expression of inflammasome genes compared to non-treated cells (Figure 2).

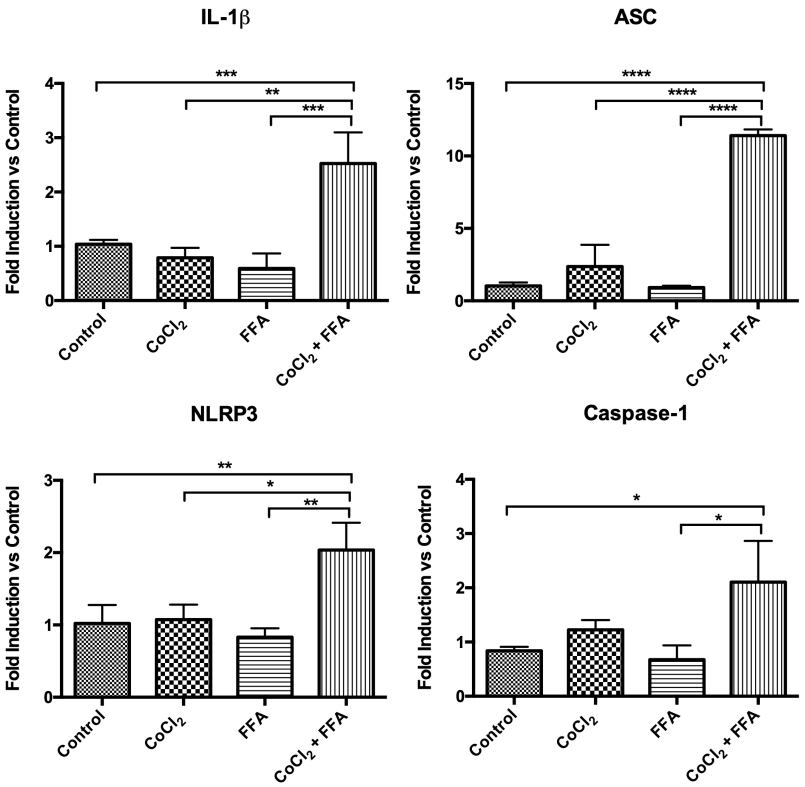

Figure 2. Hypoxia increases the expression of inflammasome-related genes in fat-laden hepatocytes. Primary hepatocytes were incubated for 24h with oleic acid and palmitic acid 2:1 (FFA) in the presence or absence of 200 µM $CoCl_2$. Gene expression of IL-1β, ASC, Caspase-1 and NLRP3 were measured as described in Materials and Methods. Data were shown as mean ± SEM (n ≥ 3) * indicates P < 0.05; ** indicates P < 0.01; *** indicates P < 0.005; **** indicates P < 0.001.

3.3 Hypoxia in fat-laden hepatocytes increases the release of extracellular vesicles that promote inflammasome activation and the inflammatory phenotype in Kupffer cells: We next tested whether EVs from hypoxic and steatotic hepatocytes promote the pro-inflammatory phenotype in KC. EVs were isolated from conditioned medium of HepG2 cells (HepG2-EV) following different treatments. EVs were characterized by their typical structure visualized by TEM and detection of the positive EV marker CD81 and the negative EV marker Bcl-2 by Western blot. In addition, size and concentration of HepG2-EV were determined by NTA. Fat-laden HepG2 cells showed a significant increase in the release of EVs compared to control, which was further increased by $CoCl_2$-treatment (Figure 3C).

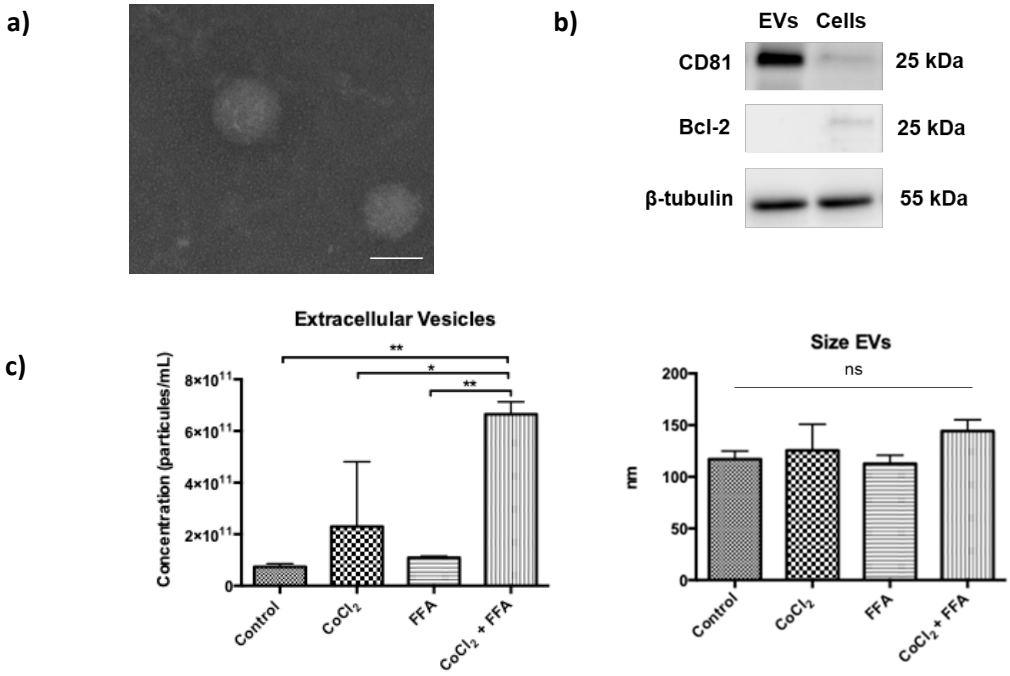

Figure 3. Hypoxia in fat-laden HepG2 cells increases the number of extracellular vesicles. EVs were isolated from conditioned medium from control HepG2 cells by a) electron microscopy; b) detection of the EV-positive marker CD81 and the EV negative marker Bcl-2 by Western blot and c) EV quantification and size determination after different treatments performed by NTA as described in Material and Methods. Data were shown as mean ± SEM (n ≥ 3) * indicates P < 0.05; ** indicates P < 0.01 ns: no statistically significant difference. Scale Bar: 100 µm.

We next investigated the effect of different HepG2-derived EVs on Kupffer cells. KCs were treated with 15 µg/ml of HepG2-EV from each treatment and gene expression of inflammasome components was evaluated. As shown in Figure 4, HepG2-EVs from steatotic+hypoxic condition significantly increased gene expression of the inflammasome components NLRP3, ASC, Caspase-1 and IL-1β in KC (Figure 4). HepG2-EVs from steatotic and hypoxic conditions also significantly increased gene expression of IL-6, iNOS and TNF-α (Figure 5). These results suggest a synergistic effect of steatosis and hypoxia on the pro-inflammatory effect of HepG2-derived EVs on KCs.

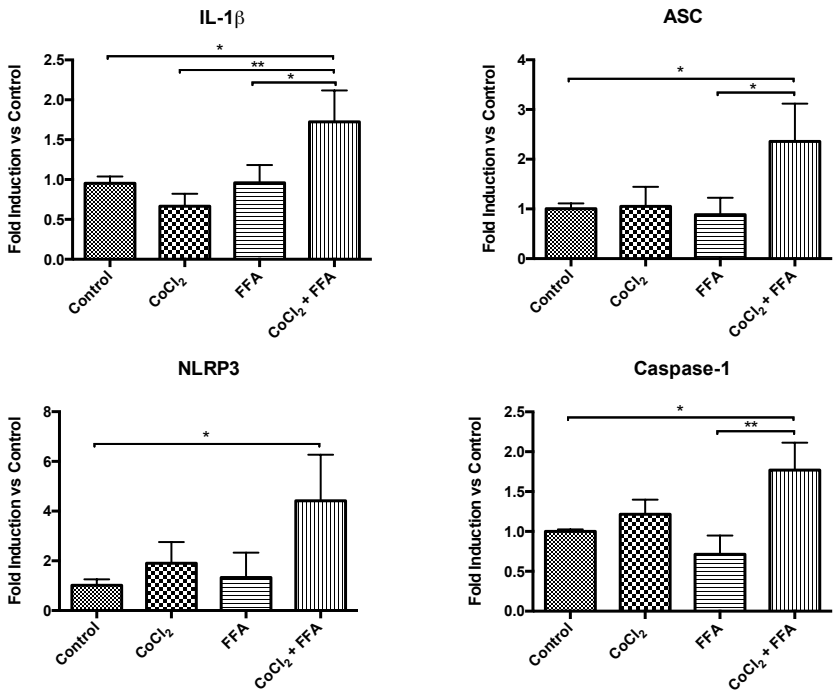

Figure 4. EVs from hypoxic, fat-laden HepG2 cells increase the expression of inflammasome components and cytokines in Kupffer cells. Kupffer cells were exposed to 15 µg of EVs isolated from HepG2 cells that had been treated with $CoCl_2$, FFA and $CoCl_2$ + FFA for 24h. mRNA levels of NLRP3, ASC, Caspase-1 and IL-1β were measured as described in Material and Methods. Data were shown as mean ± SEM (n ≥ 3) * indicates P < 0.05; ** indicates P < 0.01.

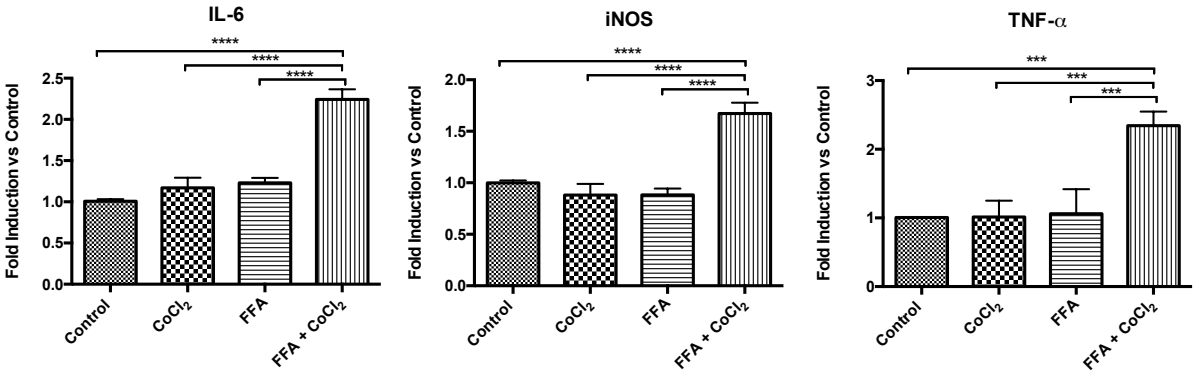

Figure 5. EVs from hypoxic, fat-laden HepG2 cells increase the expression of pro-inflammatory cytokines in Kupffer cells. Kupffer cells were exposed to 15 µg of EVs isolated from HepG2 cells treated with $CoCl_2$, FFA and $CoCl_2$ + FFA for 24h. mRNA levels of IL-6, iNOS and TNF-α were measured as described in Material and Methods. Data were shown as mean ± SEM (n ≥ 3) *** indicates P < 0.005; **** indicates P < 0.001.

3.4 Extracellular vesicles from steatotic and hypoxic HepG2 cells contain increased levels of active caspase-1: We next investigated whether EVs obtained from hypoxic and fat-laden HepG2 cells are enriched in (active) caspase-1. Protein levels of pro-caspase-1 and cleaved caspase-1 (p10 and p20) and the activity of caspase-1 were determined in purified EVs. EVs isolated from hypoxic fat-laden HepG2 cells contain significantly increased levels of active caspase-1 compared to all other groups (Figure 6).

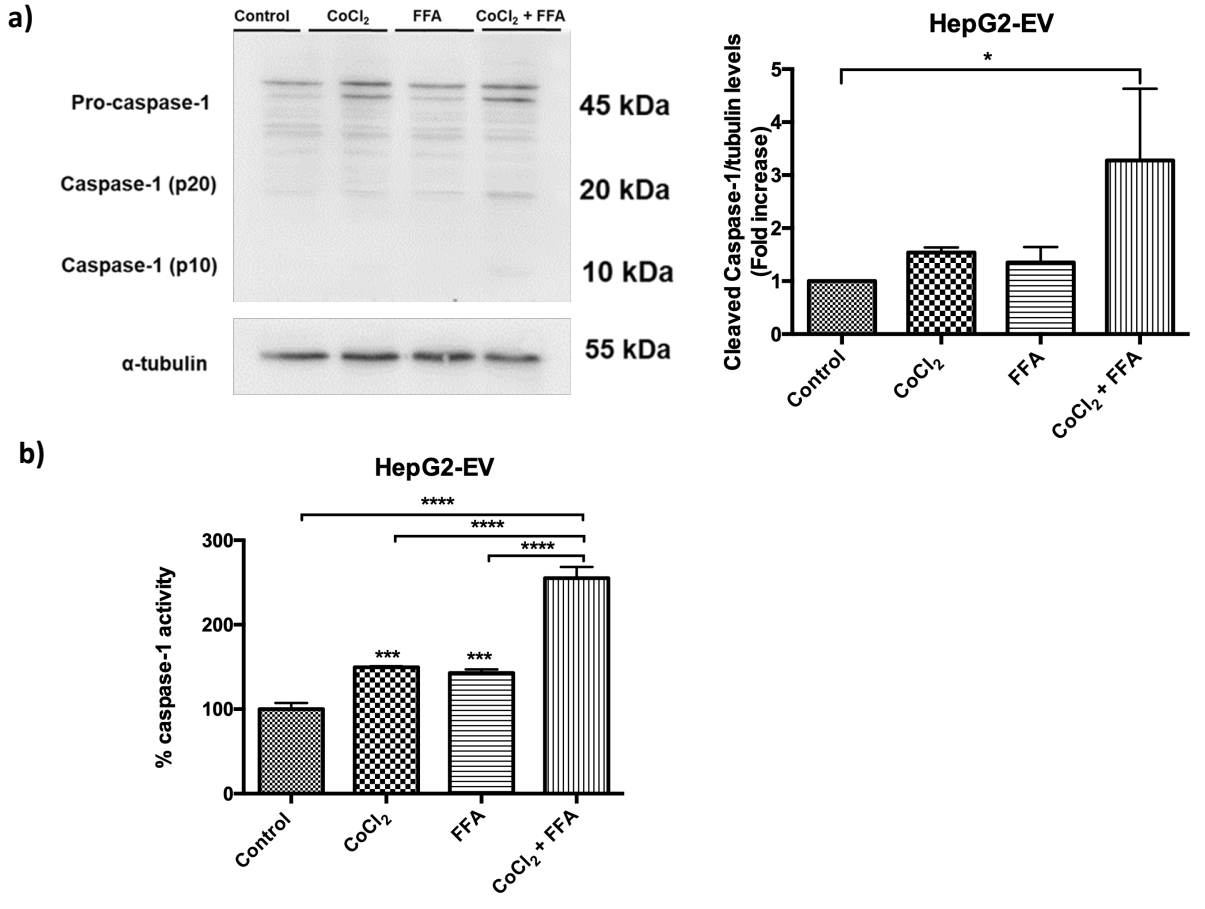

Figure 6. EVs from steatotic and hypoxic HepG2 cells have increased levels of cleaved caspase-1 and caspase-1 activity. a) Western Blot analyses of pro-caspase-1 and cleaved caspase-1 (sum of p10 and p20) and b) the activity of caspase-1 from purified EVs were measured as described in Material and Methods. Data were shown as mean ± SEM (n ≥ 3) * indicates P < 0.05; **** indicates P < 0.001.

3.5 Intermittent hypoxia in an experimental model of diet-induced non-alcoholic steatohepatitis increases levels of active caspase-1 and circulating EVs: In order to validate our *in vitro* findings, we tested the effect of intermittent hypoxia for 12 weeks in an animal model of CDAA diet-induced NASH on caspase-1 activation and levels of circulating EVs. We demonstrate that IH in mice with NASH significantly increased hepatic active caspase-1 levels and caspase-1 activity (Figure 7) as well as the amount of circulating EVs in serum (Figure 8). Finally, we demonstrate increased caspase-1 activity in circulating EVs isolated from mice subjected to IH and NASH compared to EVs isolated from all other groups (Figure 9).

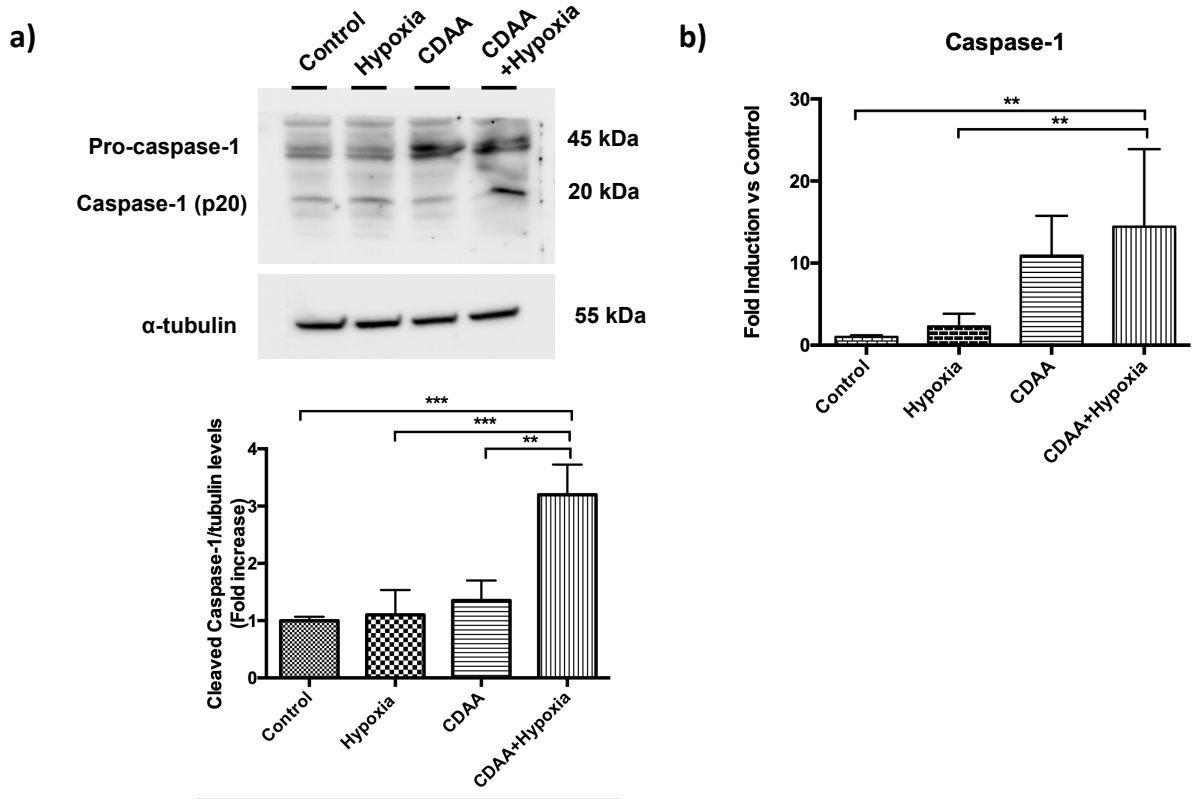

Figure 7. Intermittent hypoxia in an experimental model of diet-induced non-alcoholic steatohepatitis increased caspase-1 activation in the liver. The mice were placed on choline-supplemented L-amino acid defined (CSAA) diet as control or defined diet with choline deficiency amino acids (CDAA) for 22 weeks to induce liver injury and intermittent hypoxia (IH) or normoxia was applied for the last 12 weeks of the diet as described in Materials and Methods. a) Protein levels of pro-caspase-1 and cleaved caspase-1 (p20) were determined by Western Blot as described in Materials and Methods. α-Tubulin was used as a loading control. b) mRNA levels of caspase-1 were measured as described in Materials and Methods. Data were shown as mean ± SEM (n ≥ 3) ** indicates P < 0.01; *** indicates P < 0.005.

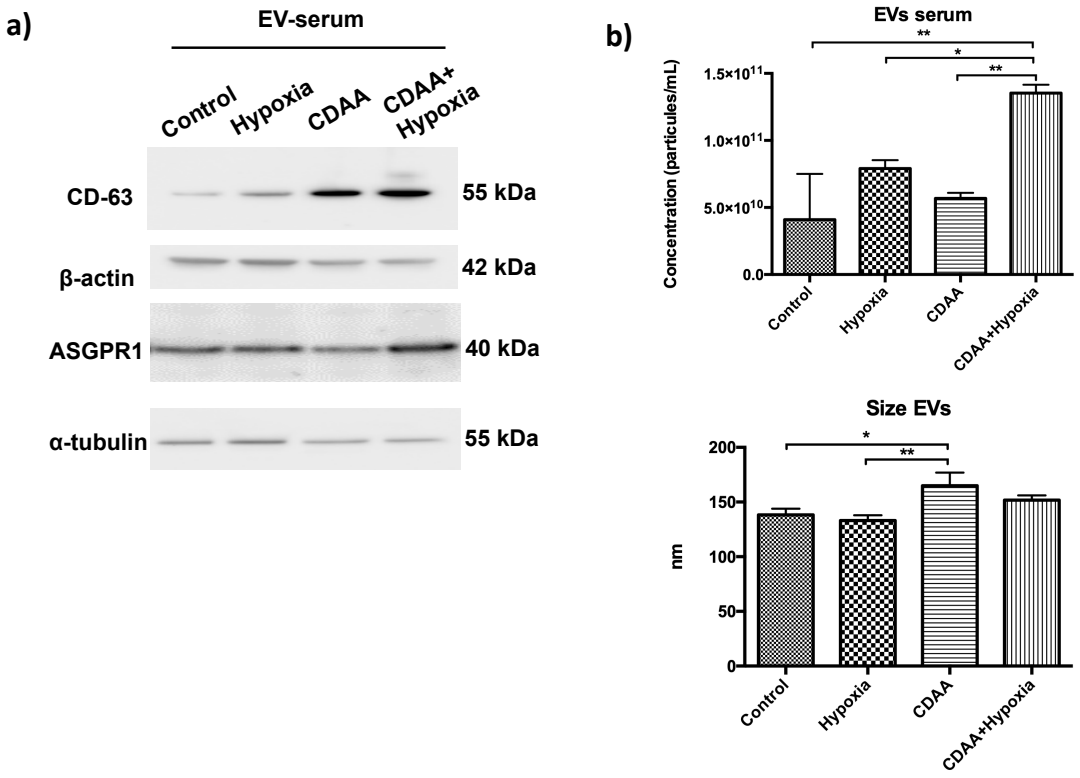

Figure 8. Intermittent hypoxia (IH) increases number of extracellular vesicles in a model of diet-induced NASH. a) Circulating EVs were characterized by detection of EV-positive marker CD63 and hepatic positive marker asialoglycoprotein receptor (ASGRP1) by Western blot and b) EV quantification and EV size by NTA as described in Material and Methods. Data were shown as mean ± SEM (n ≥ 3) * indicates P < 0.05; ** indicates P < 0.01.

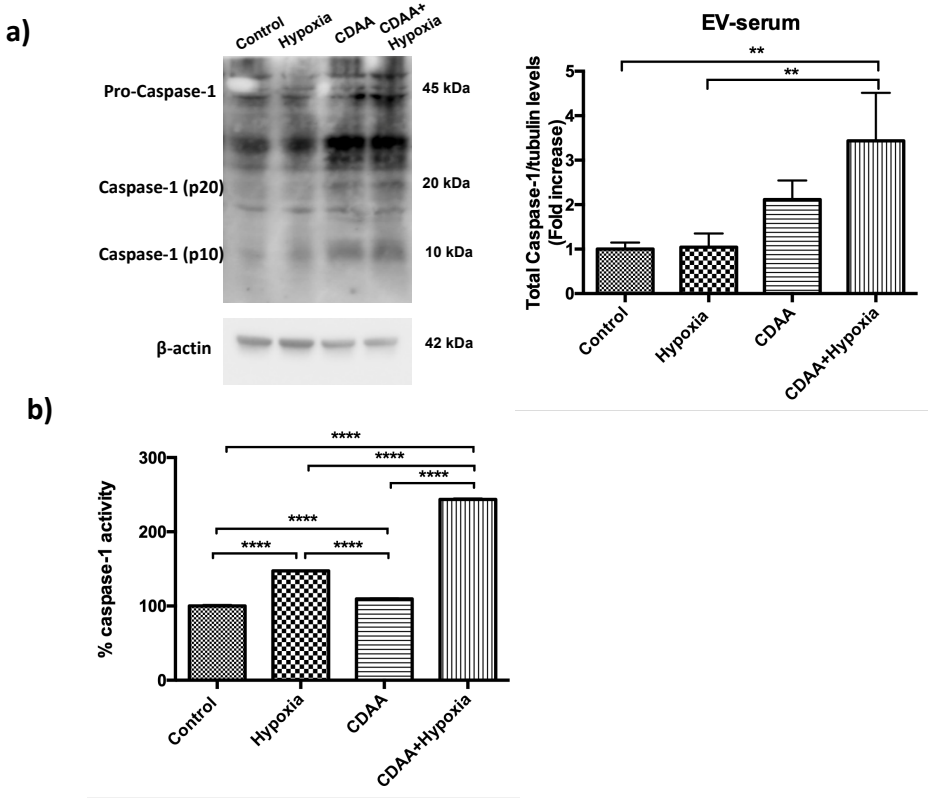

Figure 9. Extracellular vesicles from CDAA diet-fed mice subjected to Intermittent Hypoxia are enriched in caspase-1. a) Western Blot analysis of pro-caspase-1 and cleaved caspase-1 (p10 and p20) and b) the activity of caspase-1 from purified circulating EVs were measured as described in Materials and Methods. Data were shown as mean ± SEM (n ≥ 3) ** indicates P < 0.01; **** indicates P < 0.001.

4.- DISCUSSION

The principal finding of this study is that extracellular vescicles from hepatocytes play an important role in intercellular communicationin the context of NAFLD. Specifically, we have shown that EVs from fat-laden and hypoxic hepatocytes induce a pro-inflammatiory phenotype in Kupffer cells, which contributes to the initiation and progression of inflammation in NASH. The induction of this pro-inflammatory phenotype is at least in part mediated by active caspase-1, and possibly other components of the inflammasome, contained within EVs.

In recent years, different studies have provided evidence that hepatocyte injury induces a pro-inflammatory response in macrophages via the release of hepatocyte-derived EVs, thus contributing to the development and progression of NAFLD (47). The progression from simple steatosis to NASH is not completely understood. The onset and progession of NAFLD from simple steatosis to inflammation (NASH) is most likely the result of multiple factors acting in parallel or sequentially (48). The recent clinical observation that obstructive sleep apnea syndrome (OSAS) is a predictive factor for the progression and aggravation of NAFLD, prompted us to consider hypoxia, the hallmark of OSAS, as an important trigger for hepatocellular damage, excarcebating lipotoxicity and inflammation and increasing the release of EVs. We tested our hypothesis both *in vivo* and *in vitro*. Our *in vitro* study using HepG2 cells and primary rat hepatocytes demonstrates that hypoxia, mimicked by the HIF-1α stabilizer $CoCl_2$, further increases hepatocellular TG content, pyroptosis-induced cells death and mitochondrial ROS generation in FFA-treated hepatocytes. Moreover, chemical hypoxia increased mRNA levels of inflammasome components. These results are in line with our previous studies that hypoxia exacerbates apoptotic cell death determined by caspase-3 and promotes disruption of cellular membranes in fat-laden hepatocytes (Hernandez et al 2019. *Submitted under revision*). Moreover, we demonstrated an increase in the amount of EVs from conditioned medium obtained from hypoxic fat-laden hepatocytes. These EVs promoted an inflammatory phenotype in KCs as evidenced by increased mRNA expression of inflammasome components in EV-treated Kupffer cells. Via this mechanism, EVs may contribute to the inflammation associated with NASH (49,50). The inflammasome is an intracellular pro-inflammatory structure that promotes inflammatory signaling and metabolic disruption (51). The activation of inflammasomes involves activation of caspase-1 which in turn cleaves pro-IL-1β into its active secreted form, thus amplifying the inflammatory response (52). Interestingly, we observed increased caspase-1 activity in

EVs from fat-laden, hypoxic hepatocytes. In the current study we demonstrate increased caspase-1 activity in circulating EVs in mice with NASH subjected to intermittent hypoxia (IH). Previous studies have demonstrated that circulating EVs levels and inflammasome activation correlate strongly with pathophysiological changes observed during NASH development (4,27,28,53). In our previous studies, we also confirmed that IH promotes NLRP3 inflammasome activation and pro-inflammatory and pro-fibrotic signaling in the context of NASH. In line with these previous results, we have now demonstrated increased levels of circulating EVs in mice with NASH and subjected to IH and we also demonstrate that these EVs contain a higher activity of caspase-1 compared to circulating EVs from control mice. Our results are supported by studies reporting that EVs released by hepatocytes exposed to lipotoxic stress may actively contribute to pro-inflammatory responses by activating macrophages in a NLRP3 inflammasome-dependent, paracrine pathway (17) and (54-56). In particular, a recent study demonstrated the presence of the inflammasome components NLRP3, pro-caspase-1, pro-IL-1β and ASC in macrophage-derived EVs (57). Taken together, our data extend these observations by demonstrating that EVs from hypoxic fat-laden hepatocytes contain active caspase-1 that induces pro-inflammatory signaling in Kupffer cells.

In conclusion, our data clearly indicate the importance of crosstalk between hepatocytes and Kupffer cells under steatotic and hypoxic conditions. Moreover, our results suggest that this crosstalk is mediated via activated caspase-1 contained in EVs and that this is essential for inflammasome activation in macrophages. Our data provide new insights in intercellular communication and the role of inflammasomes in hepatocyte-derived EVs in the context of NAFLD.

Our findings could have implications in the development of EV-based biomarkers, delivery vehicles and therapeutics for the treatment of liver diseases.

5.-REFERENCES

1. Peters KM, Wilson RB, Borradaile NM. Non-parenchymal hepatic cell lipotoxicity and the coordinated progression of non-alcoholic fatty liver disease and atherosclerosis. Curr Opin Lipidol. 2018;29:417-422.

2. Cha JY, Kim DH, Chun KH. The role of hepatic macrophages in nonalcoholic fatty liver disease and nonalcoholic steatohepatitis. Lab Anim Res. 2018;34:133-139.

3. Arab JP, Arrese M, Trauner M. Recent insights into the pathogenesis of non-alcoholic fatty liver disease. Annual Review of Pathology Mechanisms of Disease 2018 13:1, 321-350

4. Csak T, Ganz M, Pespisa J, Kodys K, Dolganiuc A, Szabo G. Fatty acid and endotoxin activate inflammasomes in mouse hepatocytes that release danger signals to stimulate immune cells. Hepatology. 2011; 54:133-44.

5. Pan J, Ou Z, Cai C, Li P, Gong J, Ruan XZ, He K. Fatty acid activates NLRP3 inflammasomes in mouse Kupffer cells through mitochondrial DNA release. Cell Immunol. 2018 ;332:111-120

6. Tang Y, Cao G, Min X, Wang T, Sun S, Du X, Zhang W. Cathepsin B inhibition ameliorates the non-alcoholic steatohepatitis through suppressing caspase-1 activation. J Physiol Biochem. 2018;74:503-510.

7. Ho CM, Ho SL, Jeng YM, Lai YS, Chen YH, Lu SC, Chen HL, Chang PY, Hu RH, Lee PH. Accumulation of free cholesterol and oxidized low-density lipoprotein is associated with portal inflammation and fibrosis in nonalcoholic fatty liver disease. J Inflamm (Lond). 2019;16:7.

8. Trauner, M.; Arrese, M.; Wagner, M. Fatty liver and lipotoxicity. Biochim. Biophys. Acta 2010, 1801, 299–310

9. Hirsova P, Ibrahim SH, Gores GJ, Malhi H. Lipotoxic lethal and sublethal stress signaling in hepatocytes: relevance to NASH pathogenesis.J Lipid Res. 2016 ;57:1758-1770.

10. Geng Y, Hernandez A, Faber KN, de Meijier VE, Blokzijl H, Moshage H. Lipotoxicity in non-alcoholic fatty liver diseases: mechanisms and clinical implications. Bba-mol cell biol l. October 2019. *Submitted*

11. Malhi H. Emerging Role of Extracellular Vesicles in Liver Diseases. Am J Physiol Gastrointest Liver Physiol. 2019; 317: G739–G749.

12. Colombo M, Raposo G, Thery C. Biogenesis, secretion, and intercellular interactions of exosomes and other extracellular vesicles. Annu Rev Cell Dev Biol 2014;30:255-289.

13. Raposo G, Stoorvogel W. Extracellular vesicles: exosomes, microvesicles, and friends. J Cell Biol 2013;200:373-383.

14. Momen-Heravi F, Bala S, Kodys K, Szabo G. Exosomes derived from alcohol-treated hepatocytes horizontally transfer liver specific miRNA-122 and sensitize monocytes to LPS. Sci Rep. 2015; 5: 9991.

15. Hirsova, P., Ibrahim, S.H., Krishnan, A. et al, Lipid-induced signaling causes release of inflammatory extracellular vesicles from hepatocytes. Gastroenterology. 2016;150:956–967

16. Liao CY, Song MJ, Gao Y, Mauer AS, Revzin A, Malhi H. Hepatocyte-Derived Lipotoxic Extracellular Vesicle Sphingosine 1-Phosphate Induces Macrophage Chemotaxis. Front Immunol. 2018;9:2980.

17. Cannito S, Morello E, Bocca C, Foglia B, Benetti E, Novo E, Chiazza F, Rogazzo M, Fantozzi R, Povero D, Sutti S, Bugianesi E, Feldstein AE, Albano E, Collino M, Parola M. Microvesicles released from fat-laden cells promote activation of hepatocellular NLRP3 inflammasome: A pro-inflammatory link between lipotoxicity and non-alcoholic steatohepatitis. PLoS One. 2017;12:e0172575.

18. Kornek, M., Lynch, M., Mehta, S.H. et al. Circulating microparticles as disease-specific biomarkers of severity of inflammation in patients with hepatitis C or nonalcoholic steatohepatitis. Gastroenterology. 2012; 143: 448–458

19. Povero D, Panera N, Eguchi A, Johnson CD, Papouchado BG, de Araujo Horcel L, Pinatel EM, Alisi A, Nobili V, Feldstein AE. Lipid-induced hepatocyte-derived extracellular vesicles regulate hepatic stellate cell via microRNAs targeting PPAR-γ. Cell Mol Gastroenterol Hepatol. 2015;1:646-663.e4.

20. Eguchi A, Lazaro RG, Wang J, Kim J, Povero D, Willliams B, Ho SB, Stärkel P, Schnabl B, Ohno-Machado L, Tsukamoto H, Feldstein AE. Extracellular vesicles released by hepatocytes from gastric infusion model of alcoholic liver disease contain a MicroRNA barcode that can be detected in blood. Hepatology. 2017;65:475-490.

21. Li J, Liu H, Mauer AS, Lucien F, Raiter A, Bandla H, Mounajjed T, Yin Z, Glaser KJ, Yin M, Malhi H. Characterization of Cellular Sources and Circulating Levels of Extracellular Vesicles in a Dietary Murine Model of Nonalcoholic Steatohepatitis. Hepatol Commun. 2019 10;3:1235-1249.

22. Baroja-Mazo A, Martín-Sánchez F, Gomez AI. , et al. The NLRP3 inflammasome is released as a particulate danger signal that amplifies the inflammatory response. Nat Immunol 2014; 15: 738-748

23. Franklin BS, Bossaller L, De Nardo D. , et al. The adaptor ASC has extracellular and 'prionoid' activities that propagate inflammation. Nat Immunol 2014; 15 (08) 727-737

24. Wilson KP, Black JA, Thomson JA, Kim EE, Griffith JP, Navia MA, Murcko MA, Chambers SP, Aldape RA, Raybuck SA. Structure and mechanism of interleukin-1 beta converting enzyme. Nature. 1994 28; 370:270-5.

25. Beier J, Banales J. Pyroptosis: An inflammatory link between NAFLD and NASH with potential therapeutic implications. J Hepatol. 2018; 68: 643–645

26. Liao J, Yang F, Tang Z, Yu W, Han Q, et al. Inhibition of Caspase-1-dependent pyroptosis attenuates copper-induced apoptosis in chicken hepatocyte. Ecotoxicol Environ Saf. 2019;174:110-119.

27. Dixon LJ, Berk M, Thapaliya S, Papouchado BG, Feldstein AE. Caspase-1-mediated regulation of fibrogenesis in diet-induced steatohepatitis. Lab Invest. 2012; 92:713-23.

28. Wree A, Eguchi A, McGeough MD, Pena CA, Johnson CD, Canbay A, Hoffman HM, Feldstein AE. NLRP3 inflammasome activation results in hepatocyte pyroptosis, liver inflammation, and fibrosis in mice. Hepatology. 2014;59:898-910.

29. Mitra S, Exline M, Habyarimana F, Gavrilin MA, Baker PJ, Masters SL, Wewers MD, Sarkar A1. Microparticulate Caspase 1 Regulates Gasdermin D and Pulmonary Vascular Endothelial Cell Injury. Am J Respir Cell Mol Biol. 2018 Jul;59(1):56-64.

30. Mesarwi OA, Loomba R, Malhotra A. Obstructive Sleep Apnea, Hypoxia, and Nonalcoholic Fatty Liver Disease. Am J Respir Crit Care Med. 2019 Apr 1;199(7):830-841

31. Qi JC, Huang JC, Lin QC, Zhao JM, Lin X, Chen LD, Huang JF, Chen X. Relationship between obstructive sleep apnea and nonalcoholic fatty liver disease in nonobese adults. Sleep Breath 2016; 20: 529-535.

32. Petta S, Marrone O, Torres D, Buttacavoli M, Camma C, Di Marco V, Licata A, Lo Bue A, Parrinello G, Pinto A, Salvaggio A, Tuttolomondo A, Craxi A, Bonsignore MR. Obstructive Sleep Apnea Is Associated with Liver Damage and Atherosclerosis in Patients with Non-Alcoholic Fatty Liver Disease. PLoS One 2015; 10: e0142210.

33. Paschetta E, Belci P, Alisi A, Liccardo D, Cutrera R, Musso G, Nobili V. OSAS-related inflammatory mechanisms of liver injury in nonalcoholic fatty liver disease. Mediators Inflamm. 2015;2015:815721.

34. Mesarwi OA, Shin MK, Drager LF, Bevans-Fonti S, Jun JC, Putcha N, Torbenson MS, Pedrosa RP,Lorenzi-Filho G, Steele KE, Schweitzer MA, Magnuson TH, Lidor AO, Schwartz AR, Polotsky VY.Lysyl Oxidase as a Serum Biomarker of Liver Fibrosis in Patients with Severe Obesity and Obstructive Sleep Apnea. Sleep 2015; 38: 1583-1591.

35. Mesarwi OA, Shin MK, Bevans-Fonti S, Schlesinger C, Shaw J, Polotsky VY. Hepatocyte Hypoxia Inducible Factor-1 Mediates the Development of Liver Fibrosis in a Mouse Model of Nonalcoholic Fatty Liver Disease. PLoS One 2016; 11: e0168572.

36. Liu Y, Ma Z, Zhao C, Wang Y, Wu G, Xiao J, McClain CJ, et al. HIF-1alpha and HIF-2alpha are critically involved in hypoxia-induced lipid accumulation in hepatocytes through reducing PGC-1alpha-mediated fatty acid beta-oxidation. Toxicol Lett 2014;226:117-123.

37. Briancon-Marjollet A, Monneret D, Henri M, Joyeux-Faure M, Totoson P, Cachot S, Faure P, et al. Intermittent hypoxia in obese Zucker rats: cardiometabolic and inflammatory effects. Exp Physiol 2016;101:1432-1442.

38. Kang HH, Kim IK, Lee HI, Joo H, Lim JU, Lee J, Lee SH, et al. Chronic intermittent hypoxia induces liver fibrosis in mice with diet-induced obesity via TLR4/MyD88/MAPK/NF-kB signaling pathways. Biochem Biophys Res Commun 2017;490:349-355.

39. Moshage H, Casini A, Lieber CS. Acetaldehyde selectively stimulates collagen production in cultured rat liver fat-storing cells but not in hepatocytes. Hepatology 1990;12:511-518.

40. Pecoraro M, Pinto A, Popolo A. Inhibition of Connexin 43 translocation on mitochondria accelerates CoCl2-induced apoptotic response in a chemical model of hypoxia. Toxicol In Vitro 2018;47:120-128.

41. Chavez-Tapia NC, Rosso N, Tiribelli C. In vitro models for the study of non-alcoholic fatty liver disease. Curr Med Chem 2011;18:1079-1084.

42. Munoz-Sanchez J, Chanez-Cardenas ME. The use of cobalt chloride as a chemical hypoxia model. J Appl Toxicol 2019;39:556-570.

43. Pizarro M, Solis N, Quintero P, Barrera F, Cabrera D, Rojas-de Santiago P, Arab JP, et al. Beneficial effects of mineralocorticoid receptor blockade in experimental non-alcoholic steatohepatitis. Liver Int 2015;35:2129-2138.

44. Cabrera D, Wree A, Povero D, Solis N, Hernandez A, Pizarro M, Moshage H, et al. Andrographolide Ameliorates Inflammation and Fibrogenesis and Attenuates Inflammasome Activation in Experimental Non-Alcoholic Steatohepatitis. Sci Rep 2017;7:3491.

45. Verhaag, E.M., et al., Hormesis in cholestatic liver disease; preconditioning with low bile acid concentrations protects against bile acid-induced toxicity. PLoS One, 2016. 11: p. e0149782.

46. Thery C, Amigorena S, Raposo G, Clayton A. Isolation and characterization of exosomes from cell culture supernatants and biological fluids. Curr Protoc Cell Biol 2006; 3: 22.

47. Schattenberg JM, Lee M-S. Extracellular vesicles as messengers between hepatocytes and macrophages in non-alcoholic steatohepatitis. Gastroenterology. 2016; 150:815±818.

48. Tilg H, Moschen AR. Evolution of inflammation in non-alcoholic fatty liver disease: the multiple parallel hits hypothesis. Hepatology. 2010; 52:1836±1846.

49. Arrese M, Cabrera D, Kalergis AM, Feldstein AE. Innate Immunity and Inflammation in NAFLD/NASH. Dig Dis Sci 2016;61:1294-1303.

50. Schuster S, Cabrera D, Arrese M, Feldstein AE. Triggering and resolution of inflammation in NASH. Nat Rev Gastroenterol Hepatol 2018;15:349-364

51. Szabo G, Petrasek J. Inflammasome activation and function in liver disease. Nat Rev Gastroenterol Hepatol. 2015; 12:387–400.

52. Kubes P, Mehal WZ. Sterile inflammation in the liver. Gastroenterology. 2012; 143:1158–1172.

53. Amir M and Czaja M. Inflammasome-mediated inflammation and fibrosis – it is more than just the IL-1β. Hepatology. 2018; 67: 479–481

54. Baroja-Mazo A, Martin-Sanchez F, Gomez AI, Martinez CM, Amores-Iniesta J, Compan V, Barbera-Cremades M, Yague J, Ruiz-Ortiz E, Anton J et al. The NLRP3 inflammasome is released as a particulate danger signal that amplifies the inflammatory response. Nat Immunol 2014; 15: 738–748

55. Franklin BS, Bossaller L, De Nardo D, Ratter JM, Stutz A, Engels G, Brenker C, Nordhoff M, Mirandola SR, Al-Amoudi A et al. The adaptor ASC has extracellular and “prionoid” activities that propagate inflammation. Nat Immunol 2014;15: 727–73

56. Wang L, Fu H, Nanayakkara G, Li Y, Shao Y, Johnson C, Cheng J, Yang WY, Yang F, Lavallee M et al (2016) Novel extracellular and nuclear caspase-1 and inflammasomes propagate inflammation and regulate gene expression: a comprehensive database mining study. J Hematol Oncol 9: 122

57. Lipinski S, Pfeuffer S, Arnold P, Treitz C, et al. Prdx4 limits caspase-1 activation and restricts inflammasome-mediated signaling by extracellular vesicles. EMBO J. 2019;38:e101266.

Chapter 7

1. - GENERAL DISCUSSION AND CONCLUSIONS

NAFLD refers to a spectrum of histological abnormalities in the liver, ranging from isolated steatosis to non-alcoholic steatohepatitis (NASH), the aggressive form of NAFLD, which is characterized by the presence of necro-inflammatory and fibrotic phenomena in the liver (1,2). Understanding the transition from simple steatosis to NASH is a key issue in the NAFLD field. Currently, several studies have shown that OSAS, mainly via the occurrence of intermittent hypoxia (IH), predisposes to the development of NASH (3). Recent studies have also demonstrated that hypoxia can aggravate hepatocellular damage by triggering pro-inflammatory and pro-fibrotic signals (4,5). However, the pathways underlying these effects are still largely unexplored. The present doctoral thesis proposes that hypoxia may act as a relevant driver of NAFLD progression in subjects with OSAS through amplification of inflammatory and fibrotic signals in the liver. Moreover, our data suggest an important role for extracellular vesicles in the hypoxia-induced exarcebation of hepatocellular damage. We used *in vitro* models of NAFLD/NASH to explore whether hypoxia induces hepatocellular damage, hepatic inflammation and fibrosis via mechanisms that involve cellular crosstalk mediated by extracellular vesicles.

In Chapter 2, we reviewed the most recent findings concerning the role of extracellular vesicles (EVs) in mediating autocrine and paracrine intercellular communication in both ALD and NAFLD as well as their potential use as biomarkers of disease severity and progression (15-17). Considering our results on the crosstalk between hepatocytes and non-parenchymal cells, we propose a role of EVs in intercellular communication and the aggravation of damage in our NAFLD models

The principal findings in Chapter 3 suggest that hypoxia promotes lipids droplet accumulation and cell death via apoptosis, necrosis and pyroptosis in fat-laden primary rat hepatocytes. These phenomena are associated with increased oxidative stress and inflammatory signals including inflammasome/caspase-1 activation and contribute to cellular crosstalk between hepatocytes and Kupffer cells throught EVs, thus aggravating the pathological phenomena of NASH (6,7). Our *in vitro* findings correlated with our findings in an animal model of NASH induced by feeding a CDAA diet. Our results are also in line with previous studies that indicate that hypoxia, via HIF-1α, promotes lipid accumulation in hepatocytes and contributes to liver inflammation and fibrosis in rodent models of NAFLD (8-10). Our studies are the first to investigate the effects of hypoxia in an *in vitro* model of NAFLD/NASH that involves EVs (11). Interestigly, we found a synergistic effect of hypoxia and fat

accumulation in hepatocytes on the increased expression of inflammasome components, suggesting that pyroptosis is the major form of cell death observed in these conditions.

In Chapter 4 we investigated the effect of hypoxia in an *in vivo* mice model of NASH (CDAA diet). In line with our *in vitro* results, intermittent hypoxia increases steatosis, pro-inflammatory gene expression and hepatic inflammasome/caspase-1 activation in mice with NASH. It has been shown that caspase-1 activation contributes to liver damage in NASH (12,13). We also performed experiments to silence HIF-1α in hypoxic fat-laden HepG2 cells, to establish the role of HIF-1α in the pro-inflammatory crosstalk between hypoxic fat-laden hepatocytes (HepG2 cells) and Kupffer cells. We demonstrated that conditioned medium from hypoxic fat-laden HepG2 cells induced an increase in the expression of inflammasome-related genes in Kupffer cells via a mechanism that requires activation of HIF-1α. These novel results are in line with a recent study that proposes a paracrine crosstalk between Kupffer cells and hepatocytes that promotes pro-inflammatory signaling and leads to inflammatory injury (14). Taken together, we identify hypoxia and HIF-1α activation as a potential aggravating factor in the development of NASH in a mechanism that involves caspase-1/inflammasome activation and cellular crosstalk.

In Chapter 5 we demonstrated that hypoxia exarcebates hepatocellular damage in HepG2 cells. Furthermore, hypoxia promotes pro-fibrotic signaling that correlates with increased release of EVs from hepatocytes in our experimental models of NASH. Morever, EVs from hypoxic fat-laden hepatocytes evoke pro-fibrotic responses in LX-2 cells. These results are in agreement with previous studies demonstrating that EVs from lipotoxic hepatocytes induce pro-fibrogenic signals in stellate cells (18,19). Furthermore, we demonstrated increased levels of EVs in serum from CDAA-fed animals exposed to hypoxia and these increased levels correlate with histologically determined fibrosis and pro-fibrotic gene expression in the liver. In Chapter 6 we investigated the paracrine effect of EVs from fat-laden hypoxic hepatocytes on Kupffer cells throught Caspase-1 like cargo into EVs. The expression of pro-inflammatory and inflammasome-related genes was increased in Kupffer cells treated with EVs from hypoxic fat-laden hepatocytes compare to EVs from non-treated hepatocytes, similar finding that we describes in Chapter 3. These results correlate well with previous results indicating crosstalk between injured hepatocytes and Kupffer cells that involves the participation of EVs (20-23). Considering the pro-infammatory role of EVs (24-27), we also evaluated the content of EVs. We could demonstrate the presence of cleaved and active caspase-1 in EVs from hypoxic fat-laden hepatocytes and EVs from serum of CDAA-fed mice exposed to IH. Collectively, these novel findings indicate that EVs from hypoxic fat-laden hepatocytes induce pro-inflammatory and pro-fibrotic signals in Kupffer cells and LX-2 cells, respectively via a mechanism that involves activation of caspase-1 and inflammasomes. Similar results have been discovered in recent clinic studies, where

caspase-1 increased in circulating EVs from patients with stroke outcome ans traumatic brain injury (28,29). Even though there have been studies of EV cargo as suggested biomarkers of different liver diseases (15,30), this study is the firts in propose EV-caspase-1 like potential to be used as a biomarker of NAFLD and OSAS. The complete analyse of EVs was not assessed in this study and future studies to determine the importance of circulating levels of caspase-1, and inflammasome components, in EVs from damage hepatocytes and from animals with NASH in the hypoxia context are warranted. In addition, EVs are gaining interest from a therapeutic point of view, to load EVs with a desired cargo (such as siRNAs) on target cells with potential as a unique drug delivery system (30).

The experimental approaches used in the work presented in this thesis has a number of limitations that we acknowledge. The use of the cobalt chloride-induced chemical hypoxia model (that stabilizes hypoxia inducible factors 1α and 2α under normoxic conditions) is widely accepted as an hypoxia-mimicking model but does not reproduce all the features of the low oxygen-induced hypoxia and therefore ur results should be confirmed in other models. Also, the EVs isolation techniques are in constant refinemet and possible contamination of the EV fraction with lipoproteins due to similarities in size and contamination is possible. Also, in *in vivo* studies, contamination with non-hepatic EVs may also occur in spite of efforts to isolate liver specific particles using specific markers. Also, the small number of mice per group as well as the use of only 1 model of NASH are potential limitations although no ideal model of NAFLD/NASH exists. Future studies should include different models of NAFLD, e.g. high fat diet and also human studies, to confirm our findings. Also, the cargo of EVs should be further analyzed for the presence of other components in addition to inflammasome components, that may modulate the response of Kupffer cells and stellate cells to EVs. A hypoxia-specific population of EVs may also exists and deserve investigation. Of note, our findings could have potential implications in the development of novel biomarkers of NAFLD/NASH in the setting of OSAS that involve EVs or selected components of EVs, like caspase-1.

In summary, this doctoral thesis identifies hypoxia as an aggravating factor in the pathogenesis of NASH. This aggravating effect is dependent on intact HIF-1α signaling in hepatocytes and intercellular crosstalk between hepatocytes on the one hand and Kupffer cells and stellate cells on the other hand. This crosstalk is dependent on extracellular vesicles released from hepatocytes and involves active caspase-1 and inflammasomes. We demonstrate that fat-laden hepatocytes are more susceptible to the damaging effects of hypoxia than non-steatotic hepatocytes and that hypoxia increases the extent of fat accumulation, inflammation and fibrosis both *in vitro* and *in vivo*. Further characterization of EVs released under hypoxic conditions will allow the detailed delineation of their role in the promotion of steatosis, inflammation and fibrosis in the context of NAFLD and OSAS.

2. - PERSPECTIVES

The information generated in this thesis may contribute to a better understanding of intercellular communication in the pathogenesis of NAFLD and the development of novel (EV-based) biomarkers and therapies. It will also be interesting to perform similar studies in other liver diseases.

An exhaustive characterization of the content of EVs isolated from *in vivo* and *in vitro* models of NASH, using genomic, proteomic and metabolomic techniques, will allow us to identify hypoxia-specific mechanisms related to hepatocellular damage that occurs in NASH. In addition, our experimental approach should be extended to clinical samples of patients with OSA and/or NASH, in order to generate translational data. These studies should include characterization of EVs obtained from patients from blood or other bodily fluids such as urine or saliva. This non-invasive approach will allow the identification and validation of novel biomarkers and improve diagnosis and prediction of prognosis of NAFLD/NASH. Finally, non-pharmacological or pharmacological management of the levels of circulating EVs can become a new therapeutic target in the context of NAFLD and OSAS.

3. - REFERENCES

1. Younossi ZM, Koenig AB, Abdelatif D, Fazel Y, Henry L, Wymer M. Global epidemiology of nonalcoholic fatty liver disease-Meta-analytic assessment of prevalence, incidence, and outcomes. Hepatology 2016;64:73-84.

2. Arab JP, Arrese M, Trauner M. Recent insights into the pathogenesis of non-alcoholic fatty liver disease. Annual Review of Pathology Mechanisms of Disease 2018 13: 321-350

3. Mesarwi OA, Loomba R, Malhotra A. Obstructive Sleep Apnea, Hypoxia, and Nonalcoholic Fatty Liver Disease. Am J Respir Crit Care Med. 2019;199:830-841

4. Savransky V, Nanayakkara A, Vivero A, Li J, Bevans S, Smith PL, Torbenson MS, et al. Chronic intermittent hypoxia predisposes to liver injury. Hepatology 2007;45:1007-1013.

5. Savransky V, Reinke C, Jun J, Bevans-Fonti S, Nanayakkara A, Li J, Myers AC, et al. Chronic intermittent hypoxia and acetaminophen induce synergistic liver injury in mice. Exp Physiol 2009;94:228-239.

6. Schuster S, Cabrera D, Arrese M, Feldstein AE. Triggering and resolution of inflammation in NASH. Nat Rev Gastroenterol Hepatol 2018;15:349-364.

7. Arrese M, Cabrera D, Kalergis AM, Feldstein AE. Innate Immunity and Inflammation in NAFLD/NASH. Dig Dis Sci 2016;61:1294-1303.

8. Mylonis I, Simos G, Paraskeva E. Hypoxia-Inducible Factors and the Regulation of Lipid Metabolism. Cells 2019;8.

9. Mylonis I, Sembongi H, Befani C, Liakos P, Siniossoglou S, Simos G. Hypoxia causes triglyceride accumulation by HIF-1-mediated stimulation of lipin 1 expression. J Cell Sci 2012;125:3485-3493.

10. Mesarwi OA, Shin MK, Bevans-Fonti S, Schlesinger C, Shaw J, Polotsky VY. Hepatocyte Hypoxia Inducible Factor-1 Mediates the Development of Liver Fibrosis in a Mouse Model of Nonalcoholic Fatty Liver Disease. PLoS One 2016;11:e0168572.

11. Chavez-Tapia NC, Rosso N, Tiribelli C. In vitro models for the study of non-alcoholic fatty liver disease. Curr Med Chem 2011;18:1079-1084.

12. Dixon LJ, Flask CA, Papouchado BG, Feldstein AE, Nagy LE. Caspase-1 as a central regulator of high fat diet-induced non-alcoholic steatohepatitis. PLoS One 2013;8:e56100.

13. Tang Y, Cao G, Min X, Wang T, Sun S, Du X, Zhang W. Cathepsin B inhibition ameliorates the non-alcoholic steatohepatitis through suppressing caspase-1 activation. J Physiol Biochem 2018;74:503-510.

14. Zhang LY, Zhan DL, Chen YY, Wang WH, He CY, Lin Y, Lin YC, Lin ZN. Aflatoxin B1 enhances pyroptosis of hepatocytes and activation of Kupffer cells to promote liver inflammatory injury via dephosphorylation of cyclooxygenase-2: an in vitro, ex vivo and in vivo study. Arch Toxicol. 2019; 14.

15. Szabo G, Momen-Heravi F. Extracellular vesicles in liver disease and potential as biomarkers and therapeutic targets. Nat Rev Gastroenterol Hepatol. 2017;14(8):455-66.

16. Eguchi A, Feldstein AE. Extracellular vesicles in non-alcoholic and alcoholic fatty liver diseases. Liver Res. 2018;2(1):30-4.

17. Urban SK, Mocan T, Sanger H, Lukacs-Kornek V, Kornek M. Extracellular Vesicles in Liver Diseases: Diagnostic, Prognostic, and Therapeutic Application. Semin Liver Dis. 2019;39(1):70-7.

18. Povero D, Panera N, Eguchi A, Johnson CD, Papouchado BG, de Araujo Horcel L, Pinatel EM, et al. Lipid-induced hepatocyte-derived extracellular vesicles regulate hepatic stellate cell via microRNAs targeting PPAR-gamma. Cell Mol Gastroenterol Hepatol 2015;1:646-663.

19. Lee Y, Kim S, Ko E, Lee JH, Yi HS,Yoo Y, Je J, et al. Exosomes derived from palmitic acid-treated hepatocytes induce fibrotic activation of hepatic stellate cells. Sci Rep 2017; 7: 3710.

20. Momen-Heravi F, Bala S, Kodys K, Szabo G. Exosomes derived from alcohol-treated hepatocytes horizontally transfer liver specific miRNA-122 and sensitize monocytes to LPS. Sci Rep. 2015; 5: 9991.

21. Hirsova, P., Ibrahim, S.H., Krishnan, A. et al, Lipid-induced signaling causes release of inflammatory extracellular vesicles from hepatocytes. Gastroenterology. 2016;150:956–967

22. Liao CY, Song MJ, Gao Y, Mauer AS, Revzin A, Malhi H. Hepatocyte-Derived Lipotoxic Extracellular Vesicle Sphingosine 1-Phosphate Induces Macrophage Chemotaxis. Front Immunol. 2018;9:2980.

23. Cannito S, Morello E, Bocca C, Foglia B, Benetti E, Novo E, Chiazza F, Rogazzo M, Fantozzi R, Povero D, Sutti S, Bugianesi E, Feldstein AE, Albano E, Collino M, Parola M. Microvesicles released from fat-laden cells promote activation of hepatocellular NLRP3 inflammasome: A pro-inflammatory link between lipotoxicity and non-alcoholic steatohepatitis. PLoS One. 2017;12:e0172575.

24. Baroja-Mazo A, Martin-Sanchez F, Gomez AI, Martinez CM, Amores-Iniesta J, Compan V, Barbera-Cremades M, Yague J, Ruiz-Ortiz E, Anton J et al. The NLRP3 inflammasome is released as a particulate danger signal that amplifies the inflammatory response. Nat Immunol 2014; 15: 738–748

25. Franklin BS, Bossaller L, De Nardo D, Ratter JM, Stutz A, Engels G, Brenker C, Nordhoff M, Mirandola SR, Al-Amoudi A et al.The adaptor ASC has extracellular and “prionoid” activities that propagate inflammation. Nat Immunol 2014;15: 727–73

26. Wang L, Fu H, Nanayakkara G, Li Y, Shao Y, Johnson C, Cheng J, Yang WY, Yang F, Lavallee M et al. Novel extracellular and nuclear caspase-1 and inflammasomes propagate inflammation and regulate gene expression: a comprehensive database mining study. J Hematol Oncol 2016; 9: 122

27. Lipinski S, Pfeuffer S, Arnold P, Treitz C, et al. Prdx4 limits caspase-1 activation and restricts inflammasome-mediated signaling by extracellular vesicles. EMBO J. 2019;38:e101266.

28. Kerr N, et al. Inflammasome Proteins in Serum and Serum-Derived Extracellular Vesicles as Biomarkers of Stroke. Front Mol Neurosci. 2018; 11: 309

29. Kerr N, et al. Inflammasome proteins as biomarkers of traumatic brain injuryPLoS One. 2018; 13(12): e0210128.

30. Hernández A, Arab JP, Reyes D, Lapitz A, Moshage H, Bañales JM, Arrese M Extracellular Vesicles in NAFLD/ALD: From Pathobiology to Therapy. Cells. 2020; 9(4). pii: E817.

Appendices

ABBREVIATIONS

OSAS: obstructive sleep apnea syndrome

IH: intermittent hypoxia

NAFLD: non-alcoholic fatty liver disease

NAFL: non-alcoholic fatty liver

NASH: non-alcoholic steatohepatitis

CDAA: choline-deficient amino acid-defined

NLRP3: NOD-like receptor Pyrin Domain Containing 3

GSDMD: gasdermin D

KC: Kupffer cells

TG : triglyceride

IL: interleukin

TNF-α: tumor necrosis factor-alpha

HIF-1α: hypoxia inducible factor 1 alpha

EVs: extracellular vesicles

FBS: fetal bovine serum

FFA: free fatty acids

CM: conditioned medium

AUF: Arbitrary units of fluorescence

PBS: phosphate-buffered saline

LDH: Lactate dehydrogenase

NTA: nanoparticle tracking analysis

ASC: Apoptosis-Associated Speck-Like Protein Containing CARD

SUPPLEMENTARY MATERIAL

Table S1: Sequences of primers and probes used for quantitative real time PCR

Gene		Primers	Specie
NLRP3	Sense	5`-GTG CGT GGG ACT GAA GCA T-3`	Rattus
	Anti-sense	5`-CTG ACA ACA CGC AGA TGT GAG A-3`	norvegicus
	Probe	5`-AGC AGC TGA CCA ACC AGA GTT TCT GCA-3`	
ASC	Sense	5`-AGC TGT GGC TAC TGC AAC CA-3`	Rattus
	Anti-sense	5`-GAC CCT GGC AAT GAG TGC TT-3`	norvegicus
	Probe	5`-ACA AAA TGT TCT GTT CTG GCT GTG CCC T-3`	
Caspase-1	Sense	5`-CGG AGT TTC CTA CTG AAT CTT TTA ACA-3`	Rattus
	Anti-sense	5`-GAA AGA CAA GCC CAA GGT TAT CA-3`	norvegicus
	Probe	5`-ACC ACT CCT TGT TTC TCT CCA CGG CA-3`	
IL-1β	Sense	5'-ACC CTG CAG CTG GAG AGT GT-3'	Rattus
	Anti-sense	5`-TTG ACT TCT ATC TTG TTGAAG ACA AAC C-3`	norvegicus
	Probe	5`-CCC AAA CAA TAC CCA AAG AAG AAG ATG GAA AAG-3`	
IL-6	Sense	5`-CCG GAG AG GAG ACT TCA CAG A-3`	Rattus
	Anti-sense	5`-AGA ATT GCC ATT GCA CAA CTC TT-3`	norvegicus
	Probe	5`-ACC ACT TCA CAA GTC GGA GGC TTA ATT ACA-3`	
TNF-α	Sense	5`-GTA GCC CAC GTC GTA GCA AAC-3`	Rattus
	Anti-sense	5`-AGT TGG TTG TCT TTG AGA TCC ATG-3`	norvegicus
	Probe	5`-CGC TGG CTC AGC CAC TCC AGC-3`	
iNOS	Sense	5`-CTA TCT CCA TTC TAC TAC TAC CAG ATC GA-3`	Rattus
	Anti-sense	5`-CCT GGG CCT CAG CTT CTC AT-3`	norvegicus
	Probe	5`-CCC TGG AAG ACC CAC ATC TGG CAG-3`	
IL-10	Sense	5`-TGC AGG ACT TTA AGG GTT ACT TGG-3`	Rattus
	Anti-sense	5`-CAG GGA ATT CAA ATG CTC CTT G-3`	norvegicus
	Probe	5`-TCT CTG CCT GGG GCA TCA CTT CTA CCA-3`	
Arg-1	Sense	5`-AGC TGG GAA TTG GCA AAG TG-3`	Rattus
	Anti-sense	5`-TCC AGT CCA TCA ACA TCA AAA CTC-3`	norvegicus
	Probe	5`-AAT GGG CCT TTT CTT CCT TCC CAG CAG-3`	

IL-1β	Sense	5`-ACA GAT GAA GTG CTC CTT CCA-3`	Homo
	Anti-sense	5`-GTC GGA GAT TCG TAG CTG GAT-3`	sapiens
	Probe	5`-CTC TGC CCT CTG GAT GGC GG-3`	
IFN-γ	Sense	5`-ACT GTC GCC AGC AGC TAA AA-3`	Homo
	Anti-sense	5`-TAT TGC AGG CAG GAC AAC CA-3`	sapiens
TNF-α	Sense	5`-CCC TGG TAT GAG CCC ATC TAT C-3`	Homo
	Anti-sense	5`-AAA GTA GAC CTG CCC AGA CTC G-3`	sapiens
	Probe	5`-ATC AAT CGG CCC GAC TAT CTC GAC TTT-3`	
IL-18	Sense	5`-AAG ATG GCT GCT GAA CCA GT -3`	Homo
	Anti-sense	5`-GAG GCC GAT TTC CTT GGT CA -3`	sapiens
NLRP3	Sense	5`-GGG ATT CGA AAC ACG TGC AT-3`	Homo
	Anti-sense	5`-CAG GAG AGA CCT TTA TGA GAA AGC A-3`	sapiens
	Probe	5`-ATC TGA ACC CCA CTT CGG CTC ATC TCT TT-3`	
TGF-β1	Sense	5`-GGC CCT GCC CCT ACA TTT- 3’	Homo
	Anti-sense	5`-CCG GGT TAT GCT GGT TGT ACA -3`	sapiens
	Probe	5`-ACA CGC AGT ACA GCA AGG TCC TGG C-3`	
CTGF	Sense	5`-TGT GTG ACG AGC CCA AGG A- 3`	Homo
	Anti-sense	5`-TCT GGG CCA AAC GTG TCT TC- 3`	sapiens
	Probe	5`-CCT GCC CTC GCG GCT TAC CG- 3`	
α-SMA	Sense	5`-GGG ACG ACA TGG AAA AGA TCT G- 3`	Homo
	Anti-sense	5`-CAG GGT GGG ATG CTC TTC A -3`	sapiens
	Probe	5`-CAC TCT TTC TAC AAT GAG CTT CGT GTT GCC C- 3`	
Collagen-I	Sense	5`- GGC CCA GAA GAA CTG GTA CAT C -3`	Homo
	Anti-sense	5`- CCG CCA TAC TCG AAC TGG AA -3`	sapiens
	Probe	5`-CCC CAA GGA CAA GAG GCA TGT CTG- 3`	
TIMP-1	Sense	5`- CTT CTG GCA TCC TGT TGT TG -3`	Homo
	Anti-sense	5`- GGT ATA AGG TGG TCT GGT TG -3`	sapiens
18S	Sense	5`-CGG CTA CCA CAT CCA AGG A -3`	Homo
	Anti-sense	5`-CCA ATT ACA GGG CCT CGA AA -3`	

	Probe	5`-CGC GCA AAT TAC CCA CTC CCG A -3`	sapiens
TGF-β1	Sense	5`- CTC CCG TGG CTT CTA GT GC -3`	Mus
	Anti-sense	5`- GCC TTA GTT TGG ACA GGA TCT G -3`	musculus
CTGF	Sense	5`- GGG CCT CTT CTG CGA TTT C -3`	Mus
	Anti-sense	5`- ATC CAG GCA AGT GCA TTG GTA -3`	musculus
Collagen-I	Sense	5`- GCT CCT CTT AGG GGC CAC T- 3`	Mus
	Anti-sense	5` -CCA CGT CTC ACC ATT GGG G- 3`	musculus
α-SMA	Sense	5` -GTC CCA GAC ATC AGG GAG TAA- 3`	Mus
	Anti-sense	5`-TCG GAT ACT TCA GCG TCA GGA- 3`	musculus
TIMP-1	Sense	5`-GCA ACT CGG ACC TGG TCA TAA -3`	Mus
	Anti-sense	5`-ACT GTT CCT GAA CTC AAC T-3`	musculus
18S	Sense	5’-CGG CTA CCA CAT CCA AGG A-3’	Mus
	Anti-sense	5’-CCA ATT ACA GGG CCT CGA AA-3’	musculus

HIF-1α	Sense Anti-sense	5`-AGG ATG AGT TCT GAA CGT CGA AA -3` 5`-CTG TCT AGA CCA CCG GCA TC-3`	Mus musculus
TNF-α	Sense Anti-sense	5`-CCC TCA CAC TCA GAT CAT CTT CT -3` 5`-GCT ACG ACG TGG GCT ACA G -3`	Mus musculus
IL-1β	Sense Anti-sense	5`-ACT GTT CCT GAA CTC AAC T-3` 5`-ATC TTT TGG GGT CCG TCA ACT-3`	Mus musculus
IL-18	Sense Anti-sense	5`-GAC TCT TGC GTC AAC TTC AAG G-3` 5`-CAG GCT GTC TTT TGT CAA CGA-3`	Mus musculus
NLRP3	Sense Anti-sense	5`-ATT ACC CGC CCG AGA AAG G-3` 5`-TCG CAG CAA AGA TCC ACA CAG-3`	Mus musculus
Caspase-1	Sense Anti-sense	5`-ACA AGG CAC GGG ACC TAT G-3` 5`-TCC CAG TCA GTC CTG GAA ATG-3`	Mus musculus
IL-6	Sense Anti-sense	5`-TAG TCC TTC CTA CCC CAA TTT CC-3` 5`-TTG GTC CTT AGC CAC TCC TTC-3`	Mus musculus
IFN-γ	Sense Anti-sense	5`-ATG AAC GCT ACA CAC TGC ATC-3` 5`-CCA TCC TTT TGC CAG TTC CTC-3`	Mus musculus
MCP-1	Sense Anti-sense	5`- TTA AAA ACC TGG ATC GGA ACC AA -3` 5`- GCA TTA GCT TCA GAT TTA CGG GT -3`	Mus musculus

LIST OF PUBLICATIONS

• Hao S, Hernández A, Quiroz-Muñoz M, Céspedes C, Vio C, Ferreri N. Prostaglandin E2 EP3 receptor downregulates COX-2 expression in the medullary thick ascending limb (mTAL) induced by hypertonic NaCl. Am J PhysiolRenal Physiol, 2014;15:307

•Cabrera D, Wree A, Povero D, Solis N, Hernández A, Pizarro M, Moshage H, Torres J, Feldstein A, Cabello-Verrugio C, Brandan E, Barrera F, Arab J, Arrese M. Andrographolide ameliorates inflammation and fibrogenesis and attenuates inflammasome activation in experimental non-alcoholic steatohepatitis. Scientific Reports, 2017; 7:3491

•Arrese M, Hernández A, Astete L, Estrada L, Cabello-Verrugio C, Cabrera D. TGF-beta and Hepatocellular carcinoma: When a friend becomes an enemy Curr Protein Pept Sci. 2018;19:1172-1179.

• Geng Y , Hernández A, Oun A, Buist-Homan M, Blokzijl H, Faber KN, Dolga A, Moshage Protective effect of metformin against palmitate-induced hepatic cell death. H. *(BBA) Molecular Basis of Disease, 2020: 1866(3): 165621*

• Geng Y , Hernández A, Faber KN, E de Meijer, Blokzijl H, Moshage H. Lipotoxicity in non-alcoholic fatty liver diseases: mechanisms and clinical implications. *Submitted 2020*

• Kalergis A, Muñoz-Durango N, Arrese M, Hernández A, Jara E, Cabrera D. A deficiency of MR in myeloid cells reduces liver steatosis by impairing activation of CD8+T cells in a NASH mouse model. *Submitted 2020*

•Hernández A, Geng Y, Sepulveda R, Solis N, Torres J, Arab JP, Barrera F, Cabrera D, Moshage H, Arrese M. Chemical Hypoxia induces pro-inflammatory signals in fat-laden hepatocytes and contributes to cellular crosstalk with Kupffer cells. (*BBA) Molecular Basis of Disease 2020; 1866: 165753*

•Hernández A, Reyes D, Arab JP, Arrese M, Moshage H. Extracellular Vesicles derived from fat laden hypoxic hepatocytes promote a pro-fibrotic phenotype in stellate cells. BBA Molecular Basis of Disease, Jan 2020 *Submitted under revision*

•Hernández A, Arab JP, Reyes D, Lapitz A, Moshage H, Bañales JM, Arrese M. Extracellular vesicles in NAFLD/ALD: from pathobiology to therapy. *Cells 2020; 9:817*